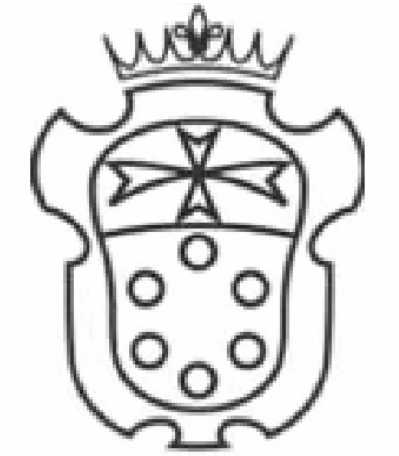

SCUOLA
NORMALE
SUPERIORE

Ph. D. Thesis, Chemistry
Tesi di Perfezionamento in Chimica

Thiol-ene functionalisation of homo- and copolymers of butadiene with L-cysteine derivatives

Candidate:
Luca Lotti

Supervisor:
Francesco Ciardelli, Professor

Pisa, academic year 2009/2010

Ai miei genitori,
che m'hanno sempre accompagnato
e sostenuto

Abstract

In the present work the functionalisation of oligomers of butadiene (liquid 1,2-polybutadiene *PBL*) and of oligomers of a random copolymer butadiene/styrene (*SBRL*) was performed by the addition of either *N*-acetyl-L-cysteine, *N*-acetyl-L-cysteine methyl ester or L-cysteine methyl ester through the thiol-ene radical reaction. Functionalisation was carried out in solution and in presence of a free radical initiator (2,2'-azobisisobutyronitrile, *AIBN*). The initial feed ratio polymer / cysteine derivative / initiator was varied, in order to highlight the occurrence of side reactions and to understand their possible influence on the reaction mechanism.

The ^{1}H-NMR determination of the functionalisation extent brought out that the addition degrees of thiols were always high, regardless of the initial initial thiol / double bond ratio; the complete conversion of the double bonds, however, was never reached because of side-reactions. In order to better understand the occurrence of the latters, reactions with AIBN or with other free radical generating species were performed, in absence of thiol; the purpose of these experiments was to reproduce the presence of macroradicals similar to those generated during the thiol addition, and to investigate their reactivity towards other macromolecules present in the reaction environment. The reaction products of these runs were characterised, and some conclusions were drawn regarding the different type of side reactions occurring with the two polymeric substrates (PBL or SBRL).

The high functionalisation degrees often caused a drastic change in the macroscopic properties of the polymers, ranging from improved solubility in hydrophilic solvents (for instance in alkaline aqueous solutions) to a remarkable increase of the glass transition temperature. Chiral properties were carried from the functionalising agents to the modified polymers; this phenomenon was evaluated by polarimetry of polymer solutions in organic solvents, and discussed with reference to the reciprocal proximity of the L-cysteine side chains. Circular dichroism measurements were also performed in order to investigate the possible presence of secondary / tertiary structures analogously to what reported in scientific literature for similar systems.

In the last part of this work, a possible use of (*N*-acetyl-L-cysteine)-functionalised products was evaluated; the hydrophilically-modified polymers showed the ability to act as coupling agents between hydrophobic polymeric matrices and inorganic, hydrophilic fillers in composite materials. The incorporation of the functionalised polymers (PBL and SBRL having various functionalisation degrees) in compounds for ground tyres was performed, and the rheological / mechanical properties of the resulting compounds were evaluated; the formulation used are highly innovative compounds including an elevated silica content.

1. INTRODUCTION

1.1 The thiol-ene reaction: recent reflowering of a long-known reaction

The thiol-ene reaction is a chemical transformation that has been extensively studied during the last decades, and has recently seen widespread use in the synthesis of various organic polymers. The main features of the thiol-ene reaction, that will be discussed in detail later in this chapter with particular reference to the addition of thiols to dienic polymers, are:

- its easy initiation by heat, UV or visible light, radical initiators, such as 2,2'-azobisisobutyronitrile (*AIBN*), or photoinitiators such as benzophenone or hydroquinone
- high yields (sometimes quantitative)
- high regio- or stereoselectivity
- lack of sensitivity to water and oxygen
- tolerance to a wide variety of solvents and functional groups.

A general scheme of the addition of a generic thiol RSH (R = H; primary, secondary or tertiary alkyl group; Ph; R'C=O; *et alii*), that can take place with electrophilic, nucleophilic or free radical mechanism, is reported in Scheme 1 (for a general review on the reaction mechanism, see ref.[1, 2]).

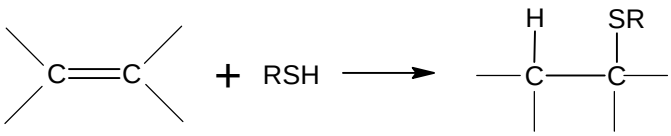

Scheme 1 – Addition of a thiol to a double bond, adapted from ref.[1]

In the absence of free-radical initiators the addition to simple olefins undergo an electrophilic mechanism, and the Markovnikov's rule is followed. (However, this reaction is usually slow and it requires severe conditions to be performed. The use of an acid catalyst speeds up the reaction; for example, it can be performed in concentrated sulphuric acid[3]). Instead, the regiochemistry of the free radical addition to double bonds leads to anti-Markovnikov products, i.e. with the sulphur atom bonded to the less-substituted carbon[4, 5]; the orientation has sometimes been used as a diagnostic tool to elucidate which mechanism is operating.

While the electrophilic attack of a proton to the carbon-carbon double bond involves the formation of the most stable carbenium ion (i.e. on the most substituted carbon; Markovnikov's rule), the radicalic attack of a thiol is obtained through prioritary addition of RS· species instead of hydrogen-related species (in particular, the concentration of hydrogen radicals in thiol-ene reactions is negligible). The reaction intermediate is a carbon radical; the most favoured one is located on the

most substituted carbon, and the reaction goes with a different regiochemistry with respect to the electrophilic proton attack. In other words, a radical addition to the double bonds follows the anti-Markovnikov rule, and the thiol-ene reaction strictly follows this rule as seen also in pioneering studies regarding the mechanism of thiol-ene additions[5]; this reaction mechanism is reported in Scheme 2.

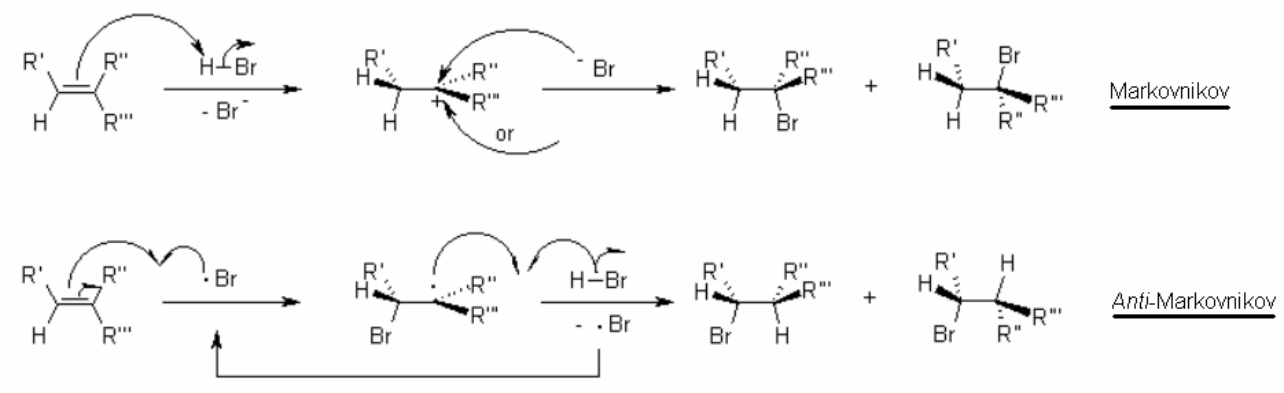

Scheme 2 – Markovnikov and Anti-Markovnikov behaviour of, respectively, i) electrophilic HBr addition and ii) free radical addition of HBr (bromine radicals are generated by an initiator; adapted from ref.[6])

In Scheme 2 the R' / R" / R"' substituents may vary. In fact, the olefins to which the thiols can be added may be internal, terminal, cyclic and carry functional groups on the sp_2 carbons such as –COOH and –COOR, $–NO_2$, sulphonic groups, *et cetera*. In the same scheme, also the stereochemistry is shown: both with electrophilic or radicalic mechanism, the racemic product is obtained.

Many thiol-ene systems could match the requirements for a reactivity to be defined as a *click* one. *Click chemistry* is a chemical philosophy introduced by Karl Barry Sharpless and co-workers in 2001[7], and describes *"chemistry tailored to generate substances quickly and reliably by joining small units together"*. According to Sharpless first works[7-11], a click reaction must have the following criteria:

- controllable and wide application in scope
- high yields
- generation of non-toxic and stable byproducts
- high regio- and stereoselectivity
- simple reaction conditions
- good availability of starting materials and reagents
- environmentally friendly solvent (preferably water)
- easy product isolation (distillation, precipitation, crystallisation…)
- strong thermodynamic driving force leading to a single reaction path.

Analogously, a *click polymer functionalisation* could be defined as a click reaction involving polymers and functionalising agents, in order to introduce particular molecules or functional groups along the macromolecular chain[12].

Through the functionalisation of polymers many objectives could be achieved, such as obtaining polymers more compatible with hydrophilic phases (metal surfaces, inorganic fillers in composite materials, *et cetera*); materials with a higher glass transition temperature (T_g); rubbers less soluble in aromatic oils; materials of improved flame retardancy properties; and so on. Later in this chapter, the objectives that were achieved in the last fifty years by using the thiol-ene reactivity in order to provide functionalised polymers will be discussed with particular reference to the used substrates.

Apart from the functionalisation of polymers, the thiol-ene photopolymerisations has recently gained, in the current decade, a growing importance for the synthesis of injectable resins, especially for biomedical uses (see, for instance, the papers[13-18] or the patents[19-21] published by Christopher Bowman and co-workers, or the publications of Charles Hoyle and co-workers[22-25]; for a review about thiol-ene photopolymerisable materials see another work of Hoyle[26]). These reactions, often *click*, occur between a tri- or tetrathiol and an alkene with three or more C=C double bonds; under light irradiation (often UV light) a photoinitiator generates thiyl radicals that attack the alkene double bonds. This results in a chain reaction, since the generated carbon radical will abstract a hydrogen radical from another thiol molecule generating a new thiyl radical. At this point, a side-reaction with a carbon-carbon double bond could occur, favouring the crosslinking of the material: a completely crosslinked material (a resin) is obtained both if the side reaction takes place or not, i.e. regardless of this side-reaction occurrence. A scheme of a typical thiol-ene photopolymerisation resulting in a resin is reported in Scheme 3.

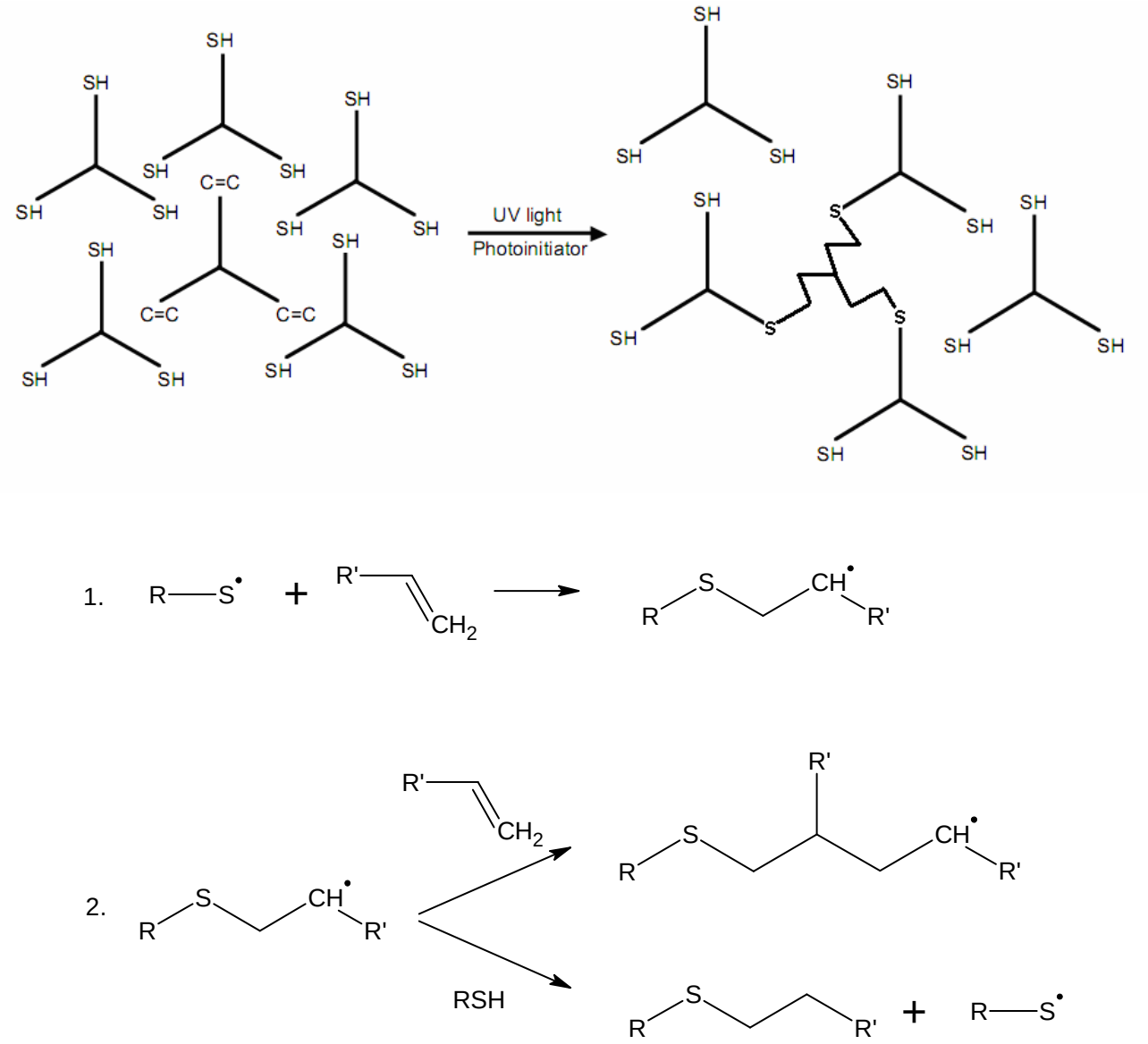

Scheme 3 – A typical photopolymerisation between a trithiol and an alkene with three C=C double bonds including a schematic reaction mechanism for the propagation step. Adapted from [15] and [23]

The hydrogen transfer reaction between the carbon radical on the polymer and the thiol is the key step for the creation of a chain reaction, and this is one of the most important features of the thiol-ene reactivity.

The thiols have always been considered ideal hydrogen transfers agents: in fact, this reaction is faster than any other possible radical reaction[27] (for instance, during resin synthesis: coupling between growing oligomers; coupling between a thiyl radical and a growing oligomer), and, in most photopolymerisations, is even faster than the crosslinking between a growing oligomer and a C=C double bond of another molecule as shown by Bowman and Cramer[28-30].

Thiol-ene *photofunctionalisation*, defined as a thiol-ene functionalisation initiated by a photoinitiator, works similarly to a photopolymerisation (i.e. a reaction the general mechanism of which is reported in Scheme 3). A polymer rich in C=C double bonds and a functionaliser (often a

poly-functional thiol, if the aim of the study is to bring some functionalities on the macromolecule) are reacted together with a mechanism involving i) the addition of the thiyl radical to the double bond, and ii) the transfer of a hydrogen atom from another thiol molecule to the carbon radical generated after the previous thiyl addition.

In thiol-ene functionalisation of polymers, the primary radicals can also be generated by thermally induced self-dissociation of initiators (e.g. AIBN, dibenzoylperoxide *BPO*, *et cetera*) or, if there is no initiator at all, by the thermal induced self-dissociation of the thiol functional group in a thiyl and a hydrogen radical (see for instance the mechanism proposed in ref.[31]). The resulting functionalised polymer is characterised by thioether bonds between the main macromolecular chain and the side groups.

The thiol-ene functionalisation has been studied mostly on diene rubbers, such as natural rubber (NR), polybutadiene (PB) or copolymers of butadiene and styrene (SBR random copolymers or SBS triblock copolymers). A generic thiol-ene functionalisation (thiol: RSH) on an unsaturation having a H_2C=CH-M structure (M = aliphatic chain; a typical unsaturation could be is a *butadiene 1,2-unit* in diene polymers) initiated by an initiator $I^{\bullet}$ is reproduced in Scheme 4 according to the general reaction scheme reported in ref.[32].

$$I^{\bullet} + RSH \rightarrow IH + RS^{\bullet}$$

$$\begin{cases} RS^{\bullet} + H_2C = CH - M \rightarrow RSCH_2 - CH^{\bullet} - M \\ RSCH_2 - CH^{\bullet} - M + RSH \rightarrow RS^{\bullet} + RSCH_2 - CH_2 - M \end{cases}$$

Scheme 4 – Thiol-ene functionalisation steps.

In Scheme 4 the propagation steps are marked on the left with a parenthesis. Thiol-ene functionalisation can be considered a chain reaction as a thiyl radical ($RS^{\bullet}$) is generated in the last step and induces another attack on another unsaturations, allowing the propagation of the functionalisation.

The termination reactions, not described in Scheme 4, could be:

- coupling between two thiyl radicals
- coupling between two intermediate polymer radicals (chain elongation / bridging)
- coupling between an intermediate polymer radical and a thiyl unit (this will lead to a α,β double-functionalised unit. It is an unlikely path because of sterical reasons. De la Campa and Pham[33], in a ^{13}C-NMR mechanicistic study performed on a thiol-ene functionalised

product, managed to recognise signals due to these units, though of very small extent. The authors do not discuss anymore this eventuality in later papers on the same subject[34, 35])

- coupling between a thiyl group and a $I^{\bullet}$ radical.

Another reaction that could affect the primary structure of the diene polymer is arises from the close disance of 1,2- units in polybutadienes (homo- and copolymers) and consists in the formation of 5- or 6-membered units[36] (Scheme 5).

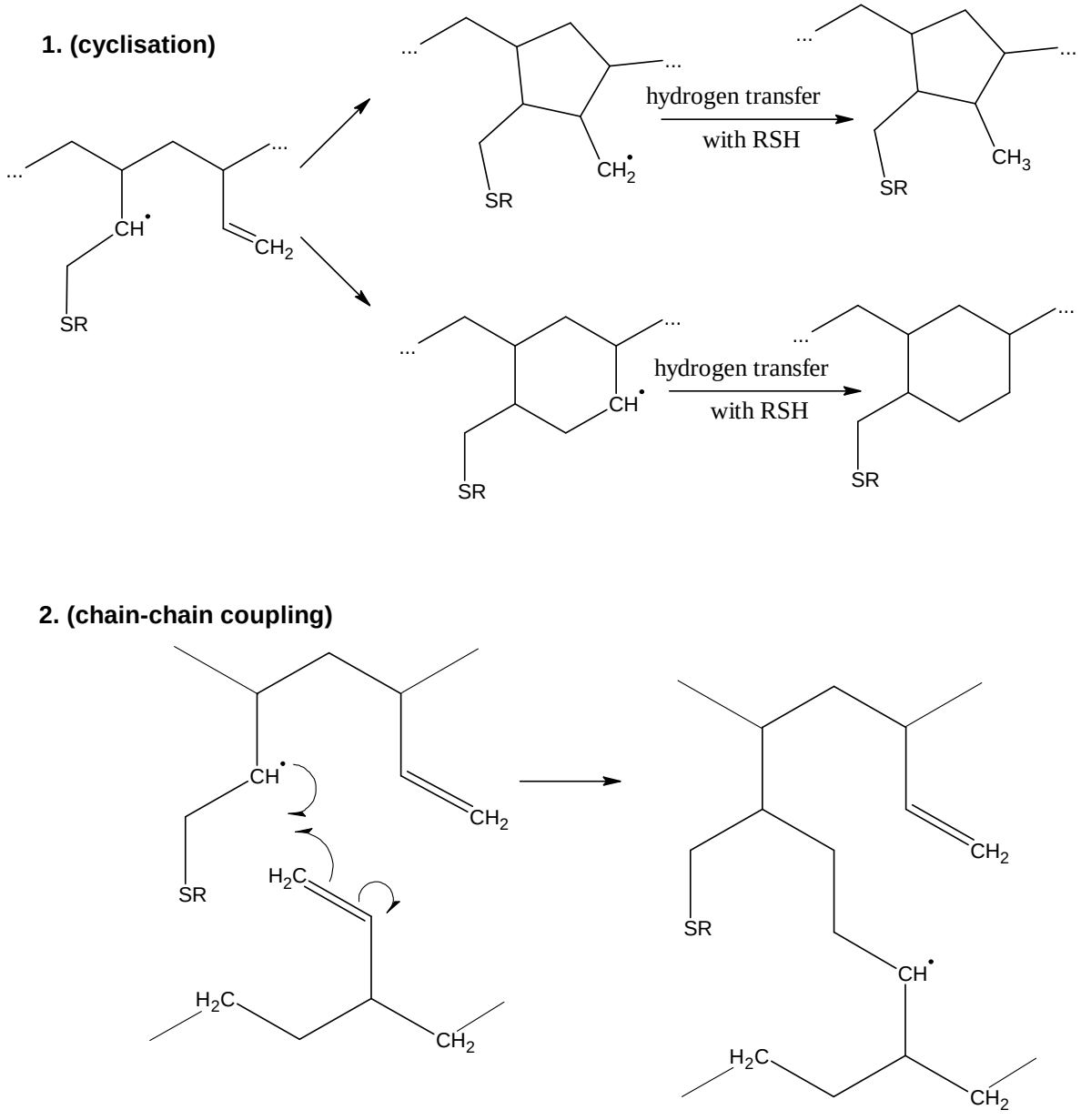

Scheme 5 – Possibile cyclisation (1.) or chain-chain coupling (2.) side reactions

In the next sub-chapters of this introduction, the prior art of polymer thiol-ene functionalisation will be described. Mechanicistic / kinetic studies (leading to reaction schemes such as that reported in Scheme 5) or characterisation of thiol-functionalised materials will be included in this description.

1.2 Diene polymers and thiols adopted in thiol-ene functionalisations

1.2.1 Pioneering work of the '50s and the '60s on various rubbers

The first thiol-ene reactions on polymers were performed on natural rubber (*NR*), that was subsequently proved to be similar to long-chain polybutadienes in terms of reactivity[37, 38]; these functionalisations were performed by Cunneen and co-workers during the '50s[39-43]. The objectives of the work of Cunneen were mainly to obtain oil- and petrol-resistant rubbers[40], or to explore new crosslinking methodologies through the addition of dithiols or dithioacids[41] or by using alkali bases on carboxy-functionalised NR (functionalised with thioglycolic acid, *TGA*)[42]. In each of his studies, Cunneen verified the occurrence of thiol-ene reaction between the studied thiol and a small molecule resembling NR molecular structure (for example: oligomers of isoprene, cyclohexene and derivatives, squalene, myrcene and derivatives).

Formation of thiyl radicals was induced by irradiating the reaction vessels with bare UV light, or by using organic peroxides under the same conditions. Cunneen performed some reactions using ascaridole (1-methyl-4-(1-methylethyl)-2,3-dioxabicyclo[2.2.2]oct-5-ene), and some in absence of any initiator. The thiol conversion degrees obtained in these pioneering works were high, ranging from 20 to 90+%; the best conversion degrees were obtained in defect of thiol with respect to the unsaturations, though the highest functionalisation degrees were obtained with higher feed ratios.

The most remarkable points of Cunneen works are:

i) *activation* of the thiyl group through a radical initiator, UV light or heating (or a combination of these) is not mandatory but preferable in order to obtain high yields
ii) the reaction shows high conversion degrees
iii) bulk properties of the functionalised products could vary in a wide range (stress-strain behaviour[41, 44], T_g and crystallisation behaviour[43], rheological behaviour[42]).

Cunneen's studies led to two patents about oil- resistant[45] or cold-resistant[46] rubbers; a summary of the most interesting results arising from the works of Cunneen is reported in Table 1. In Scheme 6 a reaction general scheme for thioacid functionalisation of NR is reported, according to the cited author[40].

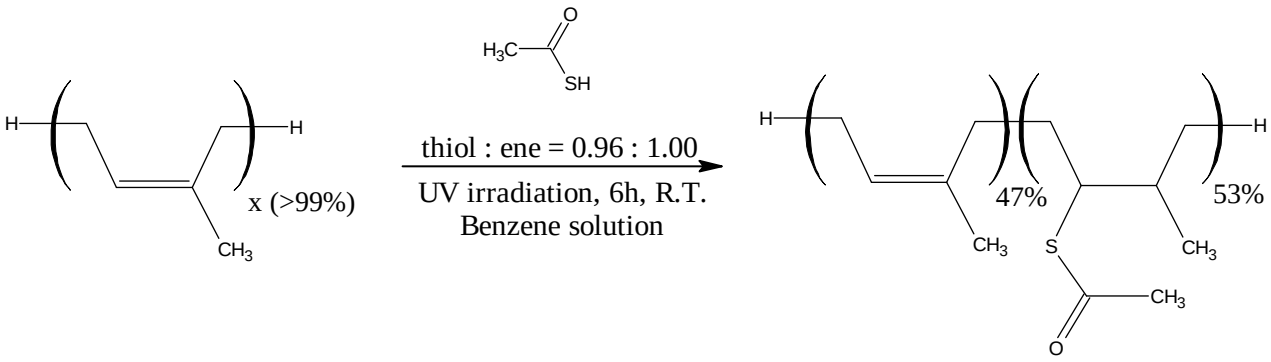

Scheme 6 – Reaction conditions and general scheme for a functionalisation of NR with thioacetic acid[40]

The subscripts in the products are normalised to ideal macromolecules of 100 monomeric units

Reagents	Reaction Conditions[c]	[Initiator]:[RSH]:[C=C]	DF %[b]	Thiol Conversion %
[39] NR / TGA / ascaridole[a]	t: 20h NR: 1 gram	0.02:0.07:1	2.66	38.0
[39] NR / thiophenol / ascaridole[a]	t: 16h NR: 1 gram	0.02:0.62:1	0.99	1.6
[39] NR / pen^{iso}SH / ascaridole[a]	t: 16h NR: 1 gram	0.04:1.31:1	2.62	2.0
[40] NR / CH_3COSH / No initiator	t: 6h NR: 1 gram	(-):0.96:1	50	52.8
		(-):2.40:1	52	21.6
[40] NR / CH_3COSH / No initiator	t: 6h NR: 15 grams	(-):0.96:1	53	55.2
		(-):1.60:1	76	47.5
[40] NR / $CH_2ClCOSH$ / ascaridole[a]	t: 6h NR: 1 gram	0.02:0.92:1	88	95.2
[40] NR / $CH_2ClCOSH$ / ascaridole[a]	t: 6h NR: 50 grams	0.02:0.93:1	56	60.0
[40] NR / $CHCl_2COSH$ / ascaridole[a]	t: 6h NR: 1 gram	0.02:0.80:1	71	88.9
[40] NR / $CHCl_2COSH$ / ascaridole[a]	t: 6h NR: 0.5 grams	0.02:1.00:1	44	44.4
[40] NR / CCl_3COSH / ascaridole[a]	t: 6h NR: 1 gram	0.02:0.43:1	43	99.8
		0.02:0.86:1	76	79.9

Table 1 – Results arising from the works of Cunneen[39, 40]

[a] = ascaridole: 1-methyl-4-(1-methylethyl)-2,3-dioxabicyclo[2.2.2]oct-5-ene

[b] = Degree of Functionalisation, defined as molar amount of grafted units per 100 monomers

[c] = all the reactions are performed in benzene, at room temperature, and under UV lighting

In the same decade, Marvel[37] and Serniuk[47, 48] investigated similar thiol-ene functionalisations in order to obtain oil-resistant rubbers; they used, as functionalisers, TGA, 2-mercaptoethanol and

other polar thiols, and they worked on 1) NR[47, 48] 2) polybutadienes[37, 48] having different primary structures and different molecular weights 3) SBR[48] 4) acrylonitrile / butadiene random copolymer, NBR[48] (the molecular structure of some of these rubbers is reported in Figure 1). These studies, again, highlighted the role played by the radical initiator: the functionalisation degrees were much higher in presence of an initiator than by using bare UV light (thiol conversion nearly doubled[40, 47, 48]).

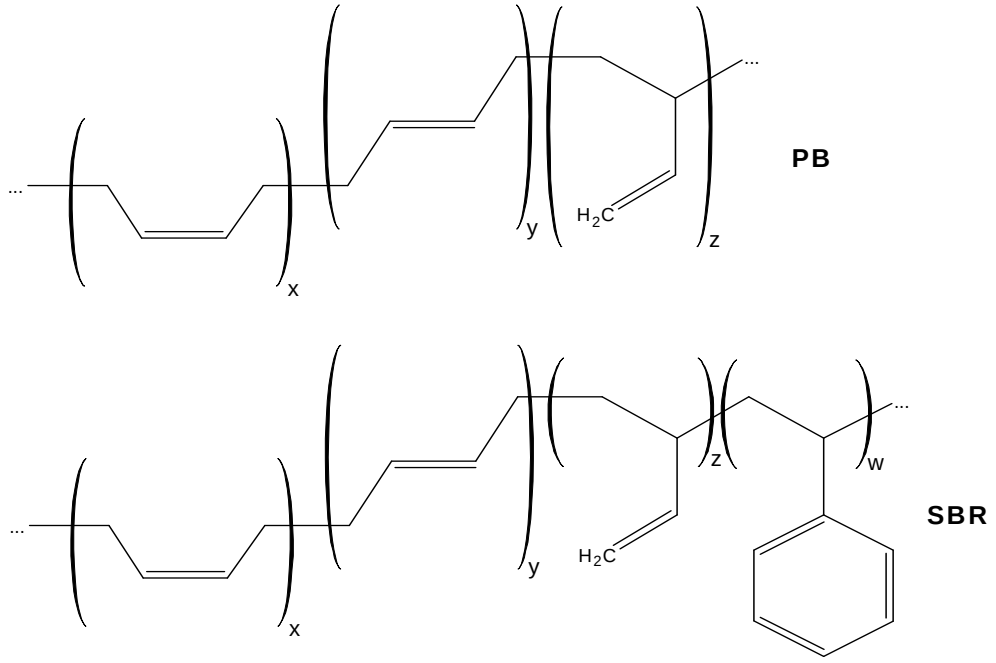

Figure 1 – Primary structure of a polybutadiene and of a SBR rubber. Typically, for long chain PBs, x > 99% (y + z ~ 1%) while PBLs may vary (in this thesis the used PBL has x = 0%, y = 9.1%, z = 90.9%). For commercial SBRs, usually w = 15-25%, x + y = 65-75% and z < 5%

These early studies all showed that the vinyl units (arising from the 1-2 polymerisation of buta-1,3-diene during PB synthesis) are more reactive toward the thiol. In any case these studies were mainly focused on the modification of long chain polymers having mostly poly(1,4-) sequences. In fact, the order of reactivity 1,2- » 1,4-*cis* > 1,4-*trans* was especially confirmed by reaction on model compounds between thiols and simple olefins resembling the structural units of polybutadiene rubbers (for instance, internal *cis*- and *trans*- olefins, or terminal ones)[38-43, 48, 49]. Later, this trend was also observed on similar model compounds[32, 50-54] or with other dienic polymers[31-35, 50-57].

Another remarkable mechanicistic aspect was a noticeable anti-Markovnikov behaviour of the addition reaction[38-40, 49, 58, 59]. This behaviour is typical of free radical additions to double bonds and it is due to the relative stability of the secondary carbon radical with respect to the primary one, as shown also in other studies (see, for instance, ref.[60] on the HBr addition to olefins in presence of free radicals for the mechanism). The anti-Markovnikov feature was observed also in the first study ever regarding the interaction between thiols and alkenes (1905)[61].

1.2.2 Functionalisation of oligomers: liquid polybutadienes

The addition of polar thiols (TGA, 2-mercaptoethanol, 2-mercaptopropanoic acid, various dithiols) to liquid polybutadienes (*PBL*s) was first studied by Alexis Oswald and co-workers during the '60s[38]. This was the first time that functionalisation was observed on a diene rubber having a noticeable amount of 1,2- vinyl units (19 mol.-%; anyway the papers of Oswald also included the functionalisation of long chain NR and SBR having a very small amount of 1,2- units). The high functionalisation degrees observed by the author (see Table 2) indicated that large amounts of polar thiols could be added to PBLs, obtaining new materials with modulated hydrophilicity.

During the '80s, Aldo Priola and co-workers functionalised PBLs in order to obtain high added-value additives for improving the paints adhesion on particular surfaces. As thiols, the authors used 2-mercaptoethanol, TGA, 3-mercaptopropanoic acid or (mercaptopropyl)trimethoxy silane (MPTS); photoinitiators under UV irradiation were used[31, 57], but Priola also investigated reactions carried out in absence of initiators analogously to what had previously been done by Cunneen.
In the works of Priola the conversion degrees of thiol were periodically evaluated, and the kinetics of the functionalisation studied. Graphs reporting thiol conversion *versus* reaction time showed a negative exponential growth up to a limited conversion value[31]; the author showed that, for short reaction times, the thiol-ene functionalisation follows the behaviour of first-order reactions. From an exponential fit of the experimental values the kinetic constants for various thiols and for different substrates were determined. In accordance with previous literature works, the reaction on PBL having 45 mol.-% of 1,2- units was remarkably faster than on PBL having around 1 mol.-% of vinyl units (with TGA, $k_{PB45} / k_{PB1} \sim 10$, where k is the pseudo-first order kinetic constant). Considering reactions with model compounds, the reaction between TGA and 1-octene was even faster with respect to the one with PBL having 45 mol.-% of 1,2- units ($k_{1\text{-oct}} / k_{PB45} \sim 3$).
The difference in reaction rate observed in this very latest case, i.e. between a model olefin and PBL, can be due to an influence of the molecular weight of the substrate on the reactivity: the diffusion of the thiol molecules in a more constraint substrate influences the reaction occurrence slowing its rate[31]. In any case the author evaluated through viscosimetry the average molecular weights of the reaction products ($<M_n>$ and $<M_w>$), and he showed that the influence of the degradation or the chain elongation reactions (Scheme 5, path 2.) was, in any case, negligible.
During late '80s, Gorski and co-workers employed octane-1-thiol[53, 55, 56] or mercaptapropyl trimethoxysilane (MPTS)[55, 56] in thiol-ene functionalisation of various PBLs to obtain products that, under particular conditions, could undergo a sol-gel process by creating a crosslinked resin.

A thiol-ene reaction with MPTS on polyisobutenes with telechelic unsaturations was also performed by the same research group[52] in order to obtain similar crosslinkable elastomeric systems; these particular systems were later studied especially by Blackborow and co-workers[62], and were the subject of European patents of both Gorski and Blackborow research groups[63-65]. Thiol-ene functionalised polyisobutenes are not diene polymers similar to those treated in the present study and related results are not pertinent and will not be discussed here.

The kinetic studies performed by Gorski on photo-induced thiol-ene functionalisations on model olefins (structural isomers of pentene) showed, again, that the kinetic constant of reaction between thiol and mono-substituted C=C double bonds is higher than internal *cis*- or *trans*- α,β disubstituted unsaturations[53] (Figure 2), and they confirmed previous literature results. The data of Gorski confirm a negative-exponential dependence of conversion from reaction time, i.e., the instantaneous concentration of thiol follows a first order law with best fit for short reaction times.

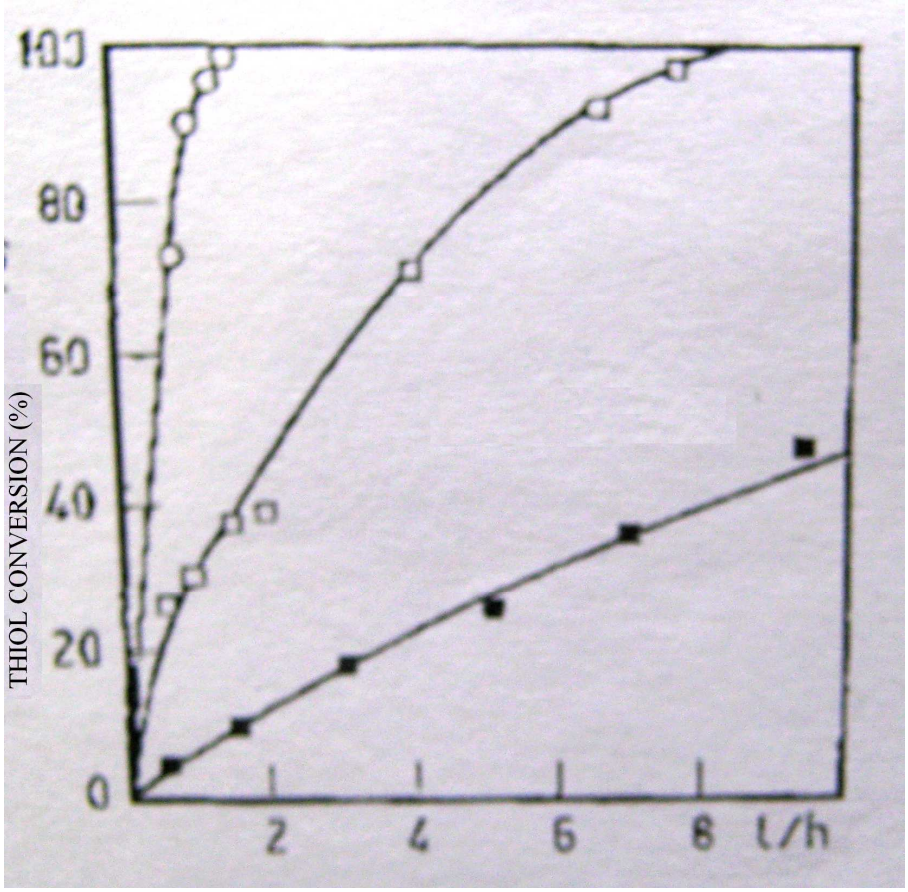

Figure 2 – Thiol Conversion (%) *versus* time for reactions between 8-mercaptoctan-1-ol and (○) pent-1-ene (□) *cis*-pent-2-ene (■) *trans*-pent-2-ene (adapted from ref.[53])
No solvent, room temperature, 1.5 wt.-% benzophenone, UV irradiation, molar thiol:ene = 1:1

Conversion data of Oswald, Priola and Gorski works, that still represent the totality of works reported so far in the scientific literature on pure PBLs, are summarised in Table 2.

Reagents	Reaction Conditions	[Initiator]:[RSH]:[C=C]	DF %	Thiol Conversion %
[38] PBL (1,2- 19%) / CH_3COSH / no initiator	15-17 °C, in bulk UV light, t: 13h	(-):0.33:1	29.3	88
[38] PBL (1,2- 19%) / $CH_3CHSHCOOH$ / no initiator	15-17 °C C_6D_6 solution UV light, t: 13h	(-):0.33:1	16.7	50
[38] PBL (1,2- 19%) / $HSCH_2CH_2OH$ / no initiator	15-17 °C CS_2 solution UV light, t: 13h	(-):0.83:1	41.6	50
[31] PBL (1,2- 45%) / TGA / no initiator	25 °C, THF solution UV light, t: up to 30’	(-):0.26:1	12.5	48
[31] PBL (1,2- 45%) / TGA / Benzophenone	25 °C, THF solution UV light, t: up to 30’	0.0086:0.26:1	21.0	80
[31] PBL (1,2- 45%) / TGA / DMFA[a]	25 °C, THF solution UV light, t: up to 30’	0.0086:0.26:1	24.3	93
[31] PBL (1,2- 45%) / $HSCH_2CH_2OH$ / no initiator	25 °C, respectively in: THF – CH_2Cl_2 – C_6H_6 UV light, t: 20’	(-):0.26:1	14.4	55 – THF
			11.7	45 – CH_2Cl_2
			8.9	34 – C_6D_6
[53] PBL (1,2- 1%) / $CH_3(CH_2)_7SH$ / Benzophenone	R.T., cyclohexane UV light, t: 24h	0.334:1:1	72.6	73
[53] PBL (1,2- 54%) / $CH_3(CH_2)_7SH$ / Benzophenone	R.T., cyclohexane UV light, t: 24h	0.334:1:1	60.0	60
[53] PB long chain[b] (1,2- 2.4%) / $CH_3(CH_2)_7SH$ / Benzophenone	R.T., cyclohexane UV light, t: 24h	0.334:1:1	62.6	63
[55] PBL (1,2- 54%) / $CH_3(CH_2)_7SH$ / BPO[c]	35 °C, *p*-xylene t: 2h	0.167:1:1	79.1	79
		0.334:1:1	81.0	81
		0.670:1:1	79.8	80
		1:1:1	79.3	79
[55] PBL (1,2- 54%) / $CH_3(CH_2)_7SH$ / BPO[c]	35 °C, cyclohexane t: 2h	0.334:1:1	76.9	77
		0.670:1:1	75.0	75
[55] PBL (1,2- 54%) / $CH_3(CH_2)_7SH$ / BPO[c]	35 °C, diethyl ether t: 2h	0.167:1:1	80.3	80
		0.334:1:1	78.2	78
		0.670:1:1	79.8	80
[55] PBL (1,2- 54%) / MPTS / BPO[c]	35 °C, cyclohexane t: 2h	0.670:1:1	crosslinked product	
[55] PBL (1,2- 54%) / MPTS / BPO[c]	35 °C, diethyl ether t: 2h	0.334:1:1	crosslinked product	

Table 2 – Results arising from Oswald[38], Priola[31] and Gorski[53, 55, 56] works

[a] DMFA = 2,2-dimethoxy-2-phenylacetophenone (photoinitiator) [b] $<M_n> \sim 2 \cdot 10^5$ Da; [c] BPO = dibenzoylperoxide

The conversion degrees reported in Table 2 are always higher than 50% regardless of the thiol used; only in one case, though, the reaction is quantitative (addition of MPTS on PBL in presence of dibenzoylperoxide[56]). As expected, the lowest conversion degrees are obtained in absence of initiator: this result is in agreement with previous works, and confirms the possibility of obtaining a certain amount of active thiyl radicals from the self-dissociation of thiol molecules.

There are no important differences in terms of thiol conversion when using different initiators; a more detailed study on the influence of initiatiors on thiol-ene functionalisation of hydroxytelechelic polybutadienes will be discussed later.

As observed in pioneering works (Table 1) the highest conversion degrees with PBLs are reached in defect of thiol (Table 2), but the highest degrees of modification occurred when the thiol was even to or exceeded the stoichiometric amount of double bonds.

Priola observed an effect of the solvent on the conversion degrees obtained functionalising PBL with TGA in tetrahydrofuran, in benzene or in dichloromethane[31]. The author suggested that the effect could be reconduced to the different diffusivity of the thiol in the reaction medium.

Gorski varied the amount of initiator on many similar experiments. On the adopted systems (octan-1-thiol / PBL / BPO, see Table 2), though, he could not observe any substantial variation in terms of conversion and functionalisation degree[55].

1.2.3 Functionalisation of oligomers: hydroxy / carboxy telechelic liquid polybutadienes

The thiol-ene functionalisation of elastomers was also used to obtain new materials for polyurethane formulations. During the ‘80s and simultaneously to many works on PBLs, hydroxyl- or carboxy- telechelic liquid polybutadienes (*HTPB* and *CTPB*, respectively), were often used as additives of solid propellants for rockets[66], or as the “polyol” part in polyurethanes[67].

The first thiol-ene functionalisations of these materials were studied since 1981 by the Pascault research team. They first showed that, in particular experimental conditions (large excess of thiol), it was possible to make an addition to all of the double bonds of a diene elastomer with aliphatic thiols[33-35].

The work of Gonzalez de la Campa and Pham[33] represents the first detailed NMR study regarding functionalised polybutadienes, and it has been cited in nearly every successive thiol-ene work. In the cited paper, a HTPB (1,2-: 20 mol.-%) was functionalised with simple thiols (n-BuSH, 4-methylthiophenol, 2,2-dimethylpropanthiol) and reaction products were characterised through ^{1}H- and ^{13}C-NMR. The authors not only confirmed the previously observed anti-Markovnikov behaviour and the different reactivity of 1,2- *versus* 1,4- units, but they also confirmed the existence of α,β dithioether units both along the macromolecular chain or in side groups. This can be

explained based on the 1,4- and 1,2- polybutadiene units that were functionalised twice (Scheme 7); as well as for the thiyl radical-ene reaction step, the double functionalisation of 1,2- units is faster than the functionalisation of 1,4- units, and the signal of the NMR spectra is reported to be more intense. The double functionalisation of a single vinyl unit has to be considered a termination reaction, as it is a coupling between two intermediate radicals.

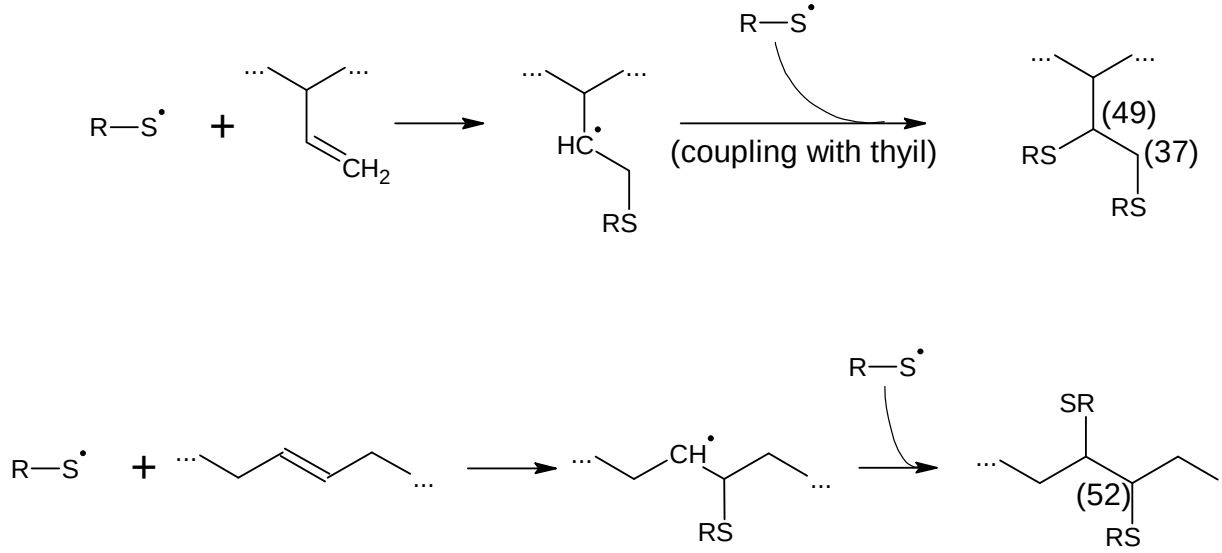

Scheme 7 – Double functionalisation of 1,2- and 1,4-*trans* units according to Gonzales de la Campa and Pham[33]
Numbers in parenthesis are ^{13}C-NMR chemical shifts of the thio-etereal carbons

In the same work, the 1,4- units geometric isomerisation, that was already observed by Cunneen on NR[43], was observed with 4-methylthiophenol; a scheme representing the amounts of units in an instance of the cited study is reported in Scheme 8 (note the composition variation in 1,4- units).

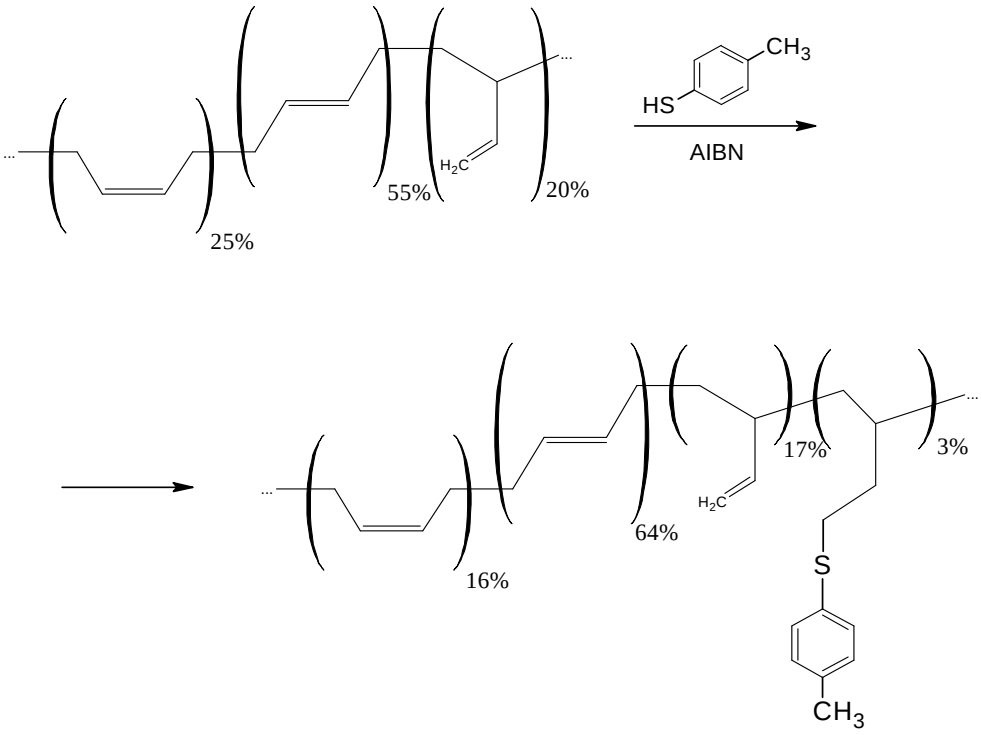

Scheme 8 – Isomerisation of 1,4- units during thiol-ene addition (scheme adapted from ref.[33])

The results of thiol-ene functionalisations performed by the Pascault research group along with those by Gonzalez de la Campa and Pham are reported in Table 3.

Reagents	Reaction Conditions	[Initiator]:[RSH]:[C=C]	DF%	Thiol Conversion %
[34] HTPB[a](1,2- 88%) / Bu[n]SH / AIBN	60°C, toluene solution t: 5h	0.0100:2:1	99	49.5
[33] HTPB[a](1,2- 20%) / Bu[n]SH / AIBN	60°C, toluene solution t: up to 54h	0.0066:3:1	94	31.3
		0.0100:2:1	84	42.0
[33] HTPB[a](1,2- 20%) / Pen[neo]SH / AIBN	60°C, toluene solution t: up to 28h	0.0066:3:1	22	8.0
[33] HTPB[a](1,2- 20%) / 4-tolylSH / AIBN	60°C, toluene solution t: up to 34h	0.0066:3:1	4	1.3
[35] CTPB[b](1,2- 90%) / Bu[n]SH / AIBN	70°C, C_6H_6 solution t: 4h	0.02:2:1	94	47.0
[35] CTPB[b](1,2- 90%) / $HSCH_2CH_2COOH$ / AIBN	70°C, C_6H_6 solution t: 4h	0.02:2:1	95	47.5

Table 3 – Results arising from Gonzalez de la Campa and Pascault works[33-35]

[a]HTPB = hydroxy telechelic polybutadiene; [b]CTPB = carboxy telechelic polybutadiene

A summary of the observations arising from these works on HTPBs and CTPBs follows.

- The steric hindrance of both the thiol and the *ene* units plays an important role as observed in previous pioneering works on NR / SBR / PB or with PBLs. Depending on the thiol, the authors observed functionalisation of the 1,2- units only (using HTPB + neo-pentyl SH, the steric hindrance around double bonds is the cause of this evidence); isomerisation and almost no functionalisation using 4-methylthiophenol (the steric hindrance around the thiol group could have caused this isomerisation instead of functionalisation).
- The kinetics of functionalisation has been studied[33]. As previously remarked by Aldo Priola for the functionalisation of PBLs[31] and by Gorski for the reaction with model compounds (see Figure 2)[53] the kinetics follows a first order law.
- The reaction does not seem to be influenced by the presence of telechelic hydroxylic or carboxylic groups on the polymer: conversion degrees with HTPBs or CTPBs are comparable to those obtained with PBLs.
- The molecular weight of the polymers has been checked by size-exclusion chromatography (*SEC*) in each of these studies, and it grows, as expected, with the functionalisation degree:

in fact, the weighted average molecular mass of the repeating unit of the functionalised products varies subsequently to functionalisation. The collected data accounts for no plausible chain-elongation or crosslinking reaction; however, the authors notice that the SEC measurement of the molecular weight of the products having the highest functionalisation degrees is not reproducible. This phenomenon is likely to be caused by the fact that the hydrodynamic volume is mainly influenced by the macromolecular chain length over the number of grafted units[35] (in the *Results and Discussion* chapter the very same phenomenon will be observed on a system presented in this thesis work).

- The anti-Markovnikov behaviour, i.e. addition of thiol on the β carbon atom of 1,2- units, is observed and confirmed in all the cited works on HTPB and CTPB thanks to detailed proton and ^{13}C-NMR characterisation of products.
- The glass transition temperature of CTPB (n-butyl SH)-functionalised samples is lowered (-40~-46 °C with respect to -22 °C of the pristine CTPB), and this is due to the possible increment of free volume around the macromolecular chain caused by the introduction of aliphatic chains. On the contrary, the glass transition temperature of CTPB functionalised with 3-mercaptopropanoic acid is raised to +4 °C, and this is probably due to the inter- and intramolecular hydrogen bonds of the carboxylic units[35].

Other studies regarding thiol-ene modification of hydroxy- and carboxytelechelic polybutadienes were performed by the research group of Bernard Boutevin[50, 51, 68-71]. The authors developed new materials for polyurethane synthesis, using fluorinated thiols[68, 70], phosphonated thiols[51] or most common thiols bearing –OH or –COOH groups[69, 71].

The authors had different aims when using the cited thiols. The functionalisation of CTPB with TGA was carried out in order to obtain a polymer carrying a modulated amount of carboxylic moieties, that could be used as a starting substrate for the synthesis of UV-crosslinkable resins[69]. In this case, the presence of a photoinitiator for the thiol-ene grafting of TGA could start the functionalisation after the deposition / casting of the elastomer and under UV irradiation. The final material, showing an elevated glass transition temperature, had the mechanical behaviour of a resin.

By using fluorinated thiols, instead, Boutevin investigated the field of fluorinated polyol parts for polyurethanes formulations (the possibility of the introduction of fluorinated polyol molecular segments in polyurethanes had previously been explored by Mueller[72] in 1984). In this case, the authors obtained new polyurethanes having good mechanical / thermal properties, though the environmental impact of the halogenated products either in gaseous phase (*CFC*) or in aromatic solid phase (*PCB*) has stopped their use in polymer formulation. Boutevin, later, shifted to the use of phosphonated thiols for the synthesis of improved fireproofing polyurethanes[51]; lately, Boutevin

explored the possible use of beta-mercapto ethanol to create base materials for polyurethane resins in which the T_g was modulated by the functionalisation degree of the polyol part[71].

Apart from a precise characterisation of the primary structure of the functionalised polymers (via ^{1}H- and ^{13}C-NMR, SEC, DSC, FT-IR spectroscopy), in the works of Boutevin and co-workers some other features of the thiol-ene functionalisation of HTPB were investigated and used.

First of all, the author observed that the kinetic order of reactivity of the thiol-ene reactions (1,2-units > 1,4-*cis* > 1,4-*trans*) could be used to obtain high conversion degrees by limiting the amount of reacting thiol to the amount of vinylic double bonds. The functionalisation of a HTPB with a fluorinated thiol ($C_6F_{15}C_2H_4SH$) in presence of a photoinitiator provided 93% of thiol conversion simply reducing the thiol:ene feed ratio to the stoichiometric amount of 1,2- units[70]. In later papers in which the author studies the reaction with different feed ratios, these observations were confirmed. This is a direct effect of the difference of the rate constants between the 1,2- *versus* the 1,4- units; the author, in his cited works, often detects (in proton NMR spectra) thiol moieties attached to 1,4-*cis* units, though the amount of 1,2- / thiol adduct units is, on average, 10-fold the amount of 1,4- / thiol adduct units (this ratio is equal to the ratio between the typically measured kinetic constants[31, 33, 53]). A scheme representing a fluorination of an HTPB, including a brief description of the primary structure of the reagent and of the product, is reported in Scheme 9, while data arising from these works are collected in Table 4.

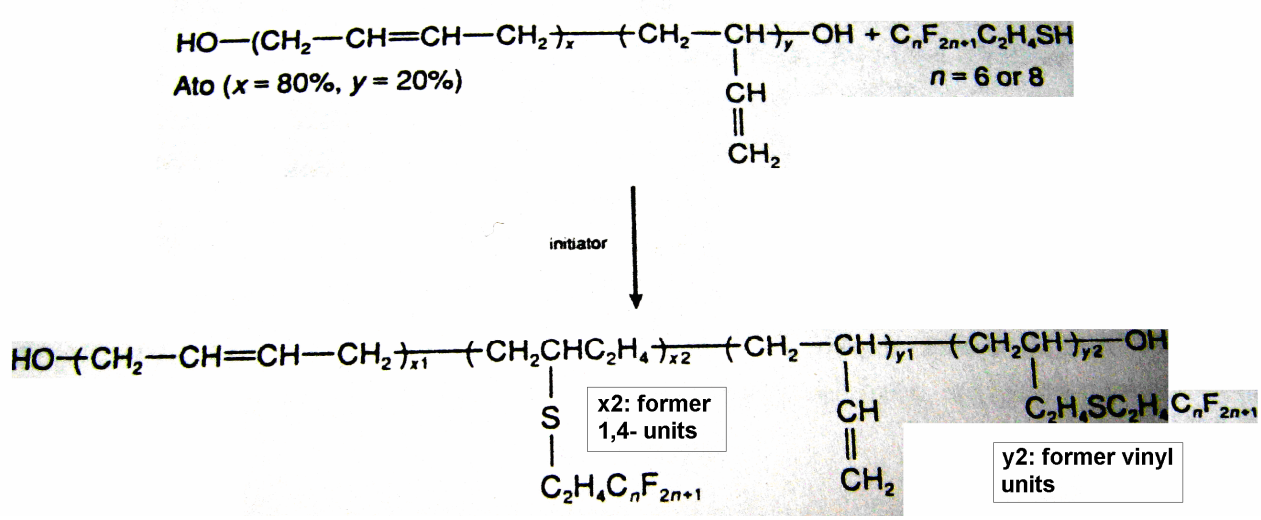

Scheme 9 – Thiol-ene fluorination performed on HTPB[68]. 0 < x2 < 1 and 3 < y2 < 11 (per 100 monomers)

Reagents	Reaction Conditions	[Initiator]:[RSH]:[C=C]	DF %	Thiol Conv. %
[69]CTPB (1,2- 20%) / TGA / AIBN	66°C, THF solution t: 5h	0.002:0.28:1	12.5	45
[70]HTPB (1,2- 20%) / $C_6F_{15}C_2H_4SH$ / benzophenone	R.T., THF solution UV light, t: up to 6h	0.0055:1.0:1	43.6	44
		0.0055:0.5:1	27.3	55
		0.0055:0.2:1	18.6	93
[68]HTPB (1,2- 20%) / $C_6F_{15}C_2H_4SH$ / Various initiators	60°C, THF sol., peroxicarbonate, 3h	0.004:0.2:1	4	20
	74°C, MEK[a] sol., Bu^tperoxypival., 3h	0.004:0.2:1	11	55
	79°C, MEK[a] sol., AIBN, t: 3h	0.004:0.2:1	7	35
	93°C, xylene sol., BPO, t: 3h	0.004:0.2:1	5	25
	135°C, xylene sol., $Bu^t_2O_2$, t: 3h	0.004:0.2:1	~ 0	~ 0
[68]HTPB (1,2- 20%) / $C_6F_{15}C_2H_4SH$ / Bu^tperoxypivalate	74°C, MEK[a] solution, t: 6h	0.004:0.2:1	11	55
		0.020:1.0:1	25	25
		0.040:2.0:1	41	21
		0.060:3.0:1	65	22
		0.080:4.0:1	59	15
[68]HTPB (1,2- 20%) $\langle Mn \rangle = 10^3$Da / $C_6F_{15}C_2H_4SH$ / Bu^tperoxypivalate	74°C, MEK[a] solution, t: 6h	0.004:0.2:1	9	45
		0.020:1.0:1	23	23
		0.040:2.0:1	19	10
[51]HTPB (1,2- 24%) $HS(CH_2)_3PO(OEt)_2$ / AIBN	66°C, THF solution, t: 6h	0.02:0.2:1	10	49
		0.02:0.3:1	15	51
[71]HTPB (1,2- 19%) / $HSCH_2CH_2OH$ / AIBN	85°C, toluene sol., t: 4h	0.00067:0.067:1	4.2	64

Table 4 – Results arising from Boutevin works[51, 68-71]. [a] MEK = methylethyl ketone, b.p. 79°C

In the same cited work about the fluorination of HTPBs[68], Boutevin systematically performed the functionalisations runs in presence of five different free radical initiators (Table 4, third major row). This study showed that there are differences in the reactivity induced by these initiators; Boutevin indicates the nature of the primary radical as a key factor for an efficient generation of thiyl radicals (in the described chemical system, the best results were obtained with *tert*-butyl peroxypivalate, followed by AIBN).

The highest conversion degrees are observed when the thiol:ene feed ratio is low, and especially when the thiol is in defect with respect to the vinyl content of the unmodified polymer (Table 4).

Boutevin was the first suggesting that 6-membered cyclic units could be formed (see Scheme 5, page 8). This eventuality was invoked in ref.[68] to explain a remarkable difference between the values of the functionalisation degree obtained by different analytical methodologies; generally, a remarkable *loss* of residual vinylic units was observed from the ^{1}H-NMR was observed.
Considering that a *lack* of residual vinyl units had occurred could have had a great impact on previous literature works, in which various methodologies of determination of the functionalisation degree led to unreproducible results[31, 33-36, 40, 41, 53, 57]. For instance, all the methodologies based on the use of the amount of residual double bonds on the functionalised products as internal standard are invalid, as well as those in which the DF was determined by difference subtracting the amount of vinyl units from the total.

The research group of Claude Bunel has been very active since late '90s in the research field of crosslinkable polyurethanes. In particular, they explored the possibilities offered by the thiol-ene functionalisations to create crosslinkable polyol parts of polyurethanes by modifying HTPB or CTPB with silane moieties, such as MPTS[73, 74]. (The authors also tried to obtain crosslinked materials through employment of other functionalising units and / or functionalisation reactivities; the created adducts having methacrylic functionalities[75] or styrene units[76], along with silane groups attached to HTPBs through urethane linkage[77, 78]).
Papers in which the MPTS silane was used in thiol-ene functionalisations, though on PBLs, were already cited in this chapter; these studies were performed by Priola[57] and Gorski[55, 56] (the results of these studies are summarised in Table 2). Bunel and co-workers, previously to their thiol-ene works, obtained polymerisable monomers carrying silane units via thiol-ene reaction on the non-polymerised monomers[79, 80], though the reduction in the conversion degrees of the polymerisation due to the presence of MPTS discouraged this pre-synthetic introduction of the silane on diene polymers.
The purpose of the modification with MPTS is to obtain crosslinkable polyurethanes by adding only a moderate amount of a crosslinking agent on the polymer, preserving, ideally, polyurethane properties. In fact, the crosslinking induced by the hydrolysis of ethoxy silane groups has a great impact on the properties of the system even if the units per macromolecule are few[81]. As Bunel and co-workers point out[73], the thiol-ene functionalisation of HTPB could be, in this case, an extremely effective and cheap reaction, since a limited amount of thiol could be added with very high conversion degrees (thiol:1,2- feed ratio ≤ 1; the feed ratio in this range represents the best reaction conditions for the highest conversion degrees, as shown from Boutevin[68, 70, 71]). Working on the same substrate of Gonzalez de la Campa and Boutevin[33, 34, 51, 68, 70, 71], i.e. a HTPB having 20 / 22

mol.-% of 1,2- units and a $<M_n>$ of 2800 Da, Bunel studied the reaction kinetics and obtained conversion degrees ranging from 80 to 100 mol.-% with 2% < DF < 14%.

Bunel reported the possibility of occurrence of side reactions involving the intermediate polymer radical. These reactions are different with respect to the cyclisation reported by Boutevin[68], though starting from the same molecule; in any case the confirmation of the presence of cyclic units is a later result achieved in the new millennium with the studies of Schlaad and others (*vide infra*).

Bunel suggests two possible reaction mechanisms involving allylic hydrogens of neighbouring 1,2- and 1,4-*cis* units[73]. The mechanism of this side reaction leading to the formation of allylic free radicals with double bonds rearrangement is reported in Scheme 10.

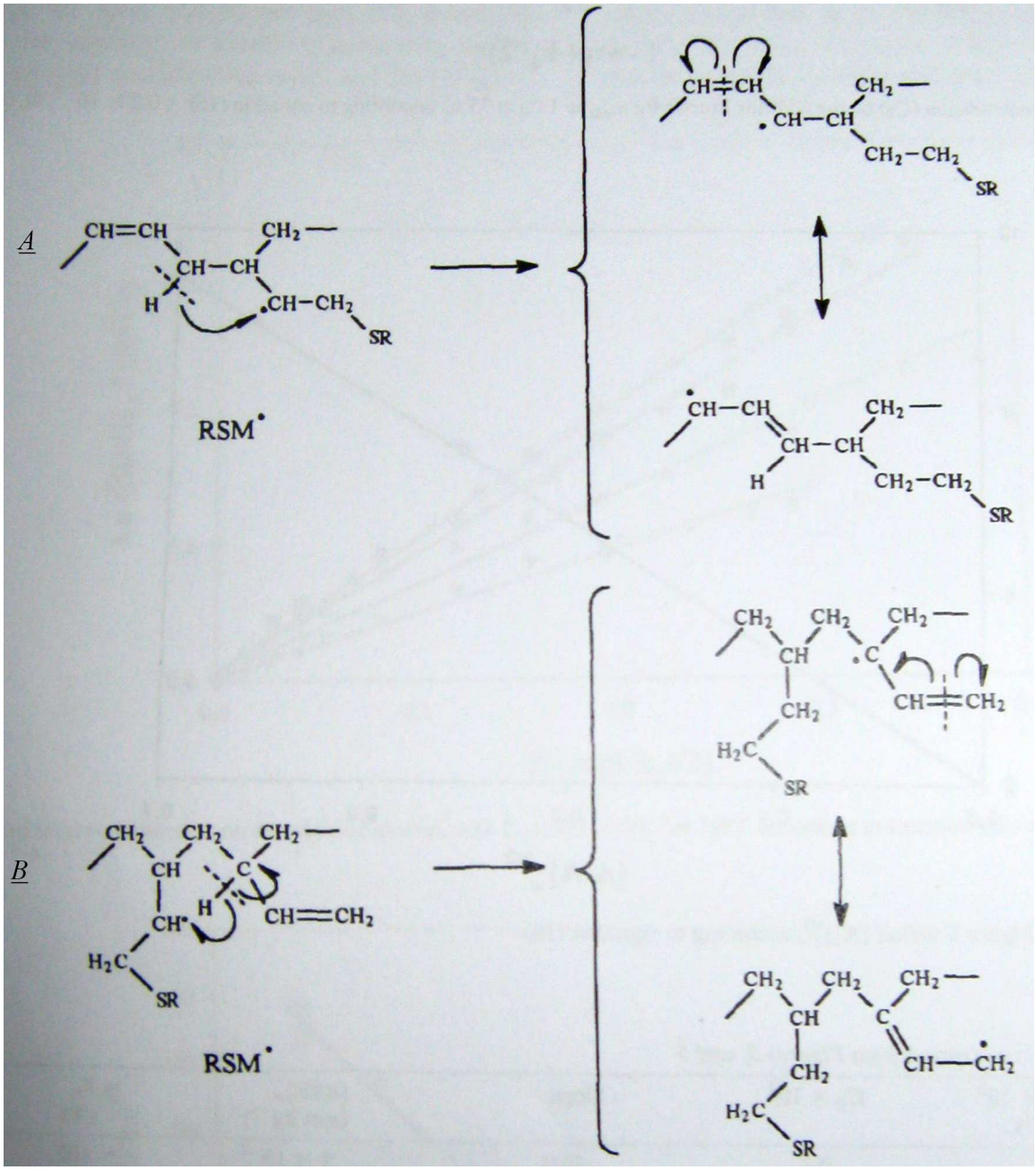

Scheme 10 – Molecular rearrangements leading to allylic radicals, suggested by Bunel et al.[73]

A: rearrangement on proximal 1,4- units, B: rearrangement on proximal vinylic units

The isomerisation should lead to a differentiated reactivity of the polymer radical towards transfer reactions or coupling termination reactions. A brief extract of Bunel kinetic considerations is here presented; only the most important equations describing the system will be presented.
The classical scheme reported in literature[31, 68, 69] for the addition of thiols (RSH) to double bonds (*M*) is shown below, and consist in various steps:

- Initiation (formation of radicals on S atom):

$$(1) I_2 \xrightarrow{k_d} 2I^{\bullet}$$
$$(2) I^{\bullet} + RSH \xrightarrow{k_a} RS^{\bullet} + IH$$

- Propagation and radical transfer:

$$(3) RS^{\bullet} + M \xrightarrow{k_1} RSM^{\bullet}$$
$$(4) RSM^{\bullet} + RSH \xrightarrow{k_2} RSMH + RS^{\bullet}$$

- Termination:

$$(5) 2RS^{\bullet} \xrightarrow{k_t} (RS)_2$$

A thermal initiator I_2 dissociates (reaction (1)) into two radicals $I^{\bullet}$; a molecule of a generic thiol RSH will react (2) with the $I^{\bullet}$ radical generating a thiyl radical $RS^{\bullet}$.
The M molecule of the reaction (3) is the unsaturated macromolecule, that forms the adduct with the thiyl radical $RS^{\bullet}$ generating a macroradical $RSM^{\bullet}$. The cycle is complete with hydrogen abstraction (transfer reaction) from a thiol to the macroradical $RSM^{\bullet}$ generating the final adduct RSMH and another thiyl radical.
As pointed out previously, these were considered the *most likely* reactions occurring; the side reactions involving $I^{\bullet}$ radicals were considered of scarce influence, since the concentration of these radicals is very small.
The formation of disulfide species (reaction (5)) due to the coupling of two thiyl radicals is not always confirmed by experimental observation: in many cases only very small amounts of disulfide species in the reaction byproducts were observed (see, for instance, ref.[33]). Bunel and co-workers

indicate the coupling reaction between radicals on the polymer as the possible main termination reaction (6) instead of thiyl-thiyl self coupling (reaction (5)).

$$(6) RSM^{\bullet} + RSM^{\bullet} \xrightarrow{k_c} RSM - MSR$$

The possible formation of allylic radicals (Scheme 10) could cause reaction (6) to be a quicker reaction than one could expect from sterically hindered polymer radicals: in fact, the radical could be re-located by allylic resonance on less hindered carbon atoms (see Scheme 10, especially the *B* path). Bunel suggests that reaction (6) could therefore had been an underestimated termination pathway; in any case, an hypothetical large difference between k_c and k_2 (the hydrogen transfer is supposed to be quicker than the coupling of macroradicals) should not allow to observe but a slight increase of the molecular weight. This would be consistent with the results of previous studies including SEC characterisations that did not highlight any extended chain-elongation / crosslinking reactions.

The kinetic formalisation including reaction (6) fits very well the kinetic experimental data collected. Bunel founds for [RSH](t) (the kinetic constants are the same of reaction 1 to 6):

$$(7) \ln \frac{[RSH]_0}{[RSH](t)} = 2k_2 \left(\sqrt{[I_2]_0 \frac{f}{k_d k_c}} \right) \left(1 - e^{-\frac{1}{2} k_d t} \right)$$

$$(8) \lim_{t \to \infty} \left(\ln \frac{[RSH]_0}{[RSH](t)} \right) = 2k_2 \left(\sqrt{[I_2]_0 \frac{f}{k_d k_c}} \right)$$

That is, the final conversion is limited by the initial concentration of the initiator and its efficiency *f* (defined as the ratio between the molar amount of $I^{\bullet}$ radicals effectively generating primary radicals $RS^{\bullet}$ and the molar amount of I_2), and depends on k_2, k_c and k_d. Knowing the value of $[I_2]_0$ and the instant concentration of [RSH] (checked with an analytical method), Bunel managed to estimate a constant comprising *f*, k_2, k_d, k_c. This constant, from (8), is defined as the "Y_∞" maximum conversion degree; this value fits well the final conversion values arising from experiments having different feed ratios. In other words, the kinetic equations comprising these side reactions lead to the conclusion that the conversion degree, depending on the feed ratio, reaches a limit value, and that the reaction cannot be complete (100% conversion of thiol), even if this value is often high (> 90%). Bunel results, including the values of Y_∞, are reported in Table 5.

Reagents	[Initiator]:[RSH]:[C=C]	DF %	Y_∞ % (see text)	Thiol Experimental Conversion %
[73]HTPB (1,2- 20%) / MPTS / AIBN	0:002:0.02:1	2.0	99.3	~100
	0.002:0.04:1	4.0	98.9	~100
	0.002:0.08:1	7.6	96.7	95
	0.002:0.16:1	14.0	90.9	89
	0.002:0.02:1	2.0	99.3	~100
	0.004:0.02:1	2.0	99.9	~100
	0.008:0.02:1	2.0	~100	~100

Table 5 – Results arising from Schapman, Couvercelle and Bunel[73] Reaction in bulk, at 75 °C; t = 24h

Boutevin's considerations about the cyclisation side-reaction could lead to an analogous kinetic expression; in fact, the amount of reactive double bonds is limited as well, and the consumption of double bonds leads to saturated $RSM^{\bullet}$ radicals. At the time of Boutevin and Bunel works there were no available data of which reactivity, between the cyclisation or the allylic proton transfer, was the most probable for the creation of less hindered polymer radicals; the cyclisation is the most likely reaction, and this has been proved by the characterisation of 5- and 6- memebers cyclic units first performed in 2005 by Schlaad and co- workers[82].

One last valuable observation arising from the cited paper of Bunel[73] is that the kinetic constants show a noticeable dependance on time, similarly to what observed by others on PBLs (Priola[31], Gorski[53]). The reduction of k_1 at elevated t (i.e. with thiol concentration straying from a first-order kinetic law) can be easily understood considering that the addition is driven by steric factors. For an incoming thiyl radical, the addition on a sterically hindered double bond (for instance a double bond next to bulky, already-functionalised units) will be more difficult, and consequently the rate of addition slows down with increasing time.

In later studies, Bunel and co-workers have chosen to add phosphonated compounds[83] or TGA[84] to HTPBs through the thiol-ene addition because of the low amount of functionaliser needed to obtain a good ignifugicity (addition of phosphonated compounds) or to obtain a certain extent of crosslinking (TGA). As said, the thiol-ene functionalisation shows good overall performances when using a low thiol:ene feed ratio (in fact the NMR measurements presented in these later studies of Bunel showed a quantitative addition of the thiols to the employed HTPBs).

1.2.4 Functionalisation of syndiotactic 1,2-PB

Deborah Carey and Gregory Ferguson studied the functionalisation of syndiotactic 1,2-PB (i.e. a PB entirely composed of vinylic units, each of which with a precise absolute configuration) having a

<M_n> of ~100 kDa[85, 86]. In these two studies, the authors tried to obtain functionalised rubber films, and they chose to performed the functionalisation runs on casted layers of 1,2-PB. The thiol and the initiator were dissolved in methanol, and the polymer film was immersed in this solution, so that the functionalisation was limited to the polymer surface; benzophenone was chosen as photoinitiator.

In a first study[85] they compare i) the thiol-ene addition of 1-mercaptopropan-2,3-diol *versus* a direct oxidation of the vinylic units into diols ($KMnO_4$ in basic ambient) and ii) the thiol-ene addition of TGA *versus* a direct oxidation of the vinylic units into carboxylic units ($KMnO_4$ in acid ambient). In both cases, the thiol-ene functionalisation led to better results with respect to the oxidation: i) it showed a greater selectivity (permanganate oxidise also in-chain units dramatically affecting the mechanical properties of the surface); ii) almost no byproducts were found (with permanganate: 1,2-diols, ketones and/or aldehydes); iii) the removal of reacted manganese in the oxidation system, found as MnO_2, with aqueous S^{2-} resulted in partial addition of sulphonated groups to the 1,2-PB (the system remains partially active, and this causes undesired, though minimal, sulphur addition); iv) using a feed ratio initiator:thiol:ene of 0.0033:0.074:1 with 1-mercaptopropan-2,3-diol and 0.0033:0.195:1 with TGA, the obtained conversion degrees were about 30 and 24% respectively, and considering that the reaction occurred only on the polymer surface, this is classified by the authors as an outstanding result with respect to the permanganate oxidation.

On a later study[86], the same authors suggested use of thioacetic acid (CH_3COSH; the first studies using thioacetic acid on PB were performed, as said, by Oswald in 1966[38]) followed by an hydrolysis to leave –SH groups on the polymer surface, so to obtain a good adhesion with metallic surfaces (gold and copper ones in particular).

These two studies showed conversion degrees similar to with those obtained on similar substrates; anyway the authors did not highlight any original feature of the reaction except the possibility of performing it on films of PB (all the other functionalisation runs were performed in the bulk or in the presence of a solvent for the polymer).

1.2.5 Functionalisation of EVA with thioacetic acid

The idea of creating new materials having –SH groups on macromolecular chains brought by a thiol-ene functionalisation with thioacetic acid and successive hydrolysis has been greatly developed by Bluma Soares and co-workers. This Brazilian research group synthesised a material rich in –SH groups in two steps with i) the reaction between thioacetic acid and a substrate of poly(ethene-co-vinyl acetate) *EVA* ii) the hydrolysis of the resulting poly(ethene-co-vinyl acetate-

co-vinyl mercaptoacetate), resulting in a polymer having –SH pending groups[87]. This material, named *EVASH*, has been tried as a compatibiliser in a large number of blends between polymeric substrates; the presence of –SH groups, in fact, could lead again to another thiol-ene reaction activated by initiators (or by the mixing heat alone) during the compounding. (The thioacetic acid is used, in this case, as a *carrier* of sulphide functionalities to create, at the end of the blending process, crosslinked products bearing thioether moieties.)

During the last two decades, Soares and co-workers published dozens of papers on these systems: they studied the interaction between phases (morphology of the phases; thermal, mechanical and rhelogical properties of final materials; use of initiators for the thiol-ene reactive compatibilisation, such as dicumylperoxide DCP; the effects of the compatibiliser on the polymer degradation and stability; influence of the thiolic agent in the blend on the vulcanisation process of the blends; and so on) in NR / poly(ethyl-co-vinyl acetate) EVA blends[88-92], low density polyethene LDPE / Nylon-6[90], poly(acrylonitrile-co-butadiene) rubber NBR / EVA[93-95], poly(styrene-co-butadiene) rubber SBR / EVA[96, 97], ethene-propene-diene-monomers rubbers EPDM / NBR[98-101], EPDM / NR[101, 102], polystyrene / EVA[103] (in which the EVASH is reacted with SBS before the addition to the blend).

Another functionalised material synthesised from the group with the same modalities is the so-called EPDMSH, in which the thiol-ene CH_3COSH functionalisation occurs on part of the macromolecular double bonds[104]. This rubber was used as well in polymer blends, NBR / EPDM[98-100, 104] and NR / EPDM[102, 105-107]; in some cases, it was mixed up with EVASH before the addition to blends[98, 100, 102].

1.2.6 Recent investigations on PBLs: evidences of cyclisation

A breakthrough in the investigation of the mechanism of thiol-ene reactivity was performed on PBLs in 2005 by Helmut Schlaad and co-workers[82]; the authors had previously published a work on thiol-ene functionalisation of a block copolymer of butadiene and ethene oxide[108]. (The thiol-ene functionalisation of copolymers of butadiene will be extensively treated in a following sub-chapter.)

Studying the mechanism of the radical addition of thiols to PB homopolymers, Schlaad used two kinds of polybutadiene: a PBL (1,2-: 93 mol.-%, 1,4-*trans*: 7 mol.-%) and a long chain 1,4-*trans* PB (99+ mol.-%); as a thiol, the author chose methyl-3-mercaptopropanoate. The functionalisation runs were carried out in presence of AIBN and in THF solution for 24h. The AIBN : thiol : ene feed ratio was strongly shifted to an excess of thiol, since Schlaad aimed to obtain a complete conversion of the double bonds (0.33:10:1, the amount of thiol was ten times the amount of unsaturations) rather

than a high conversion degree. As already remarked by Serniuk[48], Marvel[37] and others, the reaction rate of the thiol addition to 1,4- units is small, and in long chain polymers it is similar to the rate of the chain elongation side reaction; in fact, Schlaad observed gelation of the poly(1,4-) sample after only one hour, while the 93 mol.-% (1,2-) PBL remained soluble in most organic solvents after twenty four hours of reaction.

The ^{1}H-NMR characterisation of the functionalised PBL showed a DF of 82%; Schlaad suggests that the non-quantitative addition of the thiol is a direct consequence of the presence of cyclic units. This hypothesis is supported with three observations:

- ^{1}H-NMR shows no residual double bonds (belonging to 1,2- or 1,4- units)
- the measured molecular weight of the reaction product is ~ 5500 Da (MALDI-TOF mass spectrometry, the MW was estimated from the position of the maximum of the frequency distribution); assuming no occurrence of the chain elongation side reaction, this $<M_n>$ should be around 6900 Da (this is because of the increase of the molecular weight of the repeating unit); Schlaad suggests that there must be a fraction of monomer units to which no thiol was added. Note that a MALDI-TOF measurement of the $<M_n>$ does not suffer from chromatographic measurement problems due to the increased hydrophilicity of the system; Priola[31] and Laleg[35] reported that using SEC with hydrophilically-modified PBLs or HTPBs (respectively) resulted in non-reproducible measurements.
- MALDI-TOF MS spectrum also indicates the presence of monomers having a weight of 173.9 and 228.6 Da / unit; the theoretical MW of a type I adduct is 174.1 and of type II is 228.2 (see Figure 3).

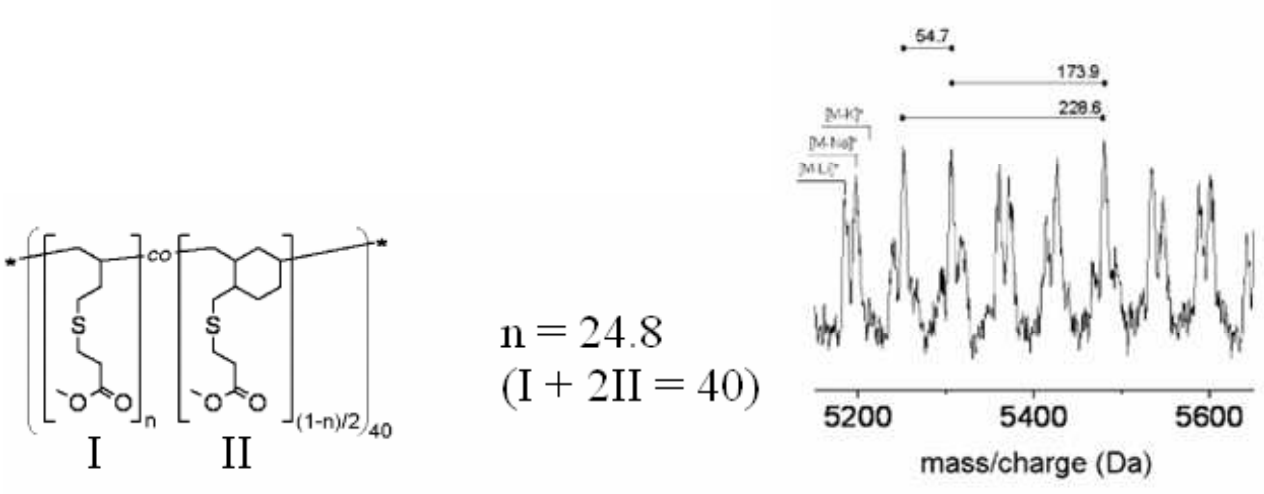

Figure 3 – Units and MALDI-TOF MS spectrum of PBL functionalised with ethyl-3-mercaptopropanoate[82]

Critically speaking, none of these observation is definitive. In fact, i) NMR measurements are affected by relatively large absolute errors, and a small amount of residual 1,2- units could remain undetected; ii) the presence of residual double bonds accounts for an unfunctionalised fraction of

monomers; iii) the molecular weight of a type I unit (Figure 3) followed by an unfunctionalised vinylic unit is exactly the same as the MW of a type II unit, and this could account for the 228.6 MS signal. In any case, the work of Schlaad is the first including a (probable) observation of cyclic units in thiol-ene functionalised diene polymers; before of his work, the presence of similar units was only supposed basing on reaction mechanisms. The conversion results obtained in these study performed by Schlaad and co-workers on PBL are summarised in Table 6.

Reagents	Reaction Conditions	[Initiator]:[RSH]:[C=C]	DF %	I:II (Figure 3)
[82]PB (1,2- 93%) / $HSCH_2CH_2COOMe$ / AIBN	70 °C, THF solution t: 24h	0.33:5:1	77	22.6:8.2
		0.33:10:1	82	24.8:7.6
		0.33:20:1	83	26.4:6.8
		0.33:40:1	86	28.8:5.6
[82]PB (1,2- 93%) / $HSCH_2CH_2COOH$ / AIBN	70 °C, THF solution t: 24h	0.33:10:1	70	16.0:12.0
		0.33:20:1	73	18.4:10.8
[82]PB (1,2- 93%) / $HSCH_2CH_2NH_2 \cdot HCl$ / AIBN	70 °C, THF solution t: 24h	0.33:10:1	79	23.2:8.4
		0.33:20:1	73	18.4:10.8

Table 6 – Addition of thiolic acid / esters / amines to PBL predominantly 1,2-[82]

Schlaad also evaluates (last column of Table 6) the ratio of type I and type I (cyclic) units, finding out that, with PBL, non-cyclic units are always from nearly two to three times the amount of cyclic ones, depending on the adopted functionalising agent.

In his last works[109, 110] Schlaad points out that the impact of the cyclisation reaction could be avoided by *increasing the distance* between the intermediate polymer radical and neighboring C=C double bonds. To verify the validity of this sentence, the authors have recently[109] carried out functionalisation runs with various thiol (methyl-3-mercaptopropanoate, 3-mercaptopropan-1,2-diol, 1-mercapto-1,2-tetrahydro perfluorooctane, thioacetic acid and 1-mercapto-2,3,4,6-tetraacetyl glucose) on poly[2-(3-butenyl)-2-oxoazoline], and they obtained functionalised products without apparent cyclisations.

1.2.7 Thiol-ene functionalisation of butadiene copolymers

The addition of thiols to random or block copolymers of butadiene has been investigated in many literature works, but not as much as the functionalisation of the butadiene homopolymer. As said, some of these systems were described in the previously mentioned works of Serniuk[47, 48] on styrene/butadiene random copolymer (SBR rubber) and Soares[93-97] on acrylonitrile/butadiene

random copolymer (NBR rubber; these recent studies of Soares, though, were poor in characterisations of the primary structure of the thiol-ene adducts and more oriented to other determinations). Serniuk, although not using any initiator, observed high functionalisation degrees, such as 23-27 mol.-% (amount of butadienic monomers in the copolymer: 87 units per 100 monomers); in the cited paper, though, there are no data regarding the 1,2- *vs* 1,4- relative ratio of the employed SBR.

Ciardelli's research group published three works[32, 54, 111] and a master degree thesis[112] about the functionalisation of SBR through thiol-ene processes. The purpose of these studies was to obtain functionalised materials with improved compatibility towards other polymers as well as organic / inorganic fillers; to observe a similar behaviour, as well as in other cases, it is not required to dramatically modify the polymer with high functionalisation degrees. For example, the functionalisation of rubbers for automotive traction descibed in patents usually achieves functionalisation degrees up to 3 *parts per hundred of rubber* (phr), usually less than 5 mol.-%.

The thiol-ene functionalisation of SBR, at the time of the first work of Ciardelli's research group, was considered appealing mainly thanks to the mild conditions and the good conversion degrees that, as seen for PBLs and HTPBs, are particularly high at low thiol-ene feed ratios.

The results arising from the first work[32], published in 1999, are summarised in Table 7. The functionalisation runs carried out in this study are aimed to the comparison of different solvent / initiator effects on the reaction.

Reagents	Reaction Conditions	[Initiator]:[RSH]:[C=C]	DF %	Thiol Conversion %
[32]SBR (1,2- 37%) / TGA / AIBN	90 °C, toluene sol. t: 2h30'	0.0008:0.15:1	3.4	27
		0.0011:0.15:1	4.0	32
		0.0015:0.15:1	4.5	37
		0.0019:0.15:1	3.4	27
		0.0023:0.15:1	3.0	25
[32]SBR (1,2- 37%) / TGA / BPO	100 °C, toluene sol. t: 2h30'	0.0008:0.15:1	1.3	10
		0.0015:0.15:1	3.0	24
		0.0023:0.15:1	2.8	23
		0.0030:0.15:1	2.8	23
		0.0038:0.15:1	3.0	24
		0.0045:0.15:1	(crosslinked prod.)	
[32]SBR (1,2- 37%) / TGA / AIBN	90 °C, dioxane sol. t: 2h30'	0.0008:0.30:1	0.9	4
		0.0015:0.30:1	3.2	13
		0.0030:0.30:1	3.8	14
		0.0045:0.30:1	4.9	19
		0.0060:0.30:1	4.4	17

Table 7 – TGA / SBR functionalisation runs carried out by Romani *et al.*[32]

In this chapter some works in which different runs were carried out changing only the reaction solvent were cited, i.e. the papers of Oswald[38], Priola[31] and Gorski[55] regarding the additon of thiols to PBLs. In these works, the obtained DF are very similar despite of the solvent, and the main conditions influencing the DF are others (temperature, reaction time, steric hindrance of employed thiols, feed ratio, primary structure of unfunctionalised polymers). Romani, instead, observed a certain dependence on the nature of the reaction solvent: the author obtained inferior conversion degrees using 1,4-dioxane instead of toluene as reaction medium.

This result regarding the differences in reaction rates using toluene or another solvent as reaction medium complies with prior works regarding radical polymerisations[113]. Despite the large number of works covering this field, there is no common agreement on the origin of the solvent effect; the explanations arising from papers are as diverse as the data, and it is not possible to generalise the findings. However, in these kinetic studies some common points were examinated:

- the possible introduction of a solvent molecule in the macromolecular chain, if possible
- chain-transfer or H· transfer reactions with solvent
- polarity and polarisability of the medium
- change in monomer reactivity by interaction of the monomer with solvents
- reversible complex formation of the propagating radical with solvent molecule
- selective solvation of polymer by monomer.

Obviously the following observations could be applied and discussed to the thiol-ene functionalisation of polymers, though this has never been done so far.

A recent study on the solvent effect on methacrylate free radical polymerisations[114] points out that in certain conditions the observed solvent effect could be ascribed to a few of the cited causes. Among these conditions the authors count: i) the absence of copolymerisation between the propagating radical and the solvent; ii) the absence of chain-transfer reactions between the same species; iii) the independence of kinetic constants from the dielectric constant ε of the solvent (the legitimation of this hypothesis on the system studied in ref.[114] was furnished by another paper on a very similar system, in which the absence of this dependence was noticed[115]).

To explain the solvent influence on propagation rate, the formation of reversible complexes between radical and solvent molecules has been considered in several publications. Since Henrici-Olive and Olive suggested the occurrence of such complexes[116, 117], a number of papers supporting this idea has been published, comprising both experimental and theoretical data. A simple scheme explaining how a similar phenomenon could affect the polymerisation rate is reported in Scheme 11, where $P_n^{\cdot}$ is the growing polymer chain, M is the monomer, S the solvent and the $P_n^{\cdot}S$ species represents a reversible complex between the polymer radical and the solvent.

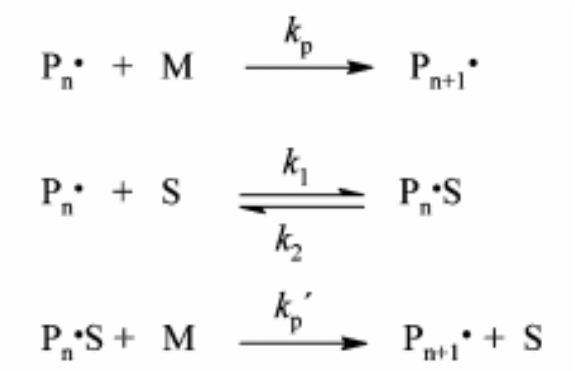

Scheme 11 – Possible solvent complexation of a growing macromolecule during a radical polymerisation

Some authors even suggested a kinetic treatment of this system[118, 119]. In the cited study of Beuermann[114], instead, the solvent effect is explained invoking possible occurrence of variations of local monomer concentrations in the proximity of the free-radical chain end; the author describes the reaction of radical transfer from the polymer chain to a molecule of solvent as an impossible one for the considered system.

The first work in which an author suggests a possible transfer reaction of a hydrogen radical from the solvent molecule to a growing polymer chain is very old (Mayo, 1943, ref.[113]); the kinetic effect of this transfer reaction has lately been invoked several times to explain solvent effect in radical polymerisations. The most common solvents for which a similar reaction has been characterised are chlorinated solvents, aromatic solvents and also thiols[120]; for review papers examinating the solvent effect based on radical transfer during free radical polymerisations, see ref. [121-124].

The authors of the cited paper about the TGA functionalisation of SBR in solution (Romani *et al.*, ref.[32]) suggest that another probable kinetic factor influencing the thiol-ene reactivity, apart from possible hydrogen transfers from the solvent to the polymer, may arise from the interaction of the solvent itself with the rubber macromolecules: the random coil macromolecular secondary structure in solution may be more or less sterically hindered depending on the solvent, thus influencing the reaction kinetics and, consequently, the functionalisation degree*.

Another aspect cited in Romani work is that crosslinking is frequently observed when AIBN:SBR ratio was high. This aspect will be analysed in detail in the next paragraphs, when the molecular weight of the starting polymer will be discussed as a key parameter for the reaction.

* As said, the influence of the kinetics on the DF for thiol-ene systems has been formalised by Boutevin and co-workers; if the solvent effect influences kinetic constants, also the Y_∞ value will change.

In the same work cited for the recent mechanicistic discoveries regarding functionalisation of PBL[82], Schlaad examines other nineteen systems regarding the thiol-ene functionalisation of PB-*b*-PEO copolymers (PB block: 92 to 97% of 1,2- units, 3 to 8% of 1,4-*trans* units, $<DP_n>$ 25 / 40 / 65; polyetheneoxide block: $<DP_n>$ varying from 75 to 273) and PB-*b*-PS copolymers (PB block: 97% of 1,2- units, 3% of 1,4-*trans* units, $<DP_n>$ = 85; polyetheneoxide block: $<DP_n>$ = 351). The added functionalisers comprised the cited methyl-3-mercaptopropanoate, the 3-mercaptopropanoic acid, the 2-mercaptoethylamine hydrochloride, the 2-mercaptoethyl diethylamine hydrochloride, the *N*-acetyl-L-cysteine methyl ester, the 3-mercaptopropan-1,2-diol (already used by Carey and Ferguson[85]), the benzylthiol, and the 1-mercapto-1,2-tetrahydro perfluorooctane (already used by Boutevin and co-workers[68, 70]). The initiator remained the same for all the experiments (AIBN); the runs were carried out with the same modalities reported in Table 6 (page 29), and with a fixed feed ratio AIBN:thiol:ene of 0.33:10:1.

Schlaad always observes very high DFs with the cited copolymers usually ranging from 70 to 85%, and the molar I:II ratio ranges from 0.6 to 7. The lowest I:II ratios (which suggest a relatively high occurrence of the cyclisation reaction) are found when using sterically hindered thiols, specifically with the *N*-acetyl-L-cysteine methyl ester, a fluorinated thiol ($C_6F_{15}C_2H_4SH$), and with 3-mercaptopropan-1,2-diol.

Starting from these results collected in the cited paper[82], Schlaad and co-workers adopted the thiol-ene functionalisation to obtain various products aimed at different purposes. In particular, he conducted extensiv investigations on secondary- and tertiary- structure of amphiphilic block copolymers in solution, especially (functionalised PB) / PEO[109, 110, 125-129]. Apart from the already used (in the previously cited explorative work [82]) 3-mercaptopropanoic acid, 2-mercaptoethylamine hydrochloride (those two compounds are then used again in ref. [126, 127, 129]), 3-mercaptopropan-1,2-diol[127], 1-mercapto-1,2-tetrahydro perfluorooctane[127], *N*-acetyl-L-cysteine methyl ester (NCysMe, [125]), the authors introduced some new compounds on PB / PEO diblock copolymers:

- Thioglucose (bringing four hydroxyl groups on the PB block)[126]
- A derivative of a dipeptide, (L,L)-cysteine phenylalanine[125] (*N*-acetyl-L-phenilalanine-L-cysteine amide)

Thanks to the high excess of thiol (Schlaad always carries out experimental runs having the already used 0.33:10:1 initiator:thiol:ene ratio except in the case of the dipeptide for economic reasons where he uses 0.33:2.5:1), the obtained functionalisation degrees are always in the range 60–80%; the formation of 6-membered cycles is always invoked as the limiting factor for the conversion, though never detected again in the works successive to ref.[82].

The original PB / PEO behaviour in water consists in the formation of spherical micelles; the functionalised diblock copolymers can show similar structures, such as in the case of the NCysMe-functionalised PB / PEO block copolymer[125]. In other cases, the copolymers may self-assemble into clusters of spherical micelles[127, 129] (addition of 3-mercaptopropanoic acid to PB-*b*-PEO), or they may have a different tertiary structure; in fact, cylindrical micelles are formed by copolymers having PB functionalised with 2-mercaptoethylamine[126] or 3-mercaptopropan-1,2-diol[129], or even more complicated micelles with structurated cores could be formed under the addition to the PB block of 1-mercapto-1,2-tetrahydro perfluorooctane[127] or the dipeptide[125]. In one of the cited works[126], more complicated structures resembling cellular membranes were synthesised using particular experimental conditions: the authors managed to create single- and poly-lamellar vescicles similar to lysosomes.

All these micelles, except the one formed by dipeptide-functionalised PB / PEO and the fluorinated one, have got an hydrophobic core formed by the PEO block and the PB main chains: hydrophilic pendant groups point to the outside of the micelle, as indicated by dynamic light scattering (DLS) scanning force microscopy (SFM) and cryo-TEM (cryogenic transmission electron microscopy) characterisations[82, 125, 126, 129]. On the contrary, when an hydrophobic thiol is added, the two blocks are inverted, and the relative stability of these emulsions is reduced[125, 127].

Very recently, Levent Demirel and Schlaad[128] performed the functionalisation of PB / PEO block copolymers with aliphatic thiols (2-ethylhexanethiol, decan-1-thiol and dodecan-1-thiol); the morphology of this copolymer in the bulk could be switched from one showing hexagonal bundles of tubular micelles to a lamellar one after the functionalisation of the PB block with thiols (and the authors noticed a dependance of the morphology from the steric hindrance of the functionalising agent).

1.3 Structural aspects of molecules influencing their thiol-ene reactivity

The molecular structure of both the functionalising agents and the diene polymer can influence the thiol-ene reactivity, and the objective of this chapter is to better explain the chemical background of the research lines drawn in the present work, with particular reference to the adopted substrates.

1.3.1 The molecular weight of the polymer

The molecular weight of the starting polymer has been reported several times as a parameter affecting its thiol-ene reactivity; moreover, the occurrence of side reactions during the functionalisation could lead to fundamental changes in the molecular weight itself.

In particular, a substantial difference between thiol-ene functionalisation and free radical grafting of molecules to polyolefin is observed. In a free radical functionalisation of thermoplastic polyolefins, on which the research group of Ciardelli worked extensively in the past (publishing papers[110, 124-134], reviews[130-132] and patents[133, 134]), the radical initiator generates free radicals on the macromolecules (*macroradicals*) and the double bonds that undergo the *macroradical-ene* reaction are located on the functionaliser molecule (maleic anhydride and maleates, usually). In these systems, the length of the macromolecular chains changes over time due to both degradation and chain extension reactions, and in order to obtain good mechanical properties of the functionalised material it has been desirable to develop methods (i.e. additon of chemical agents, modulation of the reaction temperature, *et cetera*) that could allow its control. The macroradicals are usually formed on the backbone of the macromolecular chain rather than on the short side chains because of the relative stability of the generated radical. In fact, thanks to the hyperconjugative effect, the most stable carbon radical are located on tertiary carbon atoms, and they are common on branched polyolefins such as *linear low density polyethene* LLDPE, *polypropene* PP, *polystyrene* PS. The macroradical could then undergo a *β-scission* reaction, generating two smaller macromolecules (Scheme 12); this is the most common behaviour observed when functionalising, for instance, isotactic PP. (Moreover, in the case of isotactic PP, the most suitable H· operating the saturation of the radicals generated on the side chains after the addition of double bonds comes from tertiary carbon hydrogens located on the main macromoecular chain, thus generating other β-scission points.) This has a deep influence on the molecular weight of the system, and the M_n or the M_w after a similar functionalisation can be much decreased[135].

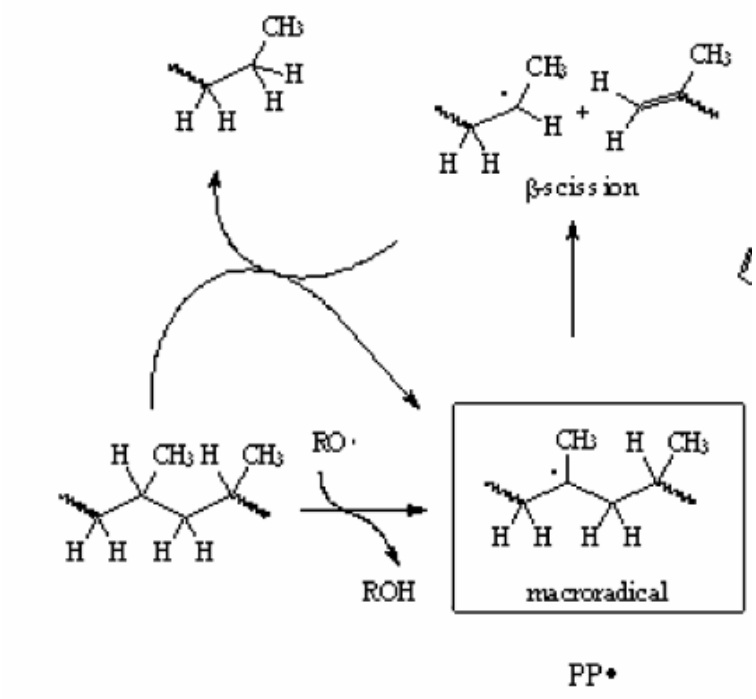

Scheme 12 – Possible self-scission of macroradicals generated on isotactic PP

During the last decade many research groups developed additives bases on substituted furan molecules to create a *spacer* from the free radical to the backbone, thus preventing degradation of the PP; for a review on the PP radical functionalisation see ref.[130].

In the case of thiol-ene functionalisation of diene elastomers, the functionalised polymers seem much more affected by the crosslinking side reaction of coupling between free radicals located on the polymer (see ref.[32, 38, 40, 41, 54, 55, 112]) rather than from scissions of the backbone. This could be explained with some considerations about the nature of the macroradical in thiol-ene reactions.
When in presence of both 1,2- and 1,4- polybutadienic units, the thiyl radical will preferably attack the 1,2- units, generating a radical located on a side-chain, as said before. As observed by Bunel and co-workers[73], this radical could migrate on the macromolecular chain originating allyl radicals (Scheme 10, page 22). If, on the other side, the addition occurs on a 1,4- unit, the situation is going to be extremely similar to the case (*A*) of Scheme 10, and an allyl radical can be formed as well. Golub and others[136, 137] observed that, when treating PBs displaying various primary structures with radicalic initiators in solution, these allyl radicals located on the backbone of elastomeric macromolecules can usually originate crosslinking reactions, but the chain scission is described as *extremely unlikely*. In fact, considering SEC measurements of the molecular weight, the authors find out a systematic increase in the MWs of the products, and this increment depends only on the amount of the added generator of radicals.
Moreover, the presence of the thiol usually avoids the creation of tertiary carbon radicals that could give β-scission. In fact, i) RSH is much more reactive than a R_3CH group toward hydrogen extraction caused by a radicalic initiator (this is a well-known property[138]); ii) the radical *RSM*· (i.e. after the thiyl functionalisation) can take four main reaction paths, as said†, and, of these, the quickest are the transfer to thiol and the cyclisation with neighboring 1,2- units (if possible[109]).

For Bunel *et al.*, the coupling of *RSM*· macroradicals is the most likely termination reaction, and they support this hypothesis with viscosimetric observations on the studied systems[73]; the molecular weight of the functionalised products will grow in any case. Four reaction paths could be described:

$$(9) I^{\bullet} + M \rightarrow IH + M^{\bullet}(-H)$$
$$(10) 2M^{\bullet}(-H) \rightarrow chain\_elongation$$
$$(11) M^{\bullet}(-H) + RSM^{\bullet} \rightarrow chain\_elongation$$
$$(12) M^{\bullet}(-H) + M \rightarrow chain\_elongation$$

† hydrogen transfer with a molecule of thiol, helping the propagation of the reaction; coupling with another $RSM^{\bullet}$ radical; cyclisation with a neighboring 1,2- unit; migration of the radical to the macromolecular backbone

Accordingly to the previously used nomenclature of equation [1…6] (page 22-23), the M molecule represents the diene elastomer macromolecule, that forms the adduct with the thiyl radical $RS^{\bullet}$ generating a macroradical $RSM^{\bullet}$. After the abduction of a $H^{\bullet}$ radical, the molecule is called $M^{\bullet}(-H)$.
Romani and co-workers[32] noticed that the obtaining of crosslinked products in SBR / TGA / AIBN systems depended mainly on the initiator / polymer ratio, so they inferred that the reaction (9) could occur, generating, as well as reaction (6), other chain elongation / crosslinking reactions (reactions 10, 11 and 12). The kinetic theoretical equation of Bunel (7) relates high conversion degrees with high amounts of $[I_0]$, but the occurrence of reaction (9) puts a limit to the usable amount of initiator; the optimal initial concentration should be determined time by time for every studied system.
Statistically, crosslinking and chain elongation were mainly observed when considering thiol-ene functionalisations on long macromolecules, and this can be explained by the fact that a hypothetically comparable number of reaction events involving the coupling of macromolecules leads to the insolubility of the material more easily if the initial MW is high.

1.3.2 Reactivity of thiols carrying carboxylic / aminic moieties vs. respective esters / amides

In the cited paper of Romani[32], two other aspects of the considered thiol-ene system are analysed with respect to the already-cited initiator concentration and solvent effects, and they are i) the effect of a peroxide initiator instead of AIBN, and ii) the influence of various functional groups carried from the thiol on the overall reactivity (specifically, a carboxylic moiety *vs* its ethyl ester).
The observation that functionalisation runs carried out in presence of BPO display smaller DFs complies with the results of the study of Boutevin[68], that used five different initiators to carry out thiol-ene additions (see Table 4, page 20).
Romani *et al.* also observe differences in the conversion degrees when using TGA *vs* its ethyl ester (ethyl mercaptoacetate, EMA) on SBR, and in particular the author observed an inferior reactivity of the acid. Similar observations were reported in the already cited works of Cunneen[42] and Schlaad[82, 108] although on other diene polymers than those of Romani (respectively, NR and PB-*b*-PEO).
The presence of free or esterified groups on the thiol has an impact on various chemical aspects of the process, such as:

- the solubility of the thiol in the reaction solvent, if present;
- the diffusivity of the thiol in the polymer (both in bulk and in solution functionalisations), and this could be mainly determined by both i) the polarity and ii) the sterical hindrance of the thiol;

- the presence of interactions between the –SH group and the unit such as cyclic intramolecular hydrogen bonding[54, 139] or deprotonation to thiolate by free amino groups[140].

The reactivity order *acid* < *relative esters* was observed, in scientific literature, only considering reactions between thiols and polymers; a systematic study on model olefins resembling structural units, that could be found in the primary structure of a PB, still has not been reported. The results achieved so far that display the lesser reactivity of acid vs esters are collected in Table 8 (values adapted from the works of Cunneen, Schlaad and Romani).

Reagents	Reaction Conditions	[Initiator]:[RSH]:[C=C]	DF %	Thiol Conversion %
[42]NR / TGA / AIBN	75°C, C_6H_6 sol. t: 24h	0.4:2.71:1	24.4	9
[42]NR / ethyl mercaptoacetate / AIBN	75°C, C_6H_6 sol. t: 24h	0.4:0.69:1	18.7	27
[42]NR / octyl mercaptoacetate / AIBN	75°C, C_6H_6 sol. t: 24h	2.6:0.62:1	21.7	35
[42]NR / ethyl mercaptoacetate / *p*MHP[a]	0 °C, latex of NR water sol. of thiol + init. t: 7d	2.0:0.14:1	12.7	91
[42]NR / butyl mercaptoacetate / *p*MHP[a]	0 °C, latex of NR water sol. of thiol + init. t: 7d	2.0:0.14:1	11.9	85
[42]NR / octyl mercaptoacetate / *p*MHP[a]	0 °C, latex of NR water sol. of thiol + init. t: 7d	2.0:0.14:1	10.5	75
[82, 108]PB_{25}-*b*-PEO_{75} / methyl mercaptopropanoate / AIBN	70°C, THF sol. t: 24h	0.33:10:1	55[108]	6[108]
			70[82]	7[82]
[82, 108]PB_{25}-*b*-PEO_{75} / mercaptopropanoic acid / AIBN	70°C, THF sol. t: 24h	0.33:10:1	77[108]	8[108]
			78[82]	8[82]
[82, 108]PB_{40}-*b*-PEO_{132} / methyl mercaptopropanoate / AIBN	70°C, THF sol. t: 24h	0.33:10:1[108]	57[108]	6[108]
		0.33:20:1[82]	72[82]	4[82]
[82, 108]PB_{40}-*b*-PEO_{132} / mercaptopropanoic acid / AIBN	70°C, THF sol. t: 24h	0.33:10:1	66[108]	7[108]
			70[82]	7[82]

[82]PB (1,2- 93%) / methyl mercaptopropanoate / AIBN	70°C, THF sol. t: 24h	0.33:10:1	82	8
		0.33:20:1	83	4
[82]PB (1,2- 93%) / mercaptopropanoic acid / AIBN	70°C, THF sol. t: 24h	0.33:10:1	70	7
		0.33:20:1	73	4
[32]SBR (1,2- 37%) / TGA / AIBN	90 °C, toluene sol. t: 2h30’	0.0008:0.15:1	3.4	27
		0.0011:0.15:1	4.0	32
		0.0015:0.15:1	4.5	37
		0.0019:0.15:1	3.4	27
		0.0023:0.15:1	3.0	25
[32]SBR (1,2- 37%) / ethyl mercaptoacetate / AIBN	90 °C, toluene sol. t: 2h30’	0.0002:0.30:1	2.0	8
		0.0003:0.30:1	5.7	22
		0.0006:0.30:1	9.7	39
		0.0009:0.30:1	8.8	36
		0.0011:0.30:1	4.4	17
		0.0015:0.30:1	(crosslinked prod.)	

Table 8 – Results of functionalisations carried out using a thiol acid and relative esters

[a] *p*HMP = *p*-menthane hydroperoxide

In his paper (ref.[42]), Cunneen notices that the different reactivity could be rationalised invoking both electronic and steric effects: i) the thiyl radical of a chemical agent containing a carboxylic proton could be stabilised by electronic effects (so the reactivity of TGA is inferior to that if the respective esters), and ii) among the esters, the less sterically hindered is more reactive (reactivity of ethyl ester > n-butyl ester > n-octyl ester). The same behaviour for acid *vs.* ester is observed in ref.[32] and in ref.[82], and was explained in the same way.

The functionalisation runs carried out on block copolymers of PB and PEO[82], however, show an opposite behaviour, with the mercaptoacetic acid being systematically more reactive than its methyl ester. The author states that perhaps the peculiar primary structure of the polymer could account for a similar difference, while the various diene polymers of Table 8 (NR, PB, SBR) behave in the same way.

1.3.3 The thiol-ene reactivity of L-cysteine and its derivatives

The latest work published by the research group of Ciardelli on thiol-ene functionalisation of SBR[54] regards the use of L-cysteine derivatives as a functionalising agent for SBR. Cysteine derivatives were recently used also, as said, by Schlaad and co-workers[82, 125, 126]; the results of these works are summarised in Table 9.

Reagents	Reaction Conditions	[Initiator]:[RSH]:[C=C]	DF %	Thiol Conversion %
[82, 125]PB_{25}-*b*-PEO_{75} / NCysMe / AIBN	70°C, THF sol. t: 24h	0.33:10:1	70[a]	7[a]
[82]PB_{40}-*b*-PEO_{132} / NCysMe / AIBN	70°C, THF sol. t: 24h	0.33:10:1	52[b]	5[b]
[125]PB_{14}-*b*-PEO_{93} / NCysMe / AIBN	70°C, THF sol. t: 24h	0.33:10:1	64	6
[125]PB_{14}-*b*-PEO_{93} / NPheCys(NH_2)[c] / AIBN	70°C, NMP[d] sol. t: 48h	0.33:2.5:1	71	28
[125]PB_{25}-*b*-PEO_{75} / NPheCys(NH_2)[c] / AIBN	70°C, NMP[d] sol. t: 48h	0.33:2.5:1	40	16
[54]SBR (1,2- 49%) / CysEt / AIBN	90°C, toluene sol., t: 4h	0.001:0.5:1	0.34	0.7
		0.002:1.0:1	0.53	0.5
		0.010:0.5:1	1.30[e]	2.6[e]
		0.020:1.0:1	1.87[e]	1.9[e]
[54]SBR (1,2- 49%) / CysEt / AIBN	120°C, Brabender mix., t: 15', 50 rpm	0.000084:0.042:1	1.0	24
[54]SBR (1,2- 49%) / NCysMe / AIBN	120°C, Brabender mix., t: 15', 50 rpm	0.000084:0.042:1	1.2	29

Table 9 – Studies on L-cysteine derivatives used as carrier of functionalities on the polymer

[a] amount of 1,2- adduct *vs* cyclic adducts: 10.0 *vs* 7.5 [b] 1,2- *vs* cyclic: 6.0 *vs* 14.8; [c] *N*-Acetyl-L-Phenilalanine-L-Cysteine amide; [d] NMP = *N*-methyl pyrrolidone; [e] measured on a crosslinked sample

The L-cysteine is a well-known amino acid, and its derivatives are comparable, in terms of thiol - ene reactivity, to other thiols as seen in Table 9. The lower reactivity of L-cysteine ethyl ester (*CysEt*) and *N*-acetyl-L-cysteine (*NCysMe*) with respect to TGA or other aliphatic thiols was explained invoking i) the higher steric hindrance of the molecule or ii) the possible formation of five or six-membered intramolecular rings[139] that could make the thiol group less available to react with primary radicals derived from AIBN, negatively affecting the addition to C=C double bonds (Figure 4).

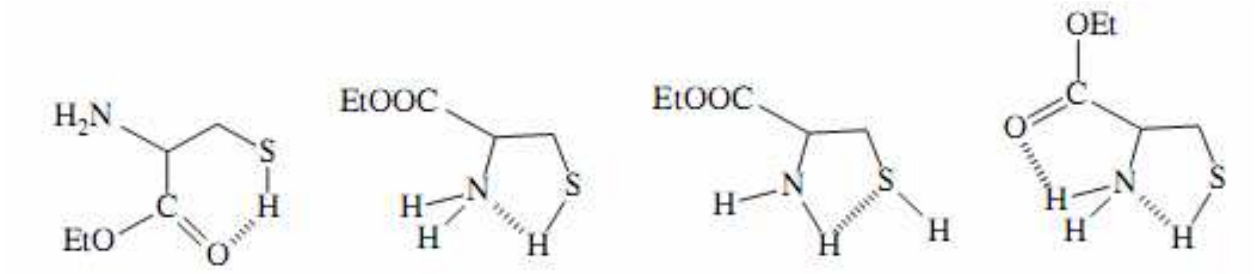

Figure 4 – Possible intramolecular hydrogen bonding of L-CysEt involving the –SH group[139]

Another important work in which a derivative of L-cysteine wad added to a block copolymer of PB and PEO was published by Schlaad and co-workers[126]; this is the only work in which a L-cysteine derivative having a free carboxylic unit was added to a polymer. Because of the absence of a solvent able to dissolve both the PB and the L-cysteine, the authors used *N*-tertbutyloxycarbonyl-L-cysteine (*NBocCys*); the protecting group was later removed by conventional hydrolysis, and a PB showing bare L-cysteine moieties attached to the macromolecular backbone was obtained.

With respect to the introduction of 3-mercaptopropanoic acid or 2-aminoethylmercapt-1-ane, the addition of NBocCys leads to lower functionalisation degrees (with thiol:ene 10:1 feed ratio, on PBL 1,2- 93 mol.-%, the authors found: 3-mercaptopropanoic acid DF 91%, conversion 9.1%; 2-aminoethylmercapt-1-ane DF 76%, conversion 7.6%; NBocCys DF 71%, conversion 7.1%). In the cited explorative work of Justynska and Schlaad[82], cysteine derivatives were, as well, the worst functionalisers in terms of obtained DF if compared to other thiols carrying single carboxylic / aminic moieties.

An interesting observation arising from the study of NBocCys addition to PB-*b*-PEO[126] is that the number of simple 1,2- adducts *vs* 1,2- cyclic adducts (I:II units, see Figure 3, page 28) is much lower if compared to the amounts found with thiols containing carboxylic or aminic units alone: 3-mercaptopropanoic acid had I : II = 82 : 9 per 100 monomeric units, 2-aminoethylmercapt-1-ane had a 52 : 24 ratio and NBocCys had a 40:30 ratio. This behaviour was observed by Schlaad also in ref.[82] when using NCysMe instead of mercaptapropanoic acid or 2-aminoethylmercapt-1-ane on PB-*b*-PEO block copolymers.

About the groups containing nitrogen, the results arising from ref.[82] and other works in which thiols carrying aminic groups or amidic ones are added to polybutadienes (SBR or PB-*b*-PEO copolymers[54, 82, 108, 126, 127, 129]) does not account for any remarkable difference in terms of reactivity between the amidic and the aminic group. A slight decrease with respect to the free primary aminic moiety is observed when using an amidic group carrying a bulky substituent (see the case of NBocCys[126] or the case of NPheCys(NH_2)[125], where the condensed group is an aminoacid). In other cases (for instance: NCysMe *vs* CysEt functionalisations[54, 112]) the reactivity leads to comparable DFs; moreover the absolute functionalisation degrees obtained with thiols

carrying aminic or amidic groups only (2-aminoethylmercapt-1-ane hydrochoride and similar compounds) is similar to the ones obtained with thiols carrying other functionalities (see Table 6, page 29).

1.4 The role of reinforcing fillers in tyre compounds

In this chapter the role of reinforcing fillers in tyre compounds will be briefly presented, highlighting chemical aspects of the rubber reinforcement and identifying major features of the improvement of mechanical properties. This section will introduce the problem of performance improvement in compounds for automotive traction, as a possible use of thiol-ene functionalised materials, that will be analysed in detail in the last chapter of the present work, is as compatibilising agent in these composite materials.

1.4.1 The reinforcing fillers: carbon black and silica

The reinforcement of elastomers by powderous fillers has been studied extensively in the past, though the subject is still much debated as it is not fully understood. The concept of reinforcement of elastomers differs from the reinforcement of thermoplastics or thermosets: in both cases it is associated to an increase of the modulus and hardness, but while in the latter materials it is accompanied by a decrease in elongation at break, in elastomers it is accompanied by an increase[141].

The most successful reinforcing agents that were adopted so far in rubber technology are carbon black (*CB*) and silica. From the beginning of the early twentieth century, CB has been employed as a reinforcing agent in automotive tyres compounds, and it is still the most important reinforcing agent for this kind of compounds; the number and quantity of carbon blacks produced for the tyres rubber industry is very high[142]. From the ‘40s and the ‘50s of the last century, CBs have been complemented by silicas in the compounds; the addition of silicas, though, presented many problems especially for the vulcanisation process. In fact, silicas interact with the chemical agents employed for the crosslinking, and, consequently, their use was limited to a few products until two major breakthroughs were obtained: (i.) the use of bifunctional organosilanes, acting as coupling agents (with the work, during the ‘70s, of researchers of Degussa[143]) and (ii.) the use of specific precipitated silica, described in a patent of Rauline[144] (Michelin S.à.S.).

Two aspects regarding each of the cited fillers will be presented in this chapter: (i.) the filler morphology and (ii.) the chemistry of the species constituting the fillers; the nature of the matrix / filler interaction will be also discussed.

The morphology of filler particles is of crucial importance because it directly defines their reinforcement ability. The surface area and the structure of both CBs and silicas were widely investigated in scientific literature by means of Transmission Electron Microscopy (TEM)[145, 146], Scanning Tunneling Microscopy (STM)[147] and Atomic Force Microscopy (AFM)[148]. TEM images of CB show irregular chain-like aggregate of spherulites; a detailed magnification of the spheres shows a layered structure made of graphenic sheets stacked together[146]. These sheets present a semi-crystalline structure with an approximate interlayer spacing of 0.35 nm (pure graphite: 0.33 nm).

Spherulites constituting CB aggregates are partially fused together; their size is of great importance, because it defines the surface of interaction between the filler and the matrix (smalle diametre = higher surface). TEM was tried as a measurement method for particles size but thousands of observations are needed, and other methods are preferred.

Electron transmission microscopy of silicas, instead, is much more difficult, particularly for silicas obtained through precipitation (that are, as said, the ones used in rubber compounds as described in ref.[144]) which tend to re-agglomerate during sample preparation or during the observation. In the (few) samples analysed in literature the appearent morphology is close to that of CB: small, chainlike, branched aggregates are observed. No spherulites can be clearly identified.

The surface area is so important that has been adopted by ASTM to designate CBs[‡]. The various determinations of surface area were tuned both for CBs or silicas, as these methods refer to the chemistry or the physical chemistry of the fillers. Among these methods, there are: the nitrogen adsorption[149] (BET-theory based method; can be extended to silicas, but has a drawback that consists in the fact that nitrogen has often access to micropores that are not accessible to macromolecules[150]); cetyl triethyl ammonium bromide (CTAB) adsorption[149]; iodine adsorption (similar to CTAB, except that the adsorpted species is I_2; this method can only be applied to CB characterisation[151]); TEM / Image Analysis (*TEM / IA*) measurements[152, 153] (difficult and time-demanding, as said).

The volume of the filler, on the other side, can be measured with other methods; in this case, TEM / IA is not a suitable method because of its bi-dimensionality. Other physicochemical methods are preferred, especially dibutyl phtalate absorption for CBs[154] (DBPA) and dioctyl phtalate absorption for silicas[155], along with mercury porosimetry[156]. The aggregate size distribution, that

[‡] ASTM D2663. CBs are divided in hundreds: 000-099 / 100-199 up to 999; diametres range up to 500 nm

is a higher-order size measurement, can be performed through TEM / IA (for both CB and silicas) but also by reflectivity measurements: a paste made from known amounts of CB, TiO_2 or ZnO and an oil such as DBP is dispersed on a solid surface and its reflectivity measured. It has been demonstrated that the obtained values will correlate with mean aggregate size and can be considered an indicator of the distribution[157].

The nature of the interaction of carbon blacks and rubber was thoroughly investigated over the past century, and it provided a base for the understanding of the silica reinforcing action. In this paragraph some aspects regarding the CB / elastomer interaction will be considered; afterwards some concepts regarding the reinforcement will be elucidated, and the sub-chapter will end with considerations regarding the reinforcement operated by silica.

A first phenomenon, consequence of the rubber / CB interaction, was observed in 1925 by Twiss[158]: a certain amount of rubber, called *bound rubber*, resulted no more separable from the CB when the compound was extracted in a good rubber solvent (for instance: toluene) over a specified period of time at a certain temperature (usually room temperature is considered).

In the following years many issues regarding the presence of bound rubber were established. A first experimental aspect that was rationalised is that the nature of the gel depends on the CB filling. A *critical filler loading* C_{crit} was defined; the amount of bound rubber grows linearly with filler loading, but at concentrations higher than C_{crit} the slope strongly decreases[159]. Moreover, the residual compound resembles an *unihomogeneous* gel below C_{crit}, and a *coherent* gel when the CB content is higher than C_{crit}; the two gels have got a completely different macroscopic aspect, being a rigid, black glass-like material in one case and a soft gel with black dots in the other. This phenomenon has been explained supposing that (i.) at low filler loadings (i.e. relatively large distances between the filler particles) the rubber chains are attached to one filler particle only, be it due to a single attachment of the macromolecule or to multiple attachment of the same macromolecule to the same filler particle; (ii.) beyond the threshold of C_{crit} one rubber molecule can connect two or more carbon black particles, and a more coherent gel is formed[159].

It has been lately established that the bound rubber content depends also on many other factors, the most important of which is the specific carbon black surface area[160-163]. Due to the elevated surface energy typical of CB[164] or to possible chemical interaction (covalent bonds; this aspect will be discussed later in this paragraph), macromolecules are adsorbed onto its surface. Even if only a part of the chains is involved in this adsorption, the mobility of many of them is reduced; elastomeric chains present a gradient of mobility coming from CB and going to the bulk[165]. The high surface area and loadings of carbon blacks used in elastomer reinforcement induce such small distances between reinforcing objects that almost any chain is in contact with at least one aggregate[163].

Moreover, because the statistical length of polymeric chains is in the range of inter-aggregate distance, close filler particles are probably bonded together by chains adsorbed on both aggregates (*coherent gel* model); the bonding of carbon black aggregates constitutes the so-called *filler network*.

The presence of oxygenated groups, due to the partial oxidation of CB of atmospheric origin, plays a role. The amount of bound rubber in compounds obtained with a *graphitised* filler (when CB is heated in inert atmosphere at more than 2700 °C all functional groups are split off[166-168]) is much smaller; on the other side, when in the '70s CBs prepared through the *furnace* method gradually replaced CBs prepared through the *channel* method (furnace CBs present ten times less acidic groups) the reinforcing ability remained unchanged or increased. Again, the synthesis of partially-oxidised CB led to a decreased reinforcement ability[169]; in conclusion the role of oxidised moieties is still unclear, though for much time it was associated to the presence of covalent bonds.

Overall, after almost a century it is still unclear whether the presence of bound rubber has to be attributed to pure adsorption effects (in which van der Waals forces and *chemisorption* play the main role), or to chemical processes involving formation of covalent / hydrogen bonds. Among the latter, the covalent bonds formation was supposed to be caused by reactions of the rubber with functional groups or aromatic hydrogens present on the CB surface[166, 167], or by the reaction of rubber radicals formed by mechano-chemical degradation (for a mechanism on degradation of SBR during processing see ref.[170]) with active sites newly formed, for instance, by the breakdown of CB structure during mixing[171]. Today, there is general agreement among most experts that although covalent bonds contribute to rubber reinforcement they are not an indispensible pre-requisite for bound rubber formation and for rubber reinforcement[172, 173].

Reinforcement models for filled elastomers include a practical definition of reinforcement: f is defined as the ratio of the viscosity η of filled elastomer and the viscosity η_0 of the pristine elastomer, or (equivalent definition) the ratio of the complex shear moduli G^* and G^*_0.

A first approximation of more complex formulae with a practical interest is the Einstein-Smallwood equation[174], whose assumption are: (i.) particles are perfectly rigid; (ii.) the matrix is incompressible; (iii.) there are no interactions between the filler particles or between them and the surrounding medium. These conditions are achieved only in very diluted compounds.

The Einstein-Smallwood equation, regarding the f given by a volume φ of a spherical filler, follows:

$$f = 1 + \frac{5}{2}\varphi$$

Guth and Gold evaluated the effect of the reinforcement including disturbances between particles at higher filler content, obtaining[175]:

$$f = 1 + \frac{5}{2}\varphi + \frac{141}{10}\varphi^2$$

As said, the reinforcement of CB (or silica, as it will be shown later in this chapter) is far from the conditions of both the cited equations especially because the filler aggregates are highly structured, and elastomeric chains strongly interact with them.
Many theoretical speculations followed to include experimental evidences in the cited equations. For instance, Kraus[176] and Medalia[177] in 1970 suggested that the *effective* volume of filler should contain a term including its structure (porosity and size of agglomerates). The new equation describing the system involved a *corrected volume fraction* φ_c instead of φ, defined as follow:

$$\varphi_c \equiv \frac{\varphi}{2}\left(1 + \frac{1 + 0.02139 \cdot DBP}{1.46}\right)$$

Where *DBP* is the measurement of structure porosity with dibutylphtalate (DBP) discussed in the previous paragraph regarding the morphology determination. The corrected volume fraction represents the "actual" size of the aggregates; i.e. it includes the filler plus a consistent volume of the polymer that is *shielded* from the deformation by the filler structure / porosity. This part of polymer is defined by Medalia as *occluded rubber*.

The physical chemistry of silica affects its reinforcement more complexely than CB, and especially the reinforcement models fail. The formation of bound rubber in filled compounds is encountered also with silicas having a surface area comparable to that of CB[178]; this bound rubber can hardly be caused by chemical reactions, if one considers the differences in surface chemistry between carbon blacks and silica (surface of semi-graphitic carbon sheets *vs* silyloxide random structure; presence of carbinolic / carbonylic / carboxylic groups *vs* siloxane groups).
Silica displaying a surface area similar to that of CBs shows a much smaller bound rubber value[179, 180]. This phenomenon, along with a very high Mooney viscosity[143], a low elastic modulus at elongation σ = 200%, and a much altered kinetics of the cure with sulphur[173] is the most evident difference between silica and CB-reinforced rubbers; other differences can be considered, in turn, affected by these. In some application areas (coloured compounds, shoe soles, *et cetera*) and especially on small objects it was possible to use silica as a reinforcer by carefully adjusting the cure system; the interaction between silica and vulcanising agents, though, remained the most

difficult problem to overcome especially in larger objects such as automotive tyres, along with scarce dispersability[181, 182]. The filler dispersion occurs by the distribution of itself in the form of pellets (micrometric dimension; these particles are called *agglomerates*) and successive erosion of them by a well-described "onion peeling" process[183]. This last event eliminates agglomerates and determines the filler structure; obviously this process depends on surface energy (the higher the surface energy, the higher are the mixing energies involved in the process to obtain a high dispersion), surface area and morphology.

The interaction between the CB dispersion and the vulcanisation process has been investigated by means of rheology and by torque measurements of the mixing instrument during vulcanisation[184-188]. Graphs regarding the *delta torque* (difference between initial torque and final torque, after the reaction) from the *filler loading* (in phr) led to the formulation of an empirical equation that showed a linear dependance of the delta torque to the filler loading:

$$\left(D_{\max} - D_{\min}\right) = \alpha\left(D_{\max,0\ filler} - D_{\min,0\ filler}\right)\frac{m_{filler}}{m_{polymer}} + \left(D_{\max,0\ filler} - D_{\min,0\ filler}\right)$$

Where $D_{max/min}$ is the maximum/minimum torque recorded by the instrument respectively after and before the vulcanisation; α is a proportionality constant; m_{filler} / $m_{polymer}$ is the filler content in phr; and the *0 filler* quantities are related to a *blank* vulcanisation run carried out in absence of filler.

The proportionality shown by this equation is observed for carbon black only; it has been shown that the α proportionality constant is indipendent of the cure system and closely related to the CB morphology[186]. In terms of reinforcement theory, the system is well-represented by the Einstein-Smallwood equation, and there is a linear contribution of the filler volume to the reinforcement. When filler concentration are higher, instead, the Guth-Gold equation (with the quadratical term) could better describe the non-linear behaviour, but after some point the re-agglomeration of CB causes the model to fail.

Instead, when the bare silica is mixed with, for instance, a SBR rubber and vulcanised, there is no linear dependance of delta torque from the filler content, and several random oscillations in the values are observed: the experiments are not easily reproducible as an non-coherent filler dispersion / vulcanisation network is achieved[189]. This effect is strictly related to the interaction of silica with vulcanisation sulphur: the previously cited linear behaviour of delta torque *vs* CB loading is not observed. On the other side, a linear behaviour can be measured when the silica-filled rubber is crosslinked through addition of peroxide initiators, such as dicumyl peroxide[190] and an empirical law, analogous to that cited before for CB, can be defined.

The composite materials including SBR and silica and vulcanised through DCP were the first to highlight the peculiarities of silica-filled, crosslinked rubbers. Many variables, starting from the α parameter of the delta torque dependence on the filler content[191], were on larger scale with respect to CB-filled compounds. On the other side, other effects of more difficult interpretation were observed: for instance, comparisons of the moduli in stress / strain graphs showed that silicas displaying similar structures are superior to CBs at small elongations (<70%) but almost do not act as reinforcing agents at 100% or higher elongations[173].

The data regarding the trend of the *tan δ vs* filler content in phr and the dynamometric experiments (stress / strain graphs, where the silica reinforcement was evident for small strains) were interpreted in terms of presence of a strong silica-silica interaction between particles; this phenomenon can be referred to the ability of silicas to form hydrogen bonds. Filler networks increase the ability of the material to resist deformation as long as the filler network remains intact; however, the filler network is destroyed under strong deformations[173]. The results regarding the tan δ measurements, obtained in dynamic stress rheometric experiments, are due, as well, to the presence of the silica network that, in these experimental conditions, shows its elasticity.

1.4.2 The development of silica coupling agents; parameters for the evaluation of reinforcement

The positive reinforcement features of the DCP-cured silica compounds cannot be obtained in sulphur-vulcanised systems especially because of the adverse effect of silica on the cure system. The research lines proposed throughout the world during early ‘70s regarded the development of new coupling agents able to (i.) avoid any possible influence the cure kinetics (ii.) promote an homogeneous dispersion of the filler (iii.) lower the amount of filler involved in filler-filler network and (iv.) strongly increase the interaction between rubber and filler[173]. Thus, researchers focused their attention on molecules carrying at least two functional groups; for a prompt reaction with the silica surface, organo silanes were investigated (alcoholysis between silanolic moieties and silyloxides is a quick reaction with scarce byproducts), while for the other functional group different possibilities were considered.

In pioneering studies of Ranney[192-196], 3-mercaptapropyl(trimethoxysilane) (*MPTS*) was used. Although the methanolysis was effective, the thiol-ene reaction led to modest yields; the presence of unreacted thiol caused i) scorch of the compound during vulcanisation (uncontrolled thiol addition to double bonds or coupling with other radicals), and ii) a disagreeable odour.

Researchers from the company *Degussa AG* (Hanau, Germany), systematically investigated the action of more than one hundred compatibilising agents; the best product in terms of overall performances is still regularly used nowadays after four decades of world-wide commercialisation:

the bis(3-triethoxysilylpropyl)tetrasulfane (*TESPT*, the structure is reported in Scheme 13). All other silanes had drawbacks regarding handling, ease of transport, storage stability, kinetics of the curing reaction, toxicological safety of the agents themselves or of the reaction products[173].

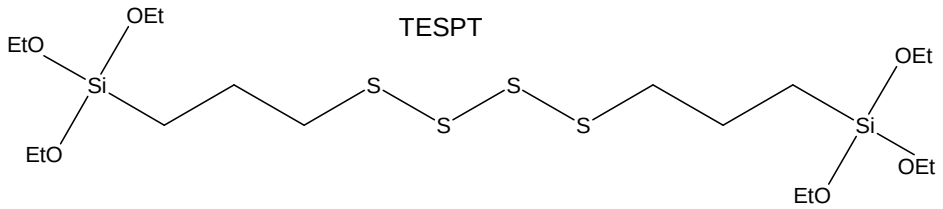

Scheme 13 – Molecular structure of bis(3-triethoxysilylpropyl)tetrasulfane (TESPT)

Among other compounds, good results were achieved also with 3-Thiocyanatopropyl-triethoxy silane (*TCPTS*)[197]; the organo silane group is the same of the TESPT molecule, though the –S–C≡N group creates monosulphidic filler-to-rubber bonds. TCPTS has not been commercially as succesful as TESPT mainly because of inferior performances of the thiocyanato-rubber reaction under vulcanisation conditions with respect to the tetrasulfane / rubber one[173]. The ethoxy moiety was chosen, in these organo silanes, as it is a good balance between quickness of alcoholysis (order of reactivity: methoxy silane > ethoxy silane > isopropoxy silane > *et cetera*) and low toxicity of reaction products.

The TESPT chemical action has been extensively investigated[198]. In a first reactive step with the silica, three or four out of six ethoxy groups react with the silica surface; in a second step the remaining ethoxy groups crosslink neighboring TESPT molecules. During vulcanisation, the tetrasulfane groups are split and react with the polymer, forming covalent filler-to-rubber bonds the most of which are poly- or disulfidic[199]. These reactions are summarised in Scheme 14.

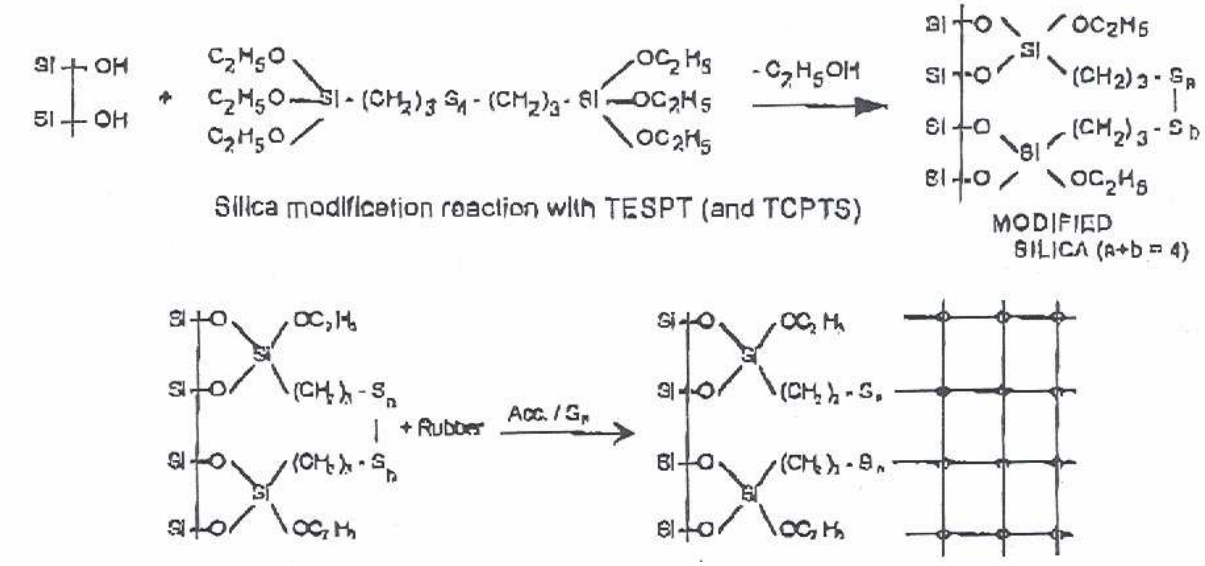

Scheme 14 – Silica modification with TESPT and interactions during the curing (adapted from ref.[173])

The *silanisation* of highly active silica leads to fundamental changes in their reinforcing action. The so-called *Payne effect* associated to the rubber compounds including silica and TESPT will be here briefly presented: this phenomenon represents and influences the performance of the material in which the reinforcing potential of TESPT-treated silica is most evident.

The Payne effect[200-202] is a particular feature of the stress-strain behaviour of rubber compounds containing fillers; the effect is sometimes also known as the Fletcher-Gent effect, after the authors of the first study of the phenomenon[203]. The effect is observed under cyclic loading conditions with relatively small strain amplitudes, and consists in a particular dependence of the viscoelastic storage modulus *G'* on the amplitude of the applied strain γ. For a strain amplitude γ > 0.1%, the dynamic storage modulus decreases rapidly from a starting value G'_0 to a G'_∞ value (for γ > 10%). At the same time, at sufficiently large strain amplitudes, the dynamic loss modulus *G"* shows a maximum, and *tan δ* too (asymmetric peak). In Figure 5, as an example, *G'* and *G"* for CB-filled polyisobutene[204] are reported; the Payne effect is more evident for the compounds containing the highest amount of CB.

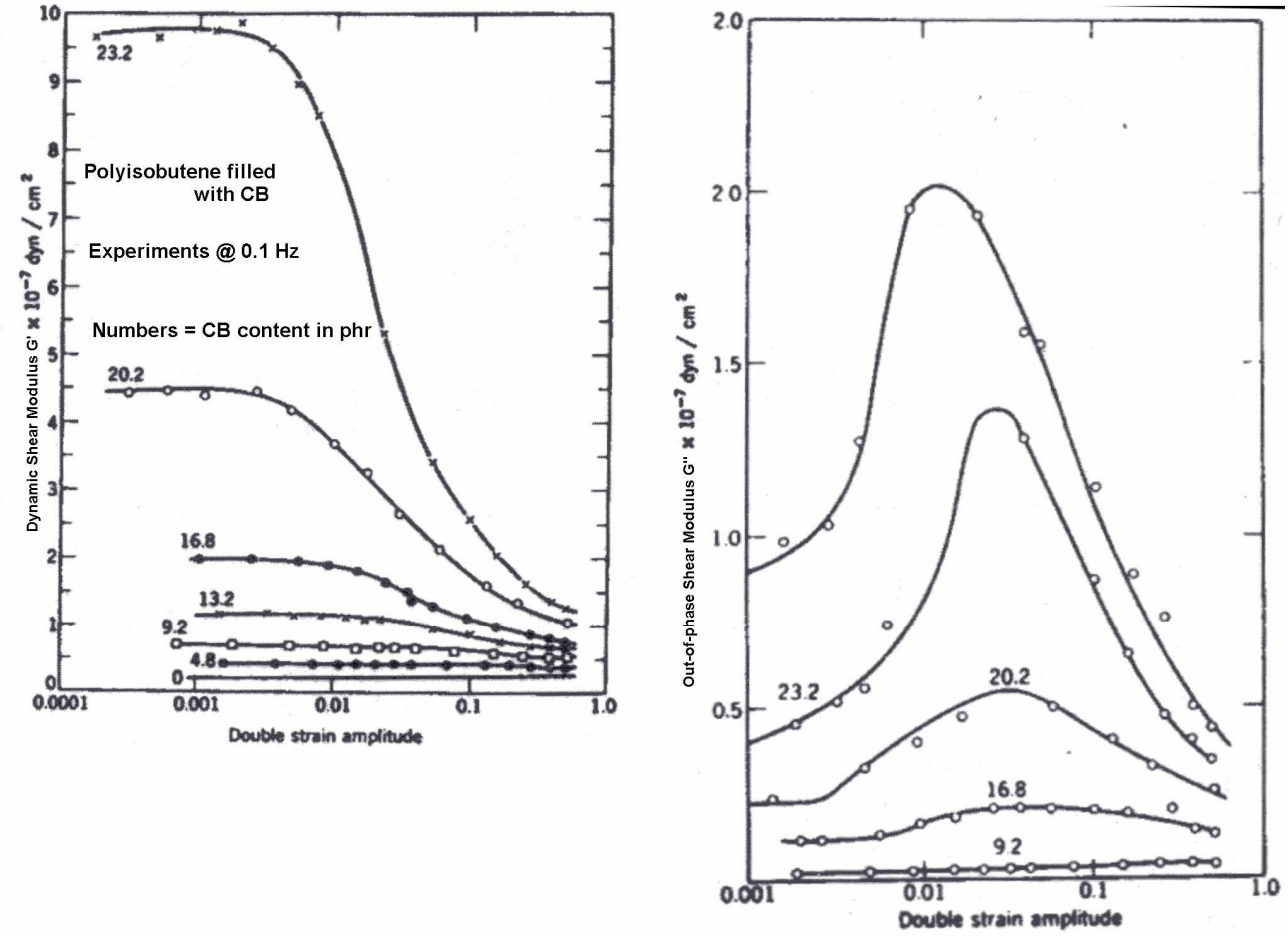

Figure 5 – G' and G" *vs* double strain amplitude in 0.1 Hz strain sweep experiments for CB-filled PIB[205]

The Payne effect, as shown, depends on the filler content of the material, and vanishes for unfilled elastomers; physically, it can be attributed to deformation-induced changes in the microstructure of the material, i.e. to breakage and recovery of weak physical bonds between filler clusters[206, 207]. The evolution of *G'* and *G"* in the range $0.1 < \gamma < 0.5$ is of particular interest because most common stress events of filled elastomer fall in this range. The expression of the hysteretic loss, that is an useful parametre as it is associated to energy dissipation, depends on the solicitation mode, and it is proportional to *G"* (constant strain), $G"/G^{*2}$ (constant stress) or *tan* δ (constant energy).

Dannenberg's *molecular slippage model* gives a good view of the mechanism responsible for the Payne effect[208, 209]; here it will be briefly presented with reference to the empirical description of the phenomenon given in Figure 5.

For low strain values, the elastomer chains remain partially adsorbed on the filler particles; when strain increases, the macromolecules bridging through filler particles are stretched and aligned (this extension is much greater than the macroscopic deformation of the material since there are zones, incorporated into filler clusters, that are not stretched; this phenomenon is called *strain amplification*). This elongation is elastic and reversible: G' is high, G" is low and constant.

When the strain passes a certain value, the elastic energy exceeds adsorption energy and elastomer chain gradually desorb from the filler surface; this desorption is not perfectly reversible. Because of this, a portion of elasticity is converted in viscous flow, i.e., G" is increased; at the same time, G' is reduced. During the strain elongations of medium intensity (Figure 5, $0.01 < \gamma < 0.1$) bridging elastomeric chains undergo adsorption-desorption cycles; at higher strains, a stabilisation of the moduli occurs (large strain properties will be described in the next paragraph).

A first consideration is that variation of moduli is determined mainly by interaggregate distances and by chain adsorption on the filler surface. Any increase in the filler loading would influence the distances between particles, and consequently the hysteresis is much increased; a first operational procedure aimed to hysteresis reduction is to obtain a good dispersion induced by prolonged processing (two-stage mixings, masterbatch techniques)[145].

Coupling agents that mask the filler surface could reduce elastomer adsorption and hysteresis of compounds; for instance, functionalised polymers having specific chemical moieties that react with the filler surface were used in a few studies[210, 211].

The high-strain properties involve different phenomena that are not usually observable under small strain conditions. A significant observation is the *Mullins effect*[212, 213]: a compounded sample is stretched, statically, to a large strain ε_m, returned to zero strain and again to ε_m; the stress-strain curve of the second strain is well below the first one, but it rejoins the final part of the first curve around ε_m (Figure 6).

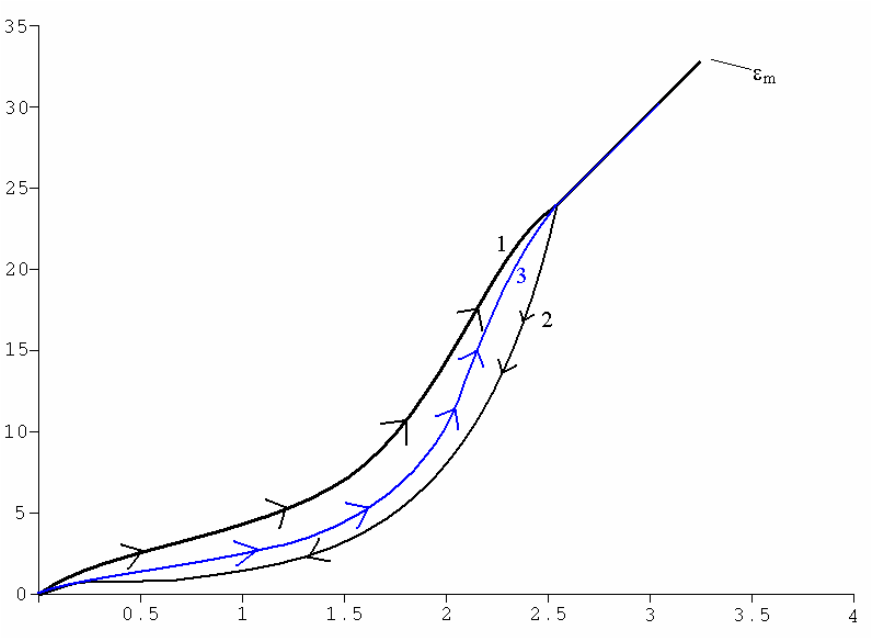

Figure 6 – The Mullins effect for large strains (taken from ref.[141])

Again, this effect can be explained by the Dannenberg adsorption / desorption model; because of its (partial) reversibility, adsorption allows elastomer – filler contact points to change continuously, allowing homogenisation of bridging lenghts. In conclusion, the stress is locally shared onto a larger amount of filler particles; on the "Payne point of view", this is reflected on another decrease of the loss modulus *G"*, along with *tan δ*, at high strains. A schematic description of the application of Dannenberg's model to the homogenisation of inter-filler chain lenghts is reported in Figure 7.

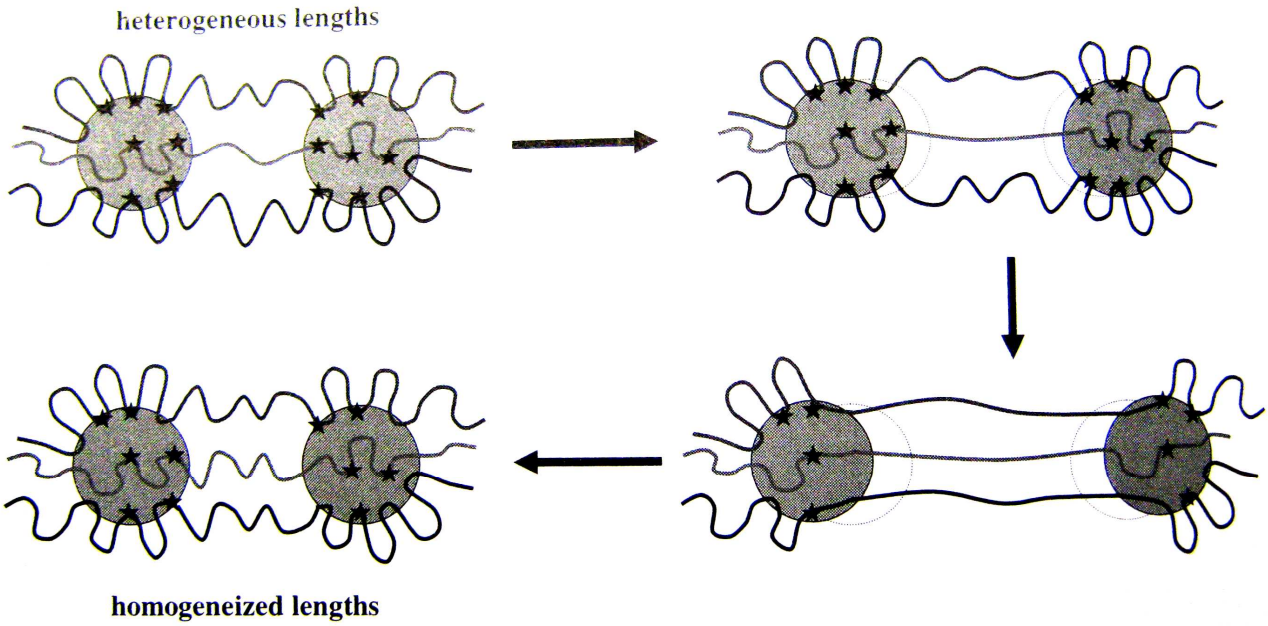

Figure 7 – Homogenisation of inter-filler lenghts caused by dynamic adsorption (taken from ref.[141]

Going back to real systems, in the case of non-compatibilised silica / diene polymer compounds the Payne effect is remarkable and often higher than in binary CB / rubber compounds. This is because rubber-filler interaction is muck weaker in silica compounds and the desorption (mid-range strains) occurs easily and irreversibly.

For compounds including TESPT-modified silica, instead, the Payne effect is much reduced; this is an effect of the compatibiliser on the surface energy and on the morphology of the filler. In fact, as said, the surface of the silica is *shielded* by the TESPT, and a silica-silica network is unfavoured. This has two effects: first, the *G'* values are low at low strains (good dispersion of silica and large inter-filler distances; according to the Dannenberg model, this allows the chains to be very mobile); second, the *G"* increment at mid-strains is reduced because of relative elasticity of the filler-rubber bonded system (when the inter-filler macromolecules are stretched and desorption of double bonds should occur, this does not happen as the filler is covalently bonded to the polymer). In conclusion, the hysteresis is decreased.

In Figure 8, as an example, two graphs are reported: three PB rubber compounds containing (i) a commercial CB (N110), (ii) a silica or (iii) a TESPT-treated silica are compared in terms of, respectively, *tan δ* and *G'*.

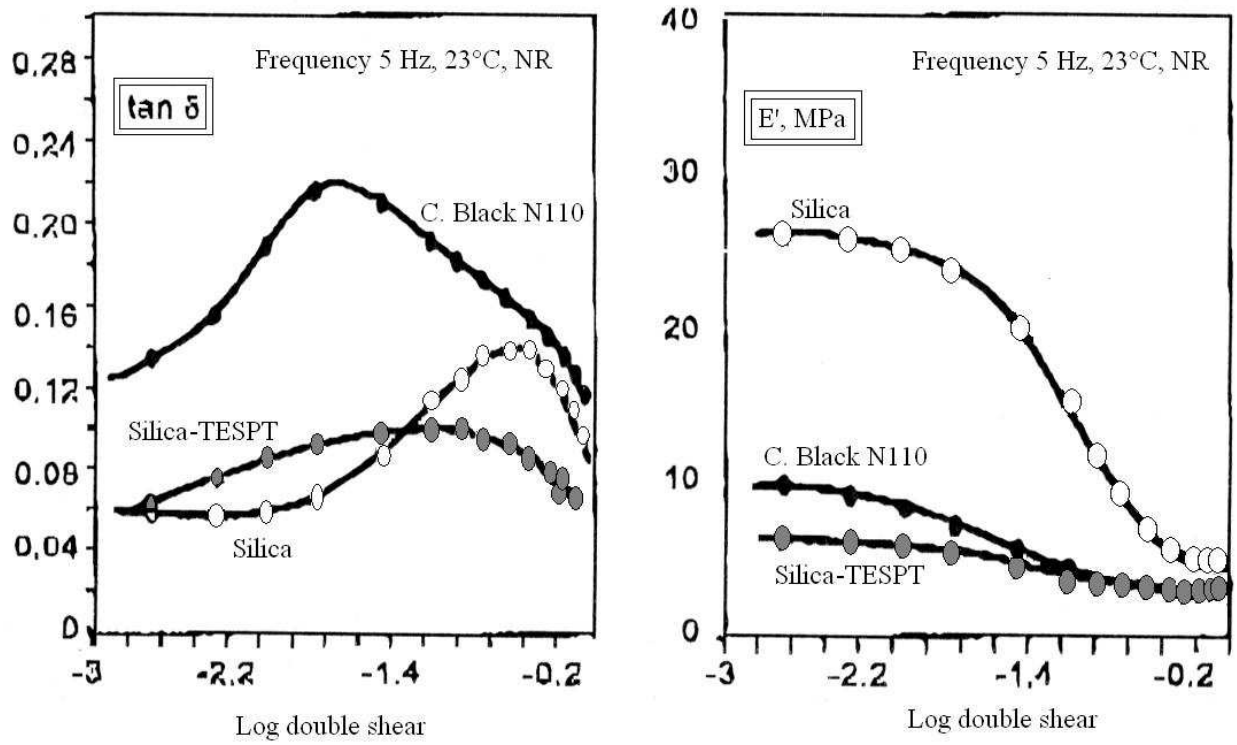

Figure 8 – tan δ and G' (respectively) *vs*. double shear graphs. Adapted from ref.[173]

The Payne effect is directly related to many ground tyre performances. In fact, as shown in the literature[214], the tread compound of the tyre is subjected to different strain patterns, including

frequencies as low as tens of Hz and as high as tens of MHz. The strain amplitude also varies widely and, consequently, the bulk of the tread may experience a strain amplitude of several percent. These stress phenomena, with particular reference to the low frequency region, are responsible for many of the tyre properties, such as rolling resistance or treadwear index[215].

There are many studies regarding the correlation between the rolling resistance of a tyre with various mechanical aspects of the different tyre components in terms of tyre production or its use. The rolling resistance depends on the tyre construction[216], tyre deformation[217], vehicle speed[218] or compound formulation[219, 220]; essentially, from the compounding point of view, small tan δ values result in a small rolling resistance[178, 180]. More in detail, the rolling resistance is mainly caused by the deformation of the tyre or the asphalt under the tyre (obviously the two deformations have a different extent), but it also depends on the wheel radius, surface adhesion and relative micro-sliding of interested surfaces. In particular, the cycle including deformation / elastic return of a tyre being periodically stressed from the contact with the ground depends on the tyre hysteresis: the higher the hysteresis, the higher the energy dissipation associated to an elevated rolling resistance. In many industrial applications the processing parameters are tuned in order to obtain a low hysteresis (strictly related and proportional to tan δ values); for instance, the filler dispersion times[221] have an influence on it, as well as many other process variables such as the adopted extruder temperatures.

Nowadays patents and scientific publications regarding innovative rubber compound formulations always refer to Payne effect measurements, as it is directly related to the rolling resistance. Rheometric measurements, performed on rotational instruments through low-frequency strain sweep experiments, give a direct measurement of the Payne effect displaying the dependence of tan δ or G' from the applied strain; in these terms, the maximum of tan δ as well as the difference between G' values at low and at high strains within a certain range of shear have become two typical values that can be found in almost every publication.

Stress-strain experiments also give a direct measurement on the reinforcing potential of fillers. Unlike for smectic-crystalline or crystalline materials, though, the linear part of the graph for rubbers is very limited; it is not easy to estimate the Young modulus, and rubber technologists prefer using the ratio $\sigma_{\varepsilon=300\%} / \sigma_{\varepsilon=100\%}$ (usually called 300/100 ratio) as a parameter of reinforcement entity.

As previously said, morphology and properties of CB / silica filled rubber compounds are greatly influenced by the filler dispersion, and many properties of tyres depend on these. The dispersion is determined by the mixing process, in which the filler networks are broken up under shear into individual aggregates and randomly distributed in the polymer matrix. On storage of the compound,

however, the filler particles slowly agglomerate to form a separated matrix: this phenomenon is called *filler flocculation*[200, 222].

Along with Payne effect evaluation and the cited Mooney viscosity / RFI measurements / stress-strain measurements of the compounds, particular rheological experiments tailored to investigate the flocculation / reaggregation of the filler have often been performed during the last decade[223-226]. It has been shown[223, 227] that an *annealing* procedure, including heating of samples between plates for various times and at different temperatures, is close to the flocculation occurring in filled rubber stocks during storage; in other words, it resembles the *ageing* of the compounds.

The Payne effect after annealing is higher than before: the entity of re-agglomeration of the filler leads to a filler network often more coherent than in the compound at the end of the mixing. As shown from researchers of *Firestone Inc.* with various CB-filled PBs[223], the difference in the dynamic storage moduli before and after the annealing depends on many variables, such as annealing time, temperature, filler loading in the composite, nature of the employed carbon black, the molecular weight of the polymer and the procedure of filler incorporation (mixing experimental parameters). In particular, the observed inverse dependence of the difference in the dynamic storage moduli before and after the annealing from the molecular weight (and, indirectly, from the polymer viscosity), characterise the phenomenon of flocculation as a diffusion-controlled process[223]. At the same time, the amount of incorporated CB and its surface properties are the most direct parameters influencing the re-formation of the filler network.

Rheometric measurements of the Payne effect can be tailored in order to investigate the effect of flocculation. In the present work a procedure, analogous to that adopted by Böhm and other researchers[223], has been adopted fruitfully in this sense; the protocol included a strain-sweep rheometrical experiment followed by annealing at high temperature and a second strain-sweep measurement.

1.5 Objectives of the work

This research aimed to investigate the thiol-ene functionalisation of polybutadiene and copolymers of butadiene and styrene with L-cysteine derivatives. A further investigation presented in this work regards the incorporation of the synthesised materials into compounds for automotive traction.

The novel materials created in the present work could act as compatibilising agents between (i.) two polymer phases, (ii.) a polymer matrix and an inorganic filler, or (iii.) metallic surfaces, or a metal and another material; in particular, a possible application in the field (ii.) is described.

It would be desirable to develop a single material acting effectively with a high number of substrates; thus, thiol-ene functionalisation using L-cysteine derivatives could be an appealing

reaction to bring on the macromolecules of a diene polymer both carboxylic / carboxylate units and amine / amide units. The simultaneous presence of acid / basic / polar moieties could potentially lead to materials with elevated and varied compatibilising capability.

Moreover, polymers functionalised with L-cysteine derivatives are recently developed materials, described in a very small number of papers and whose macroscopic properties are mostly unexplored; another target of the work is to propose a detailed characterisation of their molecular structure / properties.

More schematically, the objectives of the present work are:

- to obtain functionalised elastomers in solution or in bulk with L-cysteine derivatives: the reaction of the latter with (i.) a PBL (ii.) a liquid styrene-butadiene random copolymer (*SBRL*) (iii.) a long-chain SBR are investigated;
- to tune the experimental variables in order to obtain good yields and a low amount of byproducts. More specifically:
  - i) to understand, with model compounds, if *N*-acetyl-L-cysteine and its methyl ester are reactive towards double bonds in free radical conditions, and to compare their reactivity with existing scientific literature;
  - ii) to optimise the amount of initiator with a systematic set of runs;
  - iii) to discuss the variation in the thiol conversion degree with respect to the thiol:ene feed ratio;
  - iv) to fully characterise the products in terms of primary structure via ^{1}H-NMR, ^{13}C-NMR and FT-IR spectroscopies, along with size-exclusion chromatography (SEC) and polarimetric measurements;
  - v) to identify reaction byproducts and to identify the extent of side reactions with particular reference to the reaction conditions (feed ratio, temperature, amount of initiator, *et cetera*);
  - vi) to tune the experimental variables in order to obtain modulated properties of the functionalised materials such as, for instance, a pre-determined functionalisation degree;
  - vii) to transfer the obtained knowledge of the reaction on different substrates (for instance: long-chain SBRs) in order to draw production paths of materials with the least possible number of reactive steps. For instance: synthesising a L-cysteine functionalised SBR and then mixing it with a SBR matrix and an inorganic filler for the creation of a compound is more expensive than adding the functionaliser directly to the SBR matrix in a *one-pot* reactive mixing. (In any case, such a study should

carefully investigate if the obtained compounds display the same properties in the two situations.)

- to identify suitable systems (compounds and others) in which an amino acid-functionalised elastomer could be presumably employed as a compatibilising agent;
- to identify the best conditions to add the functionalised polymers to the existing compounding formulations. In the present work, compounds having high silica content for the construction of ground tyres were investigated; the discussed aspects were:
  i) choice of the incorporation procedure: addition in masterbatch *vs.* direct incorporation into the compound;
  ii) definition and tuning of processing parameters in order to obtain good mechanical properties of the compounds (and also: choice of Haake mixer *vs* Brabender mixer *vs* open two-rolls mill);
  iii) investigation of the action of the functionalised polymer on the mechanical properties of the compounds and dependance from the added amount;
  iv) elucidation of the mechanism of interaction between the added compatibilising agent and other compound additives (reinforcing fillers and compatibilisers, plasticisers, vulcanising agents) through experimental runs and suitable mechanical / spectroscopic characterisation.

2. RESULTS AND DISCUSSION

This thesis work is focused on the synthesis of L-cysteine functionalised compounds. In the next chapters (2.1 to 2.5 included), many functionalisation systems were investigated; a brief, schematic overview of the employed substances is reported in Table 10.

Substrate	Functionalising Agent
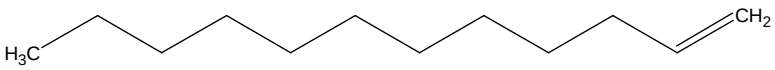 1-dodecene	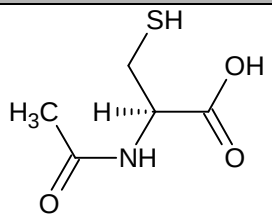 *N*-acetyl-L-cysteine
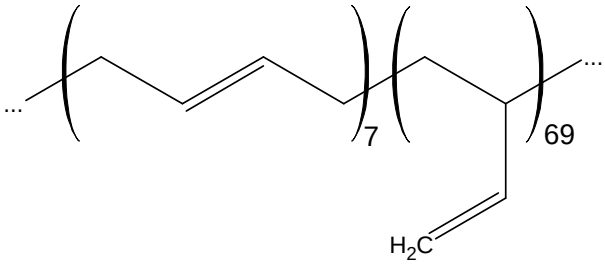 PBL (<DP_n> = 76)	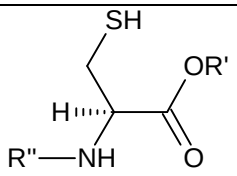 1. R' = H, R" = Acetyl 2. R' = CH_3, R" = Acetyl 3. R' = CH_3, R" = H
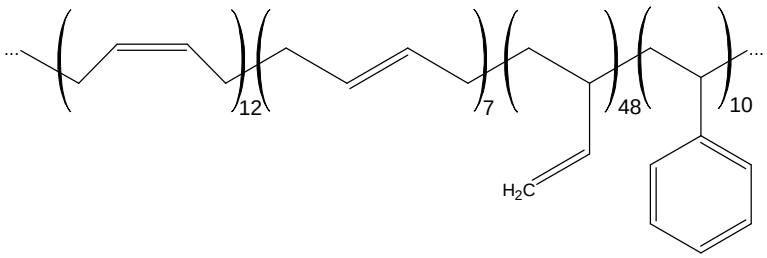 SBRL (<DP_n> = 77)	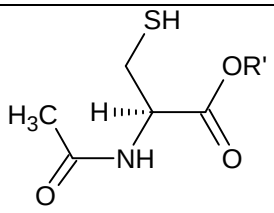 1. R' = H 2. R' = CH_3
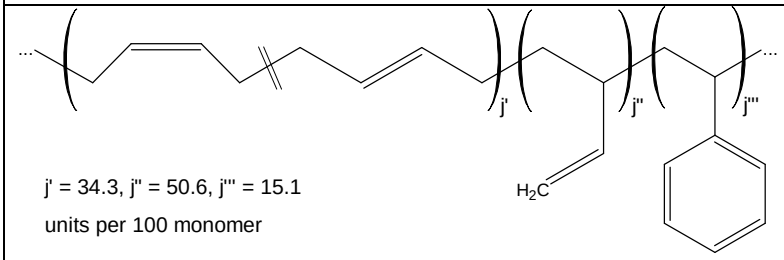 j' = 34.3, j" = 50.6, j"' = 15.1 units per 100 monomer SBR5 (<DP_n> = 7500)	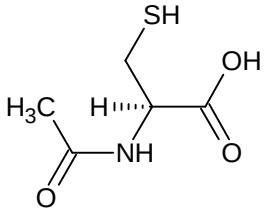 *N*-acetyl-L-cysteine

Table 10 – Olefins and thiols used fot thiol-ene functionalisations in the present work

The macromolecules whose primary structure is described in Table 10 were characterised according to existing scientific literature; other details about the polymer characterisations are reported both in the sub-chapters describing the reaction and in the experimental part. For the long-chain styrene/butadiene random copolymer (named SBR5), it has been preferred a description of primary structure in terms of units per 100 monomers; moreover, since the 1,4-*cis* units were not ditinguished from the 1,4-*trans* unit, in the structure the two units were merged in Table 10 between the same parenthesis, though this is not intended to provide informations about the monomer sequencing not the relative molar ratio 1,4-*trans* / 1,4-*cis*. All the polymers employed in the present work and described in Table 10 have a random structure without regular monomer sequencing; the latter was evaluated in the case of PBL and SBRL and both the two polymers showed a negligible regularity in the sequencing.

2.1 Addition of *N*-acetyl-L-cysteine to 1-dodecene

Thiol-ene reactions between a particular thiol and a diene polymer can be conveniently simulated by performing different reaction runs in various experimental conditions (for instance: with or without solvent, with various feed ratios) between the thiol and simple, *model* olefins having C_{12}-C_{15} alkyl chains[32, 54, 112]. The modelling consists in the location of the double bond in the olefin: terminal olefins are similar to 1,2- units of polybutadienes, while 1,4-*cis* or *trans* units of PBs are similar to internal olefins. As well as in other studies reported in literature[50-53], the characterisation of reaction products also helps identifying some typical trends in the reactivity of the thiol, such as:

- the anti-Markovnikov behaviour of the addition (this result is easily shown by the proton NMR characterisation of the thiol/olefin adducts)
- the preferred addition towards 1,2- units rather than towards 1,4- units (when a thiol-ene reaction is carried out in presence of both a terminal olefin and an internal one, the amount of recovered products reveal its preferencial reactivity with these structures)
- the preferred addition towards 1,4-*cis* units rather than towards 1,4-*trans* units
- the overall reactivity of the thiol, that is mainly influenced by its sterical hindrance or by the presence of functional groups.

Cysteine ethyl ester (*CysEt*) has been used in the past to obtain adducts on simple olefins resembling structural units of PB[54, 112], such as 1-dodecene and 7-tetradecene ([AIBN]:[CysEt]:[C=C] = 0.02:1:1, yield: 19-25 mol.-% with dodecene and 0% with 7-tetradecene). The addition reaction occurs only with 1-dodecene, and the yield was lower than in the case of addition of TGA and its ethyl ester EMA to similar olefines[32]; in order to compare the

reactivity of NCys and model olefins with the reactivity of CysEt[54] and with the reactivities of TGA / EMA[32], two reaction runs were carried out, in this work, with the same reaction conditions. A reaction having initial feed ratio [AIBN]:[NCys]:[1-dodecene] = 0.02:1:1 was performed in 1,4-dioxane. Another reaction was performed without solvent with the same feed ratio; in any case the two reactions were performed in homogeneous solutions, since both the thiol and the olefin are soluble in 1,4-dioxane and NCys is soluble in pure 1-dodecene at 90°C. The results arising from these experiments are compared to those of the previously cited study[54] in Table 11; the yield is determined by weighting the thioether obtained by removing other products by distillation under reduced pressure according to prior art[54].

Run[a]	Solvent	Reaction product	Yield (mol.-%)
1-dodecene + CysEt Toluene	Toluene	$CH_3(CH_2)_{11}SCH_2CH(NH_2)COOEt$	19[54]
1-dodecene + CysEt No solvent	None	$CH_3(CH_2)_{11}SCH_2CH(NH_2)COOEt$	25[54]
1-dodecene + NCys 1,4-dioxane	1,4-dioxane	$CH_3(CH_2)_{11}SCH_2CH(NCOCH_3)COOH$	24
1-dodecene + NCys No solvent	None	$CH_3(CH_2)_{11}SCH_2CH(NCOCH_3)COOH$	26

Table 11 – Reaction of NCys and CysEt (data of this latter case taken from ref.[54]) with 1-dodecene

[a] Reaction conditions: T = 90°C, [AIBN]:[RSH]:[1-dodecene] = 0.02:1:1

The samples described in the last two rows have an identical ^{1}H-NMR spectrum; it is reported in Figure 9, and it resembles almost perfectly a calculated spectrum obtained by ChemDraw Ultra 2002® for *N*-acetyl-*S*-dodecyl-L-cysteine, the structure of which is also reported in Figure 9.

The yield of the two reactions between NCys and 1-dodecene is similar to the yield obtained with CysEt, but lower with respect to other thiols (TGA or EMA, for example; see ref.[32]). The possible formation of intramolecular hydrogen bonds involving the –SH group[139] and the possible formation of unreactive *cistine* molecules in presence of oxygen traces[228] were invoked in the cited papers as reasonable explanations for the observed reduced reactivity.

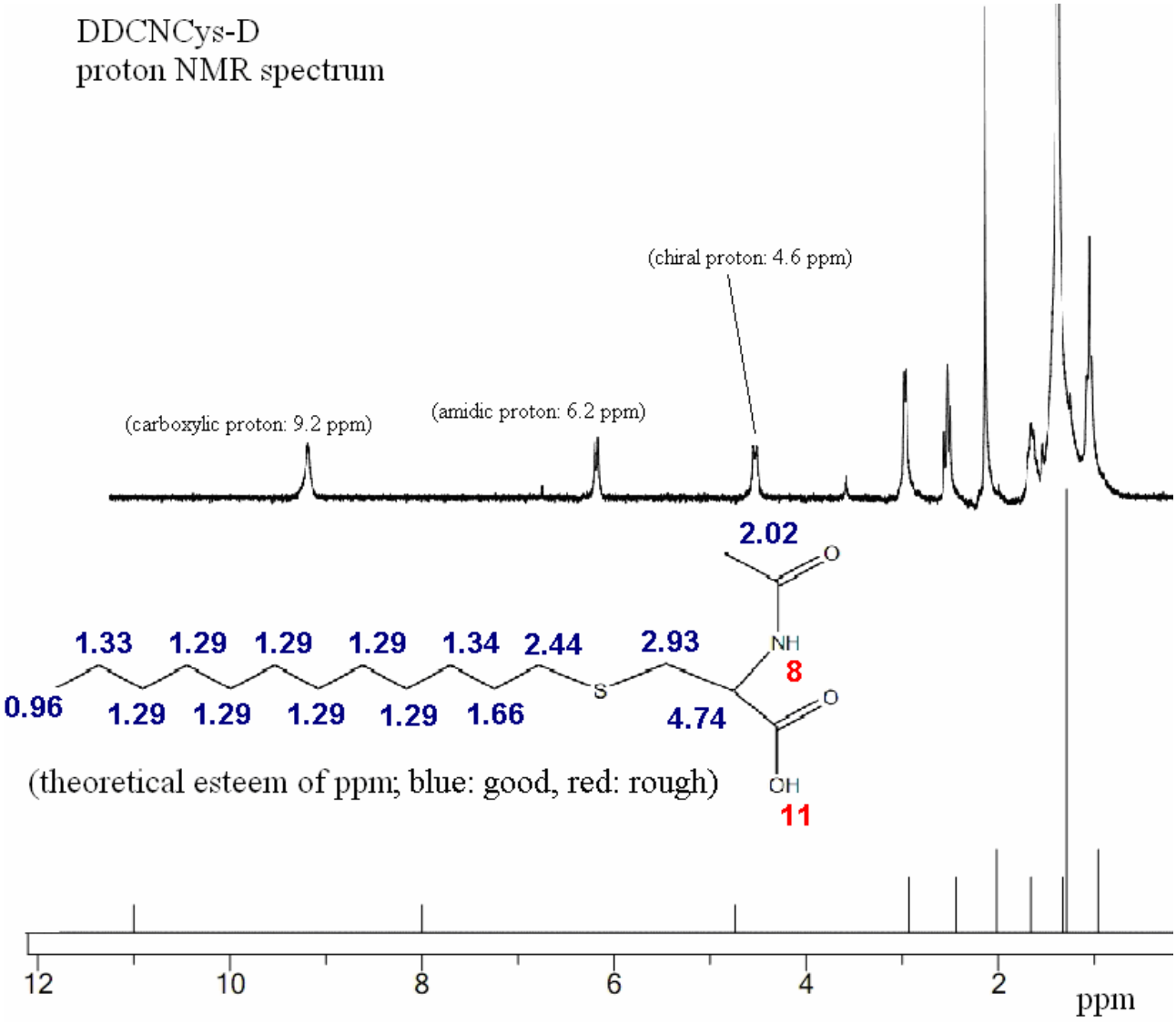

Figure 9 – Measured (above) and predicted (below) proton NMR spectrum of a 1-dodecene + NCys experiment 32 scans, 300 MHz, 25°C, $CDCl_3$

2.2 Addition of L-cysteine derivatives to liquid polybutadiene

So far the only L-cysteine derivatives that have been reported to radically add to double bonds are cysteine ethyl ester (CysEt) to SBR rubber and to model compounds[54], *N*-acetyl-L-cysteine methyl ester (NCysMe) to PB-*b*-PEO[82] and SBR[54], and two more complex *N*-cysteine amides[125, 126] on block copolymers PB-*b*-PEO. In this chapter the results achieved about the addition of NCys and NCysMe to a liquid PB in 1,4-dioxane solution will be presented; a functionalisation run using CysMe (the methyl ester of L-cysteine) was performed as well.

2.2.1 Structural characterisation of the polymer: liquid polybutadiene

A liquid polybutadiene (*PBL*) rich in 1,2- units was purchased from Sigma-Aldrich Inc. This PBL was similar to the one used by Justynska and Schlaad[82] to study its functionalisation with 3-mercaptopropanoic acid and its ethyl ester; the cited authors used a 93 mol-.% 1,2- polybutadiene, the other 7 mol.-% being 1,4-*trans* units, having a $<DP_n>$ of 40 and a $<M_n>$ of 2180 Da.

The primary structure of the PBL used in the present work has been determined via ^{1}H and ^{13}C-NMR, according to the method of Salle and Pham[229] and to other classical works on this subject[230, 231]. PBL is constituted by 90.9 mol.-% of 1,2- units and 9.1 mol.-% of 1,4-*trans* units; the content of 1,4-*cis* units, calculated from the ^{13}C-NMR spectrum, is negligible.

Considering that the $<M_n>$ of PBL is near to 4100 Da (measured by SEC in THF using a PS standards calibration curve), one can infer that a typical macromolecule of this polymer has 76 repeating monomer units, 69 of them being 1,2- ones. The ^{1}H-NMR spectrum of PBL is reported in Figure 10.

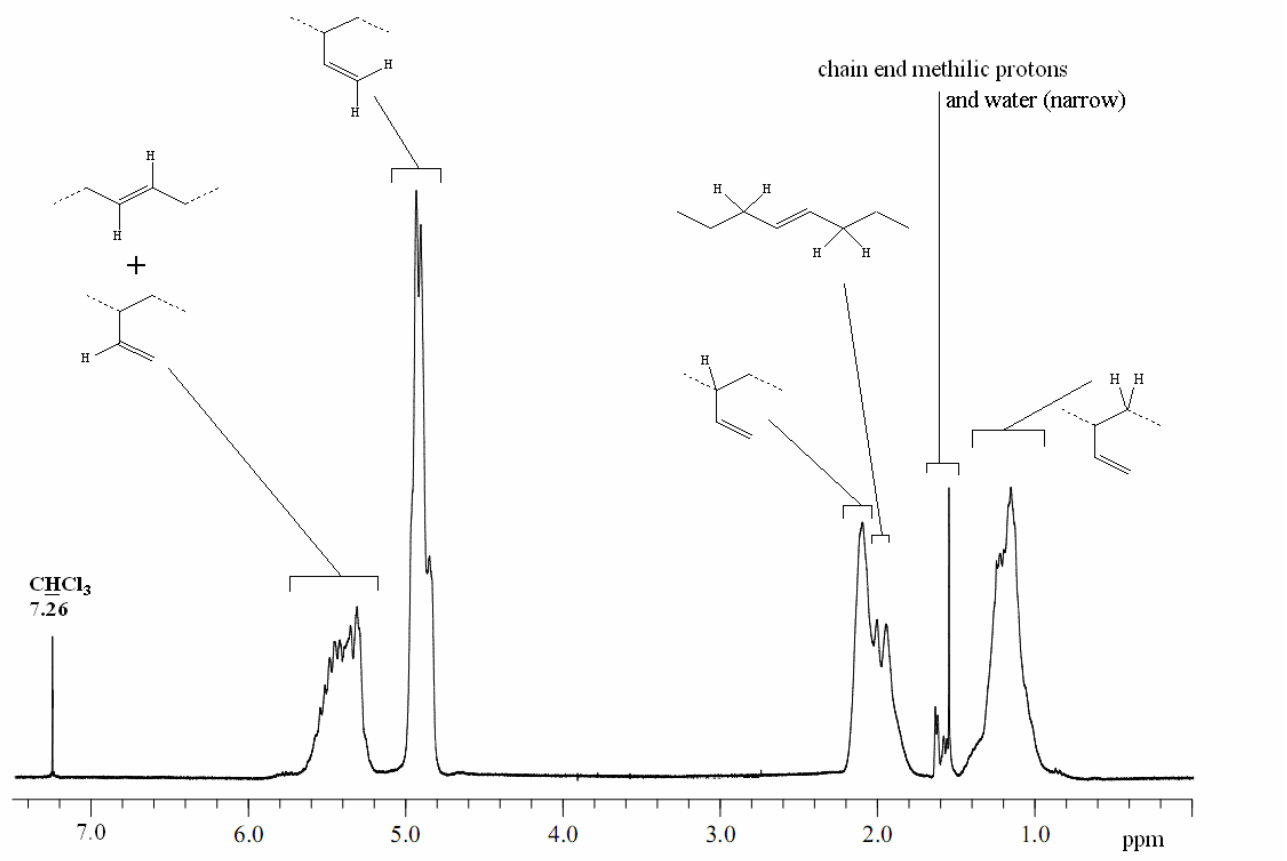

Figure 10 – ^{1}H-NMR spectrum of PBL, collected in $CDCl_3$ (32 scans, 25°C, 200MHz)

Farshid Ziaee in 2008 resolved the tacticity of a very similar polymer[232] by the deconvolution of the [113-116] ppm and the [142-144] zone in the ^{13}C-NMR spectrum. The calculations suggested by the author are time-demanding and complicated, and not useful for the present study; so far, the

tacticity of the polymer has never been reported to affect the free radical reactivity. However, the approximated calculation of Mochel was here adopted[230] to determine the amounts of triads *rr* versus *rm* or *mm* monomer triads, as well as Helmut Schlaad and co-workers did in a recent paper[233]. This nomenclature arises from the *m* (*meso*-) or the *r* (*racemo*-) diads sequence of 1,2-monomeric units: a *m* diad is composed by two neighboring prochiral tertiary carbons (belonging to vinyl units) in the same absolute configuration, while a *r* diad is composed by two neighboring units in a different absolute configuration. An isotactic triad (*mm*) is made up of two adjacent meso diads, a syndiotactic triad (*rr*) consists of two adjacent racemo diads and a heterotactic triad (*rm*) is composed of a meso diad adjacent to a racemo diad. The mass fraction of isotactic (*mm*) triads is a common quantitative measure of tacticity and it has been used in all the three cited studies[230, 232, 233].

The ^{13}C-NMR spectrum of PBL is reported in Figure 11, along with [113-116] ppm zone assignments according to Ziaee[232].

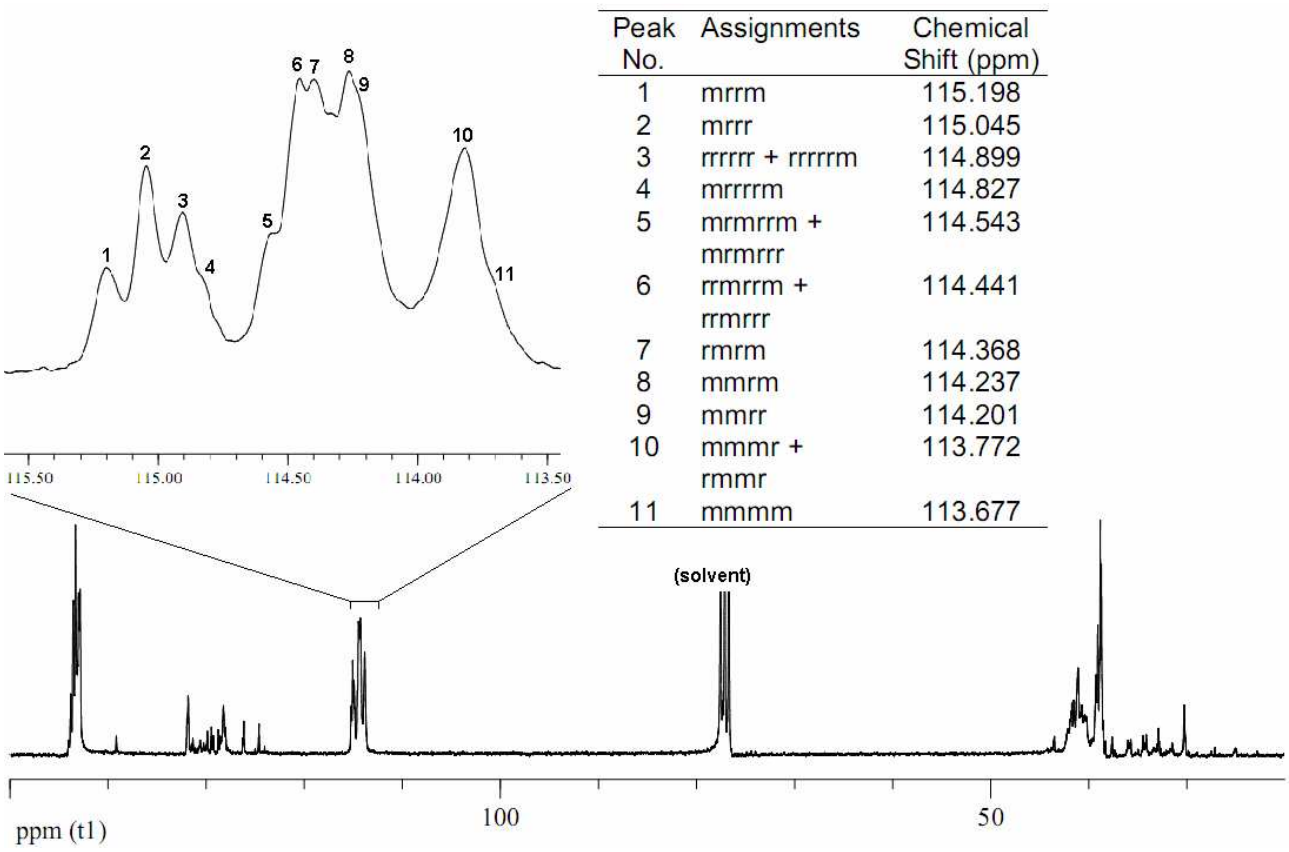

Peak No.	Assignments	Chemical Shift (ppm)
1	mrrm	115.198
2	mrrr	115.045
3	rrrrr + rrrrrm	114.899
4	mrrrrm	114.827
5	mrmrrm + mrmrrr	114.543
6	rrmrrm + rrmrrr	114.441
7	rmrm	114.368
8	mmrm	114.237
9	mmrr	114.201
10	mmmr + rmmr	113.772
11	mmmm	113.677

Figure 11 – ^{13}C-NMR spectrum of PBL, 300 MHz, 25°C, $CDCl_3$ (77.0 ppm, triplet)

The deconvolution of spectra was performed considering eleven peaks instead of the three peaks of Mochel (the author worked on a less resolved spectrum); the method was applied anyway considering that:

$$\int 1 + \int 2 + \int 3 + \int 4 = syn(rr)$$
$$\int 5 + \int 6 + \int 7 + \int 8 + \int 9 = hetero(rm)$$
$$\int 10 + \int 11 = iso(mm)$$

The considered polymer showed an *isotactic mass fraction* of 44.5%, that is a value near to the one found by Ziaee for the same substrate (46.7%)[232].

AIBN was chosen as the free radical initiator for thiol grafting due to its good solubility in the chosen reaction media (1,4-dioxane, one of the few solvents able to dissolve both the highly hydrophobic polybutadiene and the highly hydrophilic functionalising agents, along with THF as shown from Priola[31, 57], Gorski[56] and Schlaad[82, 233] in similar systems).
The absolute functionalisation degree (DF) has been defined as the molar amount of grafted molecules per 100 moles of monomeric units; the degree of functionalisation rescaled with respect to the vinyl side groups (DF_v) is defined, instead, as the molar amount of grafted functionalising molecules per 100 moles of 1,2- units. In the case of Sigma-Aldrich PBL, since the 1,2- units are the 90.9 mol.-% of the total, $DF = DF_v \cdot 0.909$.

The amount of initiator was chosen as 1 mol-.% with respect to thiol in every experimental run: this amount has been determined with three preliminar experiments of functionalisation with NCysMe. These experimental runs, summarised in Table 12, were carried out by varying the amount of AIBN, and characterised through IR and NMR spectroscopy and SEC.

Run[a]	[AIBN]:[NCysMe]:[vinyl]	Achiev. DF_v %	DF_v %[b]	Conv. %	M_n (M_w) , Da[c] PS calibr.
PB	-	-	-	-	4080 (5850)
PBNCysMe100/0.5	0.005:1:1	100	44.6	45	5270 (7310)
PBNCysMe100	0.010:1:1	100	79.2	79	6240 (9240)
PBNCysMe100/2	0.020:1:1	100	78.4	78	7920 (13540)

Table 12 – Feed ratios, DFs and avg. <M_n>(<M_w>) of the runs aimed to the choice of initiator amount

[a] Reaction conditions: T = 70°C, time 4h48', 1,4-dioxane 2 wt.-% polymer solution, under dry N_2

[b] Calculated with a ^{1}H-NMR method, see chapter 2.2.4, page 71

[c] SEC instrument with RI detector. Solvent: THF, 25°C, 1ml/min, DVB/PS Mixed-D column

In the case of TGA / EMA functionalisation reported in literature, an analogous preliminar procedure was performed[111]; it outlined a range of [AIBN]:[RSH] feed ratio values to be used in

order to maximise the conversion degree. In the present study a similar trend was obtained: small DF for low AIBN:thiol ratios, followed by a leveling of the DF_v by increasing the amount of AIBN.
In general, an increment of the MW was observed with respect to the pristine PB; this increment could be due both to the functionalisation itself (the average molecular weight of the repeating unit is increased, while the polymerisation degree is not) and to the occurrence of side reaction such as chain-chain coupling (the occurrence of side reactions will be specifically addressed in later chapters). In particular, the functionalisation degree of the PBNCysMe100/2 sample is similar to the one of PBNCysMe100, while the molecular weight increased: this is probably because of the occurrence of chain-chain coupling side-reaction. On the other side, the MW of the first two functionalised samples (PBNCysMe100/0.5 and PBNCysMe100) cannot be compared to the one of the pristine PB because of the different hydrophilic nature of the polymers, that is affecting the SEC determination.
In order to ascribe the new macroscopic properties of the products just to the presence of functionalising units, it was preferred to adopt the reaction conditions that allowed to avoid a major change in the MW while keeping a high conversion degree, and so the initial ratio [AIBN]:[RSH] = 0.010:1 (AIBN is 1 mol.-% of RSH) was chosen for all the studied thiols.

A useful parameter defined and discussed in other free radical functionalisation process (for example the grafting of unsaturated functionalisers to polyolefins not having double bonds) is the grafting efficiency G_e. It is defined as the number of grafted functionalising units per primary radical generated by the initiator or, that is the same thing, the number of addition steps per primary radical. For experimental reasons, the reaction was stopped at AIBN half-life in 1,4-dioxane at 70 °C, and in these conditions it is possible to find a convenient expression for the G_e.
The conversion degree is first defined (this variable has already been reported in the majority of the tables so far in this work, in percentage; in its definition, [*RSH*] is the concentration of grafted thiol, and it is a function of the reaction time, and C_{init} is the initial amount of the thiol RSH):

$$C(t) \equiv \frac{[RSH](t)}{C_{init}}$$

Let f be the initiator efficiency, defined, in the case of thiol-ene functionalisations, as the ratio between the molar amount of primary radicals $I^{\bullet}$ involved in the reaction with *RSH* species and the total number of generated $I^{\bullet}$. ($I^{\bullet}$ will represent the radical arising from-self dissociation of AIBN, i.e. the 2-cyano prop-2-yl radical). One could then write, for the grafting efficiency:

$$G_e = \frac{[RSH](t)}{[I^{\bullet}](t)} = \frac{C(t)C_{init}}{2f[AIBN](t)}$$

Since at half time

$$[AIBN](t_{1/2}) = \frac{1}{2}[AIBN](0)$$

And, for the chosen feed ratio

$$\frac{[AIBN](0)}{C_{init}} = \frac{1}{100}$$

One obtains:

$$G_e(t_{1/2}) = \frac{100 \cdot C(t_{1/2})}{f}$$

In the case of AIBN, often $f \sim 1$[234], so the grafting efficiency is 100 times the conversion, that is, it ranges from 0 to 100. As shown from Priola[31] and others (see, for instance, ref.[38, 40]), the grafting of thiols occurs even in absence of a radical initiator because of the self-dissociation of –SH groups generating active thiyl radicals: in this case there are no primary radicals, and the grafting efficiency cannot be defined. In the case of reaction conducted at 70°C or more in presence of AIBN or other radical initiators, the formation of thiyl radicals depends not only on the amount of primary radicals but also on the self-dissociation of –SH groups, and the conversion degree is influenced by this collateral generation of thiyl radicals. This generates an *apparent* grafting efficiency that could be related to the real G_e knowing the precise kinetics of the self-dissociation of –SH group at the reaction temperature; anyway, it will be sufficient to consider that the G_es indicated into the tables of this work are all *apparent* ones.

The hydrogen transfer from the macroradical to the thiol (Scheme 4, page 7) is a quick reaction, and it allows the G_e of a thiol-ene functionalisation to be much higher than in any typical free radical functionalisation of polyolefins with unsaturated monomers. Usually, the values of G_e arising from the functionalisations of PE and PP with, for instance, maleic anhydride derivatives go up to 15-17 (17 is one the highest value reported in literature[235], in a diethylmaleate / ethene-*co*-propene rubber functionalisation initiated by dicumylperoxide); the PBNCysMe functionalisations reported in Table 12, instead, had G_e ranging from 45 to 80.

2.2.2 Addition of L-cysteine derivatives to liquid polybutadiene

A preliminary experiment with 0.01:1:1 molar ratio AIBN / NCys / vinyl (theoretically achievable DF: 90.9%, DF_v: 100%; AIBN: 1% of the thiol), performed under the experimental conditions pointed out in Table 13 (page 68), showed that the functionalisation occurred: the purified sample dissolved quantitatively in a 10% KOH solution in water, while a mix of NCys and pristine PB was not soluble in the same solution. An analogous behaviour was also noticed for TGA-functionalised PBLs in 1984 by Priola and co-workers[31]. This run was called PBNCys100, from the substrate (PB), the functionalizing molecule (NCys) and the maximum theoretical achievable DF_v % (100).
In order to evaluate the reactivity of the cysteine derivatives, a number of experiments was carried out using different initial feed ratios (Table 13). The reactivity order of thiol / ene reaction (1,2-vinylic » 1,4-*cis* > 1,4-*trans*) should allow the attack to be selective toward the vinyl side groups, particularly for a low initial amount of thiol, as reported by Bunel and co-workers[73]. Thus, it was chosen to work in defect of thiol with respect to the total amount of double bonds, and it was preferred to optimise the experimental conditions in order to obtain high conversion degrees rather than high DFs, as already done in prior art[32, 54, 68, 70, 73].

Run[a,b]	[RSH]:[vinyl C=C]	AIBN (mol.-%)		Achievable DF_v %	DF_v %[c]	Conversion %
		To polymer	To RSH			
PB	-	-	-	-	-	-
PBNCys100	1.00:1	1.00	1.00	100	77.6	78
PBNCys075	0.75:1	0.75	1.00	75	50.8	68
PBNCys060	0.60:1	0.60	1.00	60	48.2	80
PBNCys045	0.45:1	0.45	1.00	45	31.0	69
PBNCys030	0.30:1	0.30	1.00	30	11.8	39
PBNCys015	0.15:1	0.15	1.00	15	6.9	46
PBNCys010	0.10:1	0.10	1.00	10	1.5	15
PBNCysMe100	1.00:1	1.00	1.00	100	79.2	79
PBNCysMe075	0.75:1	0.75	1.00	75	66.9	89
PBNCysMe060	0.60:1	0.60	1.00	60	53.6	89
PBNCysMe045	0.45:1	0.45	1.00	45	34.6	77
PBNCysMe030	0.30:1	0.30	1.00	30	11.4	38
PBNCysMe015	0.15:1	0.15	1.00	15	6.3	42
PBNCysMe010	0.10:1	0.10	1.00	10	3.5	35
PBCysMe100	1.00:1	1.00	1.00	100	55.0	55

Table 13 – Feed ratios, DFs and conversion degrees of functionalisation runs performed on PBL with NCys and NCysMe

[a] Samples named NCys are PBL functionalised with *N*-acetyl-L-cysteine; samples named NCysMe are PBL functionalised with *N*-acetyl-L-cysteine methyl ester

[b] Reaction conditions: T = 70°C, time 4h48', 1,4-dioxane 2 wt.-% polymer solution, under dry N_2

[c] Calculated with a ^{1}H-NMR method (see chapter 2.2.4, page 71)

In Table 13 the values for the CysMe + PBL reaction are also reported, as well as some data arising from the treatment of pure PB with AIBN only (without any thiol). This latter reaction run, with a 1 mol.-% of AIBN with respect to the vinyl double bonds, is directed toward the identification of the increase of the molecular weight in the used experimental conditions, and the ~10% average increase indicates that crosslinking should be avoided in any case if [AIBN]:[vinyl C=C]<0.01:1.

2.2.3 FT-IR spectroscopic identification of products

An infrared characterisation of every single reaction product was performed; a film of polymer was cast on a KBr disc from a 1,4-dioxane solution. IR spectra of the reaction products confirmed the presence of L-cysteine derivatives grafted to the PBL, independently from the used derivative. In Figure 12 the most characteristic IR absorption bands are shown: of the pristine PBL, of a NCys-functionalised sample (PBNCys030) and of the related functionalising agent (pure NCys). The other spectra, of samples functionalised with NCysMe and CysMe, are similar; only the intensity of bands arising from stretchings associated to L-cysteine derivatives varied among the samples having different feed ratio (and consequently DF_v).

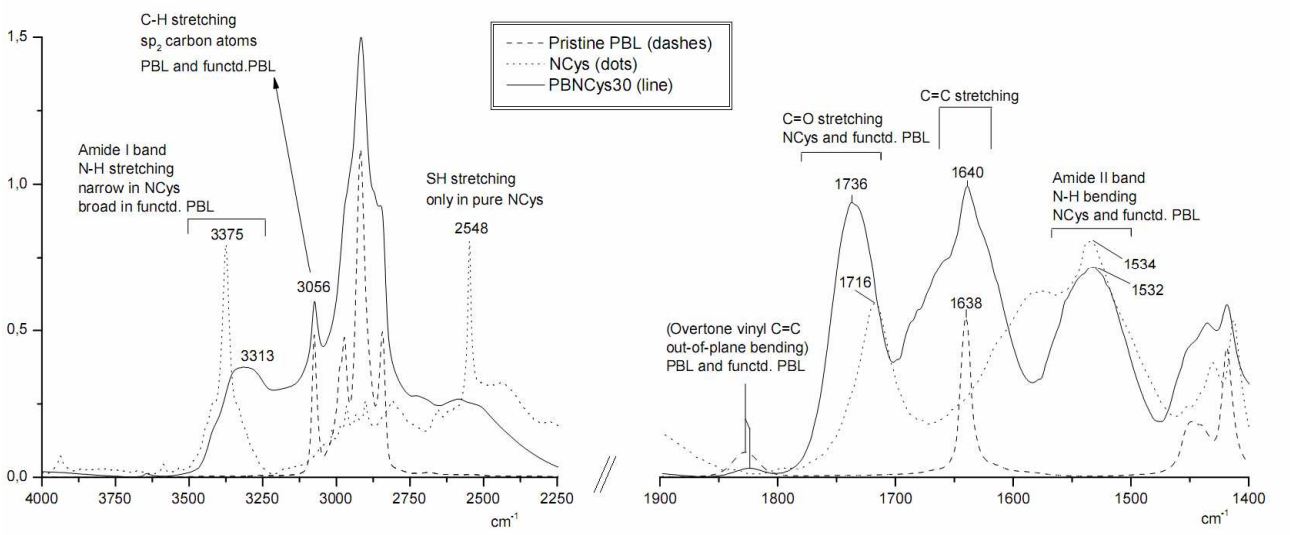

Figure 12 – FT-IR spectra in the range 4000-2250 cm^{-1} and 1900-1400 cm^{-1} of: (-------) PB film on KBr window (·····) *N*-acetyl-L-cysteine in a KBr pellet (——) PBNCys030 film on KBr window

The PBNCys030 spectrum shows the amide I and amide II absorption bands (respectively amide N–H stretching at ~3375 cm^{-1} and bending at ~1535 cm^{-1}) and, at 1736 cm^{-1}, the C=O stretching; all these bands are also present in the spectrum of the NCys functionalizing agent, but obviously not in the pristine polymer, confirming the occurrence of thiol addition and the presence of grafted amide

and carboxyl functionalities. The C=O stretching band was used, in the past, for the quantitative determination of the DF[54].

The S–H stretching band, at 2548 cm^{-1}, is recognisable only in the NCys spectrum, as expected.

The presence of residual vinyl double bonds is showed by the intense vinyl C=C out-of-plane bending at 909 cm^{-1} (which was observed but not reported in Figure 12, although its overtone at ~1820 cm^{-1} can be easily identified in both PB and PBNCys030 spectra).

A measurement of the DF using an IR method was attempted[54]; the carbonyl stretching at ~1735 cm^{-1} was used as the measuring band, being directly related to the amount of grafted thiol, and the out-of-plane 1,4-*trans* C–H bending at ~967 cm^{-1} was chosen as the reference band. A deconvolution of the signals was performed to separate all the peaks, and a calibration curve was obtained by mixing known amounts of NCys (up to 4%) with the polymer. Some IR spectra of mixtures of PB with various amounts of NCys and a brief description of the resulting calibration curve is reported in Figure 13.

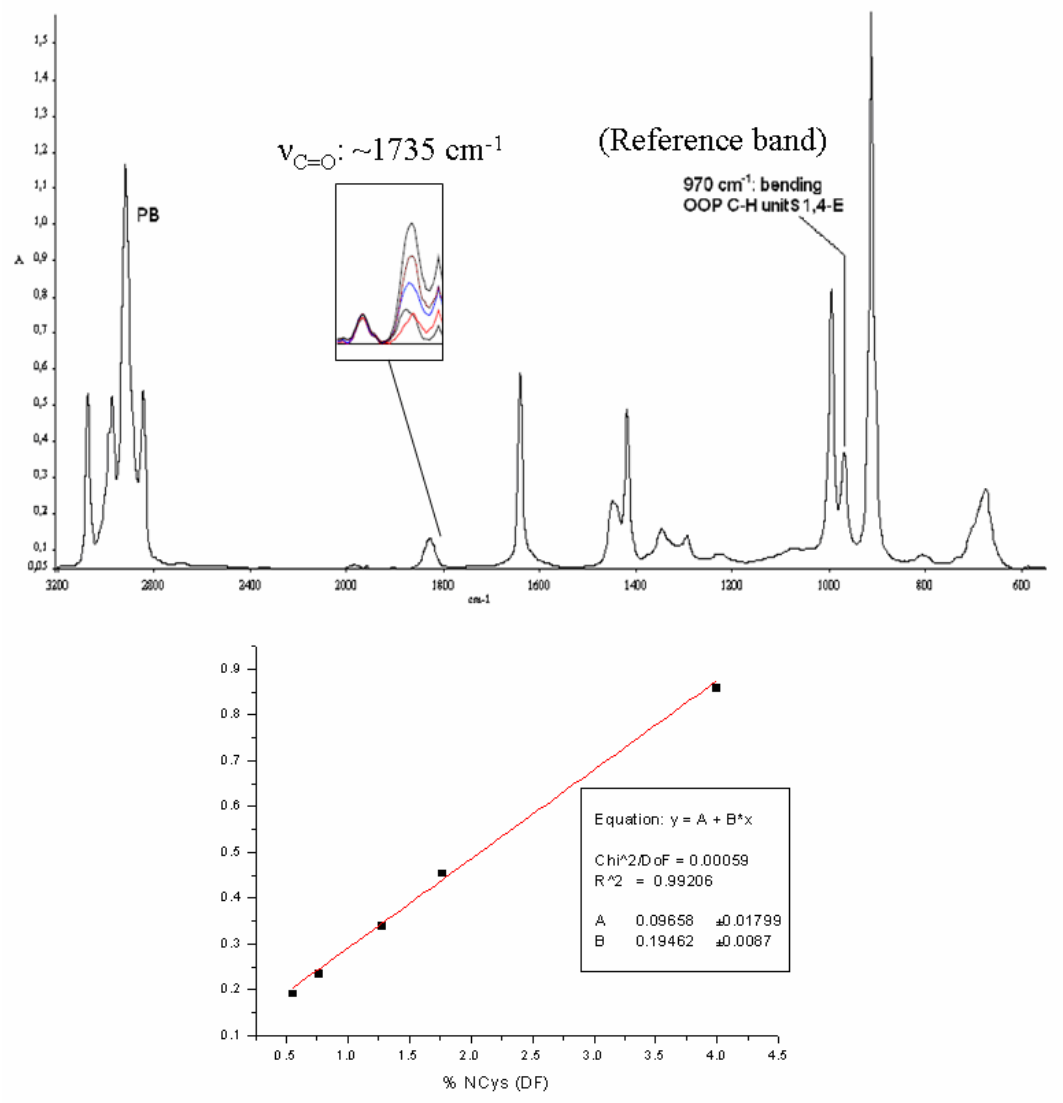

Figure 13 – IR spectra of standards samples for the creation of the calibration curve, and its description (the spectra are normalised to the band at 1819 cm^{-1} for displaying purposes)

The application of this method to the PBNCys100 sample, though, showed a DF well outside of the confidence interval of the calibration line, and probably outside of the linear range of Lambert-Beer's law as a rough estimate of the DF led to a value of 48%.

2.2.4 ^{1}H-NMR characterisation of products: determination of the DF

A complete assignment of the proton NMR peaks appearing in the spectrum of the sample PBNCys100 is reported in Figure 14.

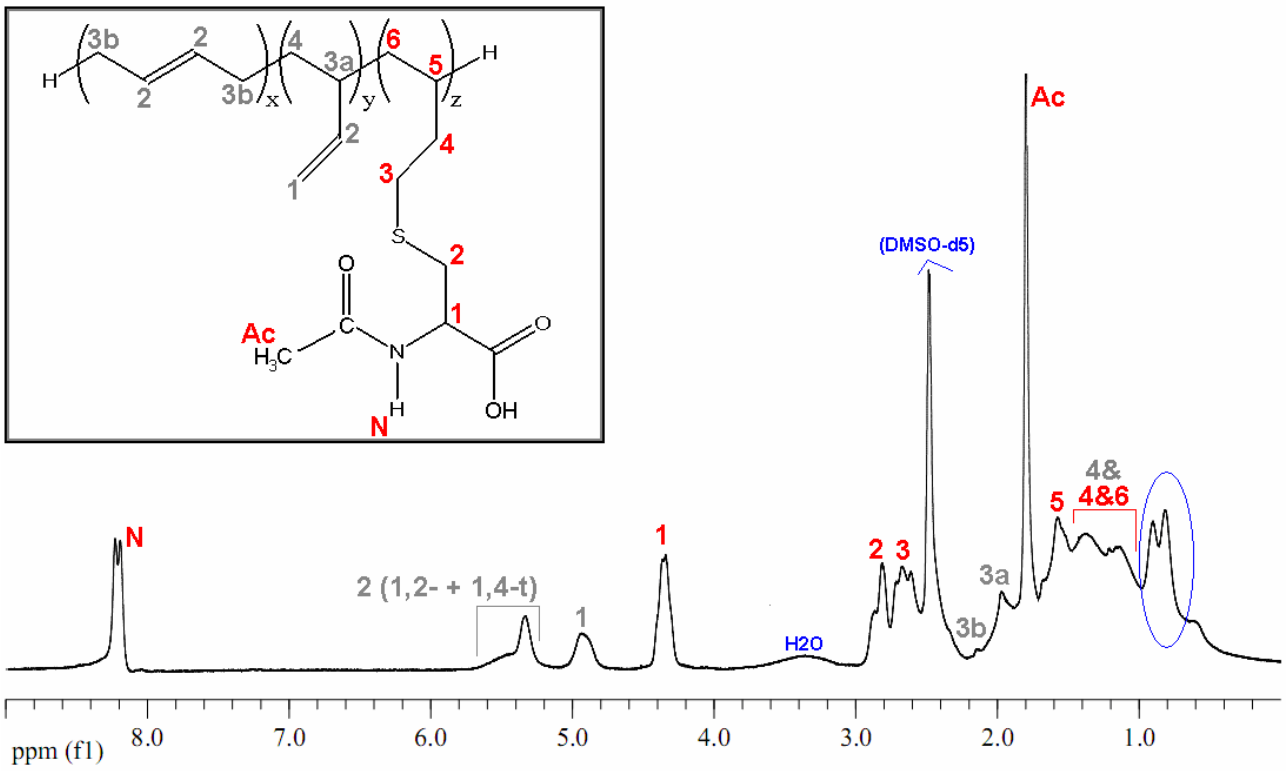

Figure 14 – ^{1}H-NMR spectrum of PBNCys100, DMSO-d_6, 200MHz, r.t., 64 scans. Blue circle: see text

The assignment of the blue-circled resonance signal at 0.9 ppm accounts for protons belonging to methyl groups probably originated by chain-chain coupling (for a possible structure see Scheme 18, page 78). The assignment will be discussed in chapter 2.2.5, page 76.

Boutevin and co-workers determined the DF of HTPBs functionalised with fluorinated thiols via ^{1}H-NMR[70]. A similar method was applied to the considered samples thanks to the presence of signals typical of the grafted units in zones of the spectra free from other non-diagnostic bands. In any case the three different cases, corresponding to the used functionalising molecule (PBNCys, PBNCysMe, PBCysMe), must be distinguished.

For PBNCys samples, the proton NMR spectra showed, in the rather clean region between 4.0 and

4.5 ppm, the signal due to protons bonded to the chiral carbon of grafted NCys units (named 1 in Figure 14). The area of this peak is proportional to the amount of grafted functionalities. The ^{1}H-NMR spectra of some of the PBNCys functionalised samples (collected in DMSO-d_6 at 25°C) are shown in Figure 15; in these spectra, the peak of the proton attached to the chiral carbon of NCys units lies at 4.4 ppm, and it increases in intensity along with the amount of grafted NCys. At the same time, the peak referring to the two vinyl terminal protons of PB (5.0 ppm) becomes smaller, as well as the peak at 5.5 ppm, accounting for the two 1,4- units sp_2 protons and the vinyl β-carbon proton.

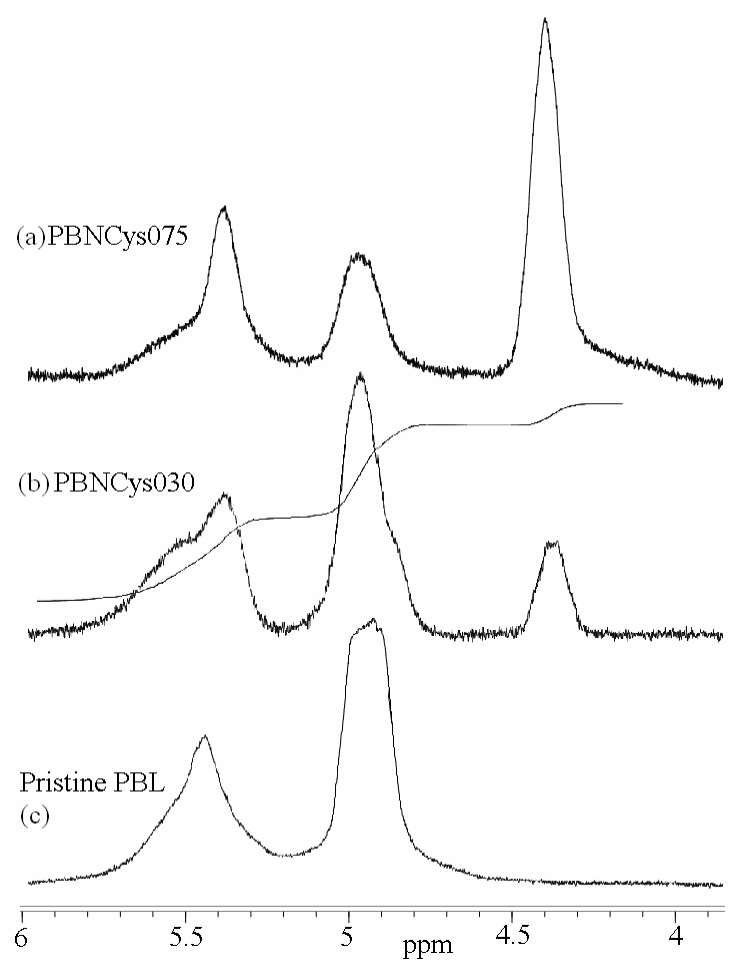

Figure 15 – ^{1}H-NMR spectrum of (a) PBNCys075 (b) PBNCys030 (both 200 MHz, 25°C, DMSO-d_6) (c) Pristine PBL (200 MHz, 25°C, $CDCl_3$)

For the PBNCysMe functionalised samples a similar method was adopted: the amount of grafted NCysMe units was evaluated considering at the same time i) the area of the 3.4 ppm peak, corresponding to the ester hydrogen units –O–C$\underline{H}_3$ and ii) the protons bonded to the chiral carbons that, in this case, overlap the 5.0 signal.

An extract of the proton NMR spectra of PBNCysMe030 is reported in Figure 16; in the spectrum of the sample named PBCysMe100 only the peak assigned to ester protons around 3.6 ppm was

observed (the spectrum is similar to the one reported in Figure 16, except for the double peak around 5.0 ppm, and it will be omitted).

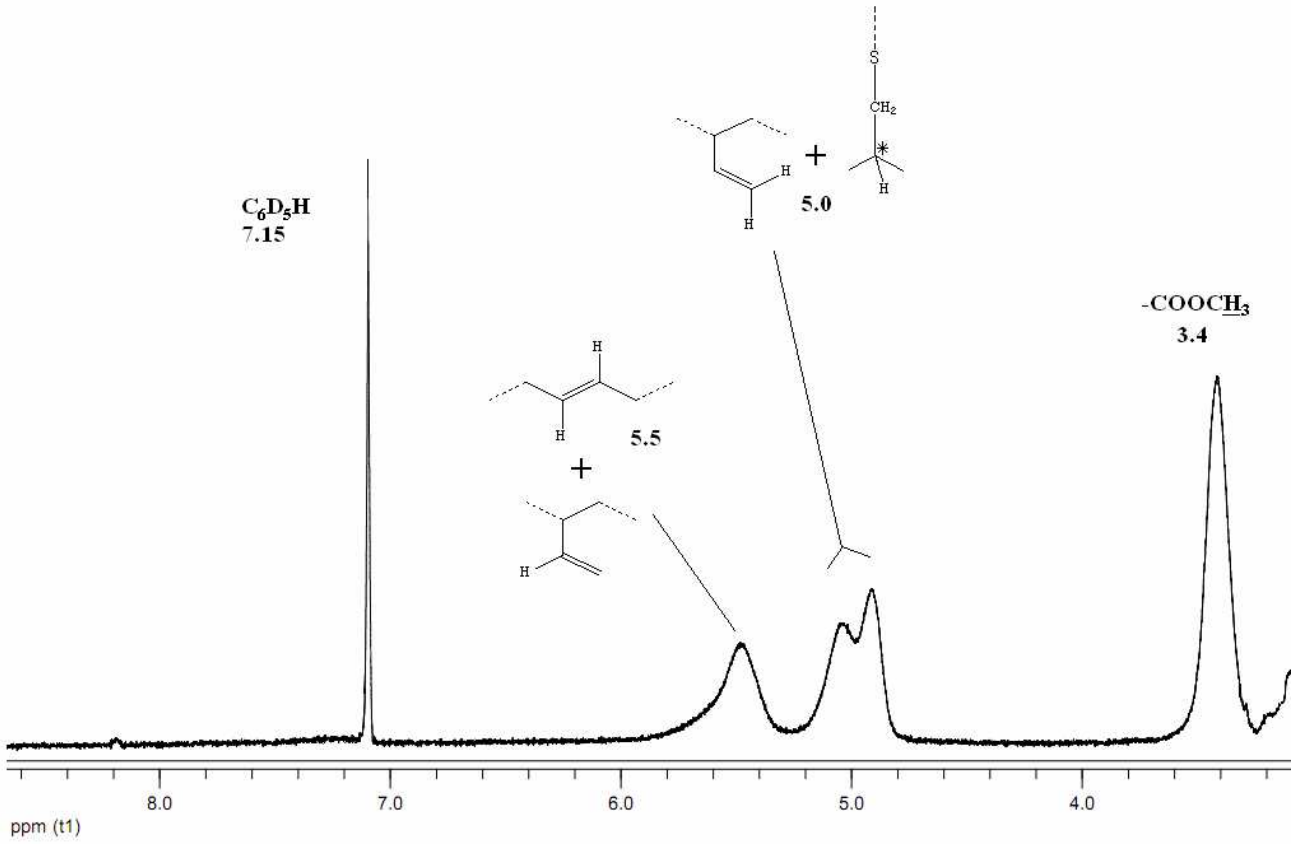

Figure 16 – ^{1}H-NMR spectrum of the PBNCysMe030 sample (200 MHz, 25°C, C_6D_6)

For clarity, the amounts of the different monomeric units in the grafted products can be named as in Figure 17.

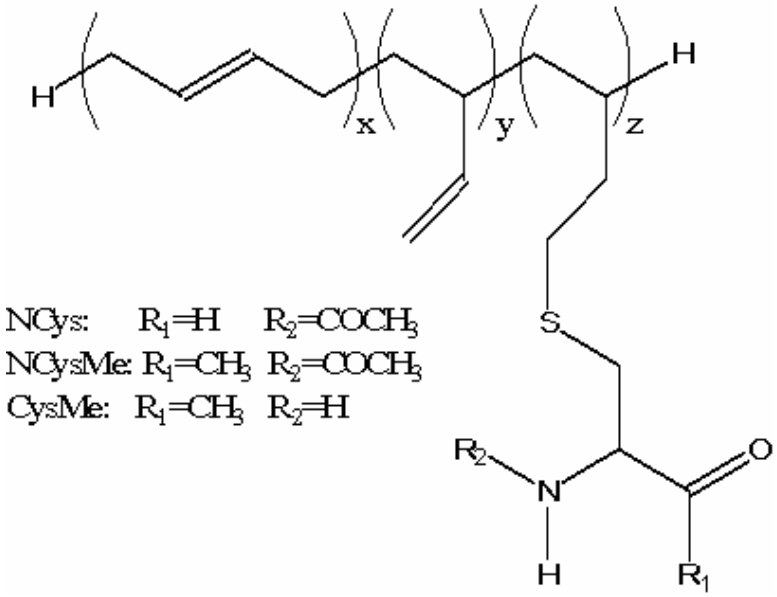

Figure 17 – Possible primary structure of PB + Cys derivatives samples

The *x*, *y* and *z* values were determined with the method suggested by Boutevin and co-workers[70],

in which the amount of the monomeric units of the products were determined through the ratio of NMR peak areas and the total area of the spectrum.

For PBNCys samples, one can say ($A_{x.y}$ is the NMR peak area at x.y ppm):

$$\begin{cases} A_{5.5} = 2x + y \\ A_{5.0} = 2y \\ A_{4.4} = z \end{cases}$$

$$DF = \frac{z}{x + y + z}$$

For the NCysMe functionaliser:

$$\begin{cases} A_{5.5} = 2x + y \\ A_{5.0} = 2y + z \\ A_{3.4} = 3z \end{cases}$$

$$DF = \frac{z}{x + y + z}$$

And for CysMe sample the system is similar to the NCysMe one, with $A_{5.0}$ = 2y (only).

The DF of the products calculated with this method often exceeded 100% both for PBNCys and PBNCysMe samples. This is probably due to an underestimation of the $x + y + z$ amount in the DF expression; a similar underestimation is likely to be caused by side reactions leading to macromolecules having less unsaturations, i.e. with a lesser content in terms of the total amount of double bonds in the products because of side reactions (cyclisation, chain-chain coupling).

A more convenient new method can be formulated considering as unchanged the amount of *x* (1,4- units) throughout the reaction; this approximation works if the thiol-vinyl reaction is considered as favoured with respect to the thiol-1,4-*trans* reaction. This hypothesis, moreover, could be supported by the observation that an analogous cysteine derivative, CysEt, showed a very pronounced preferencial addition behaviour toward terminal model olefins rather than internal ones, as noticed from Passaglia and Donati[54, 112].

By using the peaks referring to the protons of 1,4- units as an internal standard, the amount of vinyl units can be excluded from the DF calculation (*y* is not going to be considered). The method is summarised in the following scheme; for simplicity, the functionalisation degree relative to vinyl units is used (DF_v), $n_{Cys,grafted}$ is the average number of moles of L-cysteine derivative grafted, and $n_{Pol,0}$ is the initial amount of monomer units in the polymer. (The fractions arise from the initial characterization of PBL; *x* is the amount of 1,4- units, *z* is the amount of functionalised units.)

$$n_{Cys,grafted} = z$$

$$n_{Pol,0} \cdot \left(\frac{91}{1000} \right) = x$$

$$DF_v = \frac{n_{Cys,grafted}}{n_{Pol,0} \cdot \left(\frac{909}{1000} \right)} = \frac{z}{x} \cdot \left(\frac{91}{909} \right)$$

$$\triangleright\ NCys : DF_v = \left(\frac{2A_{4.4}}{A_{5.5} - A_{5.0}/2} \right) \cdot \left(\frac{91}{909} \right)$$

$$\triangleright\ NCysMe : DF_v = \left[\frac{2A_{3.4}/3}{A_{5.5} - \left(\frac{A_{5.0} - A_{3.4}/3}{2} \right)} \right] \cdot \left(\frac{91}{909} \right)$$

$$\triangleright\ CysMe : DF_v = \left(\frac{2A_{3.4}/3}{A_{5.5} - A_{5.0}/2} \right) \cdot \left(\frac{91}{909} \right)$$

The results of these calculations were reported in Table 12 (page 64) and Table 13 (page 68).

High values of DF_v were generally observed, with conversion ranging from 15 to 100% depending on feed ratio. These values are similar to those encountered in nearly every work in prior art describing thiol-ene functionalisations of PBLs[25-27, 44, 51, 52, 62, 63, 65, 67, 77, 78, 152, 153]. The comparison of the theoretically achievable DF_v and the measured DF_v is reported, for the three cases (PBNCys, PBNCysMe, PBCysMe), in Figure 18, while the conversion degrees are compared in Figure 19.

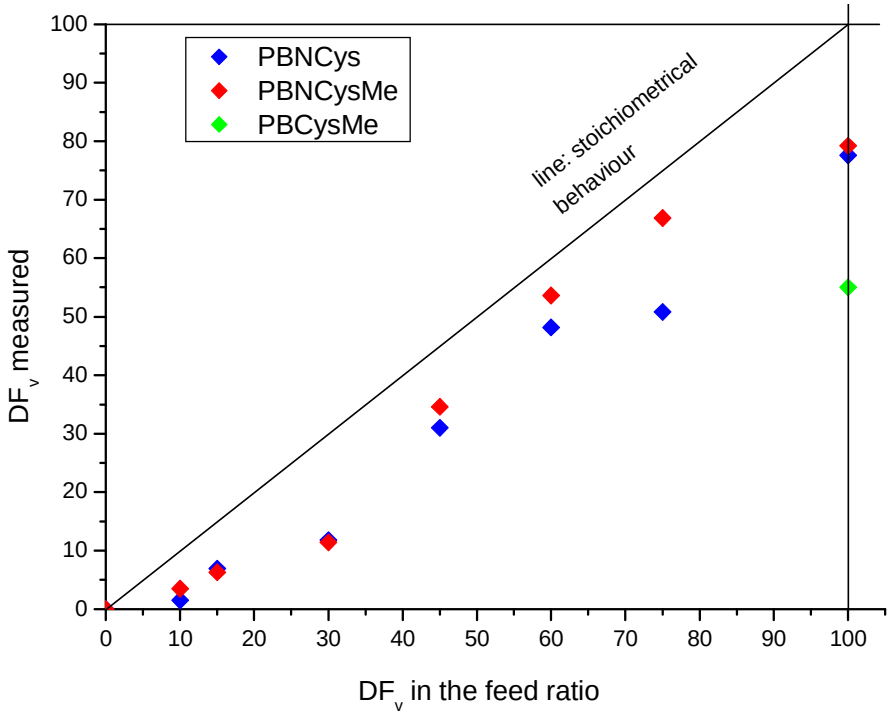

Figure 18 – Measured DF_v *vs* the feed ratio (mol.-%)

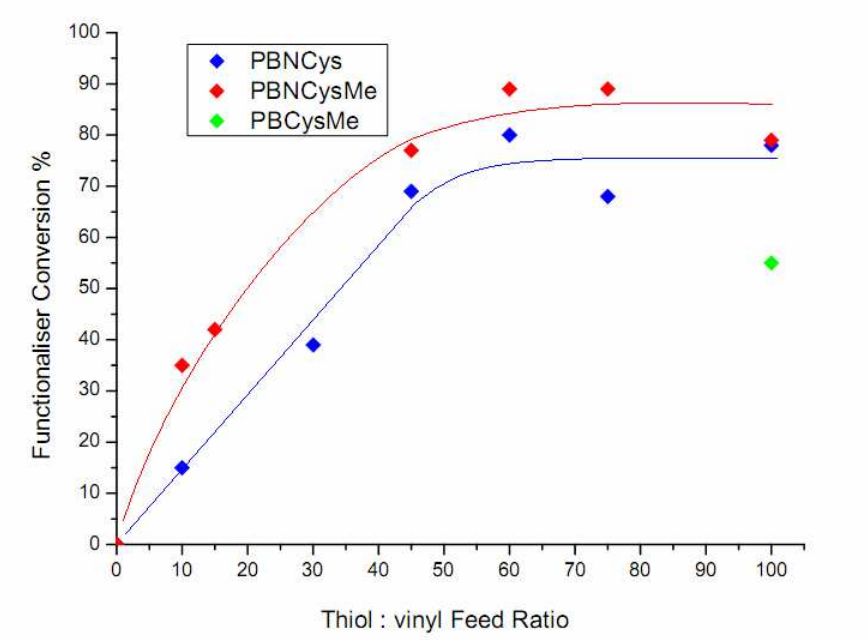

Figure 19 – Conversion (%) *vs* thiol:vinyl feed ratio (mol.-%)

The reactivity of the three cysteine derivatives is similar in terms of overall amount of grafted units; however, the PBNCysMe samples show systematically higher DFs with respect to the ones of the samples functionalised with NCys or CysMe (Figure 18). A similar trend is observed comparing the conversion degrees.

The most remarkable differences between the stoichiometrical behaviour and the experimental values of the conversion degrees (Figure 19) are at low and at high DFs. This difference could account for an influence of the side reactions when using the indicated feed ratios.

2.2.5 Side-reactions: cyclisation and chain-elongation. PBL behaviour in absence of thiol

Using the NMR method for the determination of the primary structure described by Boutevin and co-workers[70] on the samples described in the present work, a lack of vinyl units in the reaction products could be indicated as a possible factor causing an apparent increase of the amount of 1,4-*trans* units (*x*), along with DF_v exceeding 100%. This lack could be due to:

i. the intramolecular cyclisation associated to the presence of a grafted thiol (Scheme 15)
ii. other kinds of intramolecular cyclisation (Scheme 16)
iii. the chain-chain intermolecular coupling associated to the presence of a grafted thiol (Scheme 17)
iv. other types of chain-chain intermolecular coupling (Scheme 18).

The proposed mechanism for reaction i. is reported in Scheme 15, according to Schlaad and co-workers[233]. This reaction regards the formation of 5-membered and 6-membered rings in

presence of a grafted thiol; the starting macroradical is formed by the reaction of a thiyl radical with 1,2- units.

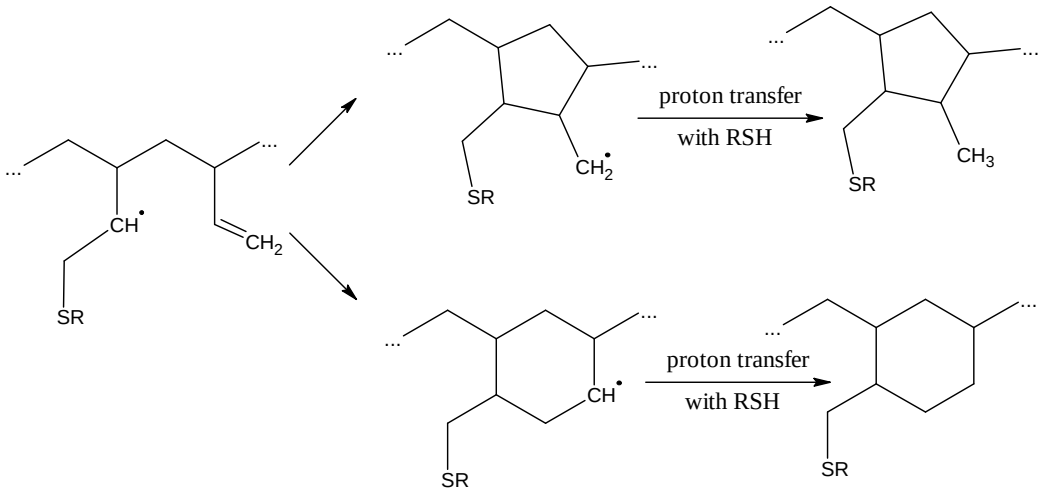

Scheme 15 – Five- and six-member rings formed during thiol-ene reactions[233]

The reaction ii. has been thoroughly investigated by Morton Allan Golub during the '70s[36, 136, 236-242] on polybutadienes treated in various conditions. As well as the intermacromolecular cyclisation due to thiol presence of Scheme 15, the reactions suggested by Golub (in absence of thiols) provide the formation of different cycles; a summary of the various mechanisms is reported in Scheme 16.

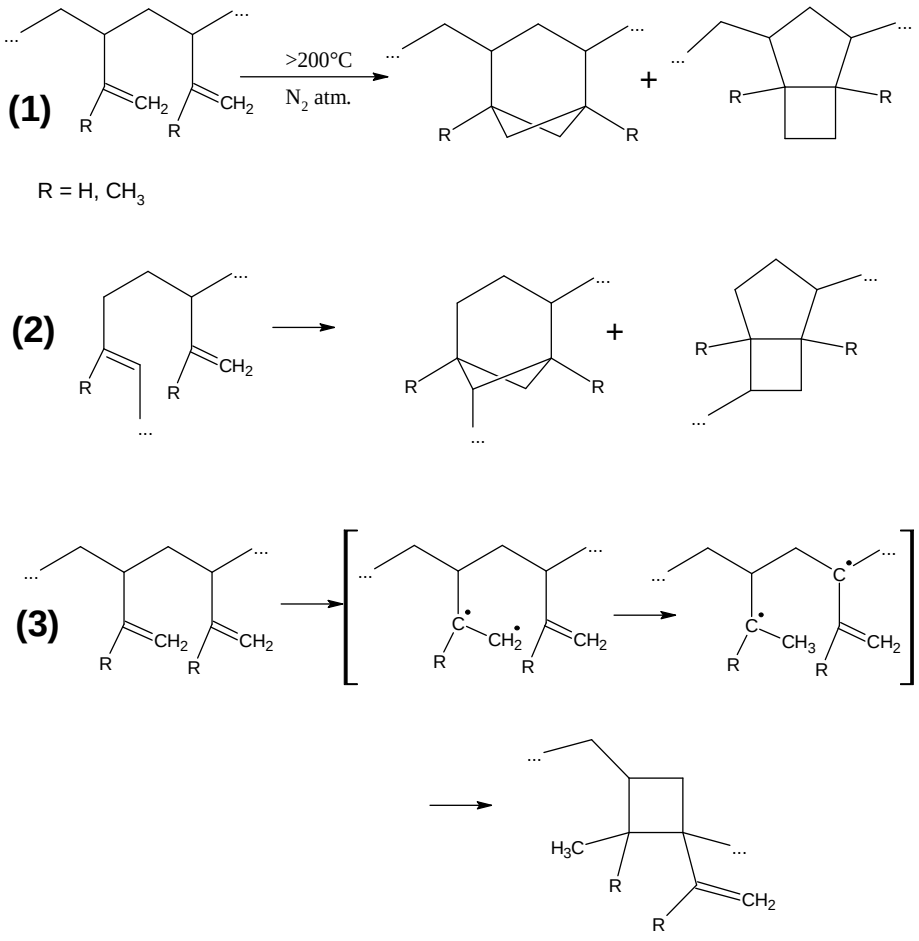

Scheme 16 – Possible cyclisations of PB-1,2 or IR-3,4 occurring under vacuum/N_2 at T>200°C[36, 242, 243]

The mechanism of reaction iii. can be described as in Scheme 17, according to the works of Schlaad and to other papers in prior art (see chapter 1.2.6, page 27).

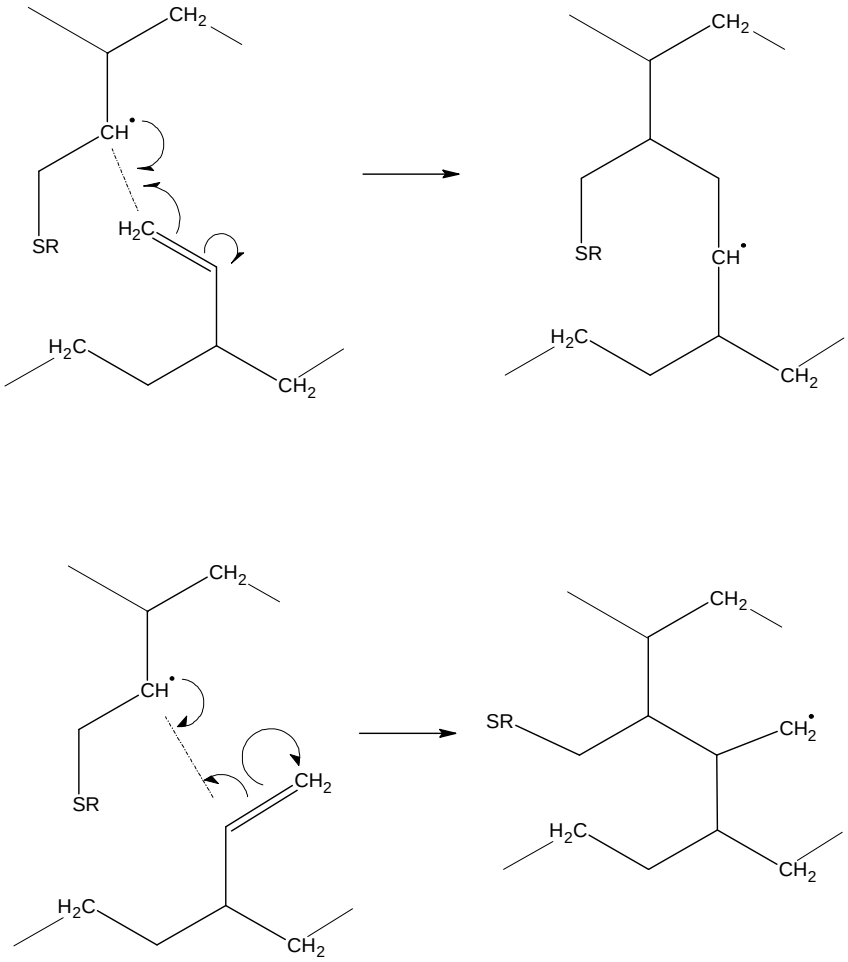

Scheme 17 – Intermacromolecular bridging due to the presence of radicals on alpha-carbon atoms of 1,2- units

The chain-elongation / crosslinking reactions occurring in absence of thiol (reaction iv.) or radical initiators were analysed in many papers; in Scheme 18 the *Grassie and Heaney* molecular rearrangement, initially proposed by the two authors[244] and often cited by Golub, is reported.

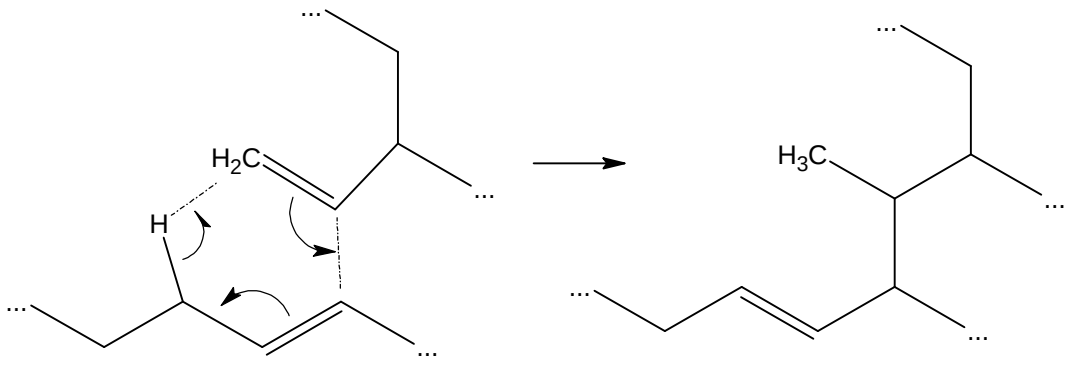

Scheme 18 – The reaction suggested by Grassie and Heaney[244] , indicated by Golub as the main chain-chain coupling event[243]

By considering the occurrence of reactions i. and ii. (cyclisations), the structure of modified polymers of the present work can be described as in Figure 20.

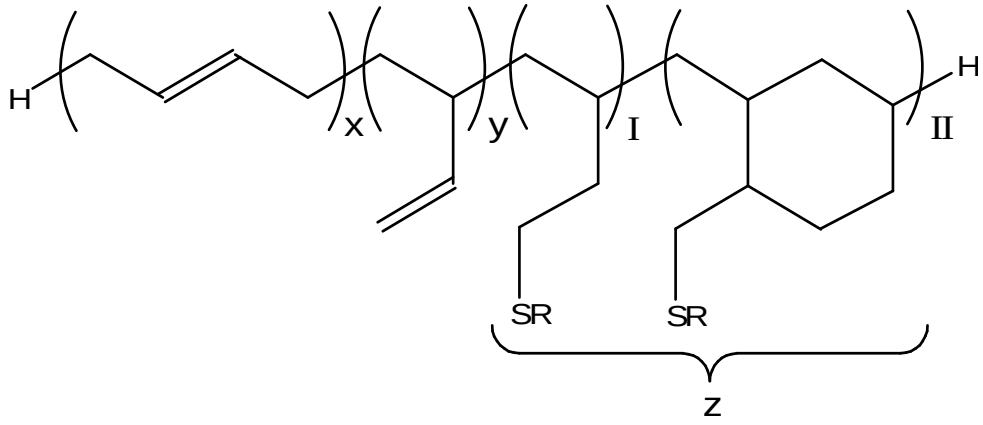

R = thiol main structure apart from -SH group

Figure 20 – Primary structure of a PB functionalised with a thiol, including cyclic units

The existence of units referred as *II* was first supposed by Schlaad and co-workers[82], that observed a remarkable lack of vinyl units (*y*) in reaction products; in the case considered by the authors, the ^{1}H-NMR spectra of the functionalised samples showed no insaturations at all. Other evidences found by Schlaad accounting for the presence of cyclic units were furnished by MALDI-TOF spectrometry; these results are already described in detail in chapter 1.2.6, page 27.

After that, a further confirmation of the presence of cycles was realised in late 2008, when Schlaad and co-workers[233] assigned a peak of the ^{13}C-NMR spectrum of a PB functionalised with methyl 3-mercaptopropanoate to methyl groups bonded to 5-member rings in the main chain (Scheme 15, reaction i.). This 5-membered cyclisation was first suggested in the cited work, though the formation of similar rings in the macromolecular backbone had already been suggested before for PB treated under pyrolitic conditions (reaction ii., Scheme 16).
In the present study, 5- and 6-membered rings were not distinguished among the type-II units (the nomenclature of Figure 20 for I and II unit types has been chosen after the paper of Schlaad and co-workers[82]). In fact, only a few of the ^{13}C-NMR spectra of the PBNCys or PBNCysMe reaction products show a peak at 18 ppm (like the one found by Schlaad[233]) accounting for the formation of 5-membered carbon rings; a qualitative comparison of a ^{13}C-NMR spectrum displaying a peak at 18 ppm from this work and one adapted from ref. [233] is reported in Figure 21.

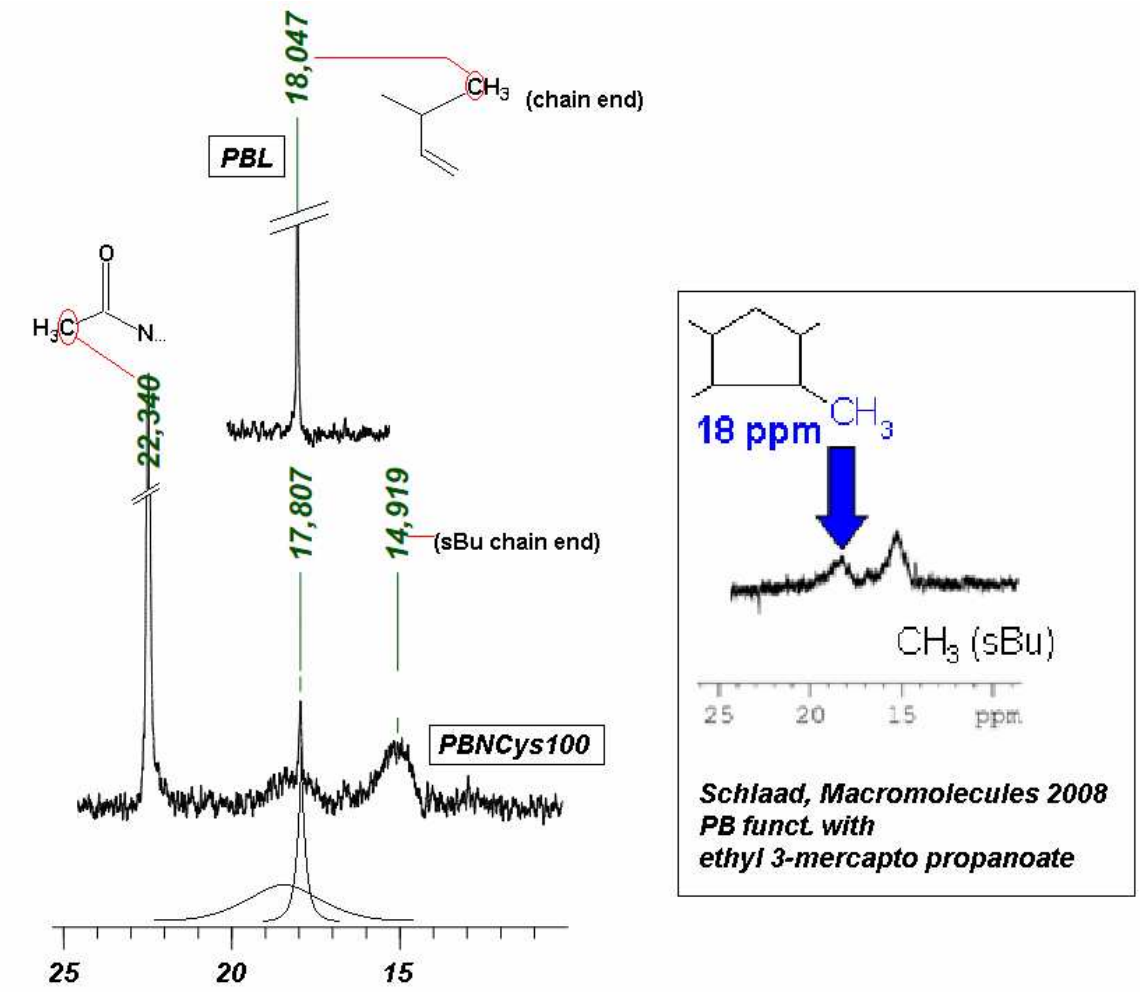

Figure 21 – [10-25] ppm zone of the ^{13}C-NMR spectra of PBL and PBNCys100 (300 MHz, 60°C, DMSO-d_6) On the right: spectrum of PB functionalised with methyl 3-mercapto propanoate (adapted from ref. [233])

The broad peak at ~18 ppm overlaps the narrow peak at 17.8 ppm, accounting for methyl chain-end groups bonded to residual vinyl units; the broad peak at 14.9 ppm accounts for methyl chain-end groups bonded to thiol-functionalised units, according to Schlaad[233].

In any case, the ^{13}C-NMR spectrum of PBNCys100 reported in Figure 21 is an exception: most of the other spectra of the functionalised products do not display a similar peak in the same zone. Moreover, Schlaad himself observes, that the amount of 5-member rings represents only the 10% of the total cyclic units (molar ratio of 5- units versus 6- units: ~1:10[233]). On this basis, the author of the present work decided to refer to type-II units as six-membered rings only.

In the previous section, an easy method to obtain the DFs using 1,4-units as internal standards was suggested. According to the adopted NMR method, by fixing *x* (1,4- units) it is possible to obtain the amount of *lacking units* by difference; in a first instance, these lacking units will be referred as cyclised ones. From the knowledge of *x*, *y* and *z* (*z* = I + II) and:

$$x + y + I + 2II = 100$$

one can obtain the values of I and II for every sample (II = 100 – *x* – *y* – *z*, I = *z* – II). The results are reported in Table 14; the structures to which the symbols refer are described in Figure 20, page 79.

Run	[RSH]:[vinylic C=C]	*x* (fixed)	*y*[a]	*z*	II[b] (cy)	I[c]	I : II ratio
PBNCys100	1.00:1	9.1	10.8	70.5	9.6	60.9	6.3
PBNCys075	0.75:1	9.1	18.9	46.2	25.8	20.4	0.8
PBNCys060	0.60:1	9.1	12.5	43.8	34.6	9.2	0.3
PBNCys045	0.45:1	9.1	16.7	28.2	50.0	?	?
PBNCys030	0.30:1	9.1	23.4	10.7	56.8	?	?
PBNCys015	0.15:1	9.1	19.2	6.3	65.4	?	?
PBNCys010	0.10:1	9.1	24.8	1.4	64.7	?	?
PBNCysMe100	1.00:1	9.1	4.9	72.0	14.0	58.0	4.1
PBNCysMe075	0.75:1	9.1	12.5	60.8	17.6	43.2	2.4
PBNCysMe060	0.60:1	9.1	14.7	48.7	27.5	21.2	0.8
PBNCysMe045	0.45:1	9.1	31.2	31.5	28.2	3.3	0.1
PBNCysMe030	0.30:1	9.1	34.4	10.4	46.1	?	?
PBNCysMe015	0.15:1	9.1	43.2	5.7	42.0	?	?
PBNCysMe10	0.10:1	9.1	43.7	3.2	44.0	?	?
PBCysMe100	1.00:1	9.1	19.1	50.0	21.8	28.2	1.3

Table 14 – *x*,*y*,*z*,I and II values for functionalised PBs. [a] $y = A_{5.0} / 2$; [b] II = 100 – *x* – *y* – *z*; [c] I = *z* - II

A remarkable result arises from the column *II (cy)* of Table 14: the number of *lacking* 1,2- units in some cases is greater than the amount of *z* (overall amount of grafted thiol), and this happens especially when the [RSH]:[polymer] feed ratio is low (samples PBNCys045, 030, 015, 010 and PBNCysMe030, 015, 010). One could expect that: i) another monomer unit, with respect to the description of Figure 20, is present, and it is a cyclic / bicyclic / polycyclic one not involving the molecules of functionaliser, or ii) a chain-elongation reaction occurred, and it involves the 1,2- units. The lack of vinyl, as said, occurs especially when the defect of thiol is pronounced; in these conditions, also the conversion degrees are lower (Figure 19, page 76). These two evidences suggest that, in defect of thiol, the side-reactions are probably competitive with the grafting.

The I:II ratio (amount of non-cyclised units : amount of cyclised units, displayed in the last column of Table 14), has been defined by Schlaad and co-workers, and analysed by the authors in some of their papers regarding the thiol-ene functionalisation[82, 109, 127]. The incidence of the cyclisation is best displayed by a graph reporting the I:II ratio *versus* the thiol/ene feed ratio (Figure 22).

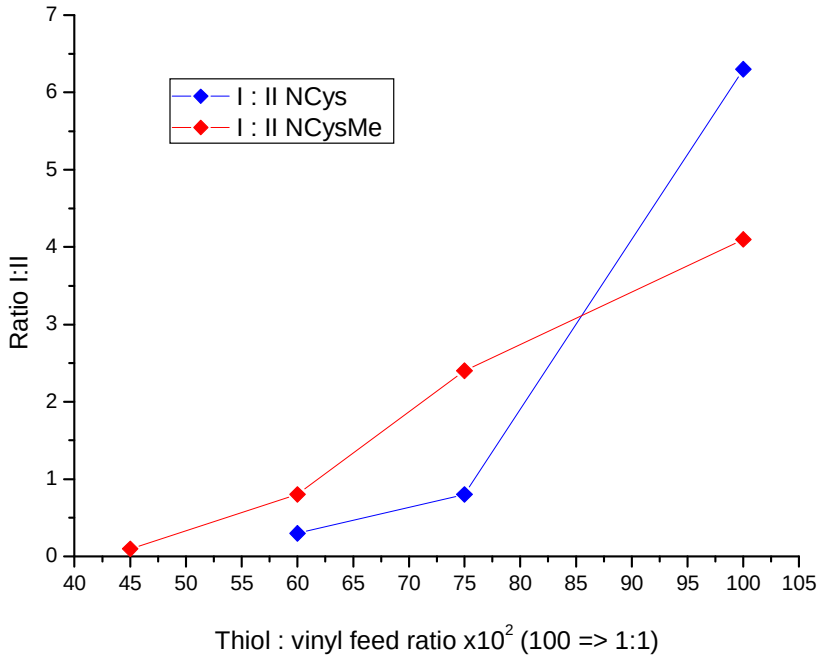

Figure 22 – I:II ratio in NCys and NCysMe samples. For lower DF_v, the ratio should be 0.

The highest values of the I:II ratio were obtained with the highest thiol:ene feed ratios, and they are very close to the values resulting from the papers of Schlaad and co-workers[82, 126]; in any case, the authors carried out runs with a large excess of thiol ([RSH]:[C=C] = 10:1) on PB-*b*-PEO copolymers with different cysteine derivatives, while in the present study the ratios remained under the stoichiometric feed.

It would be desirable to understand if simple cyclic / bicyclic / polycyclic units, not involving the functionalising agents, are present (i.e. reaction ii., Scheme 16, page 77). It would also be desirable to identify the occurrence of chain-elongation, as it is a vinyl-consumpting reaction as well as the cyclisation (reaction iii., Scheme 17, page 78, or reaction iv., Scheme 18).
In the next paragraphs a brief overview of the results of literature works describing reactions ii., iii. and iv. will be given, along with the experimental results regarding reactions carried out in absence of functionalising agents aimed to investigate the behaviour of PB.

In scientific literature several papers were published regarding the possible formation of cycles in PB, treated with heat or treated with radical initiators. The reaction conditions adopted in the present work involve the presence of thiols and a treatment of PB including heat and free radicals in anaerobic conditions; these conditions are not identical to those described in literature especially for the presence of thiols, but, in principle, some features regarding side-reactions could occur both within the reaction conditions of this study and of literature studies.

The first studies on the thermal degradation of rubbers under vacuum or under inert nitrogen atmosphere were performed by Golub and co-workers during the '70s; the authors used IR and NMR characterisation methods to evidence the structural changes in polybutadienes or polyisoprenes, with particular reference to poly-3,4-isoprene[240], poly-1,4-isoprene and poly-1,4-butadiene (where the authors observed, during anaerobic pyrolysis, also *cis-trans* isomerisations[239, 241, 242]), polypentenamers and polyoctenamers[236], poly-1,2-butadiene and poly-3,4-isoprene[36, 242], PBs having different 1,2- *vs* 1,4- content[245].

In all these studies, Golub observed changes in the relative intensities of the peaks of IR and NMR spectra accounting for a consumption of both double bonds in the main chain or double bonds belonging to vinyl units. Accordingly to the author, the observed lack of unsaturations may arise from many cyclisation reactions, along with the already cited 6- and 5-member cyclisations reported in Scheme 15 (in a thiol-free environment, the 6- or 5- member cyclisations are originated by the formation of a macroradical on the alpha-carbon of the 1,2- units). In fact, all the types of PB monomers can be involved in these reaction, and a complete reactive mechanism should include them. For instance, in Scheme 16 (page 77), reaction (1) and (3) may occur in vicinal 1,2- / 1,2- diads, while reaction (2) could occur in a 1,4-*trans* / 1,2- diad.

Golub takes into serious account the experimental conditions under which the vinyl consumption takes place, and in most of his studies this occurs during PB thermal anaerobic degradation. He also tries to obtain *ladder* polyisoprenes having polycyclic units, synthesised through cationic cyclisation induced by $TiCl_4$[240]; in this specific case, the spectroscopic characterisation of the reaction products highlighted the presence of six-membered non-polyciclic units.

Interestingly, Golub notices twice[36, 236] that all his efforts of generating a ladder polymer starting from PB by free radical initiation have been without success; a *ladder polybutadiene* has never been synthesised in presence of free radicals.

In order to understand if it was possible to obtain a PB having cyclic or poly-cyclic structures in the experimental conditions adopted for the thiol-ene functionalisation runs, a run named *PBwoRSH* was performed in absence of thiol and in presence of bare AIBN. The amount of AIBN was 1 mol.-% with respect to vinyl double bonds (the same of PBNCys100); the reaction product was dried and re-dissolved in n-hexane, and later purified by chromatography on a silica column with n-hexane as the mobile phase. This operation is necessary to remove unreacted AIBN. The purified polymer was characterised through SEC, NMR and IR spectroscopy.

The proton NMR spectrum of PBwoRSH did not show any substantial variation with respect to that of the pristine polymer: after normalisation to the 5.0 peak of the 1,2- double bonds, the area of other peaks (for instance the peak at 5.5 ppm accounting for the alpha carbon proton on 1,2-

unit plus two 1,4-*trans* protons, or the entire integral of the sp_3 protons zone at high field) is in the range of ± 0.7% with respect to the corresponding area of the spectrum of the pristine PB. Also the ^{13}C-NMR and the infrared spectra of the pristine PB and of the PBwoRSH sample are undistinguishable; from these IR and NMR data it is not possible to identify the presence of cyclic units or other differences in the primary structure.
The SEC chromatogram showed only a weak increase of the molecular weights; while pristine PBL showed a $<M_n>$ ($<M_w>$) value of 4080 (5850) Da, PBwoRSH showed a value of 4440 (6130) Da. This increment could account for minor chain elongation events that went undetected by means of NMR or IR spectroscopy.
These results comply with those found out by Golub regarding PB treated with AIBN.

An increase of the amount of methyl groups, observed in the NMR and in the IR spectra of the degradation products of PB and IR (obtained in *absence* of AIBN), led Golub to speculations about chain-elongation reactions. The author, citing a coupling reaction whose existance was suggested by Grassie and Heaney[244] (Scheme 18, page 78), inferred that this reaction could account for i. the lack of vinyl units ii. the formation of methyl groups observed in the reaction products and iii. for the extense crosslinking of the pyrolysis products.
This hypothesis was renewed only after three decades: in 2008, Farshid Ziaee and co-workers have investigated the behaviour of PBL heated under vacuum by ^{1}H-, ^{13}C-NMR and related 2D NMR techniques[232], analogously at what Golub did but with more powerful instruments and techniques.
As well as in the previous degradation studies by Golub, Ziaee and co-workers found signals suggesting the occurrence of a variation in the primary structure of the polymer; in particular, the author found an increase of the methyl groups amount and a reduction of the amount of vinyl units. Ziaee related this experimental evidence to the intermacromolecular rearrangement of Grassie and Heaney (Scheme 18, page 78). Moreover, thanks to the improved NMR techniques, Ziaee managed to ascribe the reaction events to 1,2- syndiotactic triads *rr*, that could be randomly found also in an atactic 1,2-PB, as shown by the detailed characterisation of the tacticity; the other macromolecule involved in the reaction could react with the 1,2- syndiotactic system with an allylic proton preferably from a 1,4-*trans* unit (Scheme 19). The cyclisation reactions of the pure PB (Scheme 15, where –SR is substituted with –H; and Scheme 16) are defined by the author as possible, but, still, no final evidences of similar structural units were collected even with HMQC or DEPT 2-D techniques.

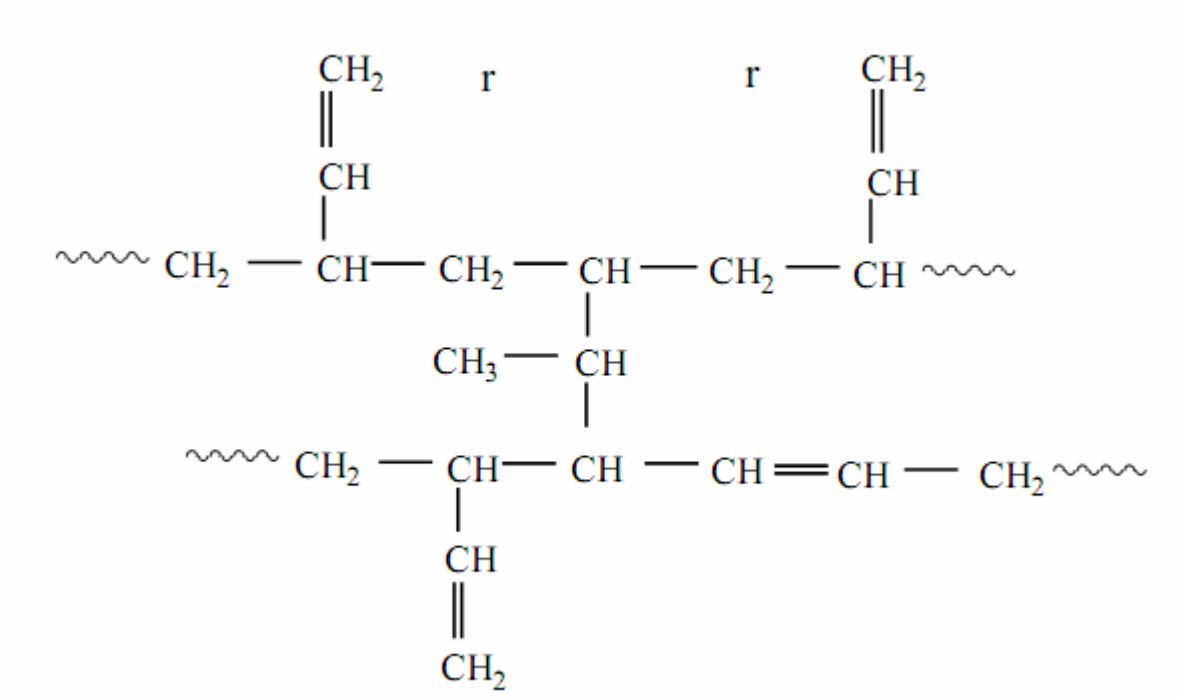

Scheme 19 – Reaction product of the Grassie and Heaney rearrangement ascribed to *rr* triads + allylic protons

In the proton NMR spectrum of PBNCys100, reported in Figure 14 (page 71), the blue-circled doublet at δ= 1.0-0.8 ppm has been observed also in other thiol-ene functionalised polymers, but it has not yet been assigned to structural units in functionalised PBL (see, for instance, ref. [233]). This doublet is not present in pristine PB (Figure 10, page 62). The use of a powerful NMR instrument allowed the assignment of this peak system to methyl groups arising from the Grassie and Heaney intermacromolecular rearrangement described in Scheme 18. Although the study of Ziaee is focused on the radical reactions occurring during pyrolitic treatment of PBL (and not during a thiol-ene functionalisation), the author used a substrate very similar to that of the present work; the blue circled doublet observed in the PBNCys100 spectrum could therefore be attributed to the presence of methyl groups associated to the 5-member cyclisation of Scheme 15 (reaction i.) or to the chain elongation of Grassie and Heaney reported in Scheme 18 (reaction iii.).

In order to further analyse vinyl-compsunting side reactions, another reaction in absence of thiol was performed. In this case, a peroxide (dicumylperoxide, DCP) generating free radicals that were proven to have the possibility to radically add to double bonds was added to PBL.

The reaction of diene rubbers with peroxides, such as DCP, has been well investigated, and it is established that the crosslinking is achieved by both the two mechanisms reported in Scheme 20: i. allylic hydrogen abstraction followed by combination of polymer radicals (as seen also on model compounds[246, 247]) or ii. addition of a peroxide radical to a double bond followed by the further

addition of the macroradical to a double bond in a nearby chain[248, 249]. The relative occurrence of the two mechanisms is dependent on the peroxide concentration and on the reaction temperature, as shown by Gonzalez and co-workers[249]. Moreover, DCP has been reported to add with an anti-markovnikov mechanism to vinyl double bonds of polybutadiene, as well as a thiol; the creation of a radical on the alpha carbon of vinyl units could lead, as said, to peculiar reaction paths typical of thiol-ene functionalisation.

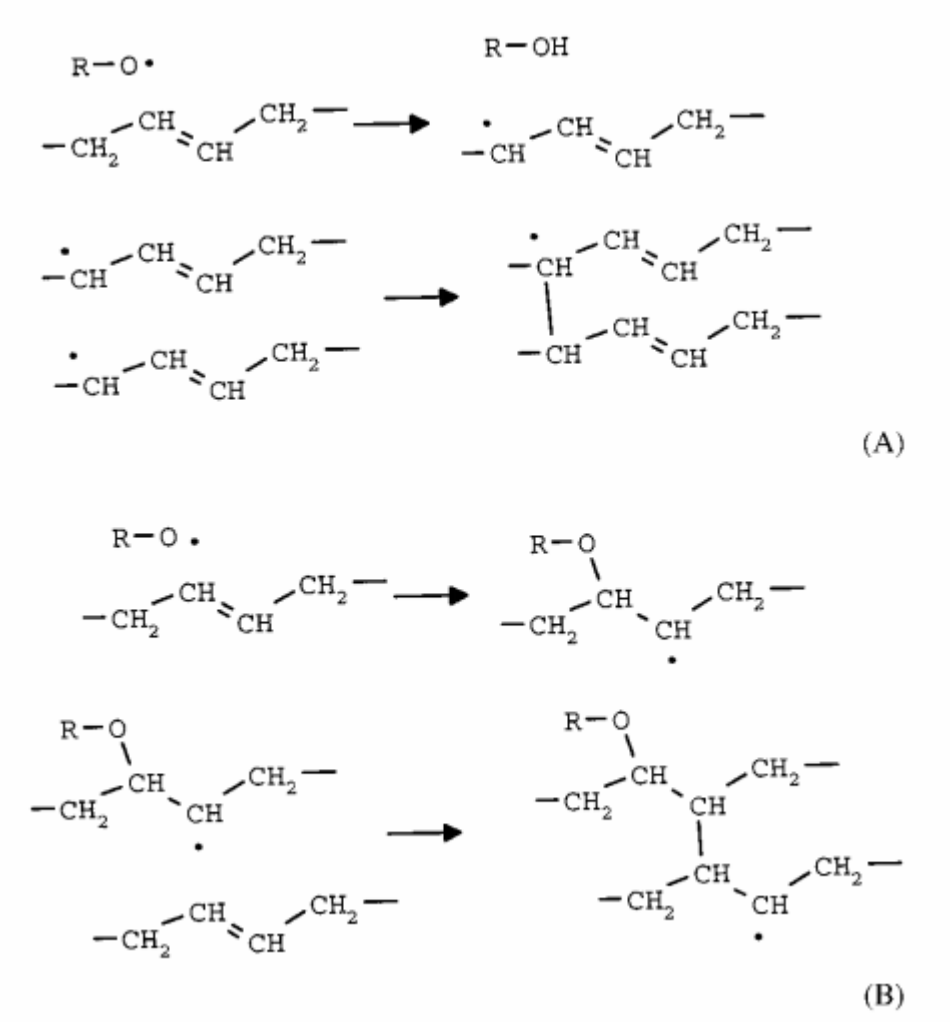

Scheme 20 – Crosslinking of PB-*cis* induced by (A) the allylic proton abstraction (B) the attack of peroxide radical onto a C = C double bond. R = 2-phenylprop-2-yl; adapted from ref.[248]

An interesting data arising from DCP vulcanisation of polybutadienic rubbers is the elevated *crosslinking efficiency*, a value defined as the ratio between the molar amount of crosslinked polymer and the molar amount of primary radicals. 1 mole of peroxide radicals often generates more than 1 mole of crosslinked macromolecules: Loan[250] reported that a 1,4-*cis* PB treated with 1 mol.-% DCP lost more than 30 mol.-% of its main chain unsaturations. In a similar study on a PB 1,4-*cis*, Van der Hoff[251] found an unsaturation loss of 25% using 0.5 mol.-% of DCP.

A reaction between PBL and DCP was performed (named *PBDCP*). With an amount of DCP of 5

mol.-% (~ 22.5 phr, *parts per hundred of rubber* = wt.-%) with respect to vinyl double bonds; by assuming a complete grafting of DCP to the polymer and a complete conversion of DCP to cumyl radicals (reaction completion time was estimated to be ten times the $\tau_{1/2}$ of DCP), one could expect a theoretical maximum functionalisation degree of 10 mol.-%. In any case, the purpose of this reaction was to investigate the PBL behaviour in presence of a concentration of free radicals adding to double bonds similar to that typically encountered in a thiol-ene functionalisation.

According to existing literature, the main reaction byproducts of the free radical reactions initiated by DCP are 2-phenylpropan-2-ol and acetophenone. The alcohol is the product of allylic hydrogen abstraction from the macromolecule, while the acetophenone has its origin in the self-decomposition of the cumyl radical (Scheme 21). The resulting methyl radical is known to be scarcely reactive towards hydrogens belonging to macromolecules; it would rather attack C=C double bonds of the diene rubber generating other adducts[252].

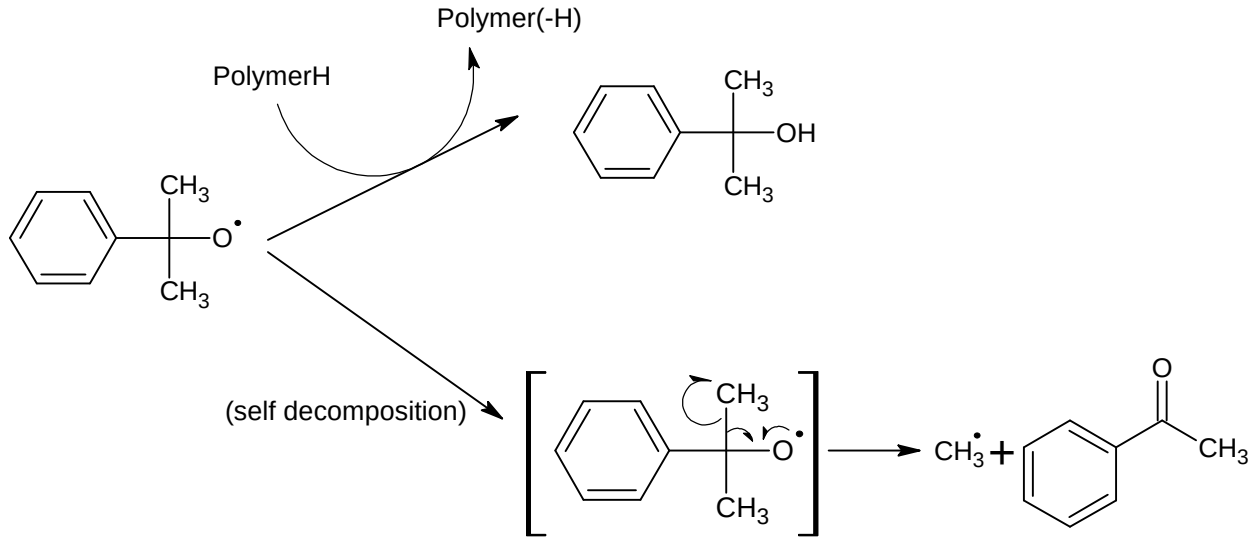

Scheme 21 – Reactions of the 2-phenylprop-2-yl radical, according to literature[246, 247]

The reaction products were fractionated, and the presence of 2-phenylpropan-2-ol and acetophenone was confirmed by FT-IR spectroscopy. The NMR spectrum of the addition products after purification is reported in Figure 23; the chemical shift of the peaks, assigned with respect to the solvent impurities (at 7.26 ppm), are attributed according to existing literature. The peak assigned to methyl protons associated to the presence of *f* units (adducts cumyl radical – vinyl units) was attributed according to a similar compound, the 2-phenylprop-2-yl ethyl ether[§].

[§] Source for the ^{1}H-NMR spectrum of 2-phenylprop-2-yl ethyl ether: Aldrich Library of NMR spectra, vol. 2

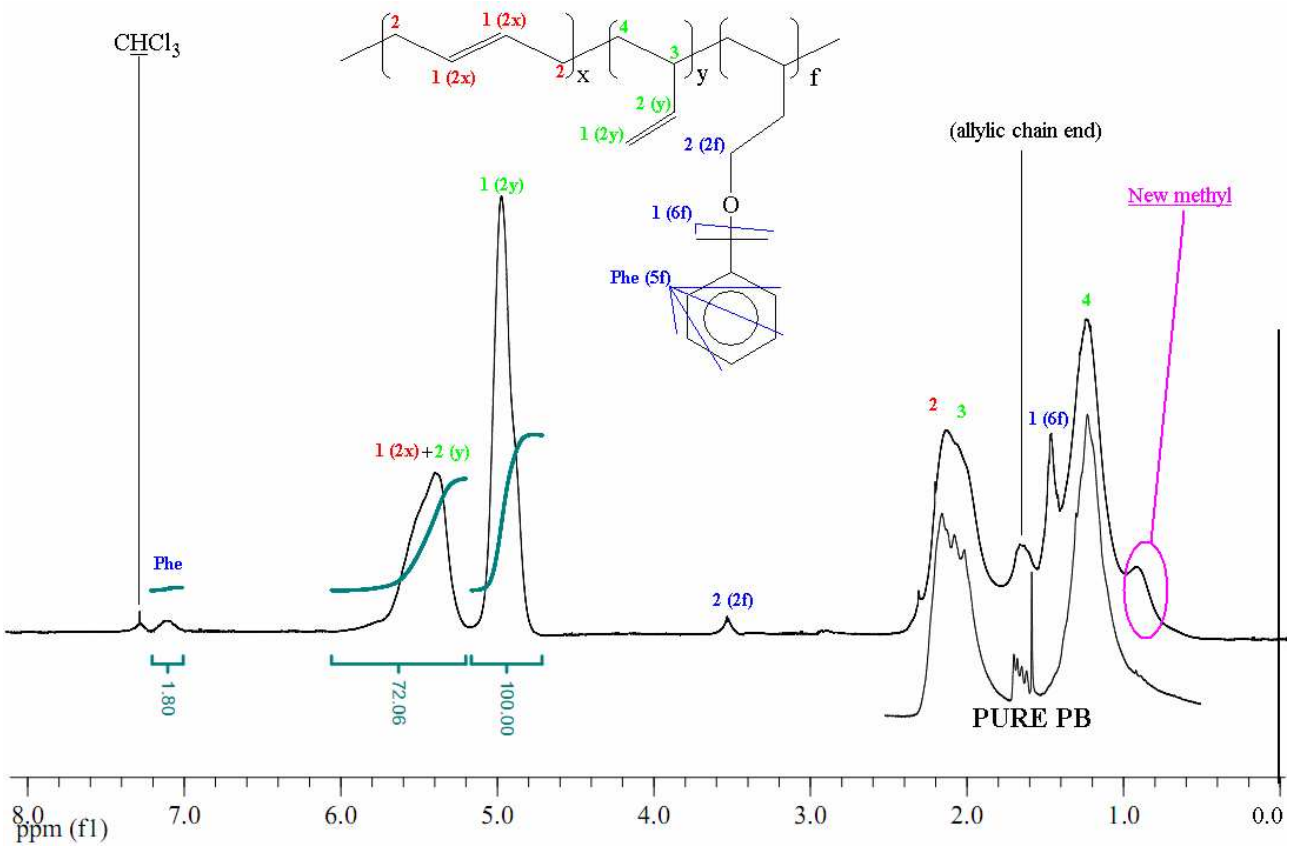

Figure 23 – Proton NMR spectrum of PBDCP. In pink: new methyl groups

The area of the peak associated to phenyl protons was used to determine the functionalisation degree. If the value *x* is fixed at 9.1 mol.-% the absolute DF is calculated as 0.4%, and could be considered as negligible.

In Figure 23, the peak at 0.9 ppm due to new methyl groups was circled in pink; this peak, already found in functionalised samples (see the blue circle in the PBNCys100 NMR spectrum, Figure 14, page 71), could account for events of chain-chain coupling (reactions iii. and iv., previous pages). Unfortunately, methyl radicals arising from the self-decomposition of the cumyl radical (Scheme 21) could as well attack the double bonds generating methyl chain-ends; this is a limit in reproducing the thiol-ene conditions due to the nature of the employed peroxide.

From the area of the 5.5 peak and from the area of the 5.0 peak, the relative amount of *x* versus *y* could be measured; as said, the amount *f* of grafted cumyl groups will be considered as negligible. The estimated *x* / *y* ratio is 0.22; according to literature on DCP crosslinking of diene rubbers[250, 251], the 1,2- units react quickly than 1,4- ones, and, by supposing unchanged the 1,4- units amount, the PBDCP composition should be 9.1% 1,4- (*y*) and 41.4% 1,2- (*x*); the calculated amount of lacking units (including functionalised ones) is 49.5%. This fraction is very high, but it is comparable to the data obtained for thiol-ene functionalised samples (see Table 14, page 81): in particular, the samples functionalised with the lowest thiol:ene feed ratio showed similar values

(e.g. the lack of units of PBNCysMe010 was 44%).

The SEC measurements confirmed the occurrence of chain-elongation events. While the pristine PBL sample showed a $<M_n>$ ($<M_w>$) value of 4080 (5850) Da, PBDCP showed a value of 4820 (8300) Da. This result, together with the increase of the polydispersity index (PDI, defined as the $<M_w>/<M_n>$ ratio) from 1.43 to 1.72, with the pronounced lacking of C=C double bonds and with the presence of new methyl groups, confirms the side reactions like cyclisation and chain elongation as seriously affecting the PB functionalisation when the formation of radicals onto the alpha carbons of vinyl units is involved.

2.2.6 Functionalisation runs carried out in absence of AIBN

Two functionalisation runs, one using NCys and the other using NCysMe, were carried out in absence of radical initiator; the chosen thiol / vinyl ratio has been 0.30. Priola and co-workers[57], as well as a lot of earlier studies about thiol-ene reactions in absence of an initiator (see for instance: Cunneen[40] on natural rubber substrates, Serniuk[48] on NR, SBR and long-chain PB), showed that the decomposition of the –SH group can start the cyclic thiol-ene reaction, and functionalisation was observed even if the DFs were much lower than in presence of a free radical generator.

The characterisation data of these two experiments are summarised in Table 15.

Run	[thiol]:[vinyl]	Achiev. DF_v %	DF_v %	(DF_v with 1% AIBN)$^{\varsigma}$	Conv. %
PBNCys030woAIBN	0.30:1	30	10.4	(11.8)	35
PBNCysMe030woAIBN	0.30:1	30	8.0	(11.4)	27

Table 15 – Experiments carried out in absence of AIBN: PBNCys and PBNCysMe. $^{\varsigma}$: see Table 13

The proton NMR characterisation of the purified reaction products showed functionalisation degrees, together with a lack of vinyl groups, near to the values determined for the runs carried out in presence of AIBN. With NCys, the amount of II (see Figure 20, page 79) is 50.4, so it is much more than the amount of functionalised units; with NCysMe, the amount of II is 36.5, and again it is larger than the number of grafted units.This behaviour is similar regardless of the AIBN presence.

The glass transition temperature of the samples will be analysed in detail in chapter 2.2.8 (page 93) and compared to the data arising from the samples synthesised in presence of AIBN.

2.2.7 SEC analysis of N-acetyl-L-cysteine methyl ester samples

The introduction of large amounts of L-cysteine units on the macromolecular backbone puts limits to the evaluation of the SEC data. With this characterisation method, polymer particles are separated based on their hydrodynamic volume, which depends on many factors such as the interaction with solvent or the molecular rigidity. The introduction of different groups along the backbone increases the molecular weight of the macromolecule, but it does not necessarily increase the hydrodynamic volume of the macromolecule in solution because of the heterogeneity of the introduced structure with respect to the original macromolecule; in particular, in this study hydrophilic units are introduced on highly hydrophobic macromolecular chains. This applies both when considering copolymers or heavily-functionalised homopolymers; as said before, the structure of an unsaturated rubber functionalised to a high extent is close to that of a copolymer.
During the '80s many methods based on the use of multiple detectors and sets of standards were elaborated[253-255] for an accurate determination of the molecular weights of copolymers. Typically, a combination of UV and RI detection is used, but other detector combinations have also been employed. However, all the multiple detector methods work well only on high MW copolymers especially because of the relative importance of different chain ends; these methods are not suitable for short-chain samples like those treated in the present work. Moreover, the peaks of the UV spectrum of the functionalised PBNCys and PBNCysMe samples could be related only to the absorbance of double bonds as the only detectable UV band for the considered samples is related to electronic transitions of these unsaturated systems; as said, it is not possible to put the double bond amount in direct relationship with the DF, and double-detector methods are based on two measurement systems one giving hydrodynamic volume and the other giving chain composition.

It has not been possible to obtain chromatograms of the PBNCys samples, since the refractive index peak on the chromatogram always overlapped the solvent one. One pure solvent and three eluting mixes were tried without observing appreciable differences: THF alone and THF / MeOH mixes 95/5, 90/10, 80/20. An analogous phenomenon was observed also by Priola[31] on samples obtained grafting TGA on liquid PB; the author related this phenomenon to the possibility of a strong self-association of PBNCys macromolecules in solution induced by the presence of carboxylic groups, regardless of the solvent. In the present work, instead, this peak superposition is not observed in the case of PBNCysMe samples.
Two sets of standards were used in order to create calibration lines: a set of polystyrene (PS) standards and a set of polymethylmethacrylate (PMMA) standards both having PDI ~ 1.

By considering no variations of the average degree of polymerisation $<DP_n>$ before and after the thiol grafting, the molecular weight of functionalised macromolecules would grow linearly with the DF; by no means, though, the hydrodynamic volume of the considered macromolecules could be supposed to display a similar direct proportionality with the DF.

In Table 16 the calculated $<M_n>$, the $<M_w>$ and the PDI of the PBNCysMe samples are compared to the measured values given by the standard calibration curve SEC method. These data can be compared to the results published in scientific literature regarding the copolymers of butadiene and an ester comonomer (for instance: polybutadiene-co-methylmethacrylate).

By examining the data of Table 16, one could distinguish between two ranges, one for samples having DF $\leq$ 10.4% and one for samples showing higher DFs.

For samples showing DF $\leq$ 10.4%, there is a good agreement between the calculated and the measured values of $<M_n>$ especially using the PMMA set of standard samples for the calibration curve. Another experimental evidence is that the M_w of these samples (evaluated with the PMMA calibration curve) is higher than the calculated value. Moreover, the PDI does not suffer great increments (from 1.44 of the pristine PBL to 1.72 of PBNCysMe010); this observation complies with an hypothesis of scarce occurrence of the chain-chain coupling reaction of Scheme 5 or Scheme 18, as it would have increased the average molecular weights along with PDIs.

Samples having higher DFs show all constant elution times. This resembles the case described earlier: two copolymer molecules having different MW and different composition but having the same hydrodynamic volume could be eluted at the same time. In the PBNCysMe samples, the number of ester groups increases with the DF, and this has two consequences: the MW increases (for the incorporation of the thiol) and, with it, the hydrophilicity of the chains. Perhaps this is enough to make the polymers having a low DF (anyway more than 31.5%) elute at the same time of polymers having a higher DF; unfortunately, this does not help in determining the PDI and the possible occurrence of the chain-elongation reaction within this DF range.

Run	DF%	Weighted MW of the rep. unit (Da)[a]	M_n (M_w), calcd.[b]	M_n (M_w) , Da PS calibration	M_n (M_w) , Da PMMA calibration	PDI[c]	
						PS calib	PMMA
PBNCysMe100	72.0	181.68	13710 (19630)	6240 (9240)	5920 (8280)	1.48	1.40
PBNCysMe075	60.8	161.86	12220 (17490)	5690 (7660)	6140 (7970)	1.35	1.30
PBNCysMe060	48.7	140.44	10600 (15180)	5410 (7620)	6030 (8060)	1.41	1.34
PBNCysMe045	31.5	109.83	8290 (11870)	5680 (7880)	6220 (8070)	1.39	1.30
PBNCysMe030	10.4	72.45	5470 (7830)	4890 (7400)	5230 (8120)	1.51	1.55
PBNCysMe015	5.7	64.24	4850 (6940)	4610 (7530)	4940 (8150)	1.63	1.65
PBNCysMe010	3.2	59.73	4510 (6450)	4340 (8330)	4890 (8420)	1.92	1.72
PBwoRSH	-	54.09	-	4440 (6130)	4510 (6280)	1.38	1.39
PB	-	54.09	-	4080 (5850)	4100 (5910)	1.43	1.44

Table 16 – SEC measurements on PBNCysMe samples, and estimate of the molecular weights

[a] $\langle DP_n \rangle$ = 75.4 repeating units (calculated on theMW of the pristine polymer), weight of functionalised unit: 231.31 Da, weight of unfunctionalised unit: 54.09 Da

[b] $\langle M_j \rangle = \langle DP_j \rangle \cdot$ MW repetitive unit; j = n, w

[c] the PDI of the calculated M_n (M_w) remains 1.43 as the $\langle DP_j \rangle$ is supposed unchanged in the pristine PBL or after the grafting

The previously cited case of the PBNCysMe runs carried out with various amounts of AIBN (Table 12, chapter 2.2.1, page 62) is noteworthy: when the AIBN:ene ratio is higher than 1 mol.-%, a PDI increase in the reaction products is observed, and this could be due to the chain-chain coupling reaction (when AIBN concentration is 1 mol.-% this increase is not observed). The amount of grafted units in the polymers cited in Table 12 is similar to that of the samples of Table 16; in conclusion, the occurrence of the chain elongation reaction is negligible for the later samples. This complies with the previous determination of lacking units (chapter 2.2.5, page 76): on highly functionalised samples the amount of lacking units was very small, if even present.

2.2.8 Calorimetric measurements of the glass transition temperature

The glass transition temperature (T_g) of the functionalised products was determined by DSC, analogously to what reported in prior art for similar polymeric substrates (thiol-ene functionalised hydroxyl telechelic polybutadienes HTPBs[34, 68], functionalised carboxy telechelic polybutadienes[35], and polyurethanes synthesised starting from thiol-ene functionalised HTPBs[83, 84, 256]). The starting T_g of the PBL used in this thesis work is -26.6 °C; the T_g of every functionalised sample, though, is much higher even at low DFs. A graph of T_g *versus* DF_v is reported in Figure 24, and it shows a remarkable increase of T_g values with increasing DF, up to 30-40%; the behaviour is similar for both systems (PBNCys and PBNCysMe).

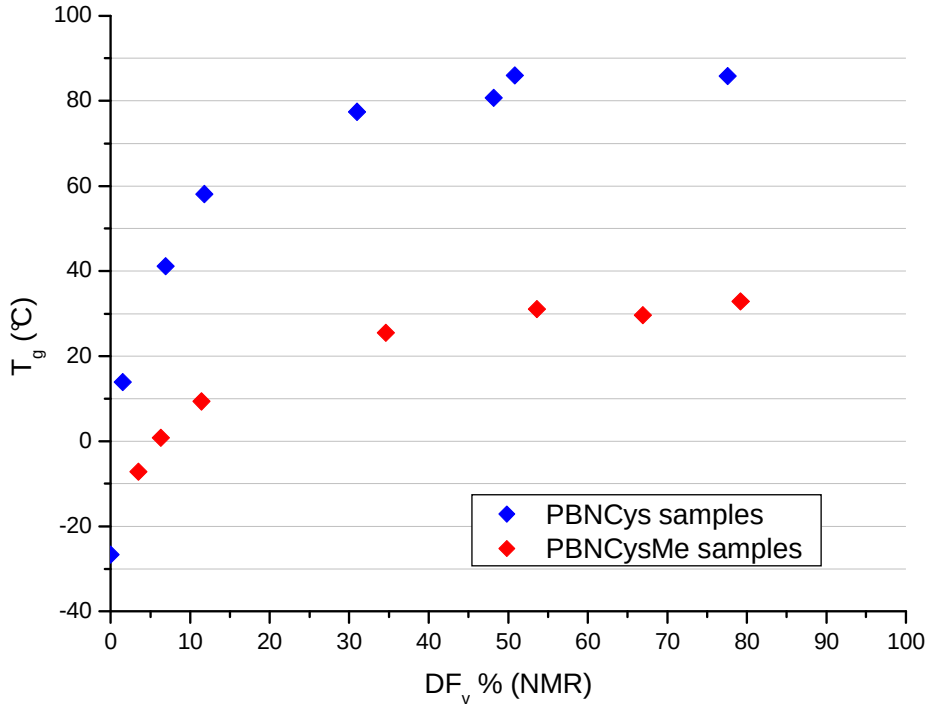

Figure 24 – T_g *versus* DF_v for PBNCys and PBNCysMe samples. DSC measurements, 10 °C/min

As an example, in Figure 25 two thermograms of pure PB and of the sample PBNCys015 are reported. The functionalised sample contains only 6.3 mol.-% of NCys, but its glass transition temperature is over sixty degrees higher than that of the unfunctionalised sample.

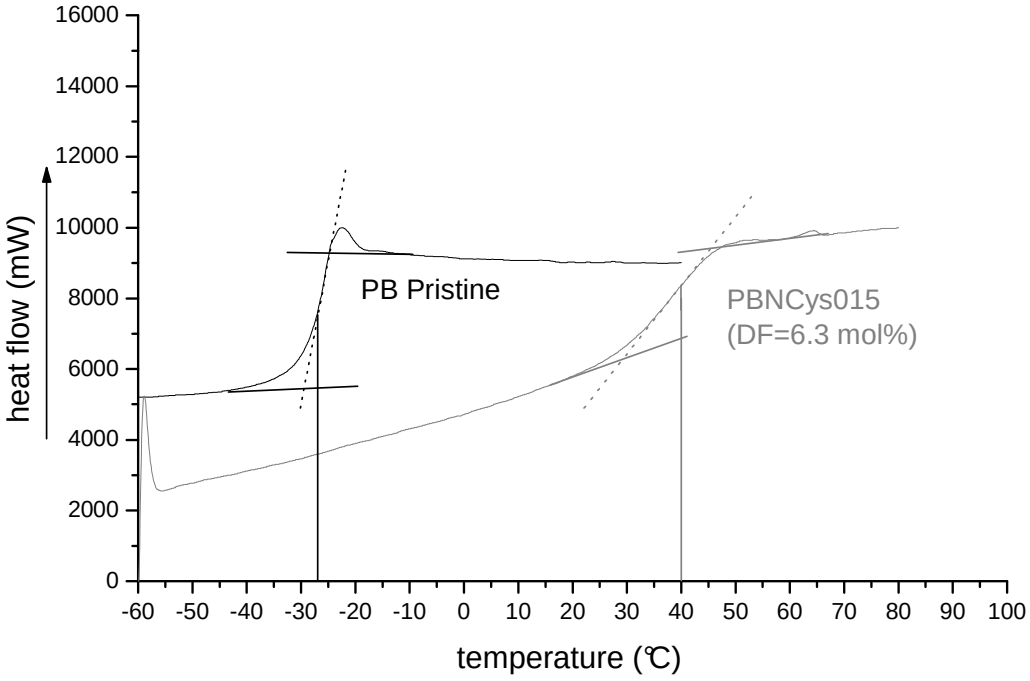

Figure 25 – Example of two thermograms, pristine PB *versus* PBNCys015 (DF = 6.3%)

Pascault and co-workers[35] found a similar behaviour when considering a carboxy telechelic polybutadiene functionalised with TGA (T_g increased from -22 °C to 4 °C at DF = 94.5%; the starting substrate was a CTPB having $<M_n>$ = 1550 Da and 90 mol.-% of 1,2- units). Ameduri[68] discovered a different behaviour with fluorinated thiols (HTPB fluorinated with linear $C_8F_{17}C_2H_4SH$, T_g shifted from -30°C to 0° only in the range [90-100%] of DF, otherwise remaining at ~ -30°C; the starting substrate was a HTPB having $<M_n>$ = 2000 Da and 88 mol.-% of 1,2-units), but the grafted chains were highly hydrophobic, thus showing only minor interactions between themselves.

In the case discussed in this thesis work, it is possible to estabilish a direct relationship between the nature of the added thiol (an acid or an ester) and the increase of the T_g. In particular, this effect could be ascribed to the presence of hydrophilic units grafted on the macromolecular chains. In particular, comparing the results reported in literature using TGA with those of the present work, higher increase of the T_g at higher grafting levels are observed, but the trend is similar. This effect is less remarkable in PBNCysMe samples: a possible explanation is that the number of hydrogen bonds thet could be formed between macromolecules or with different units of the same chain is decreased (Scheme 22) when NCysMe is used, and the T_g is consequently lower with respect to the PBNCys samples.

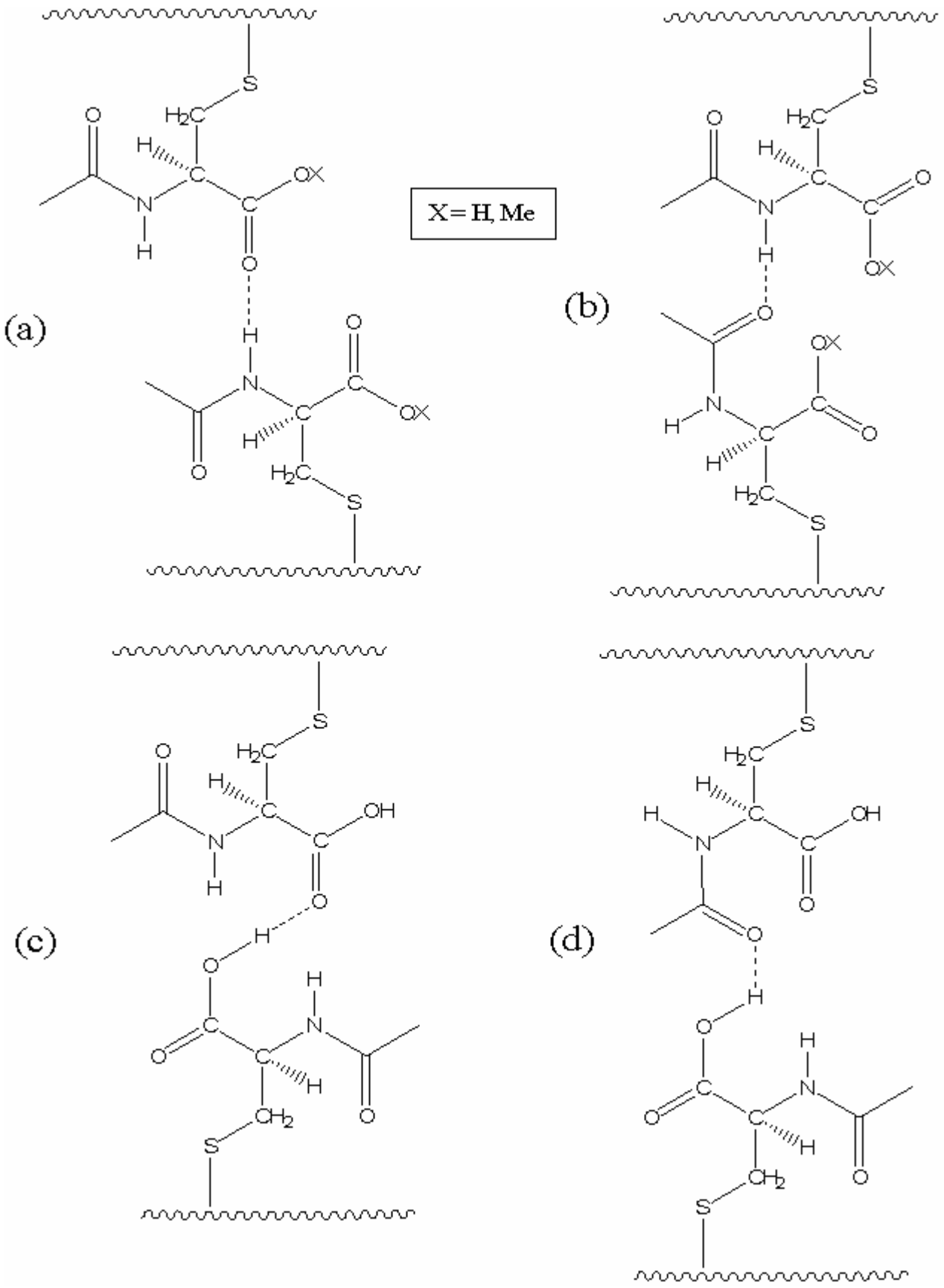

Scheme 22 – The possible hydrogen bonds between grafted NCys or NCysMe units.
The (a) and (b) situations are possible with both functionalisers; the (c) and (d) situations only with NCys

The intermacromolecular hydrogen bonds of Scheme 22 are likely to be the most important contribution to the T_g variation: in fact, the presence of hydrogen bonds (alone: the number of cyclised units in the PBNCys and the PBNCysMe samples should be quite similar, see Table 14, page 81) causes a shift in the T_g of more than fifty degrees, that is half the maximum variation obtained with PBNCys samples.

Another aspect affecting the T_g of a polymer is the comonomer distribution in a copolymer; again, like in the case of SEC, the properties of the functionalised samples studied in this thesis work are similar to those of random copolymers.

Many studies of the thermal properties of copolymers were performed since the introduction of the DSC. The first equations aimed to the prediction of copolymers T_g appeared during the '50s: the most famous ones were the Gordon-Taylor equation[257] and the Gibbs-DiMarzio[258] one. It soon became evident that the sequence distribution of comonomers must be taken in consideration; a first relevant theoretical study was published by Uematsu and Honda.

Starting from the theoretical equation of Gibbs-DiMarzio, the authors found a good agreement with experimental data by considering that the influence of the sequence distribution of comonomers on the T_g could be represented by an extra term of the equation[259, 260]. The Uematsu-Honda equation for predicting the T_g of an AB random copolymer follows:

$$T_g = \chi_{AB} T_{g,AB} + \chi_{AA} T_{g,AA} + \chi_{BB} T_{g,BB}$$

In this equation, the χ_{ij} term refer to the molar fraction of the *ij* diads, the terms $T_{g,AA}$ / $T_{g,BB}$ refer, respectively, to the T_g of the A and of the B homopolymer, and the term $T_{g,AB}$ refer to the T_g of the strictly alternating AB copolymer. In many cases the diad sequence could be determined by NMR measurements, and several methodologies were developed in order to find this value.

In 1970, Barton[261] suggested the same equation of Uematsu and Honda, and in the western world the cited equation has been known as the Barton's one. The equation proved to be succesful in many cases, and a good agreement between calculated and measured values was found in many systems (see, for instance, ref. [262-264]). Soon thereafter, the T_g of alternating copolymers of acrylonitrile and buta-1,3-diene, that are copolymers having a primary structure similar to the one of the functionalised products of this thesis work, were studied by Junji Furukawa and co-workers[265], and they compared the experimental results with those arising from the Uematsu-Honda equation. (Later Furukawa determined also the mechanical properties of similar substrates[266, 267].) In the cited studies, a good agreement is achieved between the calculated T_g values arising from the

Uematsu equation and the experimental data for various poly(buta-1,3-diene-*co*-acrylonitrile) having different composition. Furukawa and co-workers managed to vary the synthetic conditions of the copolymers in order to obtain a different amount of rotatable B / AN diads, and they observed various T_g ranging from -26 °C to -15 °C with a fixed copolymer composition (AN content: 49.0±0.3 mol%).

However, the Uematsu expression, that considered the diad sequence effect, cannot be adapted to describe the asymmetrical and even "S-shaped" T_g *vs* copolymer composition relations that sometimes had been observed. In most cases, the agreement obtained by assuming the additivity of triad sequences is substantially improved over that of diad sequences[268-270].

Hirooka and Kato formulated an empirical equation[271] that was partially put in relationship to the parameters of the Barton equation. The authors characterised the thermal properties and the primary structure (usually via NMR) of many copolymers (Sty/MMA, α-MeSty/AN, vinyl chloride/AN, Sty/MA, vinyl chloride/MA, vinyl acetate/AN, vinylidene chloride/MA, Sty/AN), having, for each couple of comonomers, different composition in terms of i. relative molar amounts ii. sequence (diad / triads). The T_g *versus* composition curve is analysed and compared to the graphs appearing in other literature works[272-274]: the authors find out that the graph could consist in a concave line, in a convex line or in a linear dependence of the T_g from the composition. Moreover, they observed an interesting relationship between this behaviour and the primary structure of the copolymer: if strictly alternating copolymers (composition of which is 50 mol.-% per comonomer) have a T_g inferior to that of random copolymers, the curve is always concave; if the strictly alternating copolymers have a T_g higher to that of random copolymers, the graph will be convex; if their T_g is similar to that of random copolymers, the dependace will be linear (and this result is regardless of the couple of employed comonomers). For *random copolymers* the authors refer to copolymers obtained in conditions not influencing the copolymerisation rates; strictly alternating copolymers are, instead, synthesised with more complex experimental methods (a general method is suggested by Hirooka in ref.[275]).

In their study, Hirooka and Kato also find that the extent of the difference of the T_g of the strictly alternating copolymer from the arithmetic average of the T_g of the homopolymers (i.e. the linear dependence, expressed by the Gibbs-DiMarzio equation) is also a good estimation of the entity of the concave/convex behaviour. If the difference is zero, the curve will be a straight line.

The empirical equation that Hirooka and Kato suggested in the cited paper can be related to the Barton equation, and an empirical constant arising from the Hirooka equation finds immediately its meaning in the extent of the *poly-A* or *poly-B sequence length*: the linear dependence of the T_g from

the molar composition is reached if the copolymer is a block one[**] (in the Barton equation, for a block copolymer, $\chi_{AB} \sim 0$). In the cited *convex* cases, the behaviour was explained by suggesting a high T_g of the strictly alternating copolymer ($T_{g,AB}$) and a relevant contribution of the χ_{AB} molar fraction, that is, the amount of AB diads is not negligible.

The data regarding the PBNCys and the PBNCysMe systems (Figure 24, page 93) show a *convex* dependence of the T_g from the polar comonomer unit, this latter being the functionalised one. This behaviour is similar to the behaviour of vinylidene chloride / MA[271, 274], Sty / AN[272] and ethene / MA[276] copolymers, while butadiene / acrylonitrile copolymers[265] and other copolymers (especially the ones containing styrene) show a linear or a concave dependance of the graph T_g *versus* hydrophilic monomer mol.-% composition. Although there are, as said, strong clues about the most relevant contribution to the T_g (that is the formation of hydrogen bonds between the macromolecules), the sequence distribution of comonomers could have an impact on the T_g. In this case, the convex T_g / composition trend should account for a random AB structure of the functionalised samples rather than a block-copolymer structure.

The T_g of samples obtained in absence of a radicalic initiator (described in chapter 2.2.6, page 89) is lower with respect to that of the PBNCys030 and PBNCysMe030 samples. The two sets of samples PBNCys and PBNCysMe display, for small DFs, a linear dependence of the T_g from the DF, and the experiments PBNCys030woAIBN and PBNCysMe030woAIBN lie below this line. In Figure 26 the T_gs of the runs carried out without AIBN are reported on a T_g *vs* DF graph.

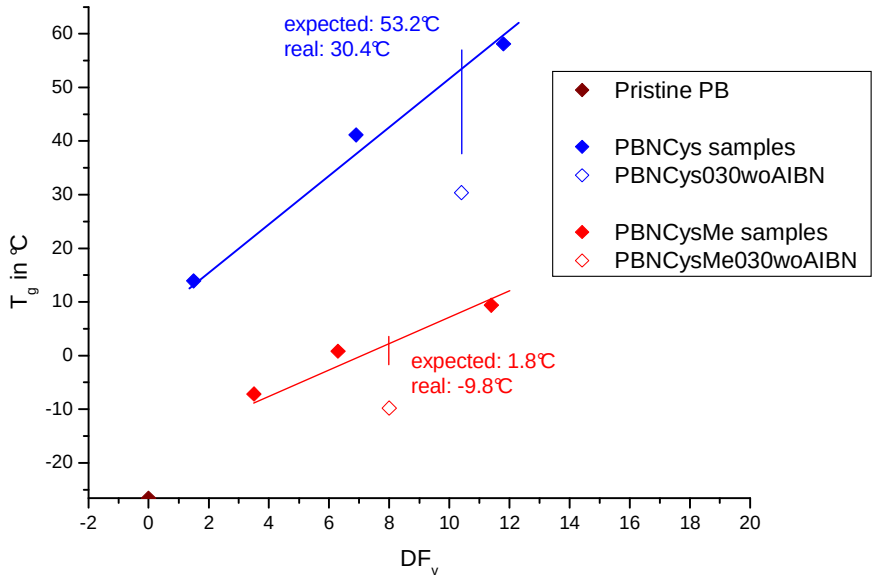

Figure 26 – Unexpectedly low T_gs of samples obtained in absence of AIBN

[**] However, when dealing with a block copolymer, other factors related to the morphology of the material occur, and they often determine the presence itself of a single or a double T_g (if any).

This result could arise from a possible lower occurrence of side-reactions, that, as seen, are particularly competitive with the thiol-ene functionalisation at these low feed ratios. The formation of cycles could raise the glass transition temperature by increasing the macromolecular rigidity; the chain elongation could as well increase the T_g because of the longer macromolecular chains.
A possible lesser extent of side reactions in absence of AIBN is not in contrast with previous results concerning thiol-ene reactivity investigated through spectroscopic methods, as the DSC measurement of the T_g is a characterisation having a different sensibility to certain structure modifications with respect to IR or NMR spectroscopies.

2.2.9 Polarimetric / circular dichroism measurements

Amino acids have been used as chiral substituents in polymers since the late '60s, with the pioneering studies of Iwakura and co-workers[277, 278]. Later many amino acids were used, such as L-alanine (extensively studied by Morcellet and co-workers[279-286]), L-phenyl alanine and L-glycine[287], L-leucine[288-291] and others (for a review of these systems and others, see ref.[292]).
Takeshi Endo and co-workers studied homo- and copolymers of L-cysteine derivatives[293, 294]; the structures of some of the synthesised polymers are reported in Figure 27.
In a first study[293], the authors polymerised the *N*-methacrylamide of *S*-trityl-L-cysteine methyl ester and methacrylic acid (see Figure 27, molecule **a**). With respect to the polymers presented in this thesis work, the amino acid is bonded to the macromolecular backbone through the amide group and not, as in the case considered here, through a sulphur atom bridging from the amino acid to the chain. The trityl group acts as a protecting group on the sulphur atom, and it was introduced in order to discourage the formation of cystine-type units in the adopted polymerisation condition; after the reaction, the authors removed the trityl group.

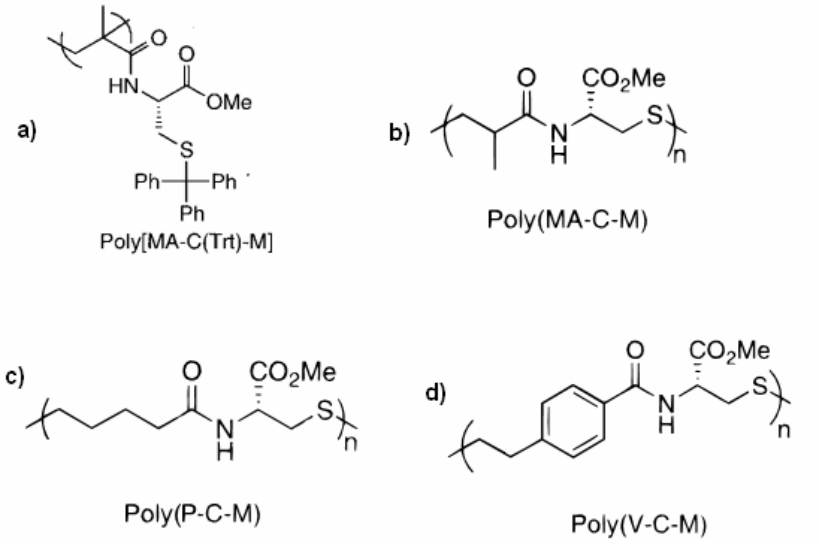

Figure 27 – Chiral polymers studied by Endo *et al.* (a[293], b c and d[294])

In the same paper, also various compositions of copolymers of the cysteine adduct and MMA are synthethised and characterised. The most interesting result concerns the specific optical rotational power [α] of the synthesised poly[*N*-methacryloyl-*S*-trityl cysteine methyl ester]-co-MMA: no linear relationship was observed with the composition of the copolymers. Endo suggested that two factors could affect the propagation of chiral properties to the synthesised copolymers: i) the steric hindrance of the incoming monomers during copolymerisation could induce an asymmetry of the polymer backbone, as seen for other copolymers of MA with bulky MA-ester comonomers[295-297] and ii) the values could have been affected by higher order structures of the polymer such as helices, as seen for other methacrylates.[297]

In the cited study of Endo[293], the second possibility is not supported by the results of circular dichroism, as well as in the majority of the other studies of the author (materials obtained polymerising *N*-methacryloyl derivatives of L-phenylalanine, L-alanine, L-glutamic acid, L-tyrosine). The tendency to form helices has been reported, however, for poly(*N*-methacryloyl-L-leucine) by the authors themselves[291], and also in a polymer of a cysteine derivative: poly(*N*-4-vinylbenzoyl-L-cysteine methyl ester)[294] (Figure 27, molecule **d**, poly(V-C-M)). The primary structure of this macromolecule, though, is quite far from the ones of the polymers presented in this thesis work; poly[*N*-methacryloyl-*S*-trityl cysteine methyl ester]-co-MMA, instead, is a polymer that could potentially show some analogies with the polymers presented in this thesis work in terms of optical properties since it shows a similar macromolecular backbone.

Polarimetric measurements on PBNCys and PBNCysMe samples in MeOH solution and in 1,4-dioxane solution (at a concentration of 1 g / 100 ml) were performed. As published in the scientific literature on similar systems, the optical rotating power of the amino acid was propagated to the products as expected, and all the samples displayed a remarkable optical rotating power. The values of the optical rotating power [α] for the PBNCys and PBNCysMe samples in MeOH or 1,4-dioxane (at C = 1) are reported in Table 17.

The *rescaled* optical rotating power [ϕ], obtained dividing the specific optical rotating power [α] for the cysteine derivative content in the polymer (DF wt.-%), would resemble the [α] of a solution of the pure amino acid; a graph displaying the value of [ϕ] *vs.* the DF wt.-% is reported in Figure 28.

Run	DF wt.-%[a]	C = 1 in MeOH		C = 1 in 1,4-dioxane	
		$[\alpha]_{589}^{25}$ [b]	$[\varphi]_{589}^{25}$ [c]	$[\alpha]_{589}^{25}$ [b]	$[\varphi]_{589}^{25}$ [c]
NCys	(-)	+9.8	(-)	+39.2	(-)
PBNCys100	68.0	-6.5	-9.5	+4.4	+6.4
PBNCys075	58.2	-5.9	-10.1	+4.7	+8.0
PBNCys060	56.9	-5.3	-9.3	+4.9	+8.5
PBNCys045	46.0	-5.0	-10.9	+4.0	+8.7
PBNCys030	24.4	-3.2	-13.1	+4.0	+16.6
NCysMe	(-)	-23.5	(-)	+31.2	(-)
PBNCysMe100	70.2	-8.6	-12.3	+6.7	+9.5
PBNCysMe075	66.6	-9.8	-14.7	+8.6	+12.9
PBNCysMe060	61.5	-9.5	-15.4	+7.6	+12.4
PBNCysMe045	50.8	-11.1	-21.8	+9.7	+19.2
PBNCysMe030	25.3	(insolub)	(insolub)	+8.9	+35.2
PBNCysMe015	15.8	(insolub)	(insolub)	+5.6	+35.4

Table 17 – Relationship between absolute DF (wt.-%) and the specific optical rotating power of samples

[a] Measured by ^{1}H-NMR; [b] Measured by a polarimetre at 25°C (C = 1 g / 100 mL); [c] $[\varphi]_{\lambda}^{T} \equiv \frac{[\alpha]_{\lambda}^{T}}{(DFwt-\%)\cdot 100}$

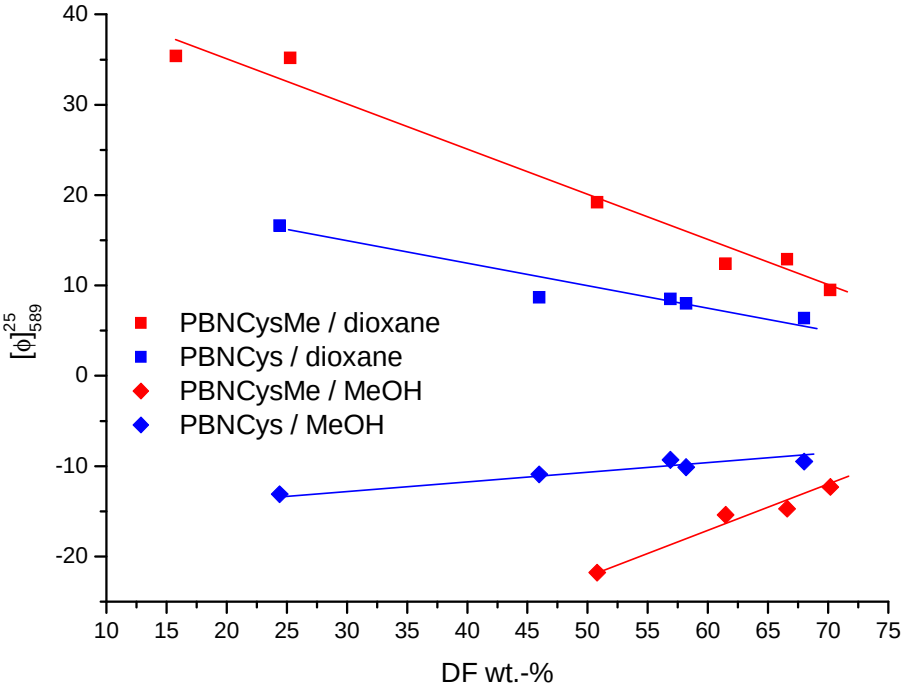

Figure 28 – $[\varphi]_{589}^{25}$ *versus* DF wt.-% for PBNCys and PBNCysMe samples at C = 1 in MeOH and 1,4-dioxane

If one assumes that the only contribution to the rotating power of the polymer solution arises from the chiral atoms belonging to the grafted units, rescaling the $[\alpha]$ should lead to a constant value of $[\phi]$ regardless of the amount of grafted cysteine; in other words, $[\alpha]$ should grow linearly with the cysteine content. As shown in Figure 28, however, the absolute value of $[\phi]$ decreases at high DFs for both sets of samples (PBNCys and PBNCysMe) and in both solvents; the values of $[\alpha]$

(Table 17), instead, display a non-linear growing behaviour with increasing DF. A possible explanation to this experimental evidence arises from the high relative proximity of the chiral units in polymers having high cysteine derivative content. In fact, the Biot law expressing the proportionality between the measured α and the concentration of the chiral species displays a linear range; the α dependance of the most concentrated solutions is far from the linear behaviour due to the micro-conformational changes happening when chiral species are close, often induced by intermolecular forces.

In the case reported in the present work, though, no spacial modelling is possible as there are no clues on the modality of occurrence of micro-conformational changes probably generating the observed behaviour; an hypothesis found in literature on other systems is a permanent variation of bond angles induced both by steric hindrance or hydrogen bond formation.

Another experimental evidence arising from the observed optical rotating powers is that the values in 1,4-dioxane are very different from the values in methanol solution, switching from positive values to negative ones for all the samples. This could be due to the possibility, for protic solvents (in this case MeOH), to establish new hydrogen bonds with amidic groups or carboxylic / carboxylate moieties; a similar interaction would affect the macromolecular structure in solution, causing the observed shift in the values of $[\alpha]$ and $[\phi]$.

In an already cited study of Endo of poly(*N*-methacryloyl-L-leucine)[291], circular dichroism spectroscopy (CD) confirmed the presence of an ordered secondary structure. In a study of Schlaad and co-workers on the addition of a dipeptide derivative of cysteine to an unsaturated polymer[125], CD showed the presence of micelles, some having a right-handed helix structure and some a left-handed one.

CD-UV spectra of polymer solutions in MeOH were collected. NCys and NCysMe solutions having a concentration of 0.0088 wt.-% displayed the best UV absorption conditions in order to avoid signal saturation; the polymer solution of the PBNCys and PBNCysMe series were created with a given amount of polymer tuned in order to maintain the cysteine derivative concentration at 0.0088 wt.-%, since the UV chromophore was the same in the functionaliser and in the polymers.

All the CD spectra of the polymers can be superimposed, and overlap themselves regardless of the DF; at the same time, the spectra of the pure amino acids showed a small translation on the X-axis with respect to the polymers (Figure 29; for simplicity, only two spectra of polymers are reported).

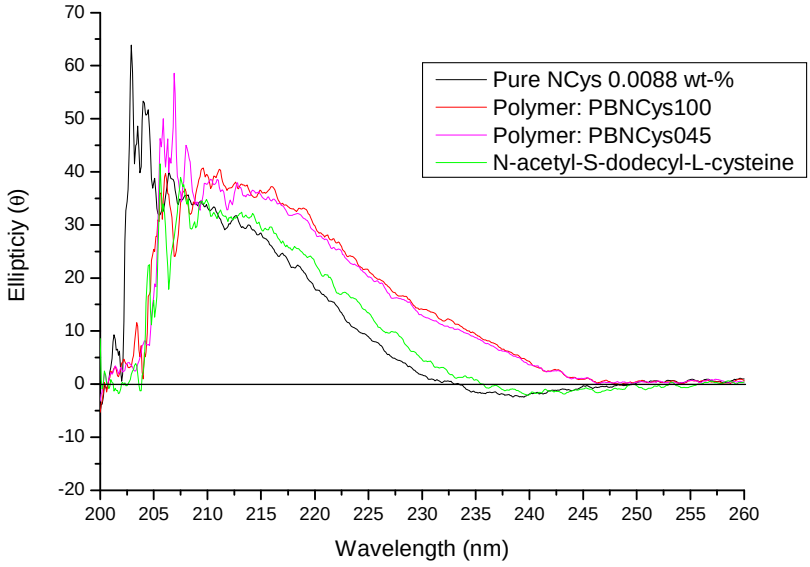

Figure 29 – CD spectra in the range 260-200 nm of PBNCys samples dissolved in MeOH with constant NCys content; room temperature, under nitrogen flux

In Figure 29 the CD spectrum of the adduct between 1-dodecene and NCys (chapter 2.1, page 59), that is *N*-acetyl-*S*-dodecyl-L-cysteine, was reported. This sample showed a CD spectrum (green line) that lies between the spectra of the pure NCys and the overlapping signals of polymer samples. Perhaps the X-axis shift of the spectra of polymers is simply a direct consequence of the presence of an alkyl substituent (in the case of polymers an entire macromoleculecular substituent is present) on the sulphur atom; this effect is smaller if the alkyl group is smaller (dodecyl group *vs* PBL).

The situation for PBNCysMe solution in MeOH is analogous, and the line shape of their spectra is not distinguishable from the one of the PBNCys samples. A graph reporting the CD of PBNCysMe samples, along with a spectrum of the pure NCysMe is reported in Figure 30.

In conclusion, no evident secondary structure in solution are found.

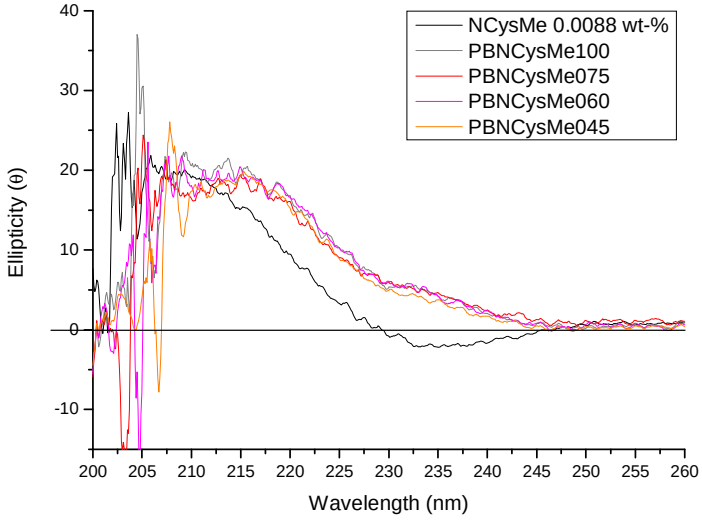

Figure 30 – CD spectra in the range 260-200 nm of PBNCysMe samples dissolved in MeOH with constant NCysMe content; room temperature, under nitrogen flux

2.3 Addition of L-cysteine derivatives to liquid styrene/butadiene random copolymer

In the most recent years, the tyre industry has been successful in reducing rolling resistance and increasing the traction of automobile tyres. By optimising the reaction conditions of compounds / mixings, the microstructural control of the employed elastomers can be considered a key-factor of new tyres development. The most used elastomers are polybutadiene rubber (PB, also named BR), poly(styrene-co-butadiene) rubber (SBR), natural rubber (NR), nitrile butadiene rubber (NBR); often these polymers are blended together in order to enhance the mechanical properties of the tyre. The combinations of the cited polymers generally do not result in a monophasic system after mixing, so the blends are often bi- or tri-phasic materials. The phase morphology controls the thermal behaviour, the resistance to oils and other macroscopic properties; tailoring the mixing conditions to obtain a particular phase morphology has then become an important production parameter.

The production process of rubber compounds is optimised to obtain a morphology in the polymer blends able to impart a good processability / mechanical properties to the materials. Other properties of the composite materials such as, for instance, a retarding of scorch times during vulcanisation, an improvement of the flexibility or other mechanical properties, a better diffusion of filler particles during compounding, water resistance in coatings and paints, *et cetera*, can be reached by using short-chain homo- and copolymers. The complete miscibility of these substrates with at least one of the two phases especially in PB / SBR blends looked appealing, since already-commercialised products could be modified without affecting too much the phase equilibra for which the production process had already been optimised.

Ricon Resins, Inc. put on the market some series of short-chain homo- and copolymers of buta-1,3-diene, that (i) could be incorporated in the formulation of polymeric blends without severely affecting the phase morphology, being miscible with at least one phase; (ii) could possibly be used alone as adhesives or coating agents for macroscopic surfaces (glass, metal plates, etc); (iii) that could act as crosslinking co-agents in other polymeric systems, such as polyurethane formulations. These substrates, moreover, could be easily modified with a variety of functional groups through radicalic functionalisations in order to meet other formulation needs.

Nowadays these polymers are produced by *Sartomer Inc.*, which commercialises not only the pristine elastomers but also functionalised derivatives under the name of “Ricon” resins. For instance, the “Ricon MA” series of products of Sartomer include maleic anhydryde (MA) functionalised polybutadienes; a Ricon MA polymer will form a crosslinked resin after being cured with diols / triols or amines in order to give flexible coatings and potting compounds. The “RicACRYL” series, instead, include various copolymers of buta-1,3-diene and acrylates; these

products, that are flexible elastomers miscible with acrylates, can be incorporated into acrylic resins.

The product “Ricon 100” is an SBR copolymer with a low MW (~ 4500 Da), typically used as scorch retarding agent during vulcanisation of rubber compounds. The supplier company defines this product as a versatile platform for various functionalisation typologies, though there are no commercially available maleinised products similar to, for instance, the Ricon MA series (functionalised PBLs). The functionalisation of this low-MW SBR copolymer with cysteine reagents was performed with the aim to introduce carboxylic functionalities.

After a characterisation of the pristine material, addition experiments of NCys were carried out similarly to the case of PB polymer. The acronym for these samples is SBRLNCys, since the starting material is a liquid SBR (SBRL).

2.3.1 Structural characterisation of the polymer: liquid styrene/butadiene random copolymer

The Ricon 100 (*SBRL*) is a liquid SBR that could undergo crosslinking if exposed to oxidants; to improve its shelf-time, the manufacturer added 100 ppm of (2,6)-ditertbutyl-4-methyl phenol (BHT) as an antioxidant. According to the supplier data sheet, the amount of BHT is very small (0.000285 mol.-%); this quantity can be considered as negligible with respect to the amount of primary radicals generated within the experimental conditions of the present work, and absolutely not affecting the radical reactivity of the considered system. Any further purification of the polymer aimed to remove the BHT before the thiol addition was avoided.

A characterisation aimed to identify the primary structure of SBRL has been performed by combining IR, proton and ^{13}C-NMR spectroscopies and SEC analysis. The thermal properties, with particular reference to the glass transition temperature, were evaluated through DSC.

In Figure 31 the infrared spectrum of SBRL, with the peak assignments, according to the Sigma-Aldrich library of IR spectra of polymers (electronic format), is reported.

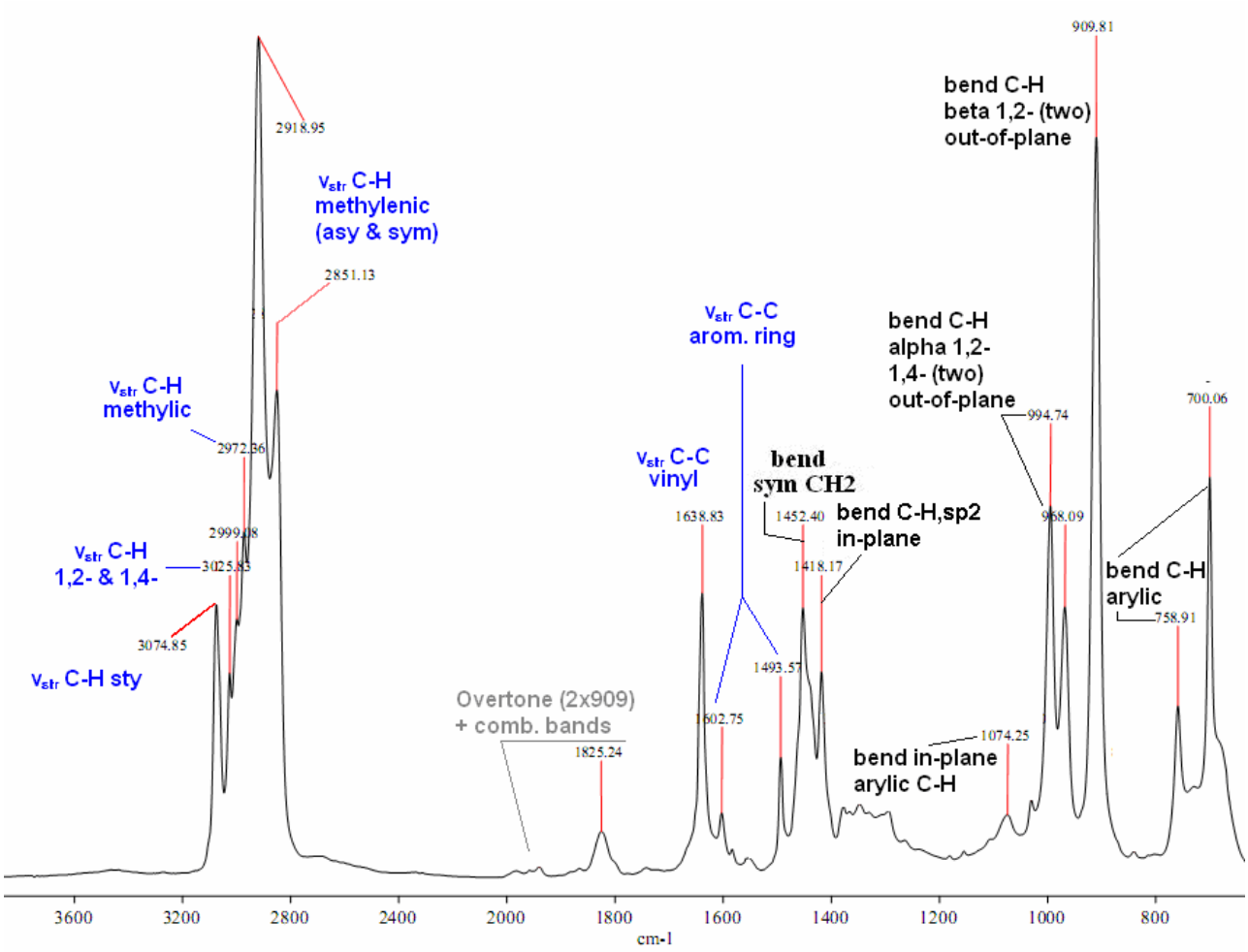

Figure 31 – IR spectrum of SBRL with peak attribution according to a Sigma-Aldrich library of IR spectra

The most relevant peaks are:

1) stretching of C-H bonds: ν_{str} C–H (styrenic): 3075 cm^{-1}, ν_{str} C–H (1,2- & 1,4-): 3025 cm^{-1}, ν_{str} C–H (methylic, end of chain): 2972 cm^{-1}, ν_{str} C–H (methylenic, respectively asymmetric and symmetric): 2919 and 2851 cm^{-1}

2) stretching of carbon-carbon double bonds: ν_{str} C=C (1,2- and 1,4-): 1639 cm^{-1}, ν_{str} C=C (aromatic rings, styrene units): 1602 and 1493 cm^{-1}, double peak

3) bendings of C(sp_3)–H bonds: δ_{sym} (methylenic): 1452 cm^{-1}

4) bendings of C(sp_2)–H bonds: $\delta_{in\text{-}plane}$ (C–H sp_2, 1,2- and 1,4- units): 1418 cm^{-1}, $\delta_{in\text{-}plane}$ (C–H sp_2, arylic): 1074 cm^{-1}, $\delta_{out\text{-}of\text{-}plane}$ (C–H sp_2, 1,2- alpha carbon and 1,4- units respectively): 994 and 968 cm^{-1}, $\delta_{out\text{-}of\text{-}plane}$ (C–H sp_2, 1,2- beta carbon): 910 cm^{-1}

No traces of BHT are evident; in particular the O–H stretching band in the 3500-3600 cm^{-1} zone, very strong and narrow in the BHT infrared spectrum[††], is missing. However, this evidence is not definitive, and this will be highlighted by NMR and SEC characterisations.

[††] Source for the BHT IR spectrum: The Aldrich Library of FT-IR Spectra, Edition II (Sigma-Aldrich Co., 1997)

In Figure 32 the ^{1}H–NMR spectrum of SBRL, collected in deuterated chloroform, is presented.

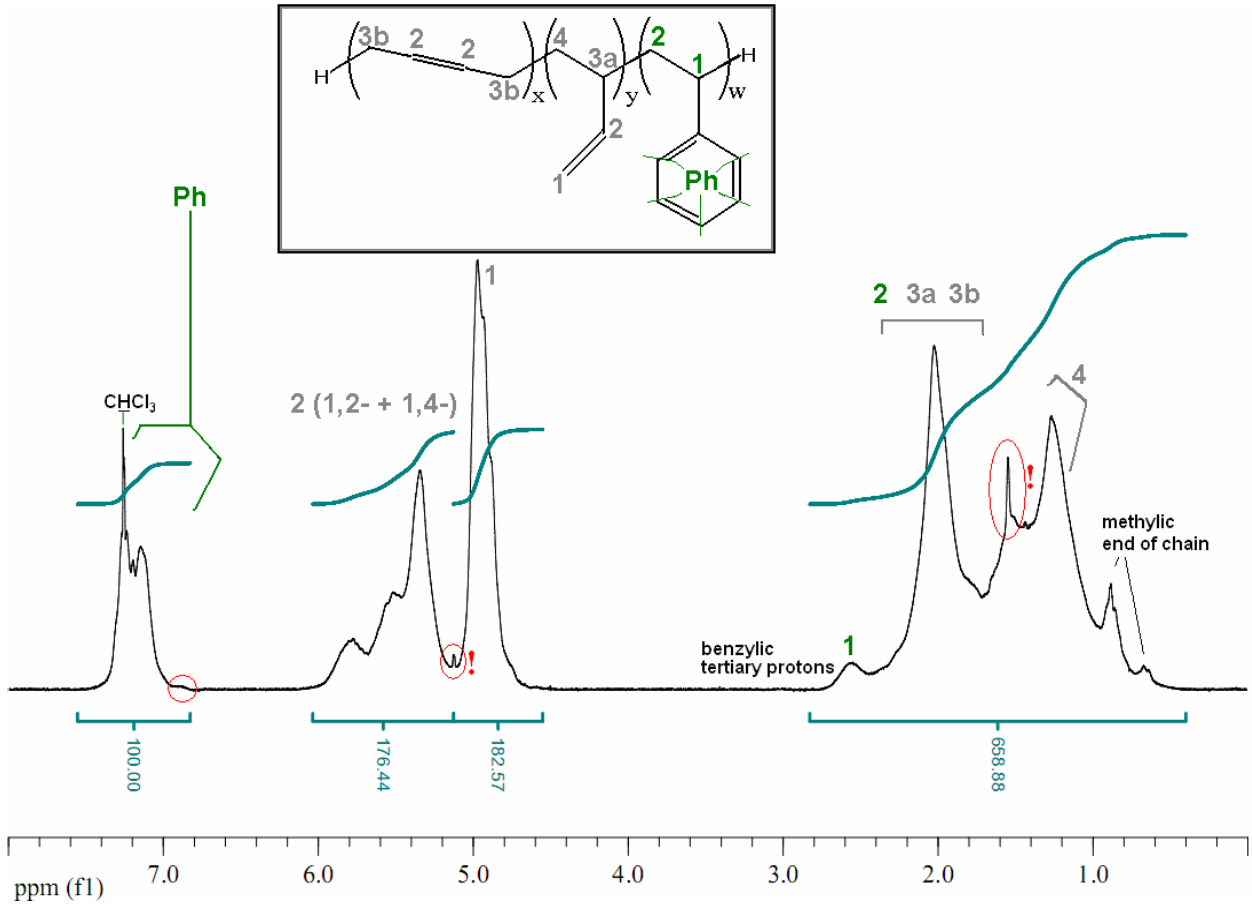

Figure 32 – ^{1}H-NMR spectrum of SBRL. Solvent: $CDCl_3$, T = 25°C, 200 MHz. !: BHT traces

The signal accounting for 1,4-*cis* sp_2 protons and 1,4-*trans* sp_2 protons in the range of 5.5-5.8 ppm is partially resolved, and the signals for the two protons are distinguishable.

Thanks to the very high resolution, typical BHT peaks (circled in red) are visible: a smaller asymmetry at ~ 6.8 ppm (accounting for the two phenylic protons), a peak at 5.1 ppm (RO*H*), and a peak at 1.3 ppm (the methylic carbons). As previously discussed, the BHT content is so small that it was not considered when calculating integrals.

According to the classical determination of the primary structure reported in literature[298], SBRL contains 62.0 mol.-% of 1,2- butadienic units, 13.1 mol.-% of styrenic units, and the remaining 24.9 mol.-% are the sum of 1,4-*cis* and 1,4-*trans* units; this complies with the supplier data sheet. The followed method does not allow to measure the 1,4-*cis vs* 1,4-*trans* units ratio; the determination could be done through ^{13}C-NMR[299-301] and details regarding this determination are furnished in the next paragraphs along with the ^{13}C-NMR spectrum.

The T_g of SBRL, measured through DSC, is -23.1 °C; it is a value higher than that of typical long chain, commercial, non-oil extended SBRs (T_gs ranging from -50°C to -30°C).

The SEC determination of the molecular weight of a copolymer is, as said before, a very difficult subject because of the nature of the macromolecules[255]. A mathematical approach to this determination, involving a two-detectors measurement (RI and UV), was described by Bernd Thratnigg[302]; although two detectors were adopted, in the present work the signal analysis was not performed as it is extremely time-demanding. In particular, the most difficult procedure consists in the determination of the constants for the use of an equation taking into account the influence of the end groups on polymers having MW up to 50 kDa[303]; the SBRL is a short-chain polymer and falls in this range, as suggested by its physical aspect (it is a liquid with low viscosity at room temperature) and by the band, of remarkable intensity, accounting for methyl groups located at the end of chains (band ay 1373 cm^{-1} of the IR spectrum, Figure 31; peaks at 0.6 and 0.8 ppm of the proton NMR spectrum, Figure 32).

SEC was performed using $CHCl_3$ as the mobile phase, and two detectors were employed: a refrective index (RI) instrument and an UV spectrometer measuring the absorbance at 260 nm. As observed by Trathnigg[255, 302], this UV band is typical of the styrene monomer units of the SBR polymer, and the response factor (Lambert Beer proportionality constant) of styrene with respect to butadienic units in this zone of the spectra is nearly 500 times higher for the styrene units[302]. If the SBR composition is random for all molecular weights, the RI chromatogram should be similar to the UV one, except for aromatic additives such as BHT (if their peak does not overlap to the polymer one). The small molecules of the stabiliser do not produce any variation of the RI, while, being aromatic, they are detected by the UV spectrometer.

The chromatograms obtained through both the RI and the UV detectors are compared in Figure 33.

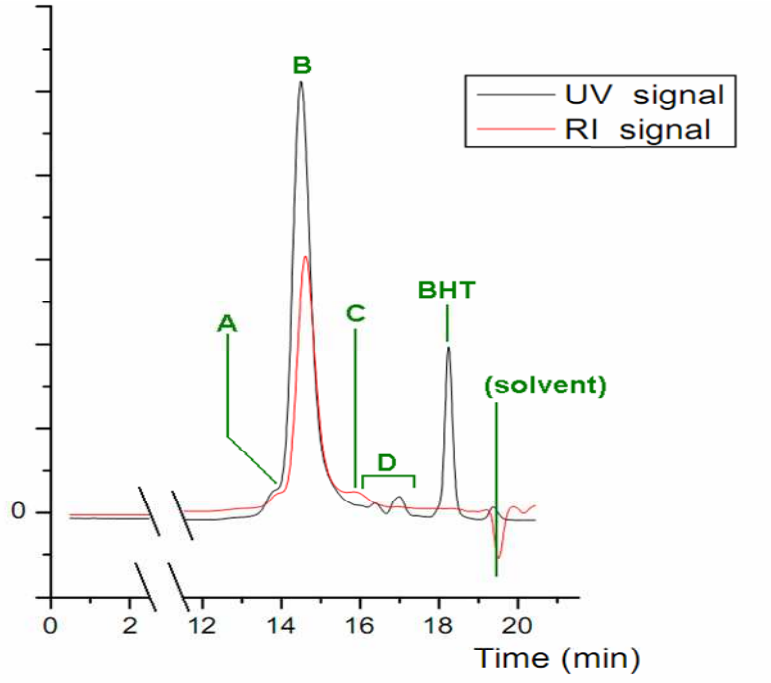

Figure 33 – SEC chromatograms in $CHCl_3$ of pure SBRL. For a description of the letters, see text

The chromatograms were converted to MW distribution graphs by using a set of PS monodisperse standards; two calibration curves, one for the UV and one for the RI, were realised. The MW determination was performed by applying a deconvolution procedure on the peak of Figure 33.
The first peak that can be observed (A) refers to long macromolecules; it is present both in RI and UV chromatogram. The most intense peak (B) comes soon after, and it shows, only in the UV chromatogram, a shoulder (C). After deconvolution, one can estimate $<M_n>$ and $<M_w>$ of A, B and C peaks (Table 18).

Peak	M_n (RI), Da	M_w (RI), Da	PDI (RI)	M_n (UV), Da	M_w (UV), Da	PDI (UV)
A	11080	11230	1.01	11050	11210	1.01
B	4970	5180	1.04	5270	5520	1.04
C	(absent)	(absent)	(absent)	1720	2030	1.18

Table 18 – Evaluation of molecular weights associated to fractions A, B and C of the chromatograms of SBRL

While it is impossible to infer the molecular structure of the A and the B fractions, one can say for sure that the C fraction is richer in butadiene units with respect to A and B; in fact, the peak C can be observed only in the RI chromatogram. A similar polymer fraction was noticed also by Thratnigg in 1992[302] in SBR samples; probably its presence, as well as the presence of the A and the B fractions, is a direct consequence of the synthetic method of the SBR copolymers (often emulsion co-polymerisation). Different copolymerisation rates between butadiene and styrene are responsible for this behaviour, and it has been shown[304] that when one of the two comonomers finishes it is possible that the residual comonomer undergoes homopolymerisation.
In the zone of the UV chromatogram called "D" (Figure 33), other less intense peaks can be observed, though their influence on the RI is negligible (no signal).

2.3.2 Reactivity of SBR towards primary radicals originated by AIBN

In order to evaluate the behaviour of SBR in the reaction conditions used for thiol-ene functionalisation but without thiol, a run called *SBRLwoRSH* was performed. This reaction run, involving only SBRL and AIBN, was carried out in order to evaluate the reactivity of the SBR towards primary radicals generated by the initiator.
After purification, the reaction product is transparent and clear, as well as the starting polymer. It is completely soluble in the most common organic solvents for unsaturated elastomers: benzene, toluene and other aromatic compounds, $CHCl_3$, n-hexane and similar hydrocarbons, acetone, 1,4-dioxane, THF.

The IR spectra of SBRL and SBRLwoRSH do not show differences in peak shifts nor in peak intensities. For intensity evaluation, a normalisation with respect to the 3074 cm^{-1} band (C–H stretching of styrenic moieties: the amount of styrene units does not change during any reaction) has been performed in order to observe changes in other absorbances.

The primary structure determination of SBRLwoRSH has been performed by using NMR, as in the case of SBRL. The proton NMR spectra of SBRL and SBRLwoRSH are similar in terms of peak shifts; only the bands related to BHT protons disappeared (the BHT was removed during the purification of the sample SBRLwoRSH). Following the described procedure for the determination of the styrene / 1,2-butadiene / 1,4-butadiene content[298], the composition of both samples was determined, and is came out that it is practically the same. The styrene content is 13.1 mol.-% in both samples; the 1,2- content is 62.0 mol.-% in SBRL and 61.5 mol.-% in SBRwoRSH; the amount of 1,4- units was 24.9 and then became 25.4 mol.-%.

The ^{13}C-NMR spectra were evaluated for the determination of the 1,4-*cis* + 1,4-*trans* content. In each ^{13}C-NMR spectrum of the SBR samples (SBRL and SBRLwoRSH) the peaks were assigned accordingly to Katritzky[300, 301] and Segre[305]. The chemical shift of each carbon atom is originated by the neighboring monomeric units, and, in the cited papers, the peak assignment is performed by considering the possible configuration of diads[300, 301] or triads[305]. The great sequential multiplicity, which can result from the different possible combinations of the four monomeric units of SBR (styrene units, “S”, 1,2- vinyl units “v”, 1,4-cis “c” and 1,4-trans “t” butadiene units) and their head-to-tail or tail-to-tail bond sequence, is evident. A more precise study in terms of peak assignment has been performed in 1989 by Tanaka and co-workers considering triads and quadriads instead of diads[306]; for the purposes of this thesis, the quicker determination method described by Segre was adopted, as it offers acceptable results in terms of c/t ratio.

In Figure 34 the peaks were named with Roman numerals in the 110-150 ppm range of the ^{13}C-NMR spectra of SBRL and SBRLwoRSH, according to Katritzky[300, 301]; Segre cites other 11 signals in the same zone, not all really evident in the spectra. The peak of $\underline{^{13}C}DCl_3$ (the used solvent) is not reported, being its triplet signal at 77.0 ppm, but it has been used as internal standard to assign all the other peaks. In Table 19 all the assignments are described in detail.

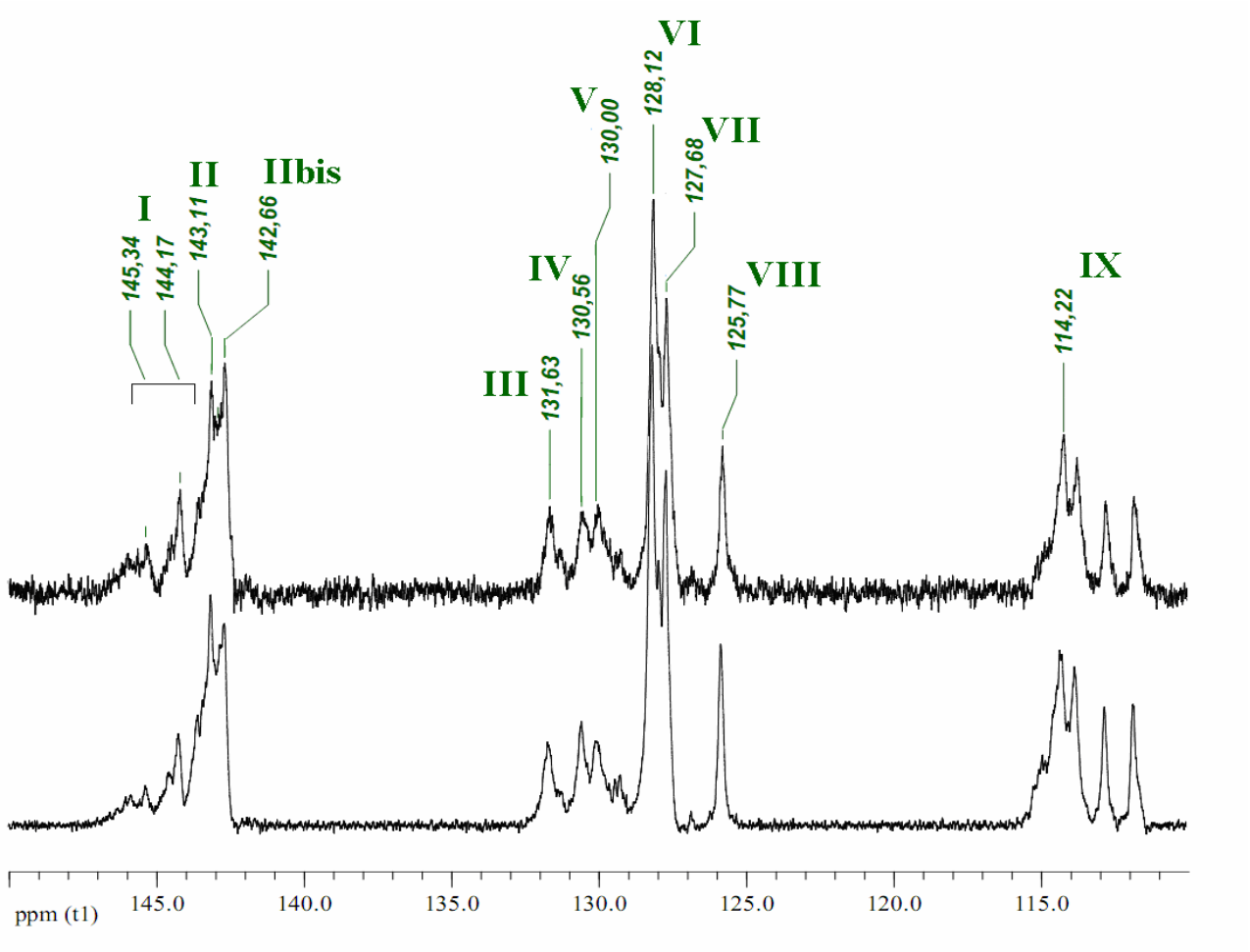

Figure 34 – 110-150 ppm zone of the ^{13}C-NMR spectra of SBRL (down) and SBRLwoRSH (top) 10^2 -10^5 scans, 25°C, $CDCl_3$

Peak	Chem.shift, ppm	Assignment	Unit (see text)	Diad(s) involved
I[a]	145.34-144.17	Ph, carbon n°1	S	All S-diads
II[a]	143.11	α-vinyl sp_2 betw. v & S	v	v-diads
II bis[a]	142.66	α-vinyl sp_2 betw. c/t & c/t	v	v-diads
III	131.63	1,4- sp_2 α near to S/v	c + t	cS, tS, cv, tv
IV	130.56	1,4- sp_2 t near to c/t	t	Tt, ct, tt, tc
V	130.00-128.50	1,4- sp_2 c near to c/t	c	Cc, ct, cc, tc
VI	128.12	Ph, carbon n°2 &6	S	All S-diads
VII	127.68	Ph, carbon n°3 & 5		
VIII	125.77	Ph, carbon n°4		
		Also 1,4- sp_2 β near to S/v	c + t	St, Sc, vt, vc
IX	114.22-111.00	β-vinyl sp_2 + NOE	v	All v-diads

Table 19 – Complete assignment of ^{13}C-NMR spectrum peaks in zone 110-150 ppm samples SBRL and SBRLwoRSH. [a]: not resolved in Katritzky[299-301], attributed according to Segre[305]

The primary structure of a SBR copolymer, in terms of molar amounts of S, v, c, t units, can be partially inferred by ^{1}H-NMR spectrum; in particular, the amount of c versus t can be determined considering that:

$$\frac{n_{cis}}{n_{trans}} = \frac{A_{130.25}}{A_{130.75}}$$

In this expression, n_x is the molar amount, referred to 100 monomeric units, of x units, with x = c (*cis*-) or t (*trans*-), and A_m is the area of the peak located at m ppm. In some early literature works the peak heights were used into the equation[305], but in 1971 Mochel suggested that a systematical application of Lorentzian deconvolution and the use of peak area instead of peak height led to more reproducible and consistent results[231].

Following the same deconvolution procedure of Mochel, the fine structure of peaks in the zone 132-129 ppm was evaluated attributing the peaks to triads according to Segre[305] (Figure 35).

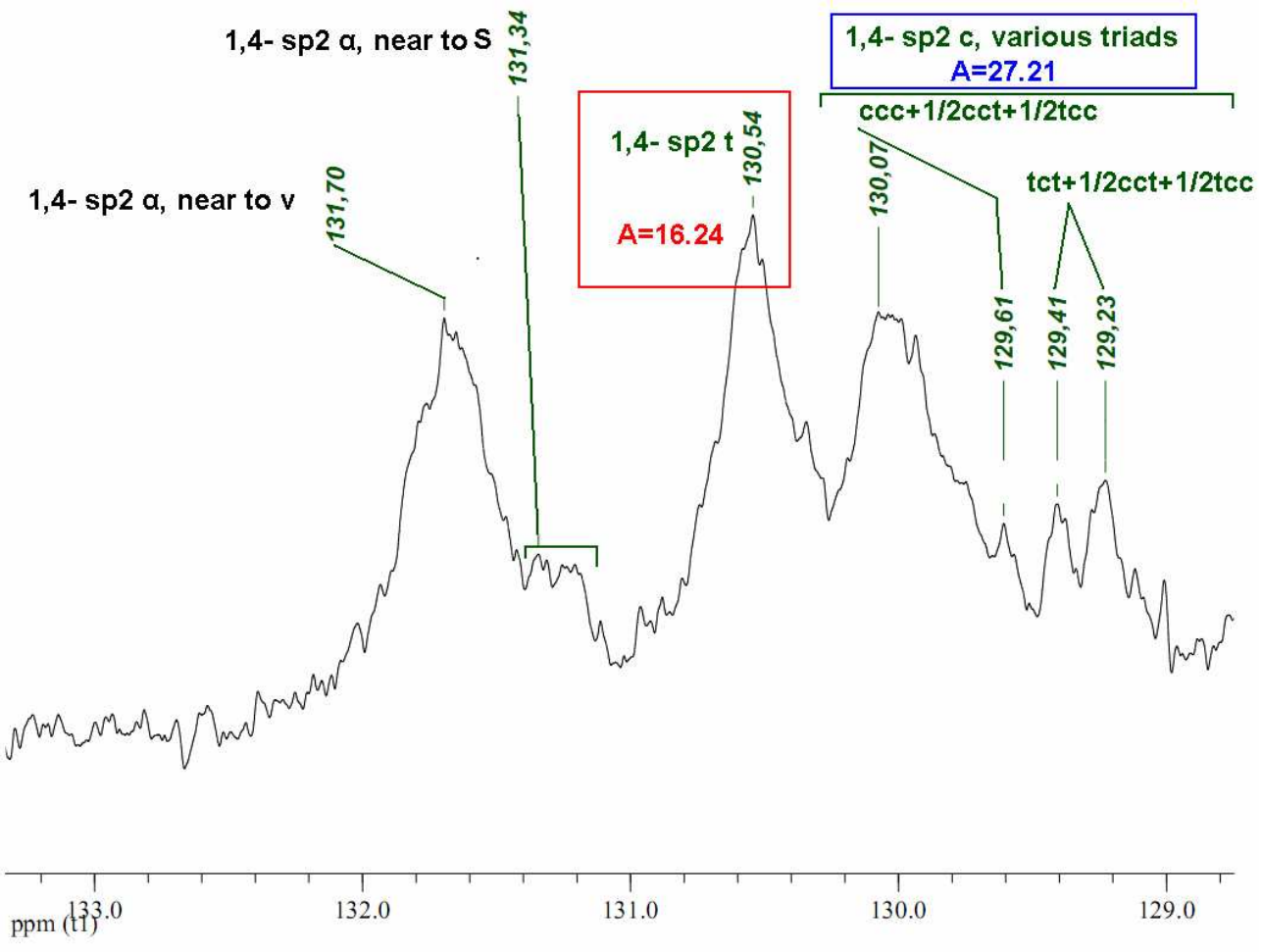

Figure 35 – Fine structure of the 133-129 ppm zone of SBRL ^{13}C-NMR spectrum

After the application of the method, the relative *cis* / *trans* ratio is 62.6 *cis*, 37.4 *trans* per 100 1,4-units. The final structure of SBRL is:

- 13.1 mol.-% styrene
- 62.0 mol.-% (1,2-)
- 15.6 mol.-% (1,4-*cis*)
- 9.3 mol.-% (1,4-*trans*)

The same method applied to the ^{13}C-NMR spectrum of SBRLwoRSH gave a relative ratio of 63.1 *cis* and 36.9 *trans* units per 100 1,4- units, which is a result close to that of SBRL. In conclusion, no appreciable variations in the proton and ^{13}C-NMR spectra account for changes in the primary structure in terms of 1,4-*cis versus* 1,4-*trans* units.

The assignment of the 50-10 ppm zone of the ^{13}C-NMR spectrum has been performed for both SBRL and SBRLwoRSH, though it has not been used for quantitative determination because of the high signal complexity and peak overlap. The peak assignement is not reported for simplicity (Segre *et al.* assigned 30 peaks in this zone, referring to as much as 152 triads[305]); again, no apparent variations in the peak shape in this zone between the SBRL and the SBRLwoRSH spectra were observed.

The T_g of SBRLwoRSH is -22.0 °C, while that of SBRL is -23.1 °C; this variation does not account for any major structural rearrangement or for the presence of degradation / crosslinked products.

The sample SBRLwoRSH showed two SEC chromatograms (UV and RI) extremely similar to those of SBRL (Figure 36).

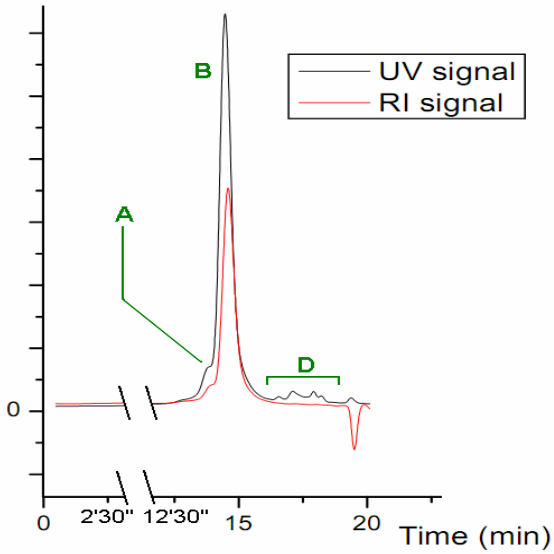

Figure 36 – SEC chromatograms in $CHCl_3$ of SBRLwoRSH

In Figure 36 one can observe the complete disappearance of peak (C) with respect to the SBRL system; the (A) shoulder of peak (B) and UV-detected impurities (D serie) are observable in both chromatograms. The MW data are reported in Table 20.

Peak	M_n (RI), Da	M_w (RI), Da	PDI (RI)	M_n (UV), Da	M_w (UV), Da	PDI (UV)
A	11240	11440	1.02	11200	11420	1.02
B	5350	5600	1.05	5400	5650	1.05

Table 20 – Evaluation of MWs associated to fractions A and B of the chromatograms of SBRLwoRSH

The disappearance of peak C probably accounts for the removal of the polymer fraction rich in PB during the precipitation in methanol of the crude reaction product. Moreover, the deconvolution and the evalutation of A and B peaks does not display any substantial variation of the MW during the treatment with AIBN; the variation of M_n and M_w of both peaks with respect to the values of Table 18 is very small suggesting that chain-chain coupling reactions did not occur.

2.3.3 Addition of N-acetyl-L-cysteine to SBRL; IR identification of products

A preliminary experiment with 0.01:1:1 molar ratio AIBN:NCys:vinyl (theoretically achievable DF: 62.0%, DF_v: 100%; AIBN 1 mol.-% with respect to the thiol) was performed under the experimental conditions pointed out in Table 21 (page 116) and called SBRLNCys100, from the substrate (SBRL), the functionalizing molecule (NCys) and the maximum theoretical DF_v % (100).
In order to evaluate the reactivity of NCys similarly to what was done in the chapter 2.2.2 (page 67) for PBL, seven experiments were carried out using different feed ratios, and were called SBRLNCys100 / 075 / 060 / 045 / 030 / 015 / 010; the number represents the maximum theoretically achievable DF_v.
The reaction products were purified by performing several times a dispersion in water and overnight stirring; after two or three re-dispersions / filtration / washing and removal of solvents under void with a pump until constant weight, the products looked white and more or less greasy depending on the feed ratio (the SBRLNCys100 → SBRLNCys030 samples were powders at room temperature).

The FT-IR characterisation of all reaction products was performed by solution casting of a film of polymer on a KBr window. The analysis of these spectra confirmed the presence of NCys grafted to the SBRL copolymer (Figure 37): amide II absorption band (N–H bending at ~1530 cm^{-1}) and, at 1735 cm^{-1}, the C=O stretching.

A pronounced decrease in the intensity of the bands related to the C–H (belonging to vinyl units) bonds out-of-plane bendings double band (909 and 996 cm^{-1}) was observed; at the same time the *1,4-* C–H out-of-plane bending band at 968 cm^{-1} decreased in a minor extent.

All the spectra of the SBRLNCys serie were different only in terms of intensity of bands arising from stretchings and bendings associated to NCys.

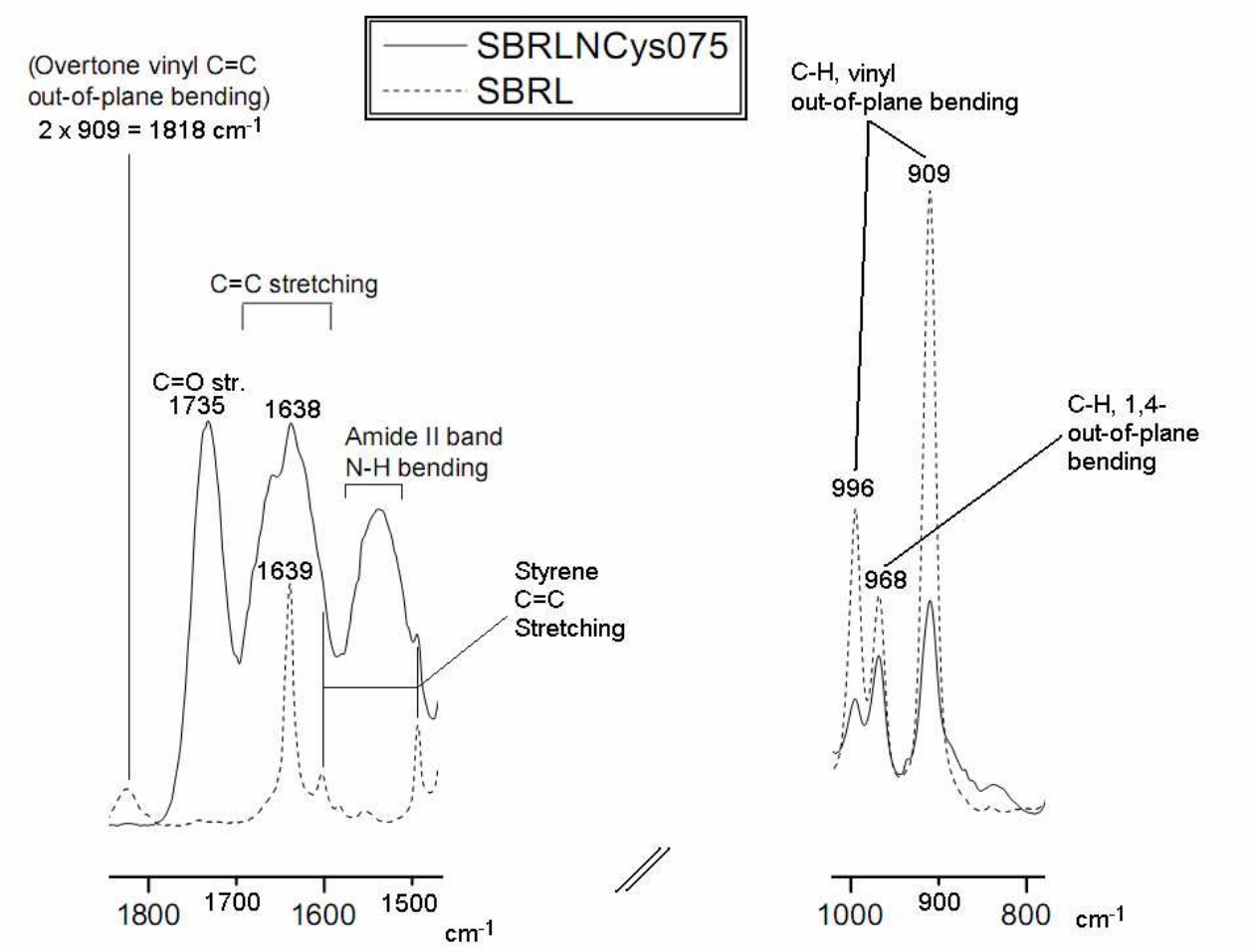

Figure 37 – 800-1000 cm^{-1} and 1500-1800 cm^{-1} zone of IR spectrum of SBRL and SBRLNCys075

To measure the DF, an IR method was adopted from a previous study focused on the CysEt thiol-ene functionalisation of long chain SBR[54, 112]. The possibility to apply this method, though, is limited to scarcely functionalised polymers; the SBRLNCys samples showed too much strong absorption bands, suggesting elevated conversion degree and rendering this IR method not suitable for a quantitative determination of cysteine derivative grafted units. The DF was therefore determined with a NMR method as in the case of PBNCys samples.

The feed ratio and the DFs determined through proton NMR spectroscopy are reported in Table 21; the data will be discussed in the next sub-chapter along with the NMR spectra.

Run[a]	[RSH]:[vinylic C=C]	AIBN (mol.-%)		Achievable DF_v %	DF_v %[b]	DF mol.-%[b] (Achiev %)	Conversion %
		To polymer	To RSH				
SBRL	-	-	-	-	-	-	-
SBRLwoRSH	-	1.00	-	-	-	-	-
SBRLNCys100	1.00:1	1.00	1.00	100	19.5	12.1 (62.0)	20
SBRLNCys075	0.75:1	0.75	1.00	75	25.6	15.9 (46.5)	34
SBRLNCys060	0.60:1	0.60	1.00	60	21.3	13.2 (37.2)	35
SBRLNCys045	0.45:1	0.45	1.00	45	18.5	11.5 (27.9)	41
SBRLNCys030	0.30:1	0.30	1.00	30	12.4	7.7 (18.6)	41
SBRLNCys015	0.15:1	0.15	1.00	15	7.9	4.9 (9.3)	52
SBRLNCys010	0.10:1	0.10	1.00	10	5.3	3.3 (6.2)	53

Table 21 – Feed ratios and functionalisation degrees of SBRLNCys samples

[a] Reaction conditions: T = 70°C, time 4h48', 1,4-dioxane 2 wt.-% polymer solution, under dry N_2

[b] Calculated with a ^{1}H-NMR method (see chapter 2.3.4, page 117)

2.3.4 ^{1}H-NMR characterisation of products: determination of the DF

A complete assignment of the proton NMR peaks shown in the spectrum of the sample SBRLNCys075 is reported in Figure 38.

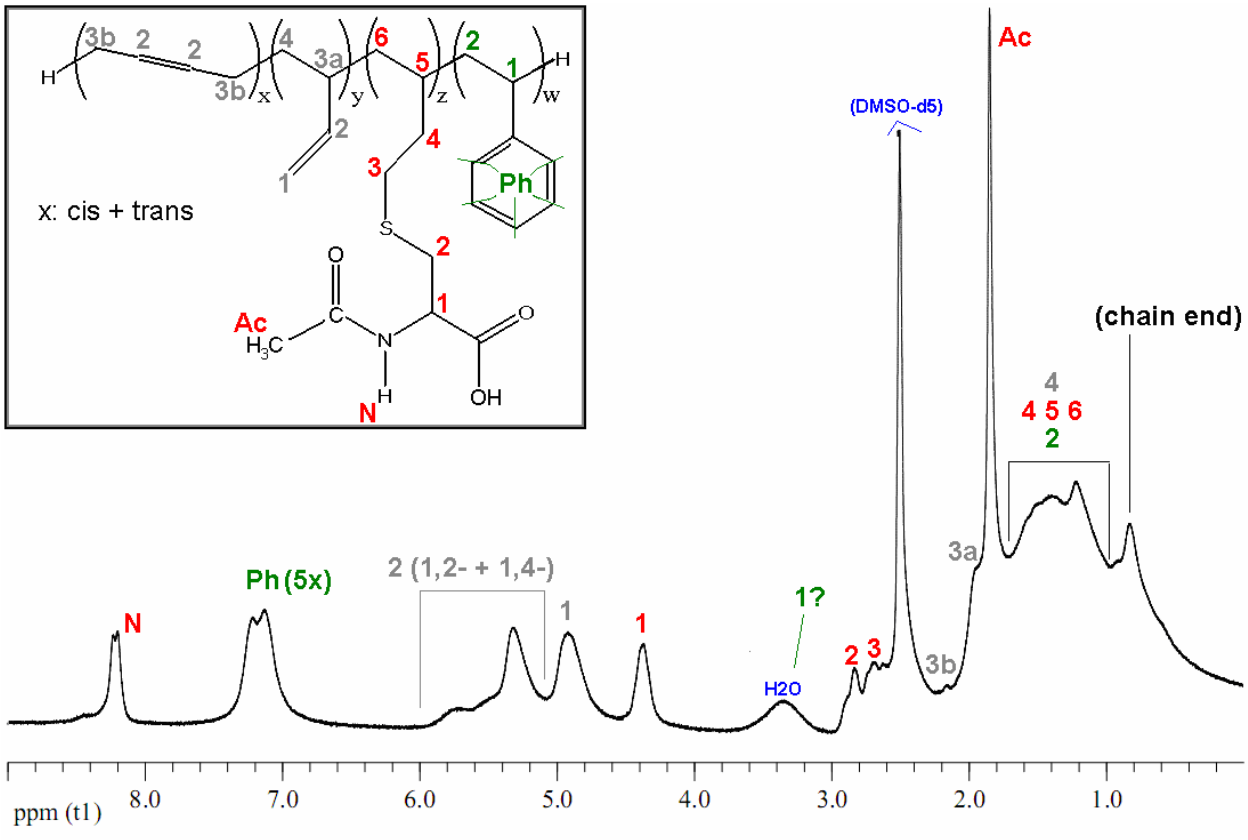

Figure 38 – ^{1}H-NMR spectrum of SBRLNCys075 (200 MHz, DMSO-d_6, 25°C)

The spectrum is very similar to that of PBNCys100 (Figure 14, page 71); in green, the five aromatic protons are in evidence at 7.0-7.4 ppm, and the methylene protons of the macromolecular backbone are located in the crowded 1.0-2.0 zone. The benzylic proton could be overlapped by the peak of water (in DMSO-d_6 the water proton falls at 3.4 ppm) due to the solvent.

The signal accounting for styrenic protons (δ = 7.0-7.4 ppm) can be conveniently used as an internal standard, since these units do not take part to the thiol-ene reaction. According to the nomenclature adopted in Figure 38, one can write:

$$\begin{cases} A_{7.2} = 5w \\ A_{4.4} = z \end{cases}$$

And, defining DF_v as the number of grafted units with respect to vinyl units (analogously to what done for PBNCys samples):

$$n_{Cys,grafted} = z$$

$$n_{Pol,0} \cdot \left(\frac{13.1}{100} \right) = w$$

$$DF_v = \frac{n_{Cys,grafted}}{n_{Pol,0} \cdot \left(\frac{62.0}{100} \right)} = \frac{z}{w} \cdot \left(\frac{13.1}{62.0} \right)$$

Where $n_{Cys,grafted}$ is the molar amount of grafted NCys and $n_{Pol,0}$ is the initial amount of monomeric units; the fraction arises from the characterisation of SBRL (chapter 2.3.1, page 105). In conclusion:

$$DF_v = \left(\frac{A_{4.4}}{A_{7.2}} \right) \cdot \left(\frac{5 \cdot 131}{620} \right)$$

$$DF = DF_v \cdot 0.62$$

Where DF is the functionalisation degree, and $A_{x.y}$ is the area of the peak of the proton NMR spectra having its maximum at x.y ppm. This calculation method is similar to the one used for PB: a non-reactive unit belonging to the macromolecular backbone is used as an internal standard.

The DF_v displayed in Table 21, collected with the described NMR method, are put into a graph in Figure 39 against the feed ratio (from 0.1:1 = 10% to 1.1 = 100%). In Figure 40 the trend of thiol conversion with the feed is represented.

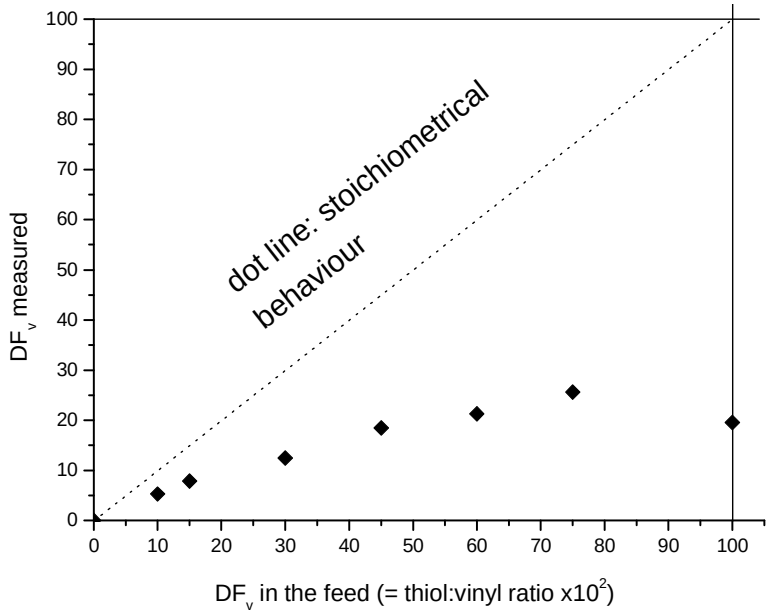

Figure 39 – Measured DF_v *vs* theoretical DF_v of SBRLNCys runs

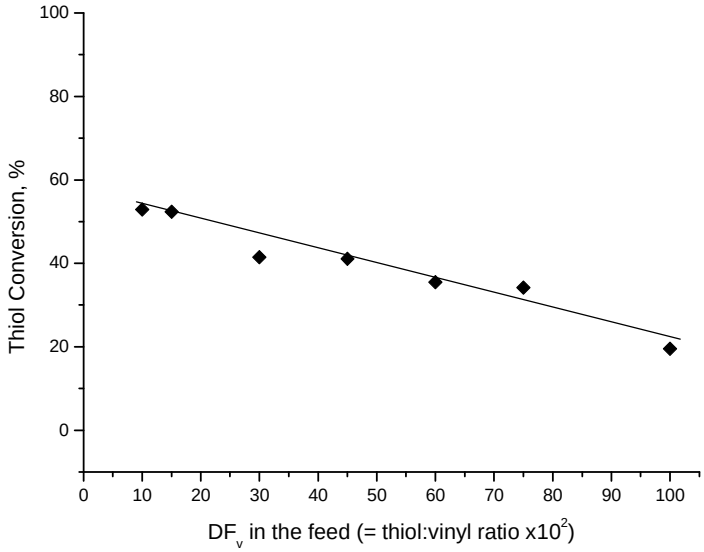

Figure 40 – Conversion of thiol *vs* feed ratio (0.1:1 = 10% to 1:1 = 100%) in SBRLNCys runs

In the first graph, the functionalisation degrees calculated for SBRLNCys samples are very small. The DF_v increases, almost linearly, up to a value of 20-25 mol.-%; this value complies with the results reported in literature[54, 112]. In the next chapters this trend will be compared with that observed with PBL; in any case, the reaction has lower yields in the case of SBRL with respect to PBL. This could be explained by the increased steric hindrance around the vinylic groups due to the presence of styrene moieties in the macromolecular backbone.

The thiol conversion, represented in Figure 40, decreases (from 53 to 20%) with the feed ratio: this suggests that the reaction is more difficult when the thiol:ene initial molar ratio is high. Probably the steric hindrance of the macromolecules being functionalised does not allow the incoming molecules of NCys to be efficiently added to the macromolecular backbone. A more accurate explanation should take into account side reactions; this will be the subject of next chapters.

2.3.5 Side reactions: cyclisation and chain-elongation

As observed by Schlaad and co-workers[109, 110], neighboring butadienic units could lead to cyclisations when treating a dienic polymer with a thiol; in order to avoid this undesirable side-reaction, a *spacer* between double bonds in the polymer backbone could lead to the complete conversion of unsaturations, and this has been demonstrated in the cited studies. In SBRL the (random) presence of styrene groups in the macromolecular chain could help avoiding cyclisations. In the considered system, such a benefit on the conversion degree could explain the high values reached especially when the thiol:ene feed ratio is low (Figure 40, values of x: 10 and 15).

Theoretically, an evaluation of the amount of vinyl-vinyl diads (whose presence is necessary for the cyclisation side reaction) could arise from the ^{13}C-NMR spectrum of SBRL; but, as observed by Sato in 1989[306], the signal of v-v diads is always overlapped to that of S-v diads and it cannot be resolved (for PB homopolymer, instead, the calculus is viable[307]).

In order to better understand the occurrence of side-reactions, an evaluation of the *lack* of vinyl units in the SBRLNCys samples is proposed here. Analogously to what done before for the PBL samples (Figure 20, page 79), the SBRLNCys primary structure is described in terms of monomer units in Figure 41. 6-membered cyclic units only were taken into account in the structure description.

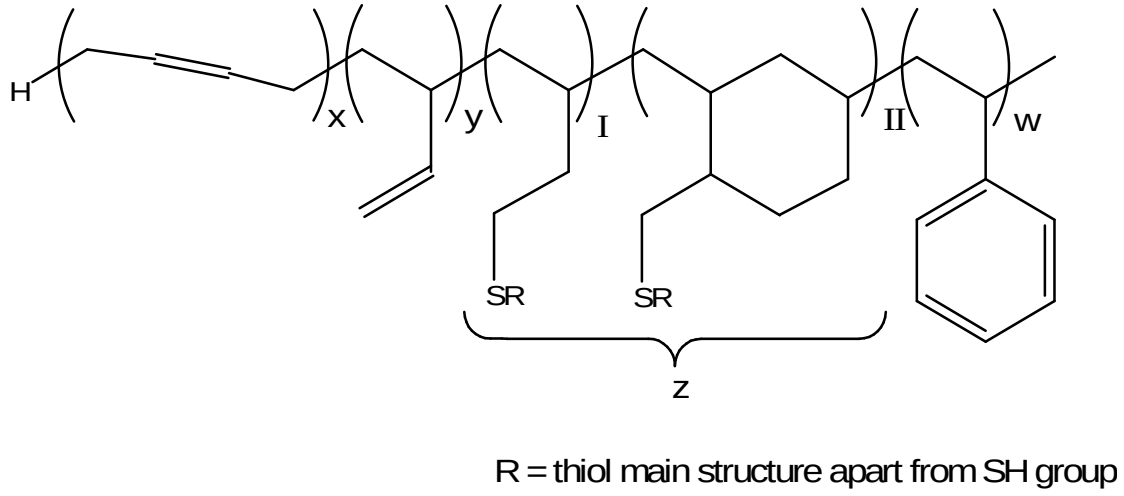

Figure 41 – Primary structure of the functionalised SBRL samples, cyclic units included

Having a good internal standard in the ^{1}H-NMR spectrum (the signal associated to the styrene protons, amount: *w*), the amount of lacking units per 100 monomers can be easily calculated as the difference (*II* = 100–*x*–*y*–*w*–*z*, *I* = *z*–*II*). The amount of different units constituting the primary structure of SBRLNCys samples, normalised to 100 monomeric units, is reported in Table 22.

Run	[RSH]:[vinyl C=C]	*w* (fixed)	*x*[a]	*y*[b]	*z*[c]	II[d]	I[e]	I : II ratio
SBRL (pure)	-	13.1	24.9	62.0	-	-	-	
SBRLNCys100	1.00:1	13.1	22.3	45.6	12.1	6.9	5.2	0.75
SBRLNCys075	0.75:1	13.1	22.5	43.1	15.9	5.4	10.5	1.94
SBRLNCys060	0.60:1	13.1	23.6	45.3	13.2	4.8	8.4	1.75
SBRLNCys045	0.45:1	13.1	23.3	48.0	11.5	4.1	7.4	1.80
SBRLNCys030	0.30:1	13.1	24.8	49.7	7.8	4.6	3.2	0.70
SBRLNCys015	0.15:1	13.1	25.0	54.4	4.9	2.6	2.3	0.88
SBRLNCys010	0.10:1	13.1	24.8	57.5	3.3	1.3	2.0	1.54

Table 22 – *x,y,z,w*, I and II values for functionalised SBRL samples.

[a] $x = (A_{5.5} - A_{5.0} / 2) / 2$; [b] $y = A_{5.0} / 2$; [c] $z = A_{4.3}$; [d] II = 100 – *x* – *y* – *z* – *w*; [e] I = *z* – II.

Let us consider the *x* column, accounting for 1,4-butadienic units (see Figure 41). The initial amount, 24.9 mol.-%, is mantained in almost every reaction, except when the DFs are high (samples 045, 060, 075, 100). In these samples, probably, a certain amount of *cis* units (less than 2.3 mol.-%, in any case) reacted with the thiol, generating 1,4-NCys adducts; in any case, the 1,4-units displayed a very limited reactivity, and their amount is almost unchanged. This confirms the previous literature results on the lower reactivity of 1,4- units *vs* the 1,2- ones.

The lack of vinyl units is small regardless of the sample: column *y* shows values similar to that of the pristine rubber (62.0 mol.-%).

In Figure 42 the values of *z* (that corresponds to the DF) and the amount of lacking units are rported *vs* the thiol:vinyl feed ratio.

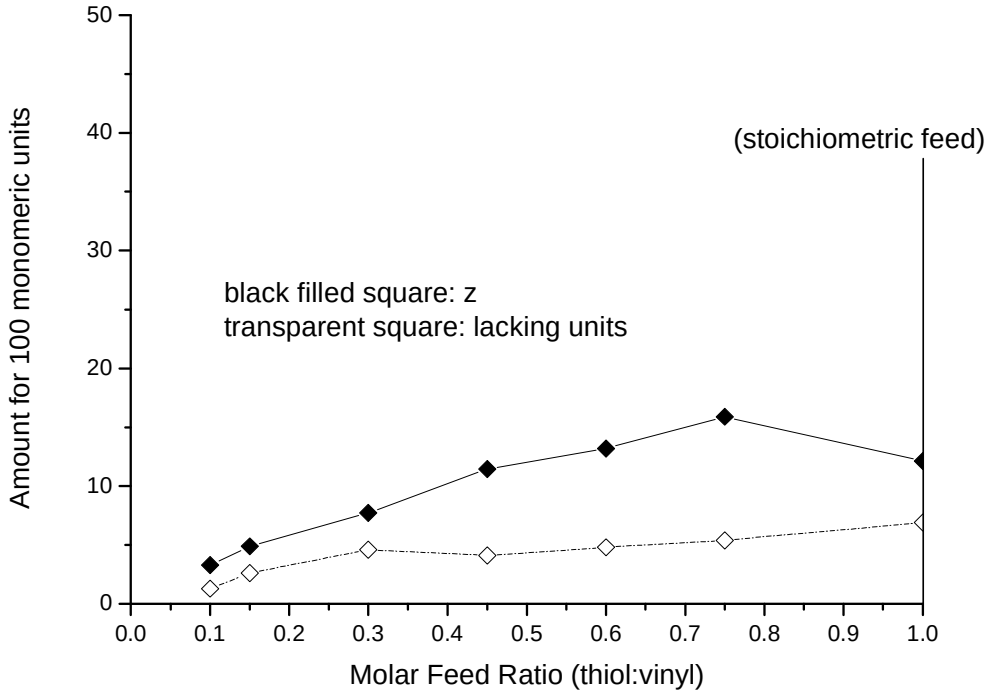

Figure 42 – Values of *z* (=DF; DF = $DF_v \cdot 0.62$) and lacking units *vs* feed ratio for SBRLNCys samples

The small amount of lacking units suggests that only a few of the initial double bonds are involved in side-reactions. Their scarce occurrence in SBRLNCys runs could be due to two main issues:

(i.) cyclisation is not favoured, probably because of the small amount of v-v diads in the SBRL macromolecular backbone as shown from the NMR characterisation (see chapter 2.3.1, page 105)

(ii.) chain-chain coupling scarcely occurs.

The primary structure of SBRL could play an important role not only in point (i.) but also in point (ii.); experiments aimed to determine the influence of SBRL structure on its sensitivity to chain elongation events were performed and will be discussed in the next paragraph.

A reaction between SBRL and dicumyl peroxide (DCP) was carried out analogously to what was done before in the case of PBL (chapter 2.2.5, page 76). The purpose of this reaction run (*SBRLDCP*) was to investigate the occurrence of side reactions involving 1,2- units, even if first evidences showed that this kind of reactions did not substantially affect the addition reaction.

The same experimental conditions of the PBDCP run were chosen: absence of thiol, nine hours in refluxing chlorobenzene, initial 0.05 DCP:vinyl molar feed ratio. The particularly low solubility in MeOH of the polymeric products of the SBRLDCP run made possible precipitating the polymer in this solvent; the soluble product, characterised through IR spectroscopy, showed traces of both acetophenone and 2-phenylpropan-2-ol, along with minor traces of SBRL.

The polymer, purified through several precipitations in MeOH and dried to constant weight with a void pump, was characterised through ^{1}H-NMR spectroscopy; the spectrum of SBRLDCP dissolved in $CDCl_3$ is reported in Figure 43.

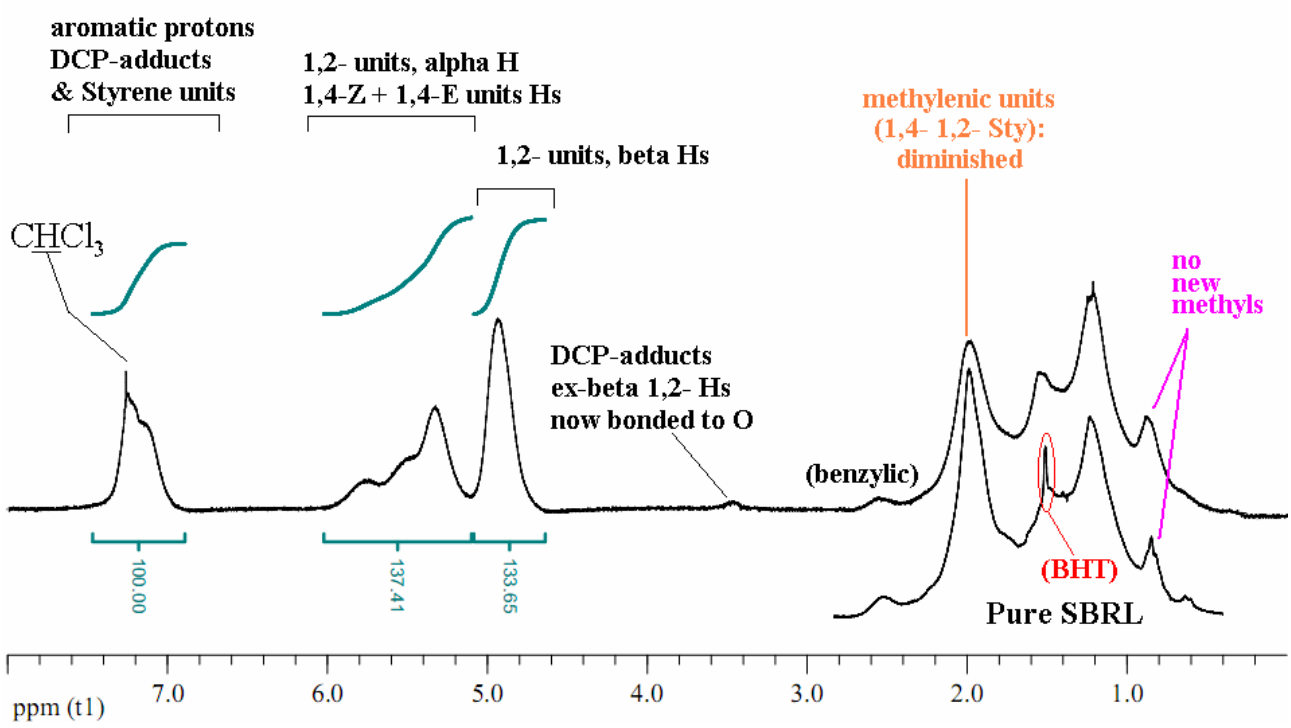

Figure 43 – Proton NMR spectrum of SBRLDCP in deuterated chloroform. 25°C, 300MHz, 64 scans

Several differences can be observed between the SBRL and the SBRLDCP spectra.

(i) The areas of peaks attributed to sp_2 hydrogens in the [4.6…6.0] ppm interval is different (in the next paragraph this difference will be quantified in terms of polymer composition).

(ii) The BHT (signal of the Bu^t protons at δ = 1.5 ppm) is removed during the polymer precipitation in MeOH, and the cited peak disappears in SBRLDCP.

(iii.) There are no new methyl groups after DCP treatment. A deconvolution of the peaks belonging

to the section [0...3] ppm of the spectra of pristine SBRL and SBRLDCP was performed: the area of the peak marked in pink in Figure 43 is nearly the same in the two spectra (-0.4%).
(iv.) The signal associated to methylenic hydrogens at 2.0 ppm is decreased in intensity.
(v.) The signal accounting for benzylic protons is decreased as well.
(vi.) A small peak attributed to adducts of cumyl radical and 1,2- units is observed at $\delta = 3.5$ ppm; a similar signal was observed in the PBDCP spectrum (Figure 23, page 88). In both cases, SBRLDCP and PBDCP, the peak area is not sufficient to estimate a functionalisation degree.

The NMR determination of the amounts of monomeric units for SBR copolymers reported in literature[298] could allow us to calculate these values for the SBRLDCP sample. The calculus is affected by an error, as seen for the case of PBDCP, PBNCys and SBRLNCys samples: if vinyl units are missing because of chain elongation / cyclisation, all the amounts of the other units (styrene, 1,4-, 1,2-) will be increased. Rescaling the values with respect to styrene groups, fixed at 13.1 mol.-%, the amount of lacking units could be estimated by difference in the usual way.
The structure of SBRLDCP is:

- 13.1 mol.-% styrene
- 23.1 mol.-% 1,4- units (sum of 1,4-*cis* and 1,4-*trans*)
- 43.8 mol.-% 1,2- units
- 20.0 mol.-% lacking units.

While the 1,4- units seem unaffected by the DCP treatment, the amount of vinyl units decreases; in any case, the results show a relatively small amount of lacking units in the SBRLDCP experiment, confirming that chain-chain coupling/ cyclisation scarcely occur in SBRL-based systems.

Another confirmation that side reactions occur in a small extent comes from SEC, although, as said before, cromatographic measurements of MW are difficult to be evaluated if performed on copolymers.

The chromatogram of SBRLDCP was collected using chloroform as the mobile phase, in the same experimental conditions adopted for SBRL characterisation (see chapter 2.3.1, page 105). Both pristine SBRL and SBRLDCP showed a bimodal distribution of MWs; the values of molecular weight are determined after performing peak deconvolution of the RI chromatogram and using a calibration curve built with PS standards.
The values are compared with those of pristine SBRL in Table 23.

	SBRL			SBRLDCP		
Peak	M_n, Da	M_w, Da	PDI	M_n, Da	M_w, Da	PDI
A	11080	11230	1.01	7210	13210	1.83
B	4970	5180	1.04	3710	6990	1.88

Table 23 – SEC evaluation of molecular weights of pristine SBRL and SBRLDCP

The values of PDI of both peaks were much increased after the DCP treatment, going from 1.01-1.04 to 1.83-1.88; moreover, the $<M_n>$ values of SBRLDCP decreased with respect to those of pristine SBRL, while the $<M_w>$ values increased.

Two reaction events could occur: (i.) some macromolecules undergo chain scission becoming low MW products; (ii.) these latter fragments undergo chain-chain coupling to become macromolecules having high MW. If the chain-chain coupling rate does not depend on the molecular weight of the molecules being coupled, a broad distribution of molecular weights is obtained.

The degradation behaviour has already been observed in SBR copolymers treated with heat or with free radical generators[170, 308]. In particular, the abstraction due to heat of a methylenic proton near to a styrene moiety could result in a reduction with molecular hydrogen elimination (Scheme 23, reaction path A) or in a chain scission reaction (reaction path B). If the $H^{\bullet}$ radical is removed by a chemical species such as a radical genereted by an initiator, path B would be favoured; the reduced amount of benzylic and methylenic protons observed in the proton NMR spectrum of SBRLDCP (Figure 43) complies with the occurrence of this chain-scission reactivity.

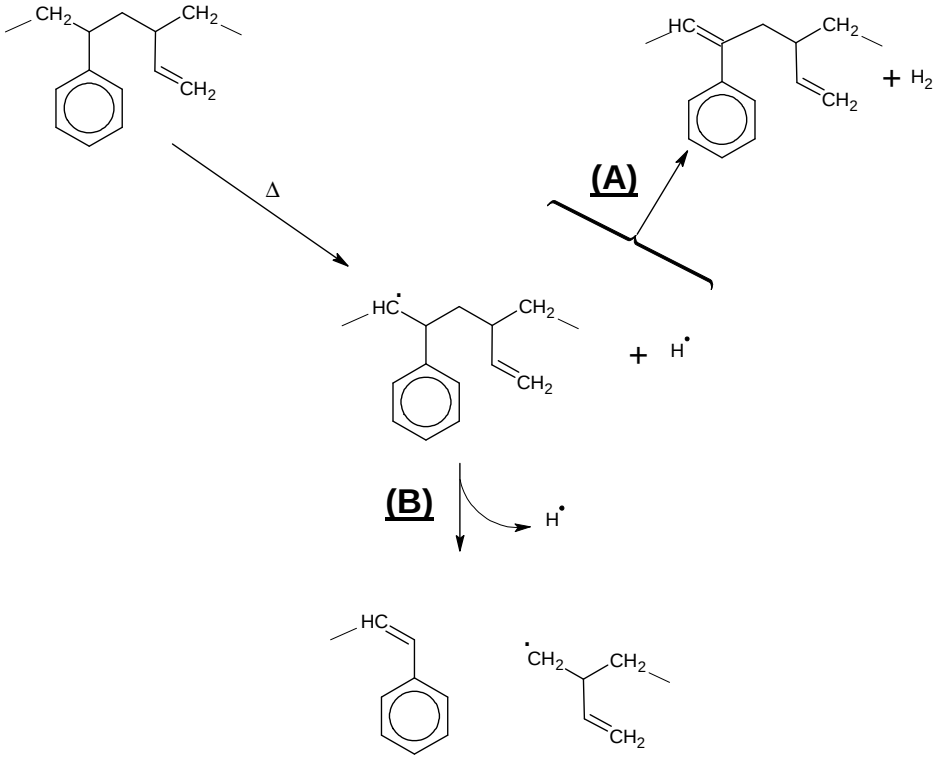

Scheme 23 – Possible paths of a S-v diad treated with heat; adapted from ref.[170]

The combination of SEC data and of the NMR data confirms that in SBRLDCP a large rearrangement of the macromolecules occur; due to the peculiar mechanism of the involved reaction paths, though, the overall double bonds disappearance extent is small, even smaller than in the case of PB functionalisation. As seen, the chain scission mechanism involves the formation of a double bond (Scheme 23, path B), while the chain-chain coupling consumes unsaturations (Scheme 17 and Scheme 18, page 78). The observed overall reduction in terms of vinyl units amount could be the result of an average occurrence of both these reactions.

2.3.6 Functionalisation run carried out in absence of AIBN

A SBRL functionalisation run using NCys has been carried out in absence of AIBN analogously at what done with PBL (chapter 2.2.6, page 89). For the SBRLNCys experiment carried out in absence of AIBN (*SBRLNCys030 woAIBN*), the chosen thiol:vinyl molar feed ratio has been 0.30.
The purified reaction product looked less powderous than SBRLNCys030, that is the sample obtained with the same thiol:vinyl feed ratio but in presence of AIBN. The DF_v of this sample was measured through the analysis of the ^{1}H-NMR spectrum, and it was 7.2% (conversion: 24%); the DF_v of SBRLNCys030 (Table 21, page 116) was 12.4% (conversion: 41%). This reduction in conversion complies with the literature data on similar systems[40, 48, 57].

2.3.7 Calorimetric measurements of the glass transition temperature

The T_g of the SBRLNCys samples was determined through DSC, analogously at what done before for PBNCys and PBNCysMe functionalised samples (chapter 2.2.8, page 93).
A graph T_g *vs* DF (DF = $DF_v \cdot 0.620$) for the SBRLNCys samples is reported in Figure 44.

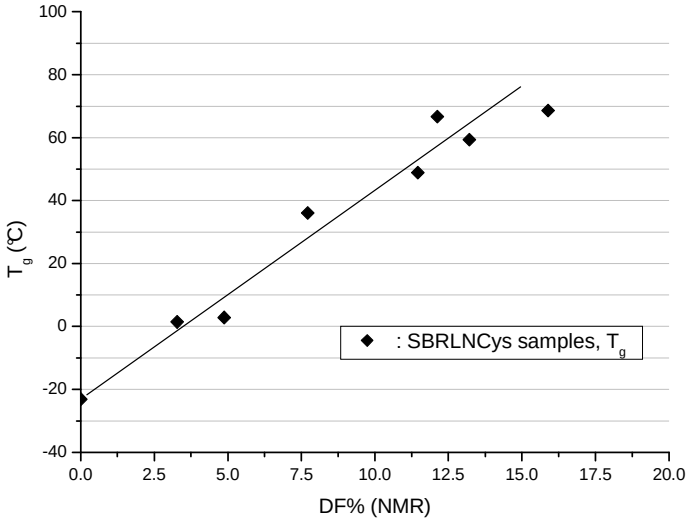

Figure 44 – T_g *vs* DF graph for SBRLNCys samples

The T_g increases almost linearly with the polymer composition within the considered DF range.

A convex graph T_g *vs* copolymer content has seldom been observed for styrene copolymers (one case is that of Sty / AN[272]); it should account for a random structure of the functionalised samples rather than a block-copolymer structure. Most styrene copolymers including polar comonomers display a concave dependence of the T_g *vs* composition (Sty / MMA[269, 270, 274], α-MeSty/ AN[271]), or a linear one (Sty / acrylic acid[309], Sty / MA[274], Sty / ethyl MA[264], Sty / butyl MA[264], Sty / octyl MA[264]). These trends, as previously observed, account for long styrene sequences in the macromolecular backbone; in any case, the graph for SBRLNCys samples has a too small *x* range to infer the concavity / convexity of the graph. As seen in literature studies, the concavity / convexity could be rather steep (graphs having a V-shape rather than a U-shape), and only a complete set of copolymers with molar comonomer composition ranging from 0:100 to 100:0 could help in identifying the behaviour[264].

The glass transition temperature of the sample *SBRLNCys030 woAIBN* is 0.5°C, similar to that of SBRLNCys samples having a similar DF_v. In Figure 45, the T_gs of this run and some SBRLNCys runs are compared on the same graph *versus* the measured DF_v of the samples.

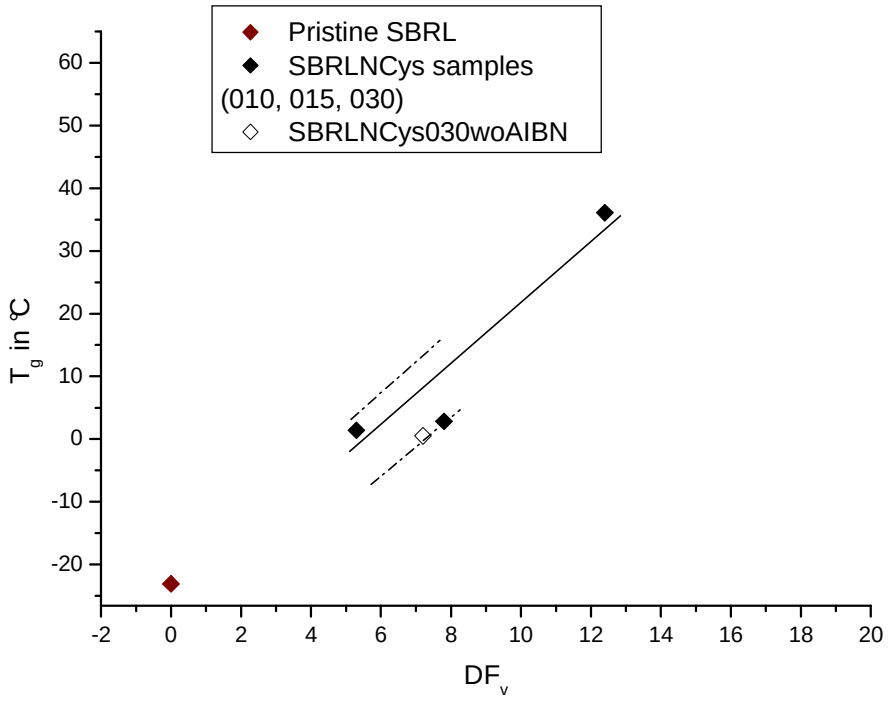

Figure 45 – T_g of SBRLNCys030woAIBN and similar SBRLNCys experiments *vs* DF_v

As said, in the case of SBRL the side reactions are not really affecting the thiol-ene reaction, both with or without the presence of AIBN; consequently, the reaction products are very similar not only in terms of primary structure but also regarding the thermal properties.

2.3.8 Polarimetric measurements

Measurements of polarimetry on SBRLNCys samples in 1,4-dioxane solution at C = 1 (g / 100 ml) were performed. The perfectly clear solutions showed rotation of the light polarisation plane; the values of [α] for the SBRLNCys samples, are listed in Table 24.

The *rescaled* optical rotating power [ϕ], obtained dividing the specific optical rotating power [α] for the cysteine derivative content in the polymer (DF wt.-%), would resemble the [α] of a solution of the pure amino acid. The [ϕ] values are reported in Table 24; a graph displaying the value of [ϕ] *vs.* the DF wt.-% is reported in Figure 46.

Run	DF wt.-%[a]	$[\alpha]_{589}^{25}$ [b]	$[\varphi]_{589}^{25}$ [c]
NCys	(-)	+39.2	(-)
SBRLNCys100	23.7	+5.3	+22.5
SBRLNCys075	29.0	+5.9	+20.3
SBRLNCys060	25.3	+5.5	+21.7
SBRLNCys045	22.7	+5.1	+22.6
SBRLNCys030	16.5	+6.1	+37.0
SBRLNCys015	11.1	+4.9	+44.1
SBRLNCys010	7.8	+3.2	+41.0

Table 24 – Relationship between absolute DF (wt.-%) and the specific optical rotating power of samples

[a] Measured by ^{1}H-NMR; [b] Measured by a polarimetre at 25°C (C = 1 g / 100 mL); [c] $[\varphi]_{\lambda}^{T} \equiv \frac{[\alpha]_{\lambda}^{T}}{(DFwt-\%)\cdot 100}$

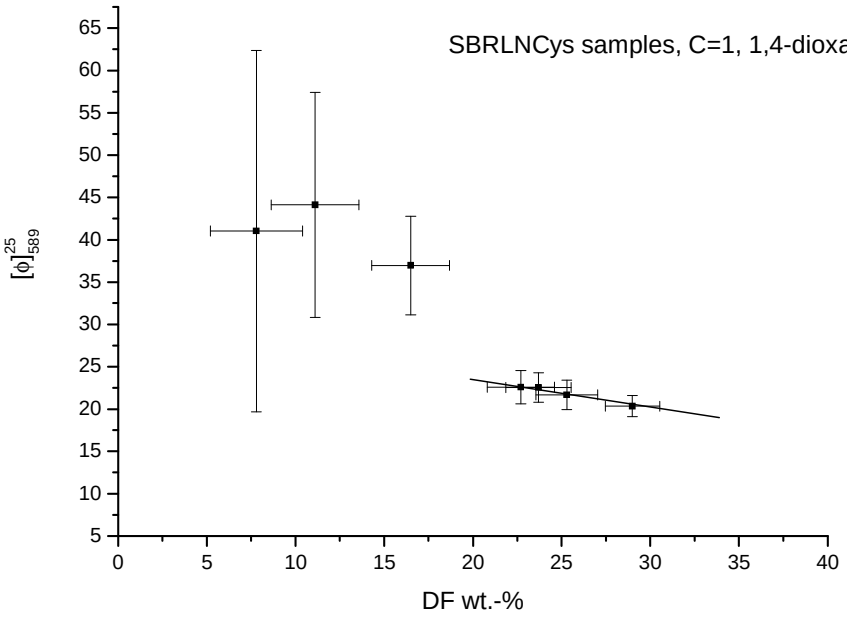

Figure 46 – [ϕ] versus DF wt.-% for PBNCys and SBRLNCys samples at C = 1 in 1,4-dioxane

The error bars appearing in Figure 46 were calculated considering a ±2% error in the DF_v determination; this is directly related to the *x* error. The value has been estimated from classical works on the ^{1}H-NMR determination of SBR primary structure[298, 310, 311].

The error arising from the NMR determination of the DF_v has also an influence on the *y* error, as it appears in the definition of $[\phi]$ along with the error on the value $[\alpha]$ (that is related to the polarimetre error).

The *x* and *y* error are small only for highly modified samples; in fact, as said, the *y* error depends not only on the polarimetre measurement error but also from the *x* error.

Considerations on the data of SBRLNCys010, 015 and 030 are difficult because of the entity of error on the measured values. For samples having higher DFs, the absolute value of $[\phi]$ decreases with increasing DF wt.-%; this trend is the same observed for PBL samples (chapter 2.2.9, page 99).

2.4 Comparison of the *N*-acetyl-L-cysteine thiol-ene reactivity towards PBL *vs* SBRL

The primary structure of PBL is rather different than the one of SBRL. Apart from the presence of styrene moieties in SBRL and from the different relative amounts of constitutive units, also the unit sequencing can be different. As said, though, this characteristic cannot be discussed because of the difficulties in the evaluation of ^{13}C-NMR spectrum of SBR copolymers.

In Table 25 the composition of PBL and SBRL are compared (units per 100 monomers).

Run	Styrene	1,2-	1,4-*cis*	1,4-*trans*
PBL	-	90.9	~0	9.1
SBRL	13.1	62.0	15.6	9.3

Table 25 – Composition of PBL and SBRL; values are normalised to 100 monomeric units

The amount of 1,2- units is smaller in SBRL than in PBL (90.9 mol.-% *vs* 62.0 mol.-%); this leads to smaller absolute functionalisation degrees. The adopted feed ratios for both series of experiments described in previous chapters (PBNCys and SBRLNCys) has been related to vinyl units; therefore the reactivity of the thiol towards the polymeric substrates will be compared by considering the DF_v, but the other properties of the functionalised samples will be evaluated with respect to the *absolute* DF, a parameter that better represents the modification of polymers. According to Table 25, for PBNCys samples, $DF = DF_v \cdot 0.909$, while for SBRLNCys samples, $DF = DF_v \cdot 0.62$.

Another difference is the amount of 1,4-*cis* butadiene units, that in SBRL is the second most common unit type after vinyl units. These units are a little reactive with thiols, as seen in scientific

literature[33] and as observed from ^{1}H-NMR units determination performed on SBRLNCys samples (chapter 2.3.4, page 117). In the cited chapter, though, the reaction between 1,4-*cis* units and NCys is only supposed basing on a measured defect of units rather than a peak assignment associated to NCys/1,4- adducts. The MWs of the substrates are similar: according to the supplier data sheet, the molecular weight of SBRL determined through SEC is 4500 Da, while for PBL the SEC data account for a MW of 4080 Da (PDI: 1.43, see chapter 2.2.7, page 90).

2.4.1 Reactivity and conversion

The DF_v *vs* thiol:vinyl molar feed ratio graphs and the conversion degree *vs* thiol:ene molar feed ratio graphs of the SBRLNCys and of the PBNCys sets are compared, respectively, in Figure 47 and Figure 48. The *x* axis of the two graphs is different: while in the first graph the objective is to compare the differences between DF_vs and the stoichiometrical behaviour (and thus the *x* axis is referred to vinyl units), in the second the aim is to compare the conversion degrees with respect to the overall feed ratio (thiol:total amount of monomeric units rescaled to 100, i.e. 0.1:1 = 10% and 1:1 = 100%). The initial primary structure of the polymeric substrate is the only property differentiating the two systems, as the functionalisation runs are carried out with the same experimental conditions.

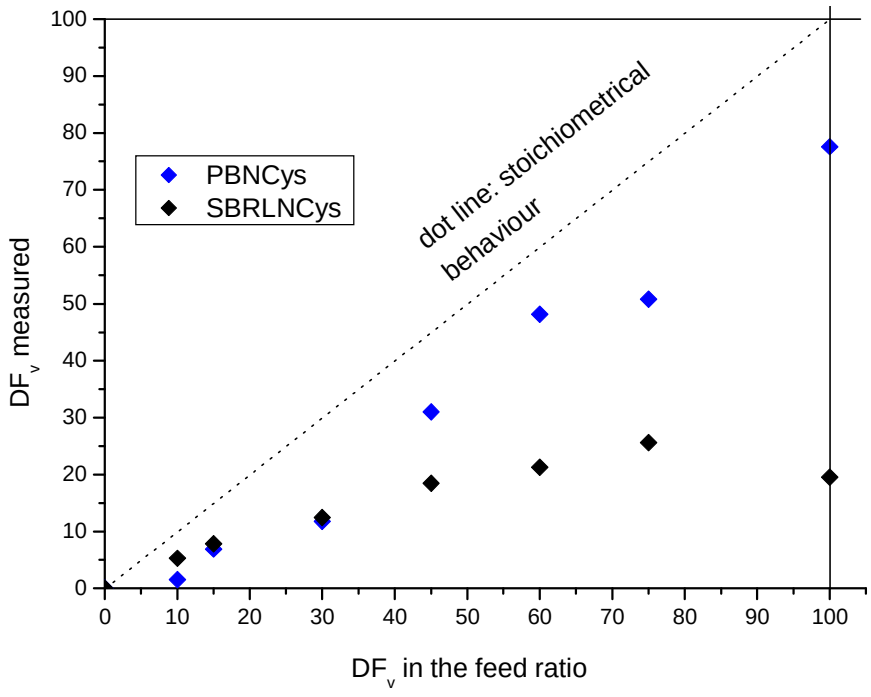

Figure 47 – Measured DF_v *vs* the molar feed ratio (%) of PBNCys and SBRLNCys runs

The functionalisation degrees for SBRLNCys samples are smaller than in the case of PBNCys. The DF_v increases almost linearly to a *plateau* around 20-25% of DF_v, while in the case of PBNCys samples the DF_v increases to much higher values (70-75%).

A possible explanation of this experimental evidence is that in the case of SBRL functionalisation the steric hindrance near to double bonds is higher than in the case of PBL. Another factor that could lower the DF is the relative stability of benzyl radicals generated by the initiator on the macromolecular chain: these radicals are stabilised by resonance and are not very reactive towards radicals or other double bonds as seen, for instance, during free radical grafting on PS[312, 313].

In Figure 48 the graphs conversion degree *vs* thiol:ene feed ratio (in percent) of SBRLNCys and PBNCys sets is compared.

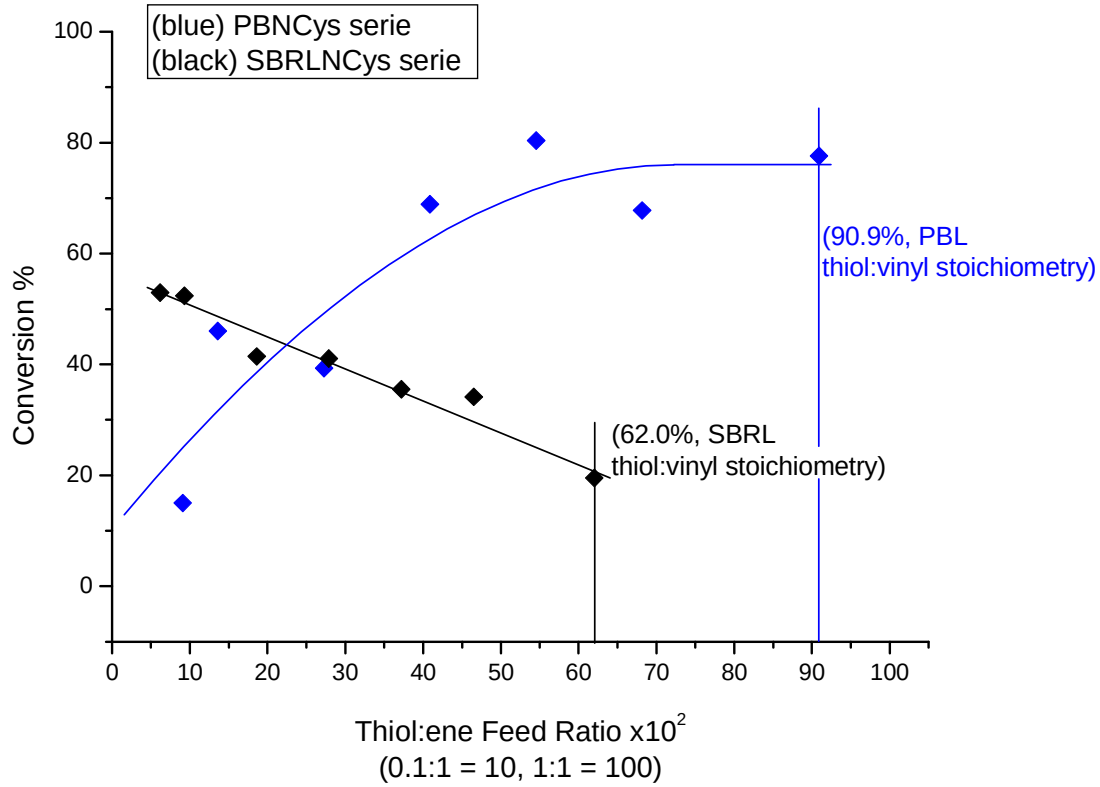

Figure 48 – Conversion of thiol *vs* thiol:ene feed ratio %: PBNCys *vs* SBRLNCys experiments

The trend of the thiol conversion is different for the two sets. In the chapter 2.2.5 (page 76) regarding PBL functionalisation, it has been shown that a considerable lack of vinyl units was observed especially for initial thiol:ene feed ratios lower than ~0.40:1. This evidence was shown to be indicative of a possible competitivity between side reaction reducing the amount of vinyl units and the functionalisation. An increase of the conversion with the thiol:ene feed ratio, in PBNCys samples, resulted into a *plateau*, and complete conversion was never reached. As previously discussed, the growing steric hindrance of the macromolecules being functionalised could limit the increase of conversion despite of the higher feed ratio.

In the case of SBRL, instead, a slight, homogeneous decrement of conversion with the thiol initial amount in the feed is observed. This behaviour could be explained by the presence of the bulky

styrene units influencing the approach of the thiyl radicals to the vinyl double bonds also in remarkable defect of thiol. The effect is even more remarkable if accompanied by the cumulative effect of functionalisation; as in the PBNCys samples, the macromolecules being functionalised become more and more sterically hindered, limiting the conversion degree to lower values even if the thiol:ene ratio is stoichiometric or nearly-stoichiometric.
As seen in chapter 2.3.5 (page 119) regarding side reactions occurring during SBRL functionalisation, the chain-chain coupling / cyclisation reaction paths are not much relevant, and cannot be invoked to explain the observed behaviour.

One of the most remarkable differences between SBRLNCys and PBNCys samples arises from the unexpected lack of vinyl units in the products: this value is quite small in SBRL samples with respect to PB samples. The amounts were determined fixing the amount of a certain structural moiety before and after the reaction; a similar internal standard (a group whose proton NMR signal remained unchanged before and after the thiol-ene reaction) was chosen as the 1,4-*trans* butadiene units for PBNCys samples and as the styrene units for SBRLNCys samples, as described in the respective chapters.
The amount of lacking units was defined as the difference between 100 and the sum of all the other groups, the amounts of which were evaluated through NMR spectroscopy and rescaled with respect to the internal standard. In Figure 49 a graph reporting both the amount of *z* (NCys-grafted units, rescaled to 100 monomers; it is equal to DF for PBL) and the amount of lacking units per 100 monomers (obtained by difference) *versus* the feed ratio in terms of thiol:vinyl ratio is reported.

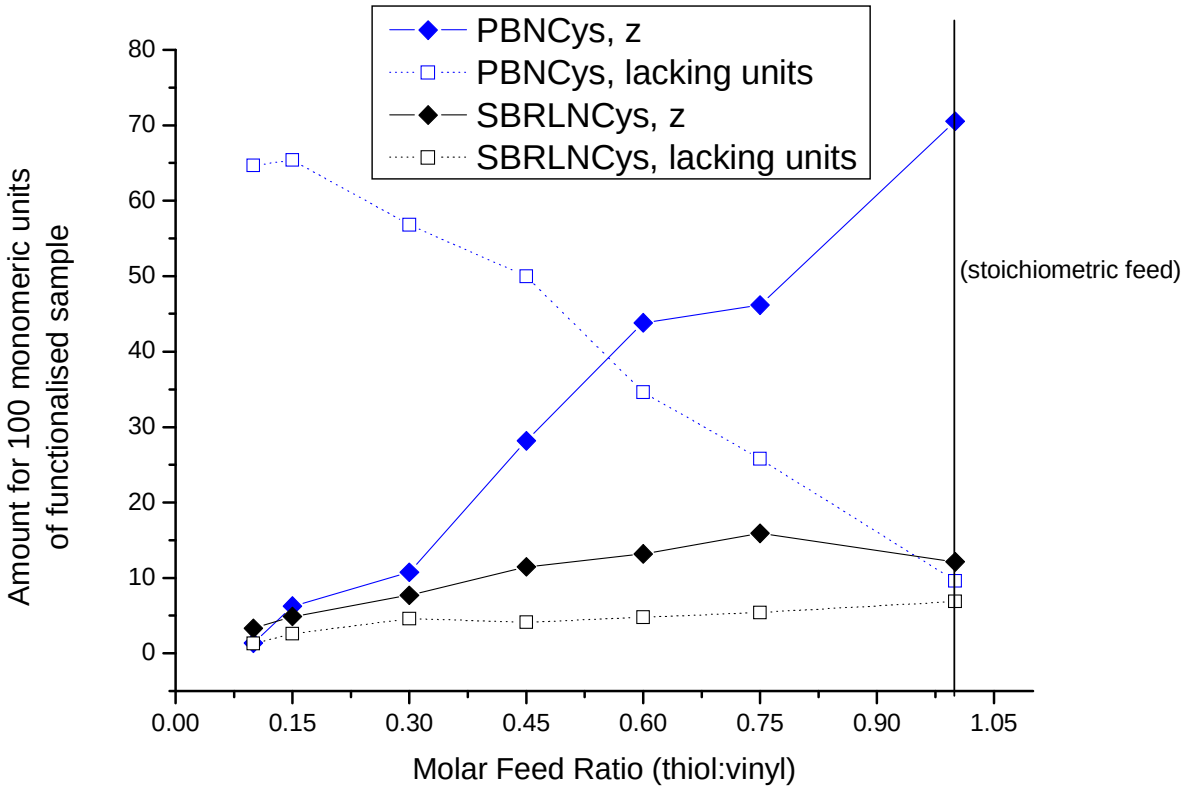

Figure 49 – Values of *z* and amount of lacking units per 100 monomers *vs* feed ratio

The difference, in terms of lacking units, between SBRLNCys and PBNCys samples is remarkable. In particular, for SBRLNCys this amount is near to the experimental error occurring in NMR determinations; in fact, the determination of type I units (Table 22, page 120) and of the I:II ratio led to results having unclear trends.

Probably many of the lost 1,2- units in PB samples were involved in cyclisation, a reaction rather difficult in SBRL because of the smaller amount of v-v diads. Moreover, the occurrence of chain scission events, a peculiarity of SBR substrates, could potentially regenerate some of the lost unsaturations, contributing to the overall amount (chapter 2.3.5, page 119).

The possibility of performing the thiol:ene addition without any radical initiator has been investigated for both PBNCys and SBRLNCys samples according to prior art[40, 48, 57].

In Table 26 an overview of the functionalisation degree data regarding the experiments PBNCys030, SBRLNCys030 and of the respective runs carried out in absence of AIBN is shown. These experiments were originally described in chapters 2.2.2 and 2.3.3 (respectively PBNCys030 and SBRLNCys030, i.e. the reactions carried out in presence of AIBN) and in chapter 2.2.6 and 2.3.6 (respectively PBNCys030woAIBN and SBRLNCys030woAIBN, i.e. the reactions carried out in absence of AIBN).

Run	[AIBN]:[thiol]:[vinyl]	DF_v %	DF%	Thiol Conversion %
PBNCys030	0.003:0.30:1	11.8	10.7	39
PBNCys030woAIBN	-:0.30:1	10.4	9.5	35
SBRLNCys030	0.003:0.30:1	12.4	7.7	41
SBRLNCys030woAIBN	-:0.30:1	7.2	4.5	24

Table 26 – Overview of the conversion data of PB and SBRL funct. runs in presence / absence of AIBN

The reactivity of NCys towards PBL is almost unchanged with or without AIBN: the thiol conversion for the first two runs described in Table 26 is similar. On the other side, the drop in the conversion observed for the SBRLNCys samples carried out in presence or in absence of AIBN seems more pronounced, going from 41 to 24%, respectively.

In conclusion, the presence of a monomer unit acting as a *spacer* in the macromolecular backbone (the styrene moieties, SBRLNCys samples) between butadienic monomers exerts different effects in terms of reactivity:

(i) lowers the occurrence of the cyclisation side reaction (small amount of v-v diads);

(ii) could potentially lead to large macromolecular rearrangements (as seen for model systems with DCP) thanks to the peculiar reaction of chain scission;

(iii) puts a severe limit to the conversion degree, especially at nearly-stoichiometric feed ratios, probably because of the steric hindrance of styrene groups.

2.4.2 Thermal properties

The glass transition temperatures of PBL and SBRL are, respectively, 246.6 K (-26.6 °C) and 250.1 K (-23.1°C). By considering the T_g of PB as 246.6 K, the T_g of PS as 373.2 K (literature value) and the copolymer composition, one can roughly estimate the T_g of SBRL applying the Fox equation:

$$\frac{1}{T_g} = \frac{w_B}{T_{g,PB}} + \frac{w_S}{T_{g,PS}}$$

where T_g is the glass transition temperature of the copolymer, $T_{g,PX}$ is the glass transition temperature of the homopolymer of the *X* monomer and w_X is the weight mass fraction of the *X* monomer in the copolymer. The T_g of SBRL should be 266.9 K (-6.2 °C), but the measured value is lower, being 250.1 K. The observed deviation from the Fox equation is a common result when

considering copolymers of butadiene, as seen in chapter 2.2.8 (page 93); probably a better estimation of the SBRL's T_g would arise from the Uematsu-Honda equation, provided the complete knowledge of SBRL diadic structure (it is necessary for the use of the equation[259, 260]).

In Figure 50 a graph T_g *vs* absolute DF for both SBRLNCys and PBNCys samples sets is reported. For both the systems an increase of the glass transition temperature is observed by increasing the number of grafted functionalities, and can be discussed in terms of intermacromolecular chain interactions in the solid amorphous state (see chapter 2.2.8 page 93).

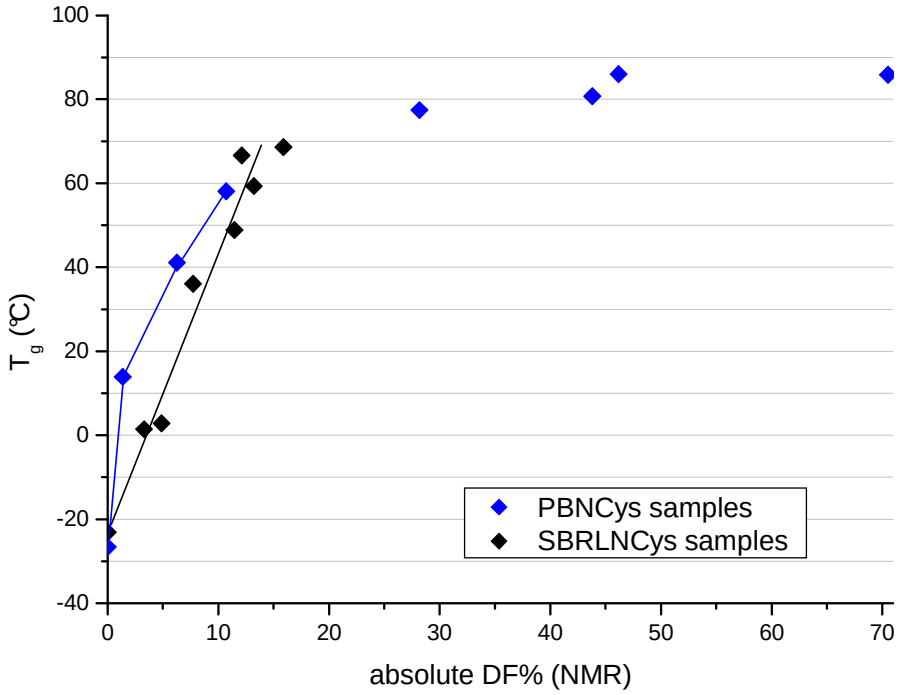

Figure 50 – T_g *vs* DF for PBNCys (blue) and SBRLNCys (black) samples.

The trend of T_gs of the SBRLNCys set is very similar to that of the PBNCys serie for 0<DF<15. Although the trend is the same, T_g values of PBNCys samples are slightly higher. This difference, observable only for the functionalised samples and not for the pristine materials, could be due to the presence of styrene moieties in SBRLNCys samples that lowers the possibility of intermacromolecular hydrogen bonding, thus increasing the molecular mobility in the products.

The linear increase of T_g in the [0…15] DF range is observed with the SBRLNCys, with the PBNCys and with the PBNCysMe sets of samples (last two are compared in Figure 24, page 93).

In the case of PB + NCys a remarkable difference was observed between the thermal properties of the samples obtained in absence or in presence of AIBN. In the case of SBRL, instead, the T_g of the sample functionalised in absence of AIBN (SBRLNCys030woAIBN) is similar to that of SBRLNCys015; this latter run was functionalised in presence of AIBN and its DF_v is similar to that of the *woAIBN* run (7.8% *vs* 7.2%).

This result, jointly with the conversion data for the experiments carried out in presence *vs* in absence of AIBN, confirms the different behaviour of PBL and SBRL in the adopted experimental conditions, especially in terms of side reaction occurrence.

With PBL, a small difference in the conversion between the *woAIBN* run and the sample carried out in presence of AIBN is accompanied by a lesser occurrence of side reactions. In the case of SBRL functionalisation, the conversion is about a half if AIBN is not used, but the extent of side-reactions is low in both cases. The T_gs of the SBRL experiments with or without AIBN is almost the same: this evidence complies with a scarce influence of side reactions influencing the molecular structure.

2.4.3 Polarimetry

The PBNCys, PBNCysMe and SBRLNCys samples showed all remarkable optical activity. In all the three sets, though, the specific rotating power of polymer solutions [α] decreased in absolute value with increasing DF, and a similar decrement was observed also for the rescaled optical rotating power [ϕ]. This value, obtained dividing the optical rotating power [α] for the cysteine derivative content in the polymer (DF wt.-%), would be the [α] of a solution of the pure amino acid. In Figure 51 a graph [ϕ] *vs* DF wt.-% in which the values for the PBNCys and for the SBRLNCys sets is reported (the values for the least functionalised SBRLNCys samples, named SBRLNCys010, 015 and 030, are omitted). The cases of PBNCys and PBNCysMe samples were further investigated through CD spectroscopy, but no clues for secondary structures were found.

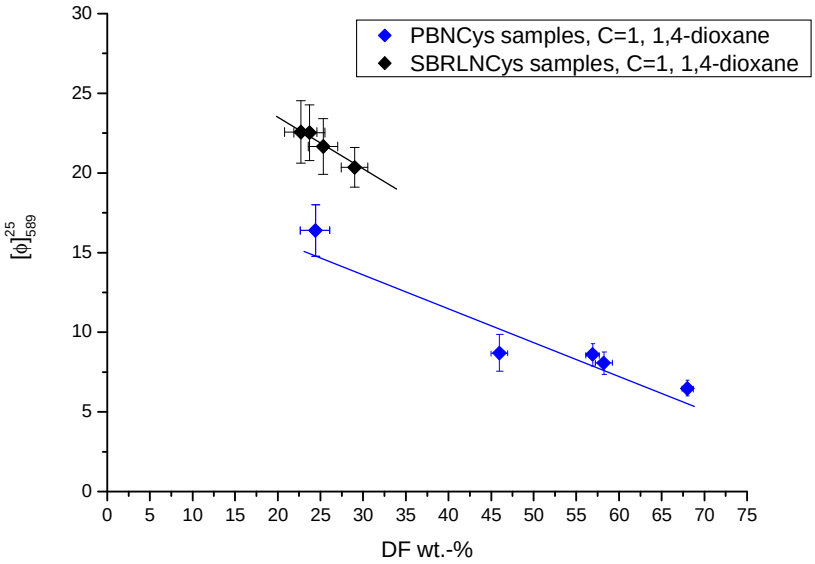

Figure 51 – [ϕ] versus DF wt.-% for PBNCys and SBRLNCys samples at C = 1 in 1,4-dioxane

The absolute value of [ϕ] decreases with increasing DF-wt.% both for PBNCys and for SBRLNCys samples. (This behaviour is also encountered with PBNCysMe samples.) The values for

SBRLNCys samples are higher; this could be reasonably due to the different polymer composition. As well as in the PB functionalised system, the [ϕ] trend in SBRLNCys samples could account for an influence of the relative proximity of the chiral units; this effect is higher especially at high modification degrees, when the chiral centres are closer to each other.

In conclusion, the SBRL functionalisation with NCys led to materials displaying a similar behaviour with respect to the PBNCys samples in terms of (i.) remarkable increase of the glass transition temperature and (ii.) optical activity. The main differences, instead, arise from the conversion degrees: the conversions for SBRLNCys samples are smaller than in the PBNCys case, probably because of the steric hindrance of the styrenic units; on the other side, for a low amount of thiol in the feed, the reaction is more effective, perhaps indicating a benefic effect of styrene moieties on the reaction (presence of a *spacer* preventing cyclisation side-reactions). Finally, the occurrence of side reactions is different, involving cyclisation and chain-elongation in the case of functionalised PBL and chain-scission and coupling in the case of functionalised SBRL.

2.5 Addition of NCys to high MW styrene/butadiene random copolymer

Analogously to previous works of the research group of Ciardelli on the thiol-ene functionalisation of diene polymers[32, 54, 112], several functionalisation runs were performed adding the cysteine derivative to a high molecular weight SBR, both in solution and in bulk. The purpose of these experiments was to investigate the thiol-ene reaction onto a rubber that has already been used as the elastomer matrix in reinforced compounds for automotive products: in fact, the direct functionalisation of the matrix of the tyre compound could represent a valid tool to achieve improved properties of the material (lower rolling resistance, better performances of the tyre on wet asphalt, *et cetera*). The addition of a cysteine-functionalised PBL or SBRL to an SBR-based tyre compound could represent an alternative method, and will be discussed in chapter 2.6, page 148.
Researchers working for *Bayer* produced a large number of patents regarding thiol-ene functionalisation of SBR during the first years of the current century. Apart from an explorative study of functionalisation of NR with various thiols[314], Scholl and co-workers at Bayer investigated the functionalisation of SBR with aliphatic thiols[315], 2-mercaptoethanol[316-318], 3-mercaptopropanoic acid[319-321], 1-mercapto-2-propanol[322] and more complex systems including different thiols[323]. Also other researchers worked on the reaction of SBR with mercapto-alcohols (patents belonging to the Goodyear group[324, 325]) and with 3-mercaptopropanoic acid (a work of Sylvie Gandon-Pain, Michelin S.à.S.[326]).

A common research line followed in the cited patents is directed towards the limitation of structural changes in the macromolecules. As seen also in previous chapters of the present work and in prior art, thiol-ene functionalisation involves chain-elongation as a side reaction; in particular, it has been observed during thiol-ene functionalisation of long-chain SBR[319-321]. With these substrates, typically, both the molecular weight and the molecular weight dispersion increased.

In patent literature, two methods are followed in order to avoid similar structural changes. The easiest workaround consists in avoiding the addition of free radical generators in the feed. As shown also in previous chapters of this work, a certain amount of thiyl radicals that are reactive toward the unsaturations are present also if no free radical generator is present. Moreover, in the case of reaction between PBL and cysteine derivatives, the presence of an initiator causes the polymer to undergo side-reactions, as shown from NMR spectra and from DSC measurements of the T_g; the runs carried out in absence of AIBN, instead, look less influenced by side reactions. On the other side, as said, the amount of grafted thiol is higher in presence of AIBN, as seen also in several literature works on PBL (Priola[31, 57], Oswald[38], Serniuk[48], and Cunneen[39, 40]).

The functionalisation of SBRL in absence of an initiator (chapter 2.3.6, page 125), instead, did not highlight conversion improvements or reduction of side reactions occurrence. However, using no initiator with a SBR substrate could be a viable possibility for avoiding chain elongation, if reaction conditions would lead to crosslinked products.

The second approach for preserving the molecular structure of the rubber consists in adding a chemical agent displaying selective quenching of macroradicals with respect to thiyl radicals, thus reducing the side reactions and not the thiol grafting. As shown from scientific literature of thiol-ene functionalisation of polymers, the side reactions are favoured by the presence of free radicals on the macromolecular chain.

In a work of 2004[326], Sylvie Gandon-Pain studied the thiol-ene functionalisation of various long-chain SBR copolymers with 3-mercaptopropanoic acid (in solution) or 11-mercaptoundecanoic acid (in the bulk, with a Banbury-type mixer). Apart from functionalisation runs carried out in solution and in absence of free radical generator, the author also performed reactions after an initial treatment of the rubber with an antioxidant (*6PPD*, *N*-(1,3-dimethylbutyl)-*N'*-phenyl-1,4-phenylendiamine), i.e. added before the introduction of the free radical generator (lauroyl peroxide) and of the thiol. *6PPD* is a well-known compound belonging to the *para*-phenylendiamine class of compounds, whose action as a radical scavenger has been thoroughly investigated during recent years[327-332]. The samples functionalised in absence of the antioxidant display both an increment of the Mooney viscosity and an increment of the PDI (measured through SEC), indicating that chain-elongation occurred. On the other side, the thiol grafting carried out on SBR previously treated with 6PPD led to products having vicosimetric parameters similar to those of the starting materials,

although the functionalisation degree was lower than in absence of antioxidant. The author suggests that 6PPD (a source of hydrogen atoms, as shown from mechanicistic and theoretical studies[327]) reacts more quickly with macroradicals rather than thiyl radicals, thus not quenching the radicals being added to the backbone.

In this chapter the results regarding several functionalisation runs carried out both in solution and in the bulk on a long-chain SBR will be discussed. The parameters for the thiol-ene functionalisation in solution were chosen after previous studies on short-chain polymers; the functionalisation runs in the bulk were instead performed under experimental conditions similar to those typically adopted in patents, though the feed ratios were chosen after those of experiments carried out in solution.

2.5.1 Characterisation of SBR Europrene SOL R-72612

A long-chain SBR, called Europrene SOL R-72612, was purchased from Polimeri Europa. This copolymer, synthesised in solution (*S-SBR*), was oil-extended by the manufacturer to improve its processability. While most of the commercial SBRs, though, include aromatic oils (*DEA*, Distilled Aromatic Extenders) whose toxicity is under discussion by international organisations, S-SBR 72612 included an innovative, non-toxic, aliphatic oil (*MES*, Mild Extending Solvent).
In recent years, researchers of the manufacturing company published some studies aimed to the development of replacements for the most used styrene-butadiene copolymers of the tyre industry[333-335]. In these studies, several experimental activities were carried out in order to investigate the effect of MES on rubber processability and vulcanizate properties, and to compare these properties with those of DEA-extended rubbers: the aims of the rubber manufacturers were to provide information to help rubber technologists (customers of the manufacturing company) to reformulate their compounds for equivalent properties. The main problem using MES-extended SBRs is the poor compatibility with inorganic fillers, with consequently a poor dispersion; at the same time, the main benefits are lower glass transition temperature and a better resilience observed during mechanical tests[334, 335]. Further studies[333] showed that a carefully chosen MES-extended S-SBR having a particular primary structure and molecular weight could well substitute a common DEA-extended S-SBR.
The rubber adopted in the present work has been chosen also because of its high vinyl content: also in previous patent literature[326] it has been shown that this value has an influence on the thiol-ene reactivity.
The acronyme of these experiments will contain the name *SBR5* to identify S-SBR SOL R-72612.

The pristine copolymer has got a pale yellow colour; a double dissolution in toluene / precipitation in MeOH removed a yellow oil (the MES) that was characterised through IR and NMR spectroscopies. The MES is composed entirely of aliphatic compounds, with no C=C double bonds nor aromatic units.

After the removal of MES, SBR5 was characterised through ^{1}H-NMR in order to determine the amounts of monomeric units in the macromolecular chains. SBR5 is composed by 50.6 mol.-% of 1,2-butadiene units, 34.3 mol.-% of 1,4-butadiene units (sum of *cis* and *trans*) and 15.1 mol.-% of styrene units.

The determination of MW of SBR5 was performed through SEC using $CHCl_3$ as mobile phase. The chromatogram of pristine SBR5 shows a bimodal distribution of MW along with a minor peak at high elution times due to the MES. The bimodal distribution is commonly observed in styrene-butadiene random copolymers synthesised in solution (see, for instance, the SEC characterisation of SBRL in chapter 2.3.1, page 105). The main peak of the SBR5 chromatogram accounts for a $<M_n>$ ($<M_w>$) of 637000 (674000) Da; a smaller peak at higher elution times accounts for a $<M_n>$ ($<M_w>$) of 462000 (541000) Da. According to this SEC determination, the molecular weight of the MES oil should be around 1000 Da, but being the MES totally aliphatic and with a molecular structure completely different with respect to the PS standard samples, this value is probably far from the real one.

2.5.2 Runs carried out in solution; determination of the DF and SEC measurements

Three functionalisation runs were carried out using NCys in a 1,4-dioxane solution of SBR5. In the first and third experiments, the chosen molar ratio between NCys and AIBN has been 100:1; the second experiment, instead, was performed in absence of AIBN. A third experiment was carried out with 100:1 NCys:AIBN molar feed ratio and in presence of 6PPD, that is *N*-(1,3-dimethylbutyl)-*N'*-phenyl-1,4-phenylenediamine.

The feed ratios of the three experiments carried out in solution are summarised in Table 27.

Run[a]	[AIBN]:[NCys]:[vinyl]	AIBN / Thiol (molar ratio)	6PPD : AIBN (molar ratio)[b]
SBR5NCys Sol	0.00045 : 0.045 : 1	0.01:1	-
SBR5NCys Sol woAIBN	- : 0.045 : 1	-	-
SBR5NCys Sol 6PPD	0.00045 : 0.045 : 1	0.01:1	1 : 1

Table 27 – Feed ratios of the SBR5NCys experiments carried out in solution

[a] Reaction conditions: T = 70°C, time 4h48', 1,4-dioxane 2 wt.-% polymer solution, under dry N_2

[b] Amount of 6PPD vs thiol: 0.656:1 (by mol.-%). Amount of 6PPD vs polymer: 0.7 phr

In terms of *phr*, that is *parts* per *hundred* of *rubber* by wt.-%, the feed ratios of the experiments are:

- 137 phr of pristine rubber (37 phr of MES, according to the supplier data sheet, are incorporated in the rubber)
- 6 phr of NCys
- 0.4 phr of AIBN (first and third row only)
- 0.7 phr of 6PPD (third row only).

The chosen thiol:vinyl ratio has been 0.045:1 for all the experiments, for a theoretical maximum DF_v of 4.5% and a theoretical maximum DF of 2.27% (1,2- units being the 50.6 mol.-% of the total). Taking into account the conversion data for the SBRL experiments (chapter 2.3.4, page 117), the 0.045:1 thiol:vinyl ratio was chosen as an optimal feed to obtain the best conversion degrees: the thiol defect is remarkable, and, as said, the NCys functionalisation on SBRL showed the best conversion degrees under these conditions.

The amount of AIBN (1.00 mol.-% with respect to NCys) was chosen according to the previously discussed optimisation of initiator / thiol ratio (performed in chapter 2.2.2, page 67).

The 1:1 molar amount of 6PPD with respect to AIBN has been chosen after the cited patent of Sylvie Gandon-Pain[326]; this amount also complies with the optimal application range suggested by the manufacturer (range: 0.5 – 1 phr; the added amount has been 0.7 phr).

The samples *woAIBN* (second row of Table 27) or *6PPD* (third row) were purified by double precipitation in methanol; this allowed to remove the MES, the unreacted thiol and the traces of unreacted AIBN and 6PPD (all these substances are soluble in MeOH). In the case of SBR5NCys Sol (first row), instead, a partially crosslinked product was obtained; after purification, the gel resulted in 41 wt.-% of the total, and the non-crosslinked fraction was characterised in the same way of the other two samples. This crosslinking occurrence will be discussed later in this chapter.

The samples were characterised through FT-IR spectroscopy for the determination of the DF, by preparing the films by solution casting. The carbonyl stretching at ~1735 cm^{-1} was kept as the measurement band, being directly related to the amount of grafted thiol; the band related to the out-of-plane 1,4-*trans* C–H bending at ~967 cm^{-1} was adopted as the reference band. A deconvolution of the signals was performed to separate all the peaks, and a calibration curve was obtained by mixing known amounts of NCys (up to 4 mol.-%) with the SBR5 copolymer after the removal of MES. Some IR spectra of mixtures of SBR5 with various amounts of NCys are reported in Figure 52, and a brief description of the resulting calibration curve is reported in Figure 53.

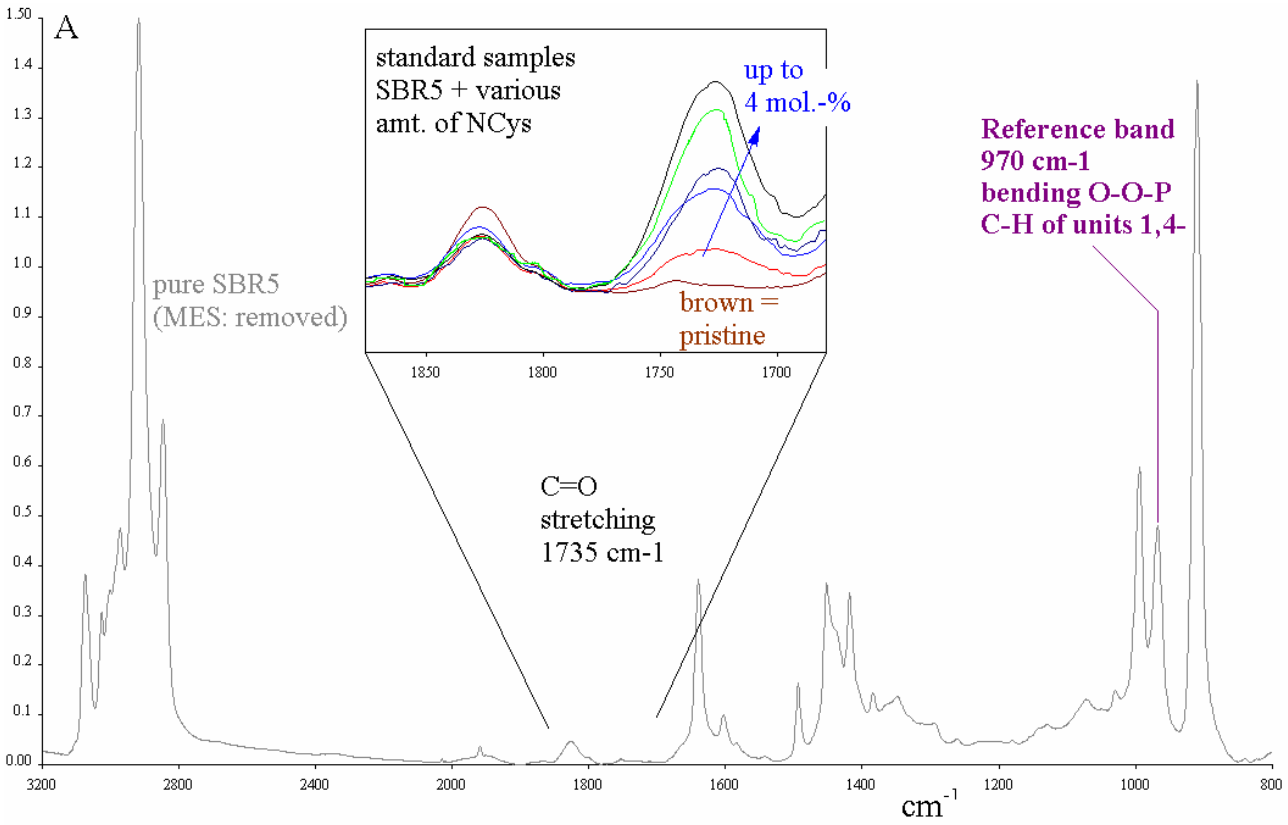

Figure 52 – IR Spectra of pure SBR5 (after MES removal) and C=O stretching band of standard samples

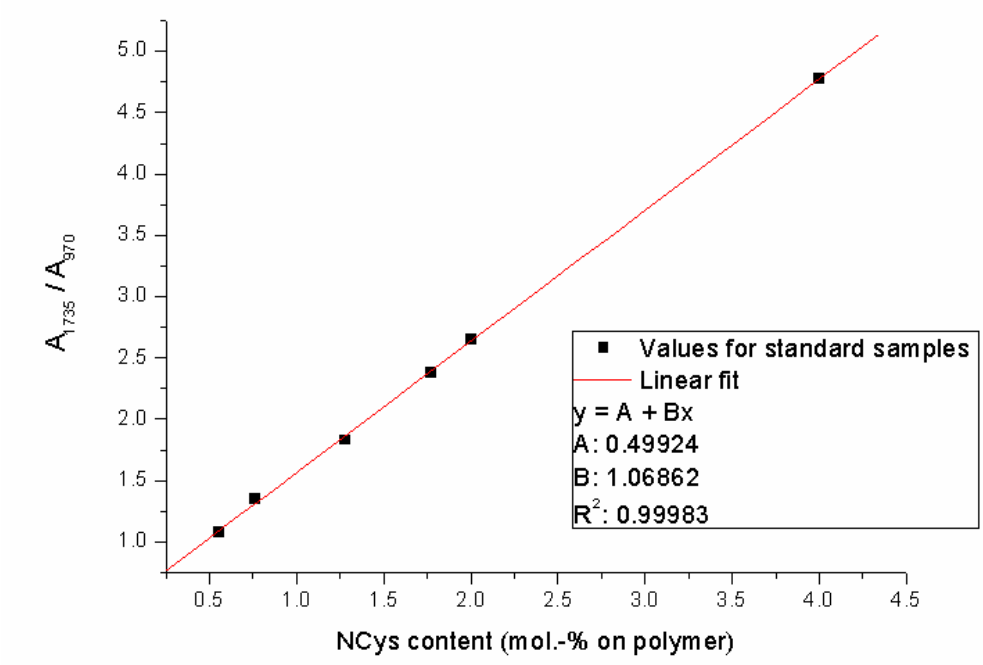

Figure 53 –Brief description of the calibration curve for determination of DF of SBR5 + NCys runs

The application of this method to the SBR5NCys samples gave the results reported in Table 28.

Run	Theoretical DF_v%	Measured DF_v%	Conversion %
SBR5NCys Sol (extracted fraction)	4.48	1.84	41
SBR5NCys Sol woAIBN	4.48	0.79	18
SBR5NCys Sol 6PPD	4.48	1.12	25

Table 28 – Functionalisation degrees (DF_v% ≡ molar amount of grafted NCys per 100 vinyl units) of the three SBR5NCys runs carried out in solution

The conversion values for the experiment *SBR5NCys Sol* are similar to those of the SBRLNCys serie of samples. The sample obtained in absence of AIBN (*woAIBN*) displays a conversion degree that is about half the conversion obtained in presence of AIBN: this result is similar to that obtained with the SBRL copolymer (see chapter 2.3.6, page 125). In that case, the conversion of the experiment carried out in absence of AIBN was 24%, while the analogous experiment carried out in the presence of the initiator gave a conversion of 41%.

In the patent of Sylvie Gandon-Pain[326], several experiments with feed ratios similar to the ones of the present work (Table 27) were carried out in solution functionalising an SBR copolymer, having 43.0 mol.-% of vinyl units and a MW of 130 kDa, in cyclohexane with 3-mercapto propanoic acid. The conversion degrees dropped from 30.5% in presence of lauroyl peroxide to 11.0% in absence of an initiator; the results of the present work comply with this behaviour.

The decrease of conversion, with respect to the AIBN + NCys sample, observed in the *6PPD* experiment is slightly less pronounced than in the *woAIBN* sample (Table 28, second row), even if comparable.

The SEC characterisation of the products has been performed, and the values for the molecular weights are compared with those belonging to pristine SBR in Table 29. All the samples show a pronounced bimodal distribution of molecular weight; therefore, the analysis of the molecular weight has been performed after peak deconvolution.

Run	Measured	High MW peak	Low MW Peak

	DF_v%	$<M_n>$	$<M_w>$	PDI	$<M_n>$	$<M_w>$	PDI
SBR5 - Pristine	-	637800	674700	1.06	462000	541800	1.17
SBR5NCys Sol (extracted fraction)	1.84	792200	821600	1.04	182600	359900	1.98
SBR5NCys Sol woAIBN	0.79	645100	702600	1.09	435200	500300	1.15
SBR5NCys Sol 6PPD	1.12	659000	691900	1.05	433000	584800	1.32

Table 29 – SEC analysis of the three functionalisation experiments carried out in solution

The extracted fraction of SBR5NCys Sol (second row) displays a narrow peak accounting for high MW, while the peak appearing at higher elution times display a low MW, and, with respect to the starting distribution in pristine SBR5, a remarkable peak broadening (PDI = 1.98).
This could be explained supposing an occurrence of both chain scission reaction events and chain-chain coupling ones. This behaviour has been observed also in liquid SBR functionalisations (chapter 2.3, page 104) carried out in presence of AIBN; on the other side, when SBR5 is functionalised in absence of AIBN (third row, *woAIBN* experiment) the PDI are mantained for both the distributions and this trend is not observed.
When the SBR5 is treated with 6PPD prior to the addition of thiol (fourth row), the effect is more complex. For the high-MW distribution, the molecular weights are similar to the starting ones along wiht the PDI; for the low-MW distribution, instead, a decrement of the $<M_n>$ and an increment of the $<M_w>$ is observed, although not in the same extent of SBR5NCys Sol. This is probably due to a selective reactivity of the anti-oxidant towards the chain elongation events, that allowed the high-MW distribution to remain on mostly unchanged values of MW.
As seen in scientific literature in studies regarding the degradation of SBR[170], the abstraction of a methylenic proton next to a benzylic unit leads to a chain-scission, and this could be strictly related to the presence of a radical abstracting protons. In the system studied in the present work, chain scission is observed when AIBN is added (SBR5NCys Sol) and not in absence of it (*woAIBN* run).
The 6PPD antioxidant avoids major increments of the MW but still allowing AIBN to generate free radicals on the thiol molecules. In particular, no gel formation was observed.

In conclusion, the thiol-ene functionalisation of long-chain SBR performed in solution is viable, though the substrate looks more sensitive to side-reactions with respect to low molecular weight diene polymers. In order to further reduce the effect of side reactions beside the optimisation of AIBN / thiol molar ratio in the feed, the addition of AIBN could be skipped, or the polymer could be treated with 6PPD prior to the thiol-ene grafting. In both two cases, though, the final DF is

reduced, and this could leave an undesirable amount of unreacted thiol in the rubber.

The purification of solution-synthesised samples has been performed through precipitation in methanol in order to better investigate the thiol grafting reaction by removing the unreacted reagents; in any case, though, it would not be desirable to purify the reaction products obtained in large amounts during industrial production. The presence of unreacted thiol could become a serious trouble when performing sulphur vulcanisation of the compound. As seen from the studies of Ranney during the '70s[193-195] regarding the creation of mercapto-silyl coupling agents between rubbers and silica, often the presence of a free thiol in the compound raises the temperature of vulcanisation generating uncontrolled crosslinking of the material with change of the scorch time. The use of a tetrasulfane compound (TESPT, bis-(triethoxysilyl)propyl tetrasulfane; a structure is reported in Scheme 13, page 49) has been the winning choice for the industrial production of rubber / silica compounds, since the tetrasulfane group displays an only moderate hexothermic reactivity towards the double bonds allowing an accurate control of vulcanisation parameters[197].

2.5.3 Runs carried out in bulk; determination of the DF and SEC measurements

Several functionalisation runs were performed in the bulk, using a Brabender-type mixer, in order to investigate the reproducibility of the thiol-ene addition of *N*-acetyl-L-cysteine to SBR5 previously performed in solution.

In tyre compounds, coupling agents between the polymer matrix and the silica filler are incorporated in the composite in many different ways; these various methodologies are adopted based on the nature of the functionalising agent and on the interaction with other chemical species. For instance, the cited TESPT tetrasulfane is usually added to the compounds in two ways: i.) it is mixed together with the filler intensively and in the desired ratio in a preliminary mixing step followed by the addition to the rubber matrix, or ii.) the coupling agent is added together with other vulcanisation reactants and with the fillers. In the latter case, the system temperature has to be carefully controlled in order to avoid extensive, uncontrolled crosslinking and scorch of the compound (this is not possible with every industrial reactor)[173].

According to previous patent literature[326] and to previous studies on cysteine derivatisation of SBR substrates[54, 112], the thiol-ene functionalisation carried out with thiols carrying a carboxylic group could conveniently be performed prior to the addition of the filler.

Six functionalisation runs were carried out in a Brabender mixer: three with a lower content of NCys (3 phr, theoretical DF_v: 2.24%) and three with a higher one (6 phr, theoretical DF_v: 4.48%). Similarly to what done for the functionalisation runs carried out in solution, i.) a first run has been carried out in presence of both AIBN and NCys; ii.) in a second one the initiator was omitted,

and iii.) in a third run the SBR was pre-treated with 6PPD, i.e. before the addition of NCys and AIBN. The addition of 6PPD before NCys and the initiator is preferred over a one-pot addition of solids: the local concentration of the radical quencher is inferior if it is well dispersed into the rubber prior to the addition of the thiol. An excessive local concentration of 6PPD could inhibit the radical creation (in the hypothesis that the radical quencher is active towards the NCys + AIBN system); on the other side, this supposition has not been proved by any means and could be the subject of further investigations.

As an example, the amounts of chemical species adopted for the synthesis of SBR5NCys 3phr 6PPD along with the addition procedure (addition phases, third column) is reported in Table 30.

SBR5NCys 3phr 6PPD							
T(℃)	time	phase	Chemical	phr	Density (kg/l)	Volume (ml)	Weight (g)
100	0'	1	SBR5 (Europrene polymer)	137	0.93	23.6860	21.0980
	1'	2	6PPD	0.7	1.02	0.1057	0.1078
	3'	3	NCys	3.0	1.00	0.4620	0.4620
			AIBN	0.1	1.00	0.0308	0.0308
	11'	4	BHT	5.0	1.00	0.7700	0.7700
~110	12'		**EXIT**	145.9	0.9341	25.0545	22.4686

Table 30 – SBR5NCys 3phr 6PPD functionalisation run. Rotor speed = 50 rpm

Starting from a temperature of 100°C, the reaction heat along with the friction of the polymer on the tools raised the temperature of the reaction chamber to 110°C in 10 minutes. The addition procedure described in Table 30 includes a pre-treatment of the SBR (introduced in phase 1) with 6PPD (phase 2); the polymer is reacted for two minutes with the anti-oxidant. Then a mixture of crystalline NCys and AIBN is added; for the experiments carried out in absence of 6PPD, this addition is phase 2 and it is performed after 1 minute from the beginning. Obviously, phase 2 comprises NCys alone in the samples carried out in absence of AIBN. The mixture of solids is used as gives best results in terms of grafting[32].

The half-life of AIBN at 100°C is nearly 7 minutes in C_6H_6; in the reaction conditions of Table 30, the AIBN will dissociate to an extent comparable to that of experiments carried out in solution.

At the end of the reaction, an anti-oxidant (BHT) is added in a large amount in order to quench any free radical, thus stopping the reaction; as seen from previous literature[32, 54, 112] and from the IR characterisation of the products, BHT is later removed during precipitation in MeOH.

The last three columns of Table 30 have an experimental purpose: they are used to estimate the filling of the mixer, and the weight of the reactants is multiplied to a *batch factor* (not reported) in order to achieve a constant filling of the reaction chamber. The most reproducible results, with the adopted Brabender mixer, are achieved when the volume of reagents is 25 ml (that corresponds to the internal capacity of the mixer).

The feed ratios of the six experiments carried out with the recipe described above are reported in Table 31. The NCys : vinyl molar ratio was the same of the experiments carried out in solution; the AIBN : NCys ratio has been raised according to existing literature[326].

Run	[AIBN]:[NCys]:[vinyl]	AIBN : Thiol (molar ratio)	DF_v (%)[b]	Conv. (%)[b]
SBR5NCys 3phr	0.00074 : 0.0224 : 1	0.0331:1	0.11	4.9
SBR5NCys 3phr woAIBN	- : 0.0224 : 1	-	0	-
SBR5NCys 3phr 6PPD[a]	0.00074 : 0.0224 : 1	0.0331:1	0	-
SBR5NCys 6phr	0.0015 : 0.045 : 1	0.0331:1	0.17	3.8
SBR5NCys 6phr woAIBN	- : 0.045 : 1	-	0	-
SBR5NCys 6phr 6PPD[a]	0.0015 : 0.045 : 1	0.0331:1	0	-

Table 31 – Feed ratios for the experiments carried out in Brabender

[a] 6PPD : AIBN molar ratio = 10 : 1; [b] Conversion and DF_v determined through FT-IR measurements

The conversion degrees obtained are much lower than in the case of reaction carried out in solution. No functionalisation is observed in four samples. In the cited patent[326] and in the other works of the group of Ciardelli[54, 112], the added thiols were more hydrophobic functionalisers with respect to NCys: in the Michelin patent the author adopted 1-mercaptaundecanoic acid, while in the reactions of SBR with cysteine derivatives, alkylic groups were esterified to the acid moiety (at room temperature, both the methyl and the ehtyl esters of L-cysteine are liquid and toluene-soluble, while NCys is a crystalline solid insoluble in aliphatic / aromatic solvents). The high hydrophilicity of NCys probably does not allow a good mixing with the polymer and a poor dispersion; thus the DF is extremely small regardless of the adopted conditions.

Another result confirming previous trends arises from SEC evaluation of the six experiments whose feed ratio has been described in Table 31. Again, all the molecular weight distributions of purified reaction products were bimodal, and analysed consequently after peak deconvolution; a summary of the MW evaluation of the chromatograms is reported in Table 32.

Run	Measured DF_v%[b]	High MW peak			Low MW Peak		
		$<M_n>$	$<M_w>$	PDI	$<M_n>$	$<M_w>$	PDI

SBR5 - Pristine	-	637800	674700	1.06	462000	541800	1.17
SBR5NCys 3phr	0.11	872200	899100	1.03	192300	375300	1.95
SBR5NCys 3phr woAIBN	0	756100	791800	1.05	315400	561300	1.77
SBR5NCys 3phr 6PPD[a]	0	818500	846600	1.03	368200	619400	1.68
SBR5NCys 6phr	0.17	798600	817500	1.02	262200	405900	1.54
SBR5NCys 6phr woAIBN	0	705000	746800	1.06	351800	572500	1.62
SBR5NCys 6phr 6PPD[a]	0	795400	826900	1.04	350800	495400	1.41

Table 32 – SEC determination of molecular weights for functionalisation runs carried out in the bulk

[a] 6PPD : AIBN molar ratio = 10 : 1; [b] DF_v determined through FT-IR measurements

The peak accounting for longer macromolecules is always shifted to shorter elution times: this effect, observable for both the 3phr and the 6phr samples, is more evident for the samples carried out with both AIBN and NCys, as expected. The chain elongation observed for the *woAIBN* samples (third and sixth row) can be attributed solely to the radicalic reactions generated by the heat and by the dynamic forces inside the reactor, since no functionalisation is observed. A similar effect is mitigated by 6PPD (row 4 *vs* row 2, row 7 *vs* row 5) but not as much as in the case of AIBN absence (*woAIBN* samples).

The peak associated to shorter macromolecules is always shifted to longer elution times (reduction of $<M_n>$) and it gets much broader (increment of the PDI). The effect is more pronounced in presence of both AIBN and NCys (row 2 and 5) with respect to the other samples.

In conclusion, *N*-acetyl-L-cysteine is not suitable for the functionalisation of SBR in the bulk. On the other side, in this chapter it has been shown that both the workarounds suggested in literature for avoiding structural changes in the rubber (the treatment of SBR with 6PPD prior to the thiol-ene grafting or the omission of a free radical generator) seem to be effective.

2.6 Incorporation of *N*-acetyl-L-cysteine functionalised oligomers in tyre compounds

In this chapter the experimental results regarding the incorporation of cysteine functionalised oligomers in rubber compounds will be discussed. These compounds, containing high amounts of silica along with carbon black, were obtained by introducing the polymeric products described in the present work as coadjuvant of main dispersing agents. A discussion of the role played by the added coupling agents in the modification of physical properties of the compounds will follow, with reference to the existing state of art; the influence of mixing parameters on the creation of the compounds will also be discussed.

2.6.1 Synthesis of SBR / silica / CB compounds and choice of compatibilising agents

The incorporation of the functionalised polybutadiene described in chapter 2.2, page 61 (from now on: *fPBL*) and of the functionalised styrene-butadiene rubber copolymer described in chapter 2.3, page 104 (*fSBRL*) in a SBR-based compound of recent formulation will be discussed in this and in the following sub-chapters.

The formulation of the SBR compound used in the present study involved different ingredients:

- Rubber matrix
- Plasticisers (introduced in order to improve compound processability)
- Reinforcing fillers (silica and carbon black)
- Vulcanisation-related agents: sulphur for the crosslinking
- Vulcanisation-related agents: accelerators
- Vulcanisation-related agents: activators
- Vulcanisation-related agents: anti-oxidants

The adopted polymeric matrix is that of chapter 2.5, page 136. The rubber Europrene SOL R-72612 is a solution-synthesised styrene-butadiene random copolymer (*S-SBR*) oil-extended by the manufacturer to improve its processability; while most of the commercial SBRs include aromatic oils (*DEA*, Distilled Aromatic Extenders), S-SBR R-72612 incorporated a non-toxic, aliphatic oil (*MES*, Mild Extending Solvent). An additional MES amount will be incorporated during processing.

The compounding method is a two-step procedure: after the first mixing a *primitive compound* is obtained (sometimes called *green compound*), and after the second step (*completion*) a *completed compound* is obtained. The formulations for the first and for the second mixing of the reference compound (*blank* run, to which no oligomeric materials are added) are summarised in Table 33; the second mixing has been performed after nearly 12 hours from the initial one, and after a two-rolls mill homogenisation of the primitive compound. The purpose of the two-step procedure is to characterise the green compounds before the introduction of vulcanising agents; the presence of

chemical agents added for crosslinking will interfere with the measurement of the true reinforcing potential of fillers, as they could act as plasticisers.

Reference Compound 1st mixing							HAAKE MIXER
T(℃)	time	phase	Chemical	phr	Density (kg/l)	Volume (ml)	Weight (g)
80	0'	0	SBR5 (Europrene polymer)	137	0.93	128.16	119.19
	1'	1	Filler: Carbon Black N330	15	1.8	7.25	13.05
			Filler: Silica Zeosil 1165	30	2.0	13.05	26.10
			Coupling Agent: TESPT X50S	10	1.344	6.47	8.70
	3'30"	2	Plasticiser: Wax	1	0.92	0.95	0.87
			Plasticiser: MES Extending Oil	8	0.91	7.65	6.96
			Activator: Stearic Acid	2	0.85	2.05	1.74
			Filler: Silica Zeosil 1165	20	2.0	8.70	17.40
~140	10'		**EXIT**	223	0.9341	174.28	194.01

Addition of vulc. agents 2nd mixing							OPEN MILL
T(℃)	time	phase	Chemical	phr	Density (kg/l)	Volume (ml)	Weight (g)
40	0'	0	(Initial Compound)	-	0.9341	144.89*	161.30*
			Activator: ZnO	2.5	5.55	0.39	1.81
			Anti-oxidant: 6PPD	2	1.0	1.74	1.74
	2'	1	Accelerator: CBS	2	1.3	1.34	1.45
			Accelerator: DPG80	2.4	1.12	1.56	1.74
			Vulcanising agent: S_8	1.3	2	0.57	0.94
~140	6'		**EXIT**				

Table 33 – Recipe for the reference compound. Rotor speed = 45 rpm; *: after removal of samples for charact.

During the first step, 137 phr of rubber (100 phr of SBR, 37 phr of MES) are mixed up with 15 phr of raw carbon black, a total of 50 phr of silica and 10 phr of TESPT supported on CB. This compound (whose commercial complete name is TESPT X50S, and it is furnished by Degussa AG) contains 50 wt.-% of TESPT and 50 wt.-% of CB; the total amount of added CB is 20 phr (15 + 5).
The addition of plasticisers (MES and an aliphatic wax) is performed after the initial *disgregation* of the fillers; the disgregation is defined as the magnitude of the degree in which the molecules of a body are separated from each other[336]. Along with plasticisers, the stearic acid is dispersed. This latter molecule acts as an activator towards other vulcanising agents, and is dispersed before the introduction of the latters; in any case, it is not going to influence the compound mechanical properties.
In the second mixing step, that is performed after the initial disgregation of the fillers and the ethanolysis of TESPT with silica, the vulcanising agents are added. In the considered recipe, the vulcanisation is performed with sulphur together with:

- accelerators (CBS and DPG80)
- activators (ZnO and stearic acid)

- an anti-oxidant (6PPD; it has already been used in this work in chapter 2.5, page 136).

The use of accelerators and activators lowers the activation energy of vulcanisation reaction to 80-125 KJ/mol from a starting value of 210 KJ/mol which is necessary if sulphur is used alone (e.g. without peroxides or other crosslinking agents)[337]. Accelerators and activators break sulphur rings, allowing a shorter length of sulphur chains bridging the polymer molecules: this has an effect on the properties of the material. Short sulfur crosslinks, with just one or two sulfur atoms, give the rubber a better heat resistance, while crosslinks with higher number of sulfur atoms, up to six or seven, give the rubber good dynamic properties but inferior heat resistance.

There are two major classes of accelerators, *primary* or *secondary* ones (also called *ultra accelerators*), that differ mainly for the induced cure kinetics. In the recipes presented in this work both a primary and a secondary accelerator are used. The first one is the *N*-cyclohexyl-2-benzothiazyl sulphenamide (commercial name: *CBS*), and the secondary accelerator is the N,N'-diphenyl guanidine (commercial name: *DPG80*; the two molecular structures are presented in Scheme 24).

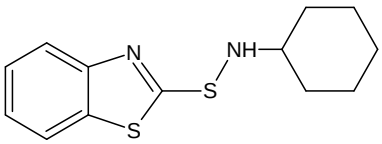

N-cyclohexyl-2-benzothyazyl sulphenamide (CBS)

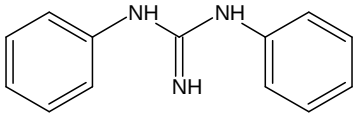

N,N'-diphenyl guanidine (DPG 80)

Scheme 24 – Molecular structure of the used accelerators (CBS and DPG80)

Some experimental parameters were varied in the functionalisation runs:

- functionalisation degree of added polymers; pristine PBL and SBRL were also incorporated in the runs, along with one sample of fPBL and two samples, having different DFs, of fSBRL.
- mixing method (use of a Haake / two-rolls mill sequence of mixing *vs* the double use of a Brabender mixer for both mixing steps)
- time of incorporation of the compatibilising agents in the recipe
- amount of compatibilising agents and mixtures of them to highlight synergistic effects.

No direct functionalisation runs with the pristine functionalising agent (*N*-acetyl-L-cysteine) were performed, since the NCys functionalisation of the employed SBR was shown as possible only in solution and not in bulk (see chapter 2.5, page 136).

Five compatibilising agents were used (Table 34). The functionalised additives were synthesised in solution and purified according to the prodecure described in previous chapters. The amount of

grafted cysteine was chosen in order to maintain a certain amount of double bonds on the polymer for the vulcanisation. The amount of NCys equivalents in fPBL and fSBRL was equal; fSBRL-L had an inferior content of NCys but it was synthesised with the same initial thiol:vinyl feed ratio of fPBL. Since the conversion degree obtained functionalising SBRL is usually lower than that obtained by functionalising PBL, in order to obtain the same amount of grafted NCys in terms of equivalents / gram of polymer a thiol:vinyl ratio of 0.75:1 has been adopted for fSBRL instead of the 0.30:1 ratio of fPBL.

Compatibilising Agent	Measured DF_v% (NMR)	DF in NCys (meq / g)	Thiol:vinyl initial feed ratio	Yield of the thiol grafting
PBL	-	-	-	-
fPBL	12.8	0.171	0.30:1	42.6%
SBRL	-	-	-	-
fSBRL	15.0	0.170	0.75:1	20.0%
fSBRL-L	11.8	0.142	0.30:1	39.3%

Table 34 – Used compatiblisers for incorporation in filled rubber compounds

2.6.2 Preliminary experiments: functionalised vs pristine oligomers

A first set of experiments was performed by introducing four out of five compatibilising agents of Table 34 (PBL, fPBL, SBRL, fSBRL-L) into the formulations; a blank run without additives was also synthesised. The name of the experiments belonging to this set of runs is the same of the added compatibilising agent. The introduction of the oligomer has been performed during phase one along with the TESPT and the fillers. As an example, the formulation of the fSBRL-L sample is reported in Table 35; 3 phr of compatibilising agent were incorporated, while the amounts of all the other chemical agents were thos of of the blank run (recipe reported in Table 33).

Compound fSBRL-L 1st mixing							**HAAKE MIXER**
T(℃)	time	phase	Chemical	phr	Density (kg/l)	Volume (ml)	Weight (g)
80	0'	0	SBR5 (Europrene polymer)	137	0.93	128.16	119.19
	1'	1	Filler: Carbon Black N330	15	1.8	7.25	13.05
			Filler: Silica Zeosil 1165	30	2.0	13.05	26.10
			Coupling Agent: TESPT X50S	10	1.344	6.47	8.70
			Coupling Agent: fSBRL-L	3	0.93	2.81	2.61
	3'30"	2	*(et cetera)…*				

Table 35 – Recipe for the run fSBRL-L

After removal of the compounds from the Haake mixer, a homogenisation process was performed

in a two-rolls mill for nearly 3 minutes; the samples were later press-molded and cut for the rheological / rubber flow index characterisation runs.

The primitive compounds were black and, macroscopically, all identical.

After incorporation of vulcanising agents, the completed compounds were homogenised in a two-rolls mill as was done with the primitive ones.

A strain sweep rhelogical experiment was performed on the five samples with a RPA2000 rotational rheometre. The routine included 1 Hz strain sweeps performed at 70°C and with a rotational, bi-conical tool geometry; the induced shear was therefore measured as a percentage of the maximum angle measurable by the instrument (90°).

A first strain sweep was performed in order to elminate the *mechanical history* of the samples; a second strain sweep, performed soon thereafter, allowed a first measurements of G', G" and tan δ. In order to highlight the agglomeration of the filler, an annealing procedure was carried out by keeping the samples for 10 minutes (i.) at 70°C (ii.) at 170°C; a final strain sweep under the same conditions of the previous strain sweeps was eventually performed. The G' *vs* shear amplitude graphs related to the second and third strain sweeps for the five compounds are reported in Figure 54 and Figure 55.

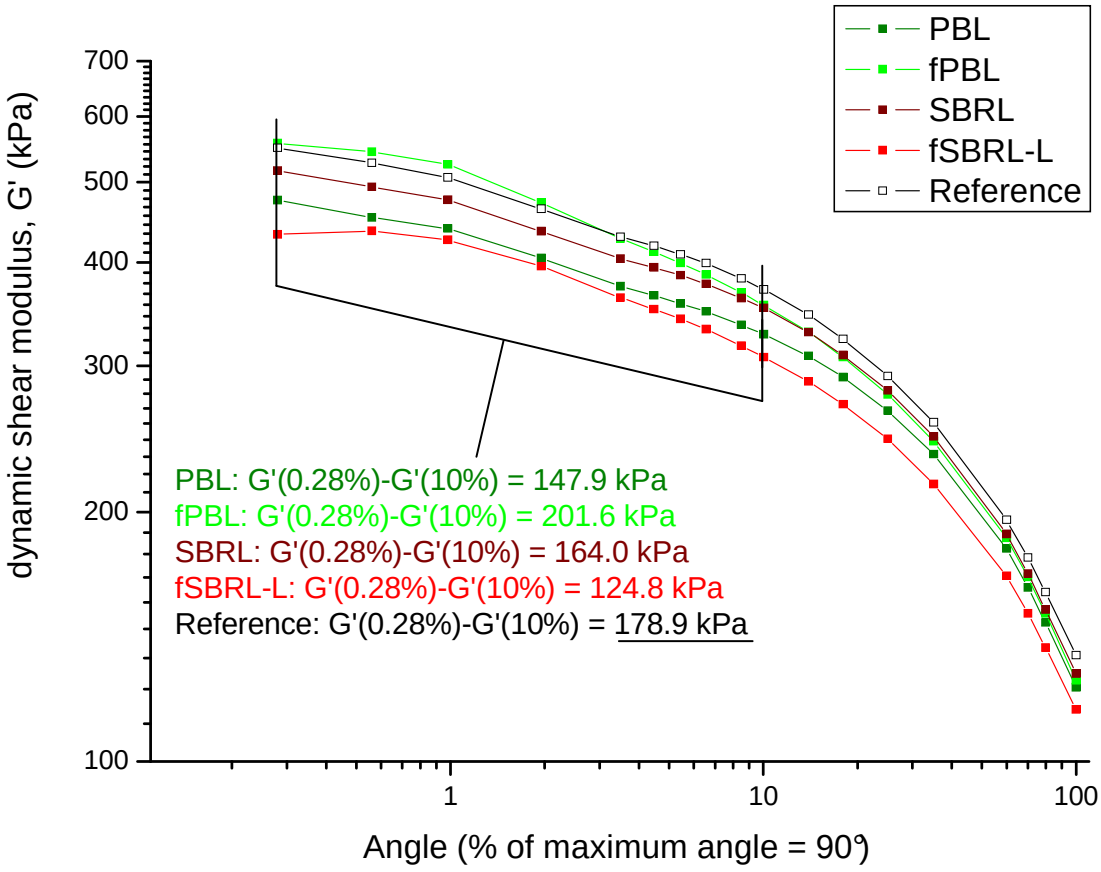

Figure 54 – G' *vs* strain graphs for the second and third strain sweeps (3rd s.s.: after annealing at 70°C)

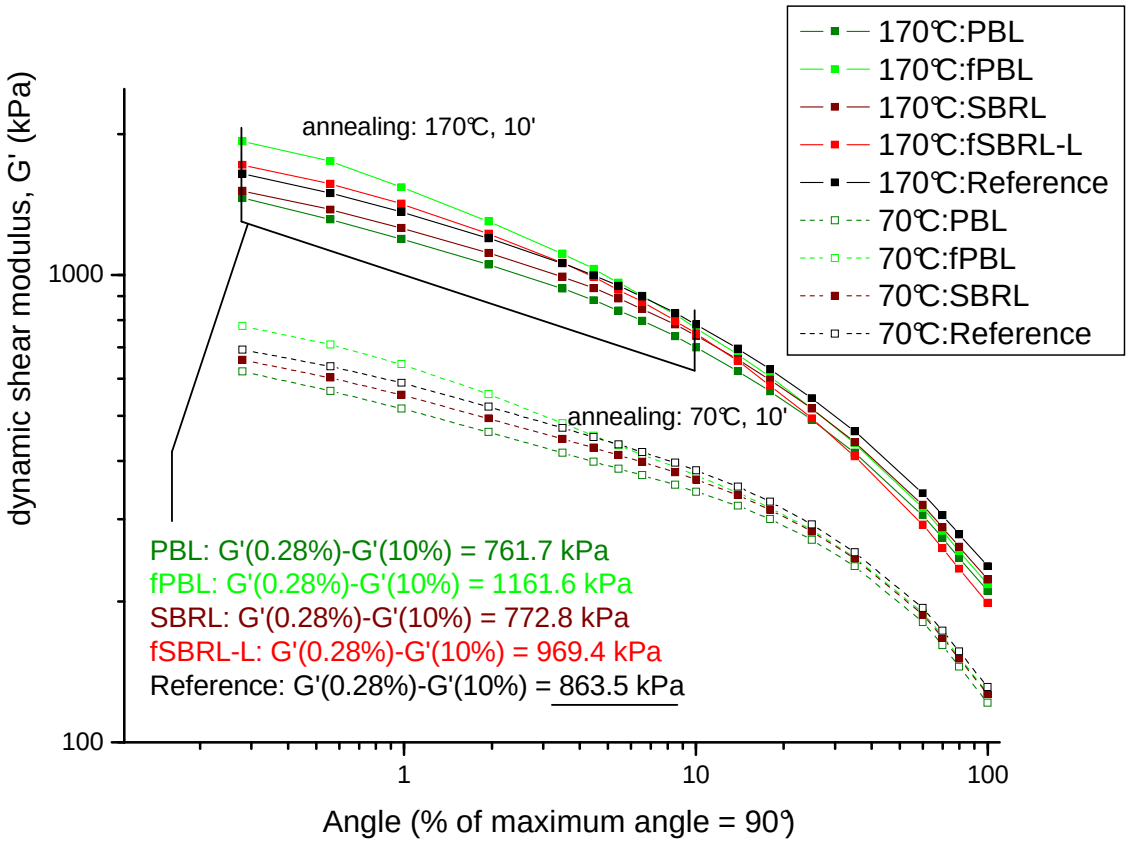

Figure 55 – G' *vs* strain graphs for the second and third strain sweeps (3rd s.s.: after annealing at 170°C)

Before the annealing, the reduction of G' is evident in all samples; in particular, a small decrease is observed with respect to the reference compound for all but the fPBL sample. A convenient quantification of the decrement of G' can be performed subtracting the G' value at an angle of 10% from the initial value at 0.28%. The decrement will highlight the occurrence of the Payne effect; this further highlights the reduction observed in samples containing oligomers (a similar evaluation of G' was performed also by Gandon-Pain in the already cited work regarding incorporation of mercapto acids in rubber formulations[326]).

After the heating at high temperature, the Payne effect is more evident; moreover is can be observed that the flocculation occurs to a major extent when the temperature is higher (Figure 55). Flocculation of filler, as observed by Böhm and Nguyen[223], Luginslad and co-workers[338] and Datta and co-workers[227], is a diffusion-controlled process which is sensitive to temperature, molecular weight of the polymer matrix, and annealing time. In the present work, since the trend of G' observed for the annealing process at 70°C is the same (but less evident) than that observed when the annealing process was performed at 170°C, in all the further rheometric measurements the annealing protocols were performed at a temperature of 170°C.

The reduction of the Payne effect in presence of pristine oligomers PBL and SBRL could be due to a local softening of the polymer matrix favouring filler disgregation. As said, in fact, the filler

flocculation is dependant on the molecular weight of the polymer resembling the matrix; moreover, if the disgregation of the filler network is reversible, the reduction of the Payne effect will be observed before and after the annealing / flocculation.

The influence of the functionalised oligomers is more difficult to be evaluated. After the annealing, the compounds named fPBL and fSBRL-L undergo a pronounced Payne effect, even more pronounced than the reference compound. (The fSBRL-L compound showed an inferior G'(0.28%)-G'(10%) value before the annealing, but the G'(0.28%) value of fSBRL-L is far from the trend indicated by the other points, and a measurement error could have occurred; see the first graph of Figure 55.) A possible explanation of this phenomenon arises from the possible disgregation / reagglomeration of a network of molecules of fPBL or fSBRL-L, i.e. the compatibilising agent could act as an additional amount of filler particles, having their own interactions. To support this hypothesis, one could invoke the presence of strong inter-macromolecular interactions observed for the functionalised PBNCys samples (to which set of samples fPBL belongs) or for the functionalised SBRLNCys samples (to which fSBRL-L belongs) respectively in chapter 2.2.8, page 93, and in chapter 2.3.7, page 125. This result could also indicate a scarce availability of the fPBL and fSBRL-L to create hydrogen bonds with the silica substrate; this phenomenon could be due to the relatively low torque values reached in the Haake mixer.

After the second mixing phase, completed compounds were obtained. The rheological measurements with the RPA2000 instrument did not show any substancial variation with respect to the first mixing procedure. The delta G' values [ΔG' ≡ G'(0.28%) – G'(10%)] of the third strain sweep, performed after the annealing procedure, are summarised in Table 36.

Run	G'(0.28%) – G'(10%) Primitive Compound, kPa		G'(0.28%) – G'(10%) Completed Compound, kPa	
	Before annealing	After annealing	Before annealing	After annealing
(Blank run)	178.9	863.5	38.9	885.7
PBL	147.9 (-17%)	761.7 (-12%)	42.1 (+8%)	732.7 (-17%)
fPBL	201.6 (+13%)	1162.2 (+35%)	100.5 (+158%)	1511.0 (+71%)
SBRL	164.0 (-8%)	772.8 (-10%)	40.9 (+5%)	771.0 (-13%)
fSBRL-L	124.8 (-30%)	969.5 (+12%)	87.2 (+124%)	1186.0 (+34%)

Table 36 – delta G' values for preliminary runs. Green = reduced / orange = increased Payne effect

Table of colours; the blank run is the reference

<-25%	<-20%	<-15%	<-10%	<-5%	<±5%	>+5%	>+10%	>+15%	>+20%	>+25%

The compounds including pristine elastomers showed, again, a reduced Payne effect while those including functionalised samples showed an increased one.

The hysteresis of these samples reflected the expected behaviour: the tan δ value undergo an increment followed by a decrement, and the values are smaller for the compounds showing a reduced G', as expected. The tan δ values of some of the completed compounds after the annealing are compared in Figure 56; the reference completed compound is compared with that including PBL (reduction of Payne effect / tan δ becomes smaller) and with the fPBL compound (increase of the Payne effect).

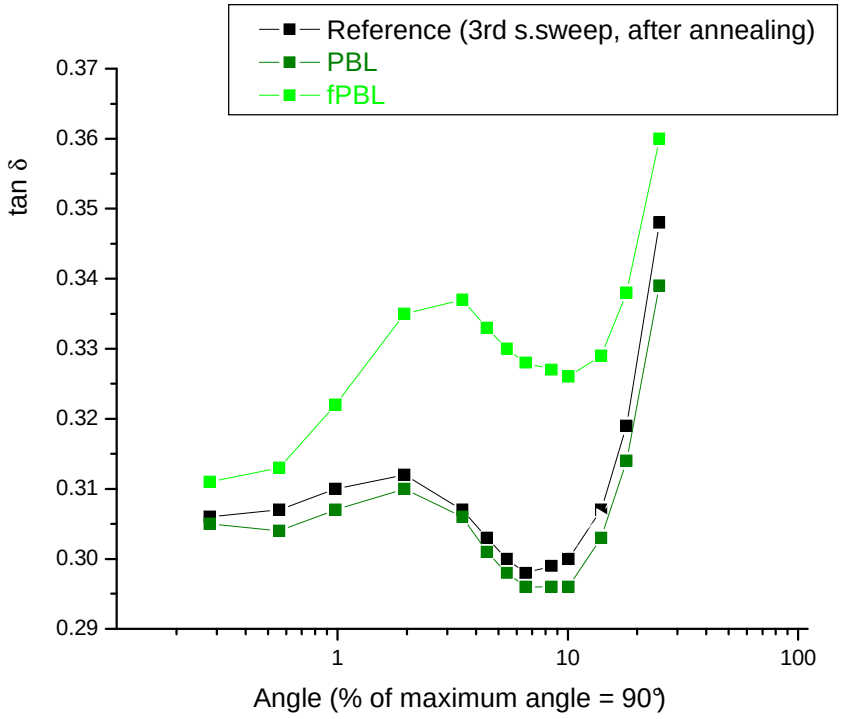

Figure 56 – tan δ *vs* log (strain) for various completed compounds (strain sweeps performed after annealing)

Dynamometric stress-strain experiments were carried out on the completed compounds according to UNI 6065 set of international rules. The ring-shaped samples were stressed vertically with a dynamometre until breaking and structure collapse; the stress-strain graphs for the five completed compounds are reported in Figure 57, along with the 300/100 value.

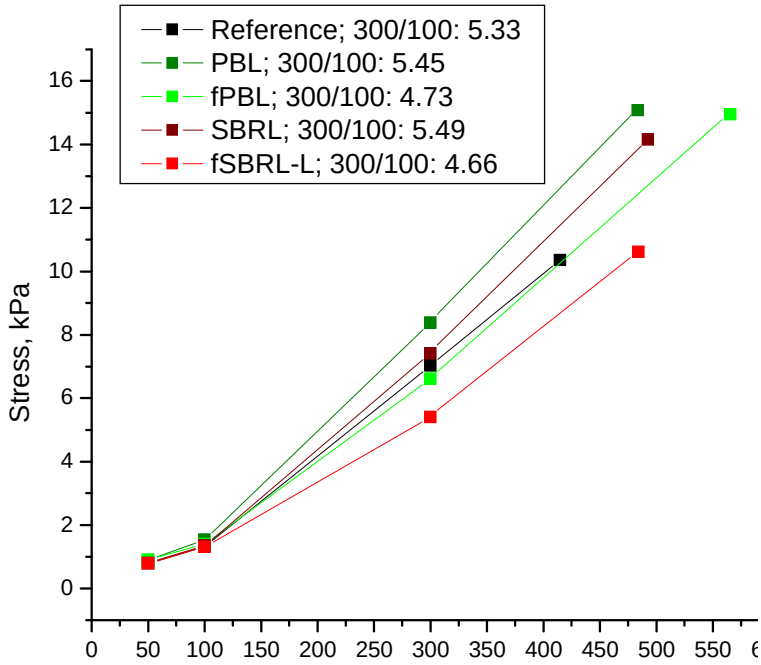

Figure 57 – Stress/strain graphs of completed compounds along with 300/100 ratios

The reinforcing effect of silica at high strains is more evident for the samples showing a limited Payne effect, i.e., the sample with PBL and the one with SBRL, as expected from the strain sweep graphs.

2.6.3 Effects of mixing energy on the dispersion of compatibilising agents

While the functionalised oligomers looked unsuitable for reducing the Payne effect, the pristine polymers seemed to favour filler disgregation thus acting positively.

The next investigation of the present work aimed at a better understanding of the influence of mixing parameters on the oligomer dispersion. As a matter of fact the fPBL and fSBRL-L oligomers have a small functionalisation degree, and, following the hypothesis that breaking a hydrophilic network would result in a good dispersion of the oligomer, a reduction of the Payne effect could potentially be achieved under those conditions.

A compound that showed a reduction of the Payne effect (additive: PBL) and one showing an increment (additive: fPBL) were chosen based on the data of previous chapter. The synthesised primitive compounds underwent two other 3-minutes homogenisation steps performed in a two-rolls mill set up with the rolls in the closest position; the torque values, although not measured, were pushed to the instreumental limit for the considered compounds. The samples were then cut from the press-molded compounds; the values of $\Delta G'$ were measured as before, with the annealing step at 170°C, and reported in Figure 58.

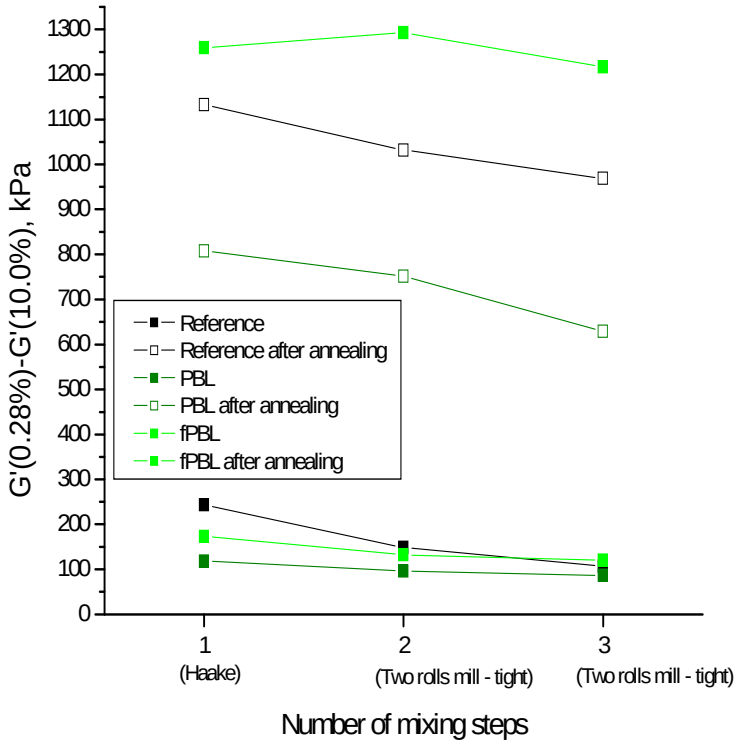

Figure 58 – Decrease of ΔG'[≡G'(0.28%) – G'(10%)] for samples that were mixed three times

The more mixing operations are carried out, the more the Payne effect is reduced, and this is true for all samples considered. In the specific case of fPBL a reduction of ΔG' was observed, and this does not comply with the previously observed increment; after annealing, though, an increase of ΔG' was observed, in agreement with the data of the previous sub-chapter.

Stress-strain data were collected on the compounds after completion, and they were similar to the previously obtained results, showing an improved 300/100 ratio for the PBL compound and a diminished one for the fPBL compound.

Although these characterisation data regarding the energy of mixing are not conclusive and do not prove that the possible disgregation of a hydrophilic network of the compatibilising agent occurs, in order to exclude similar effects all the following experiments were performed in a Brabender mixer for the synthesis of both green and completed compounds. The reaction conditions were identical to those pointed out in the formulations shown in Table 33 and Table 35, so the compounds created with the Haake mixer are directly comparable with those created with the Brabender mixer.

2.6.4 Study of the addition order of compatibilising agents

In order to confirm if the oligomers played some role as dispersive agents for the fillers, two compounds were synthesised including the compatibilising agents in a later step with respect to the addition of TESPT. Moreover the dispersive action has been directly compared with that of TESPT

by reversing the addition procedure of functionalised oligomer and of tetrasulfane.

A blank run (without any compatibiliser) was also performed, along with two runs having the formulation previously described, i.e. incorporating the oligomer simultaneously to the TESPT. A comparison of the formulations regarding the primitive mixings of the run fPBL-1.1 and the run fPBL-1.3 (fPBL added in phase 3 of the first mixing) is reported in Table 37.

			fPBL-1.1	*(primitive compound only)*			**BRABENDER**
T(°C)	time	phase	Chemical	phr	Density (kg/l)	Volume (ml)	Weight (g)
80	0'	0	SBR5 (Europrene polymer)	137	0.93	29.32	27.26
	1'	1	Filler: Carbon Black N330	15	1.8	1.66	2.99
			Filler: Silica Zeosil 1165	30	2.0	2.99	5.97
			Coupling Agent: TESPT X50S	10	1.344	1.48	1.99
			Coupling Agent: fPBL	3	0.86	0.69	0.60
	3'30"	2	Plasticiser: Wax	1	0.92	0.22	0.20
			Plasticiser: MES Extending Oil	8	0.91	1.75	1.59
			Activator: Stearic Acid	2	0.85	0.47	0.40
			Filler: Silica Zeosil 1165	20	2.0	1.99	3.98
~140	10'		**EXIT**	226	0.9341	40.56	44.97

			fPBL-1.3	*(primitive compound only)*			**BRABENDER**
T(°C)	time	phase	Chemical	phr	Density (kg/l)	Volume (ml)	Weight (g)
80	0'	0	SBR5 (Europrene polymer)	137	0.93	29.32	27.26
	1'	1	Filler: Carbon Black N330	15	1.8	1.66	2.99
			Filler: Silica Zeosil 1165	30	2.0	2.99	5.97
			Coupling Agent: TESPT X50S	10	1.344	1.48	1.99
	3'30"	2	Plasticiser: Wax	1	0.92	0.22	0.20
			Plasticiser: MES Extending Oil	8	0.91	1.75	1.59
			Activator: Stearic Acid	2	0.85	0.47	0.40
			Filler: Silica Zeosil 1165	20	2.0	1.99	3.98
	4'30"	3	Coupling Agent: fPBL	3	0.86	0.69	0.60
~140	10'		**EXIT**	226	0.9341	40.56	44.97

Table 37 – Recipes for the runs fPBL-1.1 and 1.3; the order of addition of fPBL is varied

The oligomer is added in a separate phase in the sample fPBL-1.3, named *phase three* at 4'30".

A summary of the formulations along with the ΔG' values measured through strain sweep rheometric measurements carried out on the primitive compounds are described in Table 38.

Run	Additive	G'(0.28%) – G'(10%) Primitive Compound, kPa	
		Before annealing	After annealing
(Blank run)	(no additives)	133.1	872.6
fPBL-1.1	fPBL phase 1	105.7 (-20%)	663.6 (-24%)
fPBL-1.3	fPBL phase 3	197.9 (+49%)	1112.0 (+27%)
fSBRL-L-1.1	fSBRL-L phase 1	156.3 (+17%)	961.3 (+10%)
fSBRL-L-1.3	fSBRL-L phase 3	161.5 (+21%)	963.9 (+10%)
TESPT-1.3	fPBL phase 1 + TESPT phase 3 inst. of 1	153.1 (+15%)	1106.0 (+27%)

Table 38 – ΔG' values for runs varying the order of addition. Green = reduced / orange = increased Payne effect

Table of colours; the blank run is the reference

<-25%	<-20%	<-15%	<-10%	<-5%	<±5%	>+5%	>+10%	>+15%	>+20%	>+25%

The sample fPBL-1.1 shows a reduced Payne effect regardless of the annealing, and this does not comply with the result of chapter 2.6.2 in which the Payne effect was increased for a sample having the same synthethic procedure in terms of additives and method. The two runs only differ for the used mixer (Haake *vs* Brabender); this could confirm the data arising from chapter 2.6.3, *i.e.* that mixing energies should be higher to obtain a positive effect when a functionalised oligomer is used. In the Brabender mixer the torque values are, in average, 20 to 30% higher than in the Haake mixer. This, however, is not true for the fSBRL-L samples, for which the Payne effect is always increased. The dispersion potential of the functionalised oligomers is evident only if they are added during filler dispersion: when the oligomer is added in step 3 (third and fifth row of Table 38), the Payne effect is much increased. Again, if the TESPT (the major dispersing agent in absence of other additives) is added in phase three and fPBL is added in phase 1 (sixth row), the Payne effect is increased.

In conclusion to this part:

- the use of the Brabender mixer allows a better dispersion of the functionalising agents
- a synergistic effect of dispersion between TESPT and fPBL is observed, and Payne effect is reduced if the two agents are added simultaneously
- the functionalised oligomers do not show a good dispersing capability if used alone after the incorporation of fillers and plasticisers or if replacing the TESPT

- there is still no evidence of Payne effect reduction when the compatibilising agent is a functionalised liquid SBR.

2.6.5 Synergistic effect of pristine and functionalised samples

It is possible that a dilution of the amount of functional groups brought by fPBL and fSBRL-L in the compounds could bring some benefit in terms of reducing the Payne effect. Probably the smaller Payne effect observed when adding PBL or SBRL is due to the easier diffusion of the filler into the polymer made possible by the presence of short macromolecules; this presence, however, does not cause the material to become softer (as seen from the dynamometric data) probably because of the prevalence of the reinforcing effect of the well-dispersed silica.

In order to investigate this aspect, many compounds were synthesised by including various amounts of pristine and functionalised samples for three couples of oligomers: PBL / fPBL, SBRL / fSBRL (having the same amount of functionalities per gram of material of fPBL) and SBRL / fSBRL-L. The 3 phr of added functionaliser were kept constant, but they were redistributed between the oligomers; for instance, a 100 / 0 (wt.-%) PBL / fPBL composition was examinated along with the 50 / 50 one and the 0 / 100 one, and the added amount of PBL / fPBL were, respectively, 3 phr / 0, 1.5 phr / 1.5 phr, and 0 / 3 phr.

In the case of PBL / fPBL, after investigating properties of the 50 / 50 compounds and observing a remarkable positive effect on the reduction of Payne effect, other experiments with different compositions (for instance: 75 / 25, or 90 / 10) were carried out. The successive experiments were aimed to obtain, with a certain composition, the best results in terms of ΔG'.

The formulations for the addition of PBL / fPBL are summarised in Table 39 along with the amounts of added oligomers and the ΔG' values; a graph of the latter values *vs* the content of fPBL or the amount of equivalents of NCys added to the compound is reported in Figure 59.

Run	Added oligomer in phr		G'(0.28%) – G'(10%) Primitive Compound, kPa		G'(0.28%) – G'(10%) Completed Compound, kPa	
	PBL	fPBL	Before annealing	After annealing	Before annealing	After annealing
(Blank run)	-	-	242.8	1119.5	84.1	1541.5
100/0	3.00	0.00	243.1 (<1%)	1288.9 (+15%)	109.1 (+29%)	1445.5 (-6%)
95/5	2.85	0.15	234.6 (-3%)	610.0 (-45%)	92.9 (+10%)	854.6 (-44%)
90/10	2.70	0.30	188.6 (-22%)	584.4 (-48%)	79.7 (-5%)	854.0 (-44%)
75/25	2.25	0.75	165.4 (-32%)	814.6 (-27%)	90.1 (+7%)	1160.8 (-25%)
50/50	1.50	1.50	204.5 (-16%)	1030.3 (-8%)	123.9 (+47%)	1442.8 (-6%)
25/75	0.75	2.25	248.9 (+2%)	1022.1 (-9%)	133.6 (+59%)	1674.5 (+9%)
0/100	0.00	3.00	311.9 (+28%)	1793.2 (+60%)	228.7 (+151%)	2606.5 (+69%)

Table 39 – ΔG' values for PBL / fPBL runs. Green = reduced / orange = increased Payne effect

Table of colours; the blank run is the reference

<-25%	<-20%	<-15%	<-10%	<-5%	<±5%	>+5%	>+10%	>+15%	>+20%	>+25%

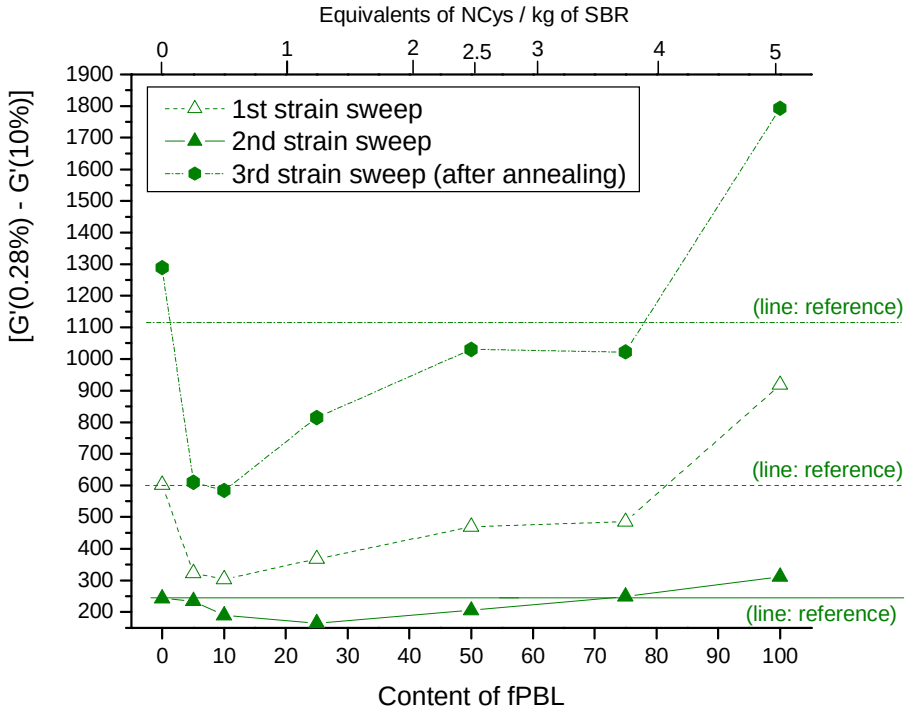

Figure 59 – Various ΔG' for primitive compounds having different amounts of PBL / fPBL

A graph for the ΔG' values for the completed compounds is not shown as the trend is very similar to that of the primitive compounds, although only for the sample 90/10 a positive effect is observed with all mixtures.

While the 100/0 compound seems to have similar properties to the reference run (without additives) and the 0/100 one suffers from an increased Payne effect, all systems with a mixture of the compatibilising oligomers display a remarkable decrease of the Payne effect. In particular, the best composition seems the 90/10 (Table 39, fourth row) that displayed not only the best ΔG' values in the green compounds, but also in the completed compounds.

The formulations for the addition of SBRL / fSBRL-L are summarised in Table 40 along with the amounts of added oligomers and the ΔG' values.

Run	Added oligomer in phr		G'(0.28%) – G'(10%) Primitive Compound, kPa		G'(0.28%) – G'(10%) Completed Compound, kPa	
	SBRL	fSBRL-L	Before annealing	After annealing	Before annealing	After annealing
(Blank run)	-	-	420.0	777.6	109.1	915.7
100/0	3.00	0.00	362.6 (-14%)	680.4 (-13%)	92.1 (-16%)	876.1 (-4%)
90/10	2.70	0.30	462.0 (+10%)	785.5 (+1%)	129.6 (+19%)	978.9 (+7%)
75/25	2.25	0.75	465.1 (+11%)	923.2 (+19%)	163.5 (+50%)	1148.5 (+25%)
50/50	1.50	1.50	479.5 (+14%)	909.7 (+17%)	152.7 (+40%)	1115.9 (+22%)
25/75	0.75	2.25	445.5 (+6%)	823.6 (+6%)	141.8 (+30%)	1061.1 (+16%)
0/100	0.00	3.00	465.0 (+11%)	907.7 (+17%)	158.7 (+45%)	1326.2 (+45%)

Table 40 – ΔG' values for SBRL / fSBRL-L runs. Green = reduced / orange = increased Payne effect

Table of colours; the blank run is the reference

<-25%	<-20%	<-15%	<-10%	<-5%	<±5%	>+5%	>+10%	>+15%	>+20%	>+25%

A graph of the ΔG' vs the content of fSBRL-L or the amount of equivalents of NCys added to the compound is reported in Figure 60.

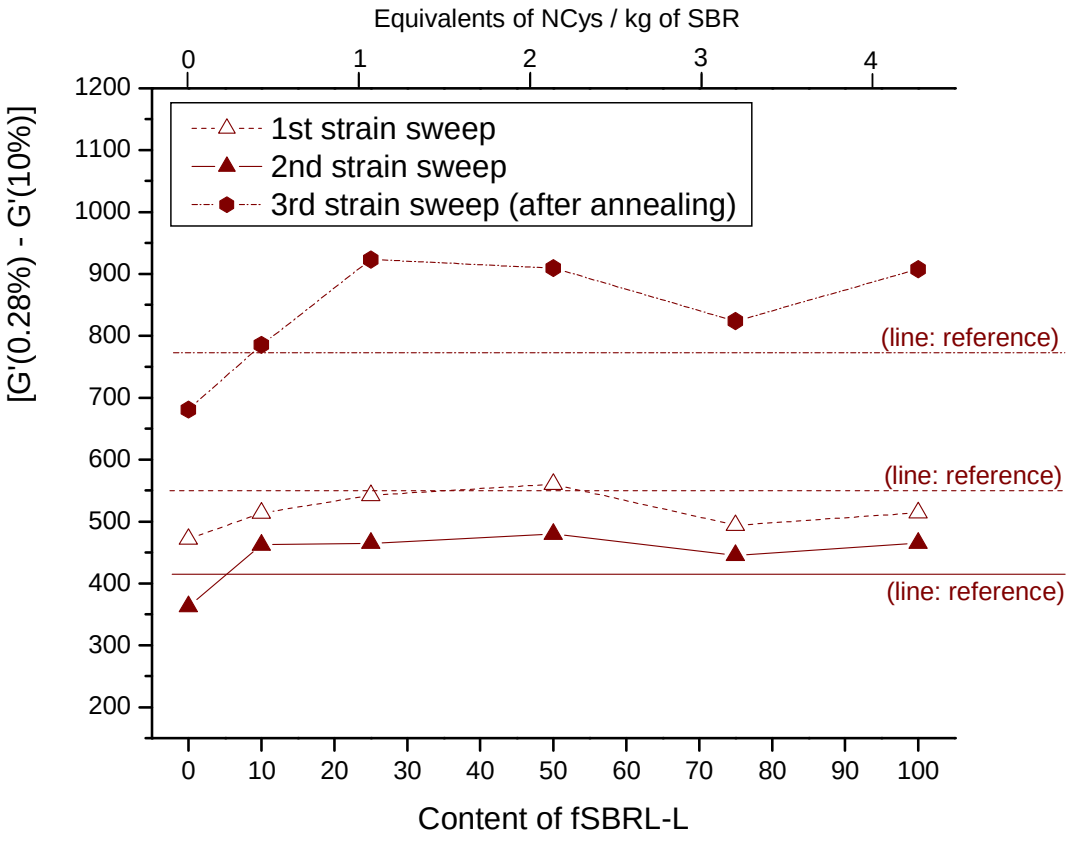

Figure 60 – Various ΔG' values for green compounds having different amounts of SBRL / fSBRL-L

Again, the substrate seemed unsuitable for reducing the Payne effect, and the only compound showing a decrease in the ΔG' values is that in which pure, unfunctionalised SBRL is used.

A last set of experiments was performed with the couple SBRL / fSBRL. fSBRL has the same amount of NCys equivalents per gram of the sample fPBL; the purpose of these experiments was to directly compare the PBL / fPBL couple with the SBRL / fSBRL couple in order to see a possible effect of NCys presence.

The formulations for the addition of SBRL / fSBRL are summarised in Table 41 along with the amounts of added oligomers and the ΔG' values.

Run	Added oligomer in phr		G'(0.28%) – G'(10%) Primitive Compound, kPa		G'(0.28%) – G'(10%) Completed Compound, kPa	
	SBRL	fSBRL	Before annealing	After annealing	Before annealing	After annealing
(Blank run)	-	-	242.8	1119.5	84.1	1541.5
100/0	3.00	0.00	170.1 (-30%)	742.2 (-34%)	75.2 (-11%)	1000.4 (-35%)
95/5	2.85	0.15	204.3 (-16%)	602.6 (-46%)	78.9 (-6%)	863.5 (-44%)
90/10	2.70	0.30	244.7 (+1%)	566.3 (-49%)	85.1 (+1%)	857.0 (-44%)
75/25	2.25	0.75	188.8 (-22%)	629.2 (-44%)	103.0 (+22%)	974.6 (-37%)
50/50	1.50	1.50	180.2 (-26%)	707.3 (-37%)	110.2 (+31%)	1192.9 (-23%)
25/75	0.75	2.25	232.4 (-4%)	969.5 (-13%)	129.4 (+54%)	1513.1 (-2%)
0/100	0.00	3.00	239.5 (-1%)	1018.7 (-9%)	144.7 (+72%)	1546.8 (~0%)

Table 41 – ΔG' values for SBRL / fSBRL runs. Green = reduced / orange = increased Payne effect

Table of colours; the blank run is the reference

<-25%	<-20%	<-15%	<-10%	<-5%	<±5%	>+5%	>+10%	>+15%	>+20%	>+25%

A graph of the ΔG' vs the content of fSBRL or the amount of equivalents of NCys added to the compound is reported in Figure 61.

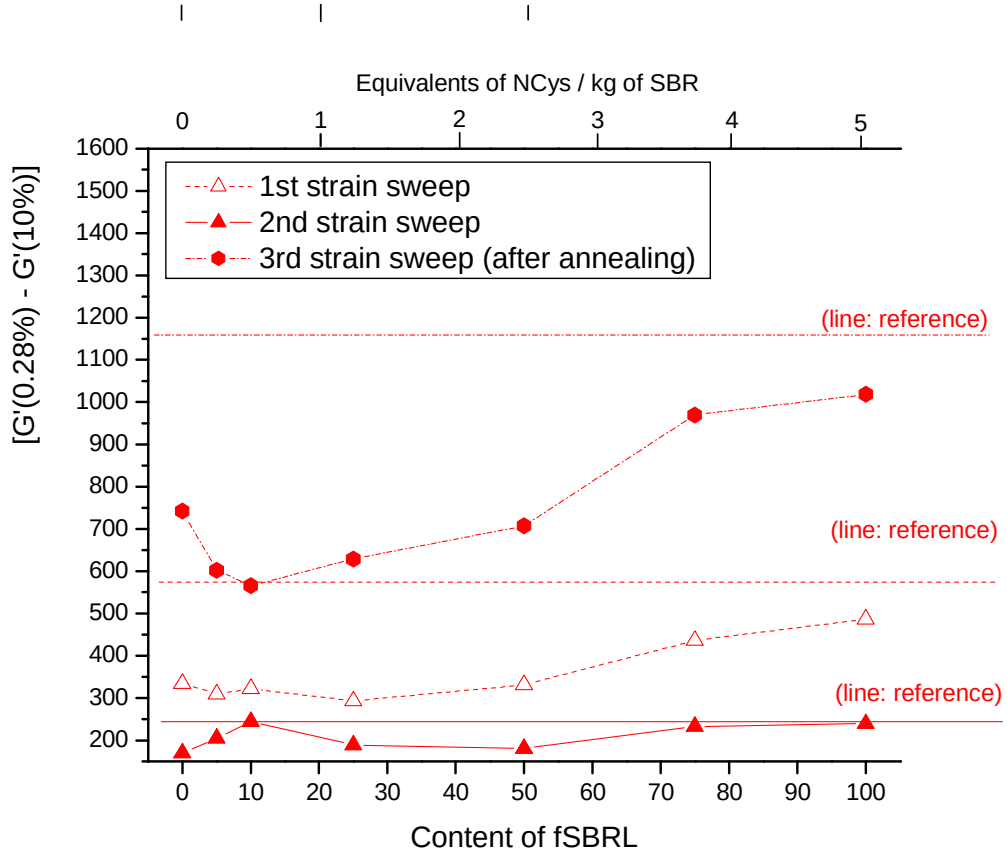

Figure 61 – Various ΔG' for primitive compounds having different amounts of PBL / fSBRL

These data are remarkably different than those obtained with the couple SBRL / fSBRL-L; this can be explained by considering the three colour tables and the graphs.

Before the completion of the compounds (second mixing), the rheological behaviour of primitive compounds is influenced by the presence of the added oligomers and the fillers. As said, the reduction of molecular weight of the polymeric part of the compound (an oligomer is being added) could favour the filler dispersion as it is a diffusion-controlled process, thus obtaining a reduced Payne effect along with a reinforcement (chapter 2.6.2, page 151). When a functionalised sample is added, probably a poor dispersion of it is responsible of an augmented Payne effect: this can be seen from the lowest rows of all the three coloured tables (Table 39, Table 40 and Table 41) when the added oligomer is *mainly* the functionalised one.

After flocculation of the pristine compounds (second column of the tables), the ΔG' value decreases, and this is usually followed by a further decrease (Table 39 rows 3, 4, 5 and 6; Table 40 row 2; Table 41 from row 2 to row 7 included). This could be a further characteristic of the mechanism of better dispersion induced by the presence of the oligomers: if the functionalised oligomer (fPBL / fSBRL / fSBRL-L) gets physically adsorbed on the silica particles covering them during the initial dispersion, this could reduce filler aggregation during flocculation, and the resulting compounds will display a smaller Payne effect.

The mixing conditions adopted in the present work are not sufficient to start the vulcanisation reaction during the completion of the primitive compounds. A partial vulcanisation, however, can be observed during the annealing of the completed compounds, and the final values of ΔG' are influenced by this phenomenon. In fact, if the flocculation occurs during the first minutes of annealing along with a certain extent of crosslinking, a coherent mass of filler will be constraint into a crosslinked rubber, and this will discourage filler disaggregation (in a successive strain-sweep routine) as it is a diffusion-controlled process. This is confirmed by comparing the ΔG' values of reference compound: after annealing the ΔG' values for completed compounds is much higher than for primitive compounds (first rows of Table 36, Table 39, Table 40 and Table 41).

In any case, for the compounds with the oligomers, the trend observed with the primitive compounds is reproduced after the completion: a decrement of the ΔG' values is observed also after completion. The values of the third columns of Table 39, Table 40 and Table 41, regards ΔG' of the second strain sweep (before the annealing step); these values are closer to the reference compound, but this effect is probably a *bias* generated by the very low absolute values of ΔG'.

Another rheometric value that can be obtained from the strain sweep experiment described above is the value *max tan δ*, defined as the maximum value of tan δ in the range [0%-10%] of strain. This value together with ΔG' is considered a good measure of the Payne effect as it is a direct measure of the hysteresis.

The *max tan δ* values for the samples considered in the present sub-chapter follow the trend of ΔG'; the values obtained for the SBRL / fSBRL samples are reported in graph *versus* the amount of added functionalised oligomer in Figure 62; for simplicity they are not reported in numbers.

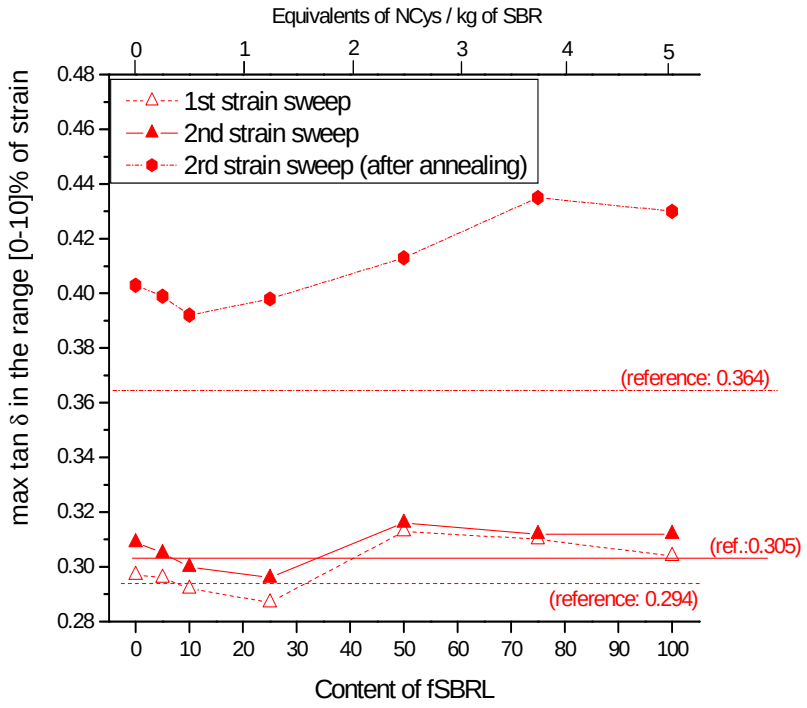

Figure 62 – Max tan δ values for the samples in which SBRL / fSBRL is added

With respect to the blank run, a decrease of the max tan δ samples is observed only for a few samples. In particular, for the PBL / fPBL series the decrease is observed only for the samples displaying the best ΔG' values (95/5, 90/10); at the same time, for the system SBRL / fSBRL-L there are no improvements except for the 100/0 run.

For the SBRL / fSBRL system the situation is similar but on a larger scale. More than one sample display a reduced hysteresis; a convenient description for this system is presented in a colour table (Table 42).

Run	Added oligomer in phr		Max tan δ Primitive Compound		Max tan δ Completed Compound	
	SBRL	fSBRL	Before annealing	After annealing	Before annealing	After annealing
(Blank run)	-	-	0.305	0.364	0.373	0.154
100/0	3.00	0.00	0.309 (+1.3%)	0.403 (+10.7%)	0.352 (-5.6%)	0.140 (-9.1%)
95/5	2.85	0.15	0.305 (0%)	0.399 (+9.6%)	0.361 (-3.2%)	0.144 (-6.5%)
90/10	2.70	0.30	0.300 (-1.6%)	0.392 (+7.7%)	0.360 (-3.5%)	0.148 (-3.9%)
75/25	2.25	0.75	0.296 (-3.0%)	0.398 (+9.3%)	0.360 (-3.5%)	0.146 (-5.2%)
50/50	1.50	1.50	0.316 (+3.6%)	0.416 (+14.3%)	0.391 (+4.8%)	0.157 (+1.9%)
25/75	0.75	2.25	0.312 (+2.3%)	0.435 (+19.5%)	0.382 (+2.4%)	0.182 (+18.2%)
0/100	0.00	3.00	0.312 (+2.3%)	0.430 (+18.1%)	0.388 (+4.0%)	0.181 (+17.5%)

Table 42 – Max tan δ values for SBRL / fSBRL runs. Green = reduced / orange = increased Payne effect

Table of colours; the blank run is the reference

<-15%	<-12%	<-9%	<-6%	<-3%	<±3%	>+3%	>+6%	>+9%	>+12%	>+15%

The last column of Table 42, related to values of completed compounds, displays very small values of max tan δ for all the samples, possibly indicating that a partial crosslinking (vulcanisers agents were added) occurred during the high-temperature annealing. In any case the situation is the same of the PBL / fPBL samples, with the compositions having a small amount of functionalised oligomer displaying the most remarkable improvements.

Unfortunately the stress-strain experiments performed on the completed compounds showed poor mechanical properties for all samples. This is in apparent contrast to what was reported in sub-chapter 2.6.2 for analogous compounds (the recipe for the sample PBL and SBRL-L in section 2.6.2 is identical to that of homologous runs reported in Table 39, Table 40 and Table 41 of the present sub-chapter); on the other side, the older samples were created with a Haake mixer and completed with an open two rolls mill and the results are not really comparable.

The various 300/100 ratios for stress-strain experiments performed on the completed compounds of this sub-chapter are reported in graph *vs* the compatibiliser composition (wt.-% fraction of functionalised oligomer introduced in the compound) in Figure 63.

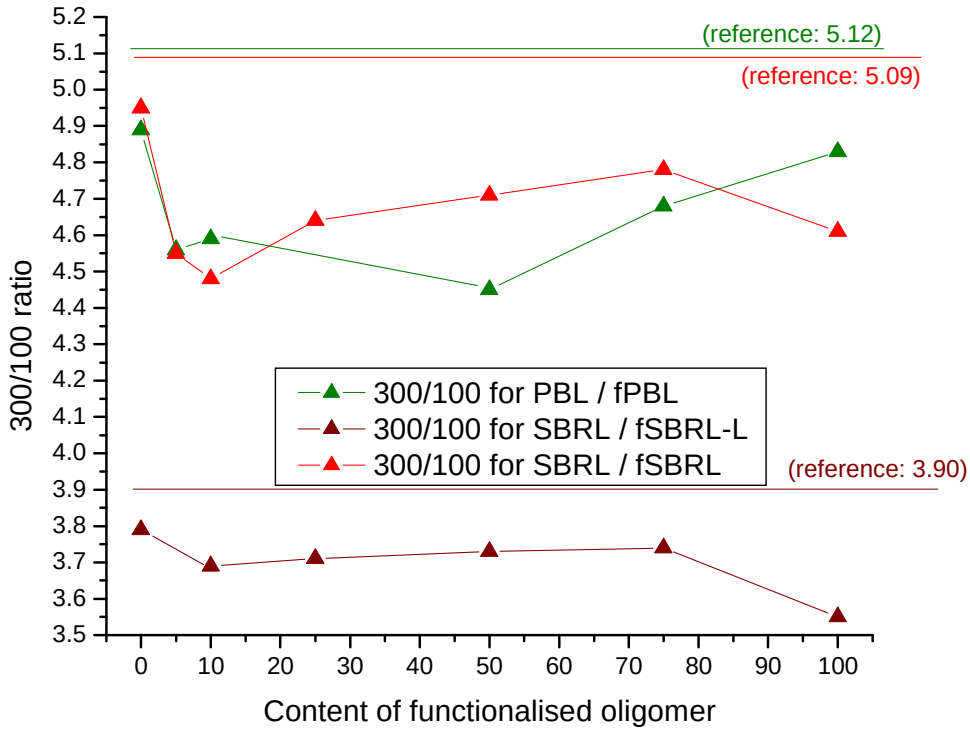

Figure 63 – 300/100 ratio for the comounds of the present sub-chapters

Especially in the first part of the graph (content of functionalised oligomer in the range [0-10]) it is evident that the 300/100 ratio is very small. Since the Payne effect for these values is inferior to the reference compounds in the considered zone (see Figure 59, Figure 60 and Figure 61), one could expect that the reinforcing action of silica could lead to an improvement of the 300/100 ratio in this zone, but an opposite behaviour is instead observed. A possible explanation of this experimental evidence could be that the effect of the addition of a low-molecular weight polymer to the compound (causing reduction of the material elasticity) prevails on the effect of a better distribution of the reinforcing filler (that should lead to better mechanical performances of the material).

3. FINAL REMARKS

In the present thesis work the synthesis, through a thiol-ene reaction, of added-value elastomers (butadiene homo- and copolymers with styrene) having grafted amino acidic side chains (L-cysteine derivatives) has been performed. New materials were obtained; these materials showed different bulk properties as a function of conversion level.

As a preliminary study, according to the investigation methodologies expressed in scientific literature on similar functionalisations, the reactivity of the L-cysteine derivatives with model olefins was checked and confirmed. An initial setup of experimental conditions was established and tried in order to establish a base from which experimental variables could be tuned and modified with later experiments in order to obtain better reaction performances.

The functionalisation degree of the synthesised samples starting from short-chain copolymers was evaluated through ^{1}H-NMR providing generally high yields (in terms of thiol conversion) and relatively high grafting degrees (up to 80%), modulated and controlled by feed ratios. The accurate structural characterisation of products confirmed the substantial chemical inactivity of 1,4- units towards thiol (the L-cysteine derivatives), and provided that chain extension reactions can be avoided by choosing appropriate ratios between the amounts of thiol and radical initiator (AIBN). At the same time an unexpected lack of residual 1,2- units in the products was observed and attributed to a cyclisation side reaction already reported in literature.

The T_g values of functionalised liquid polybutadiene samples and poly(styrene-co-butadiene) random copolymers increased with the number of grafted functionalities up to DF of about 30%. The T_g thus levels off to a constant value; this increment is especially remarkable considering the *N*-acetyl-L-cysteine functionalised samples (T_gs reach a maximum value of ~ 80°C) rather than in the case of the *N*-acetyl-L-cysteine methyl ester functionalised samples (~ 30°C), and it is probably due to the different possible interactions involving acid or ester groups.

All modified polymers displayed a remarkable optical activity, while the pristine polymers are non-chiral. Thus, it has been demonstrated that the thiol-ene reaction can be intended as an innovative approach to obtain optically active polymer by simply transferring this property from a chemical species (the L-cysteine derivative) to the polymer.

This last aspect, jointly with the selectivity of the reaction (almost only the vinyl double bonds are reactive) and the possibility to keep under control side reactions, opens the way to the synthesis of new materials starting from unsaturated polyolefins with different primary structure like SBS and SBR copolymers. One should take into account that structural differences between substrates have an impact on the reactivity: in the case considered in the present study, similar evidences were in

evidence both for the homopolymer of butadiene and for the copolymer SBR. In particular, the presence of a styrene moiety in the macromolecular chain (i.) limited the conversion degrees (ii.) limited the cyclisation side reaction and (iii.) limited the chain elongation thanks to possible chain-scission paths (these effect, as discussed, are related to styrene sterical hindrance and peculiar reactivity of tertiary carbons bonded to benzylic moieties).

The functionalisation of long-chain SBR copolymer led to good yields in solution, although the substrate seemed more sensitive to chain elongation reactions (presence of crosslinked products). Two workaround strategies, already adopted in the literature, were used to avoid chain elongation; while being effective in that sense, the conversion degree dropped to low values. When the functionalisation was carried out in bulk, the grafting yield was very low (probably because of the scarce compatibility / dispersibility of the functionalising agent into the elastomer) and associeted to chain elongation; the addition of an antioxidant (6PPD) or the initiator (AIBN) removal led to a lower occurrence of side reactions but also to no grafting. In conclusion, the addition of L-cysteine derivatives to rubbers in bulk seemed overall uneffective; a possible variation of the derivative (for instance: with the introduction of a hydrophobic spacer between groups, or an hydrophobic ester moiety) could lead to a better dispersion and better results.

The last part of the present work is focused on the incorporation of various functionalised or unfunctionalised samples into rubber / carbon black / silica ternary compounds (along with classical silica / elastomer compatibilisers and processing agents) whose formulation came from the ground tyres industrial sector. The compatibilising oligomers, that were introduced through mechanical mixers into the compounds, changed their rheological properties causing improvements or worsenings. In particular, the best reduction of the Payne effect (often associated to an improvement of the hysteretic behaviour of the compounds along with a reduced rolling resistance of tyres) was obtained by adding particular amounts of both functionalised and unfunctionalised oligomers. This evidence was discussed in relation to the molecular principles of the Payne effect, and highlighted that a possible synergistic action of the two compounds occurred: while the unfunctionalised polymer led to local softening of the polymer matrix encouraging filler diespersion, the functionalised one could help in the disgregation of filler aggregates / agglomerates. On the other side, though, while most rheological properties were improved the tensile properties underwent an unexpected worsening of the hardness, suggesting that the reinforcement due to fillers was moderated by some factor. Probably the addition of short-chain polymers such as those used in this thesis part played a role in this negative effect that exceeded a better filler dispersion witnessed by the improved rheological properties.

4. EXPERIMENTAL SECTION

4.1 Materials

4.1.1 Diene polymers and model olefins

- 1-dodecene (Aldrich) was purified by reflux in a Claisen flask and distilled over sodium; it was kept in a dry nitrogen atmosphere at room temperature.
- A commercial liquid 1,2-polybutadiene (Sigma-Aldrich) was used as received. The polymer has been named PBL in the present work, and its reactivity is discussed especially in chapter 2.2 (page 61). The ^{1}H-NMR spectrum of this PBL, dissolved in $CDCl_3$ at room temperature, was evaluated according to literature[229] for the determination of primary structure: 90.9 mol.-% of 1,2- vinyl units and 9.1 mol.-% of 1,4-*trans* units were found. The content of 1,4-*cis* units is negligible. The average molecular weight of the polymer, according to SEC measurements evaluated with a polystyrene calibration curve, is $<M_n>$ = 4080 Da ($<DP_n>$ = 75 units), and the polydispersity index is PDI = 1.43.
- A commercial liquid styrene-*co*-butadiene random copolymer (*Ricon 100,* Sartomer Inc.) was used as received. The polymer has been named SBRL in the present work, and its reactivity is discussed especially in chapter 2.3 (page 104). The ^{1}H-NMR spectrum of SBRL dissolved in $CDCl_3$ at room temperature was evaluated according to literature[298] for the determination of primary structure. SBRL contains 62.0 mol.-% of 1,2- butadienic units, 13.1 mol.-% of styrenic units, and the remaining 24.9 mol.-% are the sum of 1,4-*cis* and 1,4-*trans* units; this complies with the supplier data sheet. The followed method does not allow to measure the 1,4-*cis vs* 1,4-*trans* units ratio; the determination was performed through ^{13}C-NMR[299-301] in $CDCl_3$ at room temperature (the exact procedure is described in chapter 2.3.2, page 109). SBRL is composed by: 13.1 mol.-% styrene, 62.0 mol.-% (1,2-) butadiene units, 15.6 mol.-% (1,4-*cis*) butadiene units, 9.3 mol.-% (1,4-*trans*) butadiene units.

  According to SEC measurements, SBRL has a multimodal molar mass distribution as seen in chapter 2.3.1 (page 105). The average molecular weight of a first fraction is $<M_n>$ = 11080 Da (PDI = 1.01), for a $<DP_n>$ of 171 units; for the second population, $<M_n>$ = 4970 Da (PDI = 1.04), for a $<DP_n>$ of 76 units; a third population is made from butadiene homopolymer and it is oligomeric ($<M_n>$ = 1720 Da, PDI = 1.18, $<DP_n>$ of 31 units). According to the supplier data sheet and to relative intensity of RI and UV peaks of the SEC, the most important population is the second one, having $<M_n>$ = 4970 Da and a

$<DP_n>$ of 76 monomeric units.

SBRL, moreover, contains 100 ppm of BHT as evidenced in the FT-IR and proton NMR spectra; this amount of antioxidant was not removed from the polymer as much inferior to the amount of initiator added for the thiol-ene functionalisation.

- A commercial long-chain styrene-*co*-butadiene random copolymer (*Europrene SOL R-72612*) was purchased from Polimeri Europa, and used as received. The substrate was named SBR5 and functionalised in solution or in bulk with L-cysteine derivatives (chapter 2.5, page 136) or either used as a matrix for the formulation of high-silica compounds (chapter 2.6, page 148). SBR5 was precipitated twice in methanol to remove aliphatic oil extenders (MES); these oils were characterised through IR and ^{1}H-NMR spectroscopy. Spectra accounted for aliphatic compounds, with no C=C double bonds nor aromatic units.

  After MES removal, SBR5 was characterised through ^{1}H-NMR in order to determine the amounts of monomeric units in the macromolecular chains. SBR5 is composed by 50.6 mol.-% of 1,2-butadiene units, 34.3 mol.-% of 1,4-butadiene units (sum of *cis* and *trans*) and 15.1 mol.-% of styrene units, for a weighted average MW of the repeating unit of 61.65 Da.

  The determination of the molecular weight of SBR5 was performed through SEC using $CHCl_3$ as the mobile phase. The chromatogram of pristine SBR5 shows a bimodal molecular weight distribution; the main peak of the SBR5 chromatogram accounts for a $<M_n>$ ($<M_w>$) of 637000 (674000) Da; a smaller peak at higher elution times accounts for a $<M_n>$ ($<M_w>$) of 462000 (541000) Da.

4.1.2 Functionalising Agents, L-cysteine derivatives

N-acetyl-L-cysteine (NCys, >99%) and its methyl ester (NCysMe, >99%) were supplied from Sigma-Aldrich and used as received.

L-cysteine methyl ester (CysMe) was synthesised through L-cysteine esterification according to existing literature[339] in two steps: (i.) synthesis of CysMe hydrochloride and (ii.) of CysMe.

(*Synthesis of L-cysteine methyl ester hydrochloride*) A three neck, 1-litre flask equipped with a mechanical stirrer on the central neck and dipped in a $CO_{2(s)}$ / $MeOH_{(l)}$ bath thermostated at -78°C is vacuum-degassed and filled with 400 ml MeOH. 40.00 grams (0.330 mol) of L-cysteine is then suspended; 28 ml (0.384 mol) of $SOCl_2$ is added dropwise. The L-cysteine slowly dissolves to form a clear solution. The solution is stirred overnight at room temperature. The solvent is volatilised under vacuum to yield CysMe · HCl as a colourless, sticky syrup (56.8 g, 95.5% yield). The product solidified upon standing.

(*Synthesis of L-cysteine methyl ester*) CysMe · HCl (5.00 grams) is dissolved in 200 ml of water (HPLC grade) and neutralised dropwise by the addition of NaOH 0.1 N. The resulting solution is washed with 5 fractions of 200 ml of ethyl acetate in a separation funnel; the ethyl acetate fractions (nearly 1 liter) are dried overnight with $Na_2SO_{4(s)}$, filtered and put into rotating evaporator. After solvent evaporation, the resulting yellow oil is distilled under reduced pressure (boiling point of the fraction: 17 mmHg, 39.5°C) and kept in dry nitrogen atmosphere at -20°C. Conversion: 32.5 wt.-%.

4.1.3 Free radical initiators

2,2'-azobisisobutyrronitrile (AIBN, Carlo Erba) and Dicumylperoxide (DCP, Aldrich) were monthly re-crystallised from ethanol and stored under dry nitrogen atmosphere at -20°C.

4.1.4 Additives for rubber compounding

- Radical scavenging agents. 2,4-di(*tert*butyl)hydroxytoluene (BHT, 99+%) was purchased from Sigma-Aldrich and used as received; *N*-(1,3-dimethylbutyl)-*N'*-phenyl-1,4-phenylendiamine (6PPD, 97%) was kindly supplied by Westco (Western Reserve Chemical Corporation, Stow, Ohio, USA) and used as received.
- As fillers, N330 Carbon Black (Degussa AG, Düsseldorf, Germany) and Silica Zeosil 1165 (Rhône-Poulenc, Courbevoie Cedex, France) were purchased and used without any further purification.
- As compatibilising agent, TESPT X50S (Degussa AG, Düsseldorf, Germany) was used as received. It consists in a 1:1 by weight mixture of bis(3-triethoxysilylpropyl)tetrasulfane (TESPT) and N330 Carbon Black.
- As vulcanisation-related agents, Stearic Acid, Zinc Oxide, elemental Sulphur (purchased from Sigma-Aldrich) *N*-cyclohexyl-2-benzothiazyl sulphenammide (CBS, Westco, Stow, Ohio, USA) and *N,N'*-diphenyl guanidine (DPG80, Safic-Alcan Italy) were used as received.

4.1.5 Solvents and multi-purpose chemicals

1,4-dioxane (Baker) and chlorobenzene (Carlo Erba) were distilled over sodium / potassium alloy and kept in a dry nitrogen atmosphere; water, ethanol and methanol, n-hexane, ethyl acetate and chloroform were HPLC standard grade (Baker) and used without further purification.

The silica gel used for the PBDCP and the SBRLDCP runs purification was supplied from Merck GmbH; the mean particle size was between 0.040 and 0.063 mm. The silica was used without any purification.

Anhydrous $Na_2SO_{4(s)}$ (Baker) was purchased and immediately used without any further purification.

4.2 Procedures

4.2.1 Addition of N-acetyl-L-cysteine to 1-dodecene (chapter 2.1, page 59)

(In presence of 1,4-dioxane as a solvent) 10 ml of 1,4-dioxane, 3 ml (13.6 mmol) of 1-dodecene, 2.219 g (13.6 mmol) of NCys and 0.0446 g (0.272 mmol) of AIBN are introduced into a two-necked flask under nitrogen atmosphere. The resulting mixture is stirred and heated at 90°C for 4h and then cooled down to room temperature. The reaction product containing the unreacted 1-dodecene, the unreacted NCys and the resulting thioethereal compound is recovered by evaporation of the solvent (dioxane) and analysed by means of IR and NMR spectroscopies. The addition product (*N*-acetyl-*S*-dodecyl-L-cysteine) is isolated by removing other products (essentially unreacted olefin and NCys) by distillation under reduced pressure. The residue (2.41 g) is characterised by IR and ^{1}H-NMR (the NMR spectrum is reported in the text, page 61).

(1-dodecene used as a solvent) Into a two-necked flask, 4.5 ml (20.3 mmol) of 1-dodecene and 3.331 g (20.3 mmol) of NCys are introduced under nitrogen atmosphere. After stirring for 1 hour, 0.0666 g (0.203 mmol) of AIBN is added and the resulting mixture is heated at 90°C for 4h. The reaction product and the unreacted reagents were separated by distillation under reduced pressure; the residue (3.85 g), that consists in the addition product, was characterised by means of IR and ^{1}H-NMR.

4.2.2 PBL: thiol-ene functionalisation reactions performed in solution (chapter 2.2.2, page 67)

In a typical experiment, 1 g of PBL (18.49 mmol) is put into a 250 ml Schlenk flask immersed into a thermostated oil bath and equipped with a magnetic stirrer. The system is vacuum-degassed at 60°C for 4 hours at ~10^{-2} mbar; after ~1 hour degassing, no more bubbles evolve from the surface of the liquid polymer. The reactor is then cooled to 25°C, and ~50 ml of distilled 1,4-dioxane is added under dry nitrogen flux with a hypodermic syringe to obtain a 2 wt.-% solution of polymer in dioxane. The system is then stirred overnight at room temperature. On the next day, the thiol (NCys, NCysMe or CysMe) is added; the thiol concentration was varied from 10 mol.-% to 100

mol.-% with respect to the vinyl double bonds (from 9.09% to 90.9% with respect to the total amount of double bonds). After the occurrence of thiol complete dissolution, 1 ml of a 1,4-dioxane solution of AIBN is added. The amount of AIBN was chosen as 1 mol.-% with respect to the thiol, regardless from the RSH / double bonds initial ratio. The Schlenk tube is eventually closed and immersed into an oil bath at 70°C for 4h and 48', that is the half-life time of AIBN at 70°C.
At the end of the reaction, the solvent is immediately removed with a Büchi Rotavapor, and the residual polymer is dispersed in 250 ml of water and stirred overnight to remove the unreacted thiol. Then, the polymer is recovered by filtration with a glass filter into the form of small polymer blocks (more or less "greasy" depending on reaction conditions) and purified again by dispersion in 250 ml of water and successive filtration. This procedure has been repeated twice for all samples; the water filtered from the last operations was dried and checked for the presence of residual thiol with a FT-IR spectrometer. If any, another washing of the polymer was performed to remove residual unreacted thiol. The functionalised samples are lately kept at 50°C under vacuum until constant weight. No insoluble polymer fractions were collected. The samples were then characterised through FT-IR, ^{1}H-NMR, DSC analysis, along with polarimetric measurements in solution. The PBNCysMe samples were also characterised by SEC in order to determine their MW.

4.2.3 PBwoRSH and PBDCP (chapter 2.2.5, page 76)

These two experiments are carried out simply treating the liquid PB with a free-radical generator.

(PBwoRSH) 1 g of PBL (18.49 mmol) is put into a 250 ml Schlenk flask immersed into a thermostated oil bath and equipped with a magnetic stirrer. The system is vacuum-degassed at 60°C for 4 hours at ~10^{-2} mbar; after ~1 hour degassing, no more bubbles evolve from the surface of the liquid polymer. The reactor is then cooled to 25°C, and ~50 ml of distilled 1,4-dioxane is added under dry nitrogen flux with a hypodermic syringe to obtain a 2 wt.-% solution of polymer in dioxane; the polymer is swollen overnight. On the next day the Schlenk flask containing the polymer is thermostated in an oil bath to 70°C; in the meanwhile 30.4 mg (0.1849 mmol) of AIBN is dissolved in ~2 ml of 1,4-dioxane and then quantitatively added to the Schlenk flask containing the polymer (a washing with 1,4-dioxane of the container of the 2 ml solution of AIBN could be conveniently performed in order to remove all the AIBN traces from the container. The washing solution is added to the Schlenk flask containg the polymer as well). The flask is eventually closed and kept into an oil bath at 70°C for 4h and 48', that is the half-life time of AIBN at 70°C.
The reaction product is dried from the solvent and re-dissolved in n-hexane; later it is purified by chromatography on a silica column using n-hexane as the mobile phase. This operation is

necessary to remove unreacted AIBN. The purified polymer was characterised through SEC, NMR and IR spectroscopy.

(PBDCP) 1 g of PBL (18.49 mmol) is put into a 250 ml three-neck flask equipped with reflux condenser, magnetic stirrer and immersed into a thermostated oil bath. The system is vacuum-degassed at 60°C for 4 hours at ~10^{-2} mbar; after ~1 hour degassing, no more bubbles evolve from the surface of the liquid polymer. The reactor is then cooled to 25°C, and ~50 ml of chlorobenzene is added; the polymer is dissolved overnight. On the next day, 249.9 mg (0.9245 mmol) of DCP is added with a spatula in the flask containing the polymer solution. The reaction is carried out for nine hours at the solvent reflux (~137°C) under inert atmosphere; the crude, brown reaction product is dried with a rotating evaporator and re-dissolved in n-hexane. Later the product is purified by chromatographic separation on a silica column using n-hexane as the mobile phase. The resulting fractions are characterised through ^{1}H-NMR, IR spectroscopy and SEC.

4.2.4 PB(NCys/NCysMe)030woAIBN (chapter 2.2.6, page 89)

The reactions are carried out exactly as in presence of AIBN (see part 4.2.2), except for the addition of AIBN that is not performed. The reaction begins at the complete dissolution of the thiol in the polymer solution in 1,4-dioxane, and stopped after 4h48'. The reaction work-up is performed in the same way of the experiments carried out in presence of AIBN.

4.2.5 SBRL: thiol-ene functionalisation reactions performed in solution (chapter 2.3.3, page 114)

The experimental procedure is identical to that of PBL, except for the employed amounts of rubber. 1 g of SBRL consists in, by considering the molecular weight of the repeating unit as 61.6 Da, 16.23 mmol; the amount of thiol and of initiator are dosed with respect to the double bonds molar amount. The only functionaliser adopted for SBRL is the NCys instead of NCys, NCysMe and CysMe.

4.2.6 SBRLwoRSH (chapter 2.3.2, page 109)

1 g of SBRL (16.23 mmol) is put into a 250 ml Schlenk flask immersed into a thermostated oil bath and equipped with a magnetic stirrer. The system is vacuum-degassed at 60°C for 4 hours at ~10^{-2} mbar; after ~1 hour degassing, no more bubbles evolve from the surface of the liquid polymer. The reactor is then cooled to 25°C, and ~50 ml of distilled 1,4-dioxane is added under dry nitrogen

flux with a hypodermic syringe to obtain a 2 wt.-% solution of polymer in dioxane; the polymer is swollen overnight. On the next day the Schlenk flask containing the polymer is thermostated in an oil bath to 70°C; in the meanwhile 26.7 mg (0.1623 mmol) of AIBN is dissolved in ~2 ml of 1,4-dioxane and then quantitatively added to the Schlenk flask containing the polymer (a washing with 1,4-dioxane of the container of the 2 ml solution of AIBN could be conveniently performed in order to remove all the AIBN traces from the container. The washing solution is added to the Schlenk flask containg the polymer as well). The flask is eventually closed and kept into an oil bath at 70°C for 4h and 48', that is the half-life time of AIBN at 70°C.
The reaction product is dried from the solvent and re-dissolved in n-hexane; later it is purified by chromatography on a silica column using n-hexane as the mobile phase. This operation is necessary to remove unreacted AIBN. The purified polymer was characterised through SEC, ^{1}H-NMR, ^{13}C-NMR and IR spectroscopy, and DSC calorimetry.

4.2.7 SBRLDCP (chapter 2.3.5, page 119)

1 g of SBRL (16.23 mmol) is put into a 250 ml three-neck flask equipped with reflux condenser, magnetic stirrer and immersed into a thermostated oil bath. The system is vacuum-degassed at 60°C for 4 hours at ~10^{-2} mbar; after ~1 hour degassing, no more bubbles evolve from the surface of the liquid polymer. The reactor is then cooled to 25°C, and ~50 ml of chlorobenzene is added; the polymer is dissolved overnight. On the next day, 219.3 mg (0.8115 mmol) of DCP is added with a spatula in the flask containing the polymer solution. The reaction is carried out for nine hours at the solvent reflux (~137°C) under inert atmosphere; the crude reaction product is dried with a rotating evaporator and re-dissolved in n-hexane. Later the product is purified by repeated precipitation in MeOH / filtration / dissolution of the residual fraction in n-hexane. After having performed this task thrice, the polymer is dried to constant weight with a vacuum pump and characterised through ^{1}H-NMR spectroscopy.

4.2.8 SBRLNCys030woAIBN (chapter 2.3.6, page 125)

The reactions are carried out exactly as in presence of AIBN (see part 4.2.5), except for the addition of AIBN that is not performed. The reaction begins at the complete dissolution of the thiol in the polymer solution in 1,4-dioxane, and stopped after 4h48'. The reaction work-up is performed in the same way of the experiments carried out in presence of AIBN.

4.2.9 SBR5: thiol-ene functionalisation reactions performed in solution (chapter 2.5.2, page 139)

In a typical experiment, 13.7 g of SBR5 (222.3 mmol) is put into a 1000 ml 3-neck flask immersed into a thermostated oil bath and equipped with a mechanical stirrer (on the central neck). The system is vacuum-degassed at 60°C for 4 hours at ~10^{-2} mbar. The reactor is then cooled to 25°C, and ~500 ml of distilled 1,4-dioxane is added under dry nitrogen flux with a glass syringe, in order to obtain a 2 wt.-% solution of polymer (13.7 grams of SBR5 account for 10.0 grams of pristine SBR and 3.7 grams of extending aliphatic oil MES). The system is stirred overnight; on the next day, the solution results as a pale yellow liquid. 0.600 grams of NCys (3.6 mmol, 6 phr) is added; dissolution of this amount of NCys at room temperature takes a few minutes. After complete dissolution, three cases are distinguished: in a first instance (i) the reaction is started without any further addition; in another instance (ii) a free radical initiator (AIBN) is added; in a third instance (iii) both the free radical initiator (AIBN) and a radical-scavenging agent (6PPD) is added. In case (i), the flask is closed and heated in an oil bath at 70°C for 4h and 48'. In case (ii), ~5 ml of a 1,4-dioxane solution of AIBN (of known concentration) is added; the amount of AIBN is chosen in order to keep the AIBN / RSH molar ratio constant and equal to 1 mol.-% according to the previously discussed optimisation of initiator / thiol ratio. In instance (ii) 0.040 g of AIBN are added in the same way; the flask is then closed and heated in an oil bath at 70°C for 4h and 48'. In instance (iii) the procedure is identical to (ii), but before closing the flask, 0.070 g of 6PPD is added (in cases (ii) and (iii) the dissolution of the AIBN or 6PPD is almost immediate).
The samples *woAIBN* (instance (i)) or *6PPD* (instance (ii)) were purified by double precipitation in methanol; this allowed to remove the MES, the unreacted thiol, traces of unreacted AIBN and 6PPD. In instance (ii), a partially crosslinked product was obtained; after purification by room temperature multiple washings with 1,4-dioxane, the gel resulted in 41 wt.-% of the total (mass balance). The non-crosslinked fraction was purified by double precipitation similar to what was done with non-crosslinked products, and characterised in the same way.

4.2.10 SBR5: thiol-ene functionalisation in bulk (chapter 2.5.3, page 144)

This set of reactions was performed in a Brabender Plastograph 2-rolls mechanical mixer having a 30 ml chamber and thermostated tools. The instrument was also equipped with a torque measurement system that measured strains applied to its rotors.
Six functionalisation reactions were carried out: three having a lower content of NCys (3 phr) and three with a higher one (6phr). In a first instance (i) the run has been carried out in presence of both AIBN and NCys; in a second instance (ii) the initiator was omitted, and (iii) in a third run the

SBR was pre-treated with 6PPD, i.e. before the addition of NCys and AIBN. A typical formulation for the addition procedure is reported in Table 43.

SBR5NCys 3phr 6PPD							
T(℃)	time	phase	Chemical	phr	Density (kg/l)	Volume (ml)	Weight (g)
100	0'	1	SBR5 (Europrene polymer)	137	0.93	23.6860	21.0980
	1'	2	6PPD	0.7	1.02	0.1057	0.1078
	3'	3	NCys	3.0	1.00	0.4620	0.4620
			AIBN	0.1	1.00	0.0308	0.0308
	11'	4	BHT	5.0	1.00	0.7700	0.7700
~110	12'		**EXIT**	145.9	0.9341	25.0545	22.4686

Table 43 – Recipe for the SBR5NCys 3phr 6PPD functionalisation run. Rotor speed = 50 rpm

Starting from a temperature of 100°C, the reaction heat along with the friction of the polymer on the tools raised the temperature of the reaction chamber to nearly 110°C in 10 minutes. Before the addition of SBR5 (phase 1 for all the experiments), the Brabender's chamber is filled with nitrogen through a dispenser (with an purge valve) of pure N_2. Then the polymer is added as small stripes.

The formulation of Table 43 refers to instance (iii), and includes a pre-treatment of the SBR (introduced in phase 1) with 6PPD (phase 2); the polymer is blended for two minutes with the anti-oxidant before the addition of the functionalising agent. Then a mixture of crystals of NCys and AIBN is added; for the experiments carried out in absence of 6PPD (3phr, instance (i) and (ii), 6 phr, instance (i) and (ii)), this addition is phase 2 and it is performed after 1 minute from the beginning of the stirring. Obviously, phase 2 comprises NCys alone in the samples carried out in absence of AIBN (instance (ii)).

After the addition of chemicals (NCys alone, NCys + AIBN, 6PPD + NCys + AIBN), the mixer is closed with a steel cone and kept in these conditions up to minute 11. Then, a fixed amount of BHT is added, which is a moderate excess with respect to the introduced AIBN (50:1 by weight, 30:1 by mol). If no AIBN is present, BHT is also introduced, in the amount of 5 phr.

The last columns on the right of Table 43 have an experimental purpose: they are used to estimate the filling of the mixer, and the weight of the reactants is adjusted in order to achieve a constant filling of the reaction chamber. The most reproducible results with the Brabender mixer are achieved with a total volume of 25 ml.

After the finish of the reaction, i.e. when the rotors are stopped, the raw product is immediately dissolved in 1,4-dioxane and re-precipitated twice in MeOH similarly to what was done in the case of the functionalisation carried out in solution (paragraph 4.2.9, page 178). No insoluble products were collected; the purified polymers were filtered, washed and dried to constant weight under vaccum (oil pump), and were characterised in the usual way (IR, SEC).

4.2.11 High-silica rubber compounds creation (chapter 2.6, page 148)

This set of syntheses was performed with various instruments located at Pirelli Tyres or at Pirelli Labs in Milan.

For the recipes adopted in paragraph 2.6.1 (page 148), the following sequence was adopted:

- creation of the green compound (Haake Mixer)
- homogenisation of the green compound (2-rolls open air mill)
- (removal of samples for characterisations)
- addition of vulcanisation-related agents
- homogenisation of the final compounds (Brabender Mixer)
- (characterisation of the final compounds)

The recipes described in chapter 2.6 (page 148 and following) are reported in Table 33 (page 149) and in Table 35 (page 151) especially regarding the amount of added chemical substances, the timings of the operations and the temperature of the mixing chamber.

In an typical experiment, the mixer (Haake-type or Brabender-type) is allowed to rotate for two minutes under nitrogen flux for the calibration of rotors and of thermocouple. Then the polymer is added in stripes until the weight written on the recipe is reached; the mixer is then closed (with an electrical engine-driven *V-shaped* steel closure). Then *phase 1* of formulations is added: the silica and the CB are mixed in the solid state and slowly introduced into the mixing chamber. This operation needs some care as a quick addition could cause polymer disgregation and formation of small particles of polymer covered by silica / carbon black; in this case, the torque values drop to zero and no further mixing is possible (the entire operation of mixing need to be performed again). The addition of the second and other phases to the mixer is performed in the same way of phase 1: the closure is opened, the chemical agents are poured into the chamber and the system is closed again. At the end of the procedure, the rotors are stopped, the mixing chamber is opened and the raw polymer is recovered and cooled to room temperature.

The open-air 2-rolls mill homogenisation occurs through a finite number of passages between two-rolls termostated as 60°C. The homogenisation occurs by passing the crude compound into the rolls from the upper side to the down side. Progressively shorter distance is given to the rolls; for ~160 grams of compounds, a starting value of 2 centimetres as inter-rolls distance is used. The distance is then lowered to 0.5 cm by getting the rolls closer; this operation is performed throughout approximately two dozen of passages of the compound into the machine.

The samples for stress-strain experiments and rheological characterisation are cut from the sheet of the compound, whose thickness is 0.5 cm.

4.3 Instruments

4.3.1 Infrared analysis

Infrared spectra were collected by a Fourier transform spectrometer “Perkin Elmer FT-IR 1750” on films cast from 1,4-dioxane / n-hexane / chloroform solutions of the samples on a KBr window. Characterisation of reagents (e.g. NCys or other crystals) was performed after dispersion in KBr dishes.

4.3.2 NMR analysis

Proton magnetic resonance spectra were collected in solution by using a NMR spectrometer “Varian Gemini 200 MHz” or “Varian Gemini 300 MHz”; spectra of NCys functionalised PBL and SBRL (PBNCys and SBRLNCys experiments) were recorded in DMSO-d_6, spectra of NCysMe functionalised PBLs (PBNCysMe experiments) in C_6D_6. In all cases the chemical shifts were assigned in ppm using the impurities of C_6D_5H and DMSO-d_5 as internal standards. 32 scans were performed for all samples, at room temperature.
^{13}C-NMR experiments were performed in solution using the same instruments. $CDCl_3$ or DMSO-d_6 were used as solvents. Usually 8 hours of scans (delay between the scans: 1000 ms) were used as a standard procedure; spectra were collected at room temperature for $CDCl_3$ or at 60°C for DMSO-d_6.

4.3.3 Differential scanning calorimetry

DSC analysis was performed with a “Perkin Elmer DSC7” instrument in the temperature range from -60°C to 120°C at a scanning rate of 10°C/min. Calibration was carried out using mercury (m.p. -38.4°C) and indium (m.p. 156.2°C) standards.

4.3.4 Polarimetric analysis

The optical activity measurements for both L-cysteine derivatives and functionalized polymers were performed with a digital polarimeter “Jasco DIP-360” at C = 1 mg / 100 ml in different solvents with respect to the analysed molecule. Ten measurements at 25.0°C were collected and averaged before reporting the value.

4.3.5 Circular Dichroism analysis

The circular dichroism spectra were obtained using a “Jasco J-715” UV-CD spectrometer in the range 340-200 nm with quartz *cuvettes*. The concentration of pure NCys or pure NCysMe in MeOH was 0.0088 g/L. The concentration of polymers in MeOH varied throughout the samples in order to maintain the NCys or NCysMe concentration at 0.0088 g/L.

4.3.6 Size-exclusion chromatography

The molecular weights of the PBNCysMe samples were obtained by using the instrument as follows: Jasco PU-1580 equipped with Jasco 830-RI as refractometer, Jasco 830-UV as ultraviolet spectrophotometre and two columns PL gel mixed-D 5m (Polymer Laboratories). Analyses were performed on tetrahydrofuran diluted solutions (0.1 wt.-%) of selected samples. The calibration curve was obtained 1) with polystyrene standard samples and 2) with polymethylmethacrylate standards. The other polymers (functionalised SBR5, SBRL) were evaluated within the same experimental conditions; $CHCl_3$ was used as eluent and PS calibration curve was used.

4.3.7 Rheometric measurements on rubber compounds

The rheometric measurements on the rubber compounds samples (chapter 2.6, page 148) were performed with a rheometre called RPA 2000 by Alpha Instruments Inc. A picture of the particular measurement chamber of this instrument is reported in Figure 64.

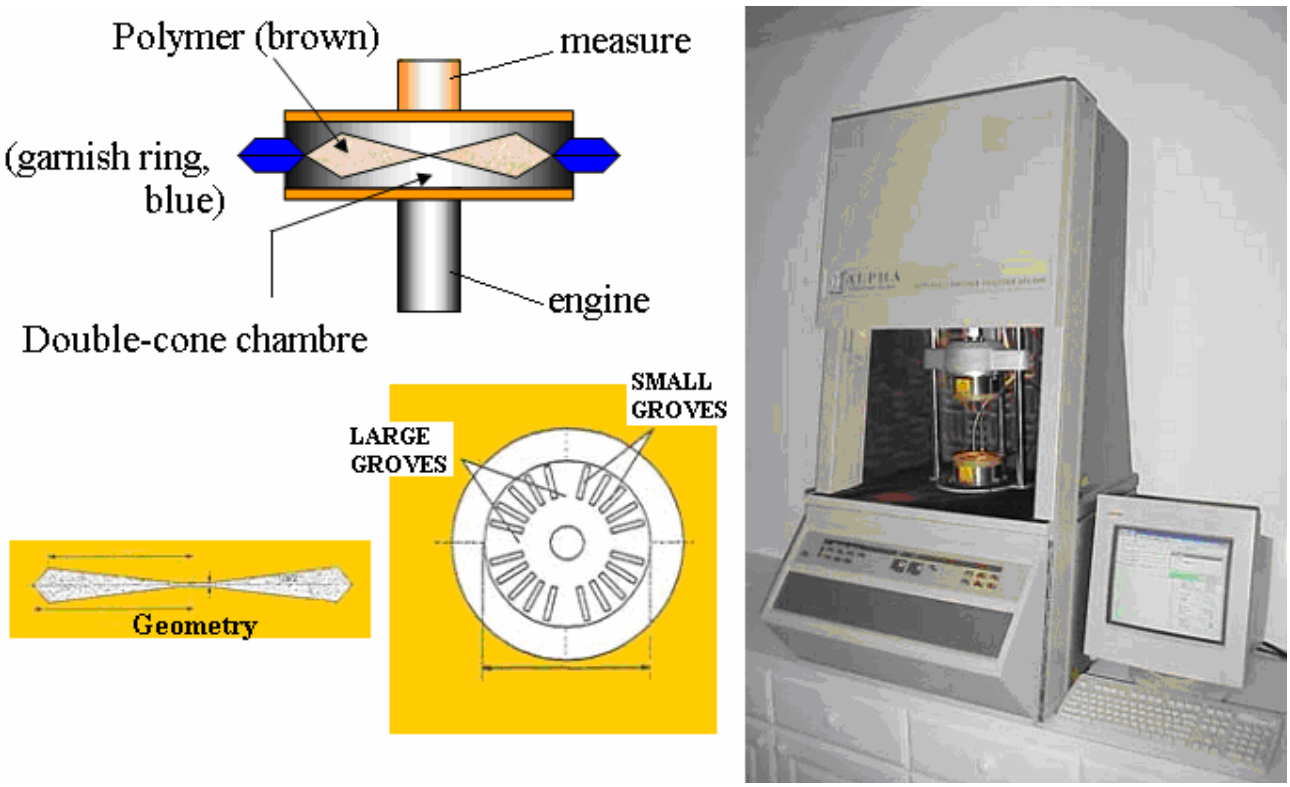

Figure 64 – Description of RPA 2000 and its chamber

The instrument fustellates the samples automatically by pressing the upper part of the chambre on a disk (having a thickness of 0.5 cm) placed in the centre of the lower tool. The disk must have a weight of 2.5 grams to ensure reproducibility and fill perfectly the measurement chamber.

After sample creation, a procedure is started. In the present work, the strain sweeps on the rubber (with a constant strain frequence of 1 Hz) were performed at 70°C; the induced shears of the samples were measured on the top tool as percentage of the maximum angle measurable by the instrument (90°).

A first strain sweep was performed in order to cancel the *mechanical history* of the sample; a second strain sweep, performed soon thereafter, allowed a first measurements of G', G" and tan δ. In order to highlight the agglomeration of the filler, an annealing procedure was carried out by keeping the samples for 10 minutes i) at 70°C ii) at 170°C; a final strain sweep, in the same conditions of the previous strain sweeps, was eventually performed. At the end of measurement, the samples were discarded.

4.3.8 Stress-strain dynamometric measurements on the vulcanised compounds

Dynamometric measurements were performed on the vulcanised compounds; these measurements referred to the standard UNI 6065. The instrument was a Tinius Olsen Testing Machine Co. Inc. U-

Serie 300 kN, and the samples were prepared by cutting, with a pneumatic die-cutter, a ring-shaped portion of the compound. The diametre of the ring was 4 cm and the section was a square 5 mm x 5 mm; during the experiments, the rings broke always in the middle part of the sample. The basis of the average measurement was five samples per run.

5. REFERENCES

[1] M. B. Smith, J. March, in *March's Advanced Organic Chemistry (Sixth Edition)* (Ed.: J. Wiley), Wiley, New York, **2007**, pp. 687.

[2] G. E. Wardell, in *Patai, "The Chemistry of the Thiol Group", Vol. 1* (Ed.: J. Wiley), Wiley, New York, **1974**, pp. 169.

[3] A. Shostakovskij, R. Kul'bovskaya, N. D. Gracheva, G. Laba, L. M. Yakushina, *Journal of General Chemistry of the USSR (English version)* **1962**, *32*, 707.

[4] K. Griesbaum, *Angewandte Chemie, International Edition* **1970**, *9*, 273.

[5] A. A. Oswald, K. Griesbaum, in *Organic Sulphur Compounds, Vol. 2* (Eds.: Kharasch, Meyers), Pergamon, New York, **1966**, pp. 233.

[6] M. J. Janssen, in *Patai Series* (Ed.: Interscience), New York, **1969**, pp. 720.

[7] H. C. Kolb, M. G. Finn, K. B. Sharpless, *Angewandte Chemie, International Edition* **2001**, *40*, 2004.

[8] Z. P. Demko, K. B. Sharpless, *Angewandte Chemie, International Edition* **2002**, *41*, 2110.

[9] Z. P. Demko, K. B. Sharpless, *Angewandte Chemie, International Edition* **2002**, *41*, 2113.

[10] H. C. Kolb, *Abstracts of Papers, 221st ACS National Meeting, San Diego, CA, United States, April 1-5* **2001**, ORGN.

[11] W. G. Lewis, L. G. Green, F. Grynszpan, Z. Radic, P. R. Carlier, P. Taylor, M. G. Finn, K. B. Sharpless, *Angewandte Chemie, International Edition* **2002**, *41*, 1053.

[12] L. M. Campos, K. L. Killops, R. Sakai, J. M. J. Paulusse, D. Damiron, E. Drockenmuller, B. W. Messmore, C. J. Hawker, *Macromolecules* **2008**, *41*, 7063.

[13] J. E. Boulden, N. B. Cramer, C. N. Bowman, *Polymer Preprints (American Chemical Society, Division of Polymer Chemistry)* **2008**, *49*, 1157.

[14] C. N. Bowman, N. B. Cramer, T. Y. Lee, J. A. Carioscia, *Abstracts of Papers, 233rd ACS National Meeting, Chicago, IL, United States, March 25-29* **2007**, PMSE.

[15] J. A. Carioscia, H. Lu, J. W. Stanbury, C. N. Bowman, *Dental Materials* **2005**, *21*, 1137.

[16] J. A. Carioscia, J. W. Stansbury, C. N. Bowman, *Polymer* **2007**, *48*, 1526.

[17] T. Y. Lee, J. Carioscia, Z. Smith, C. N. Bowman, *Macromolecules* **2007**, *40*, 1473.

[18] H. Lu, J. A. Carioscia, J. W. Stansbury, C. N. Bowman, *Dental Materials* **2005**, *21*, 1129.

[19] C. Bowman, K. Anseth, B. Hacioglu, C. Nuttelman, (The Regents of the University of Colorado, USA). Patent: WO 2003031483 A1, **2003**, p. 23.

[20] C. N. Bowman, J. Carioscia, H. Lu, J. W. Stansbury, (The Regents of the University of Colorado, USA). Patent: WO 2005086911 A2, **2005**, p. 34.

[21] C. N. Bowman, H. Lu, J. W. Stansbury, (The Regents of the University of Colorado, USA). Patent: WO 2005041807 A1, **2005**, p. 35.

[22] C. E. Hoyle, *Polymer Preprints (American Chemical Society, Division of Polymer Chemistry)* **2008**, *49*, 155.

[23] T. Y. Lee, T. M. Roper, E. S. Jonsson, C. A. Guymon, C. E. Hoyle, *Macromolecules* **2004**, *37*, 3606.

[24] Q. Li, H. Zhou, D. A. Wicks, C. E. Hoyle, *Journal of Polymer Science, Part A: Polymer Chemistry* **2007**, *45*, 5103.

[25] T. M. Roper, T. Kwee, T. Y. Lee, C. A. Guymon, C. E. Hoyle, *Polymer* **2004**, *45*, 2921.

[26] C. E. Hoyle, T. Y. Lee, T. Roper, *Journal of Polymer Science, Part A: Polymer Chemistry* **2004**, *42*, 5301.

[27] G. S. Whitby, *Synthetic Rubber*, 1st ed., John Wiley, New York, **1954**.

[28] N. B. Cramer, C. N. Bowman, *Journal of Polymer Science, Part A: Polymer Chemistry* **2001**, *39*, 3311.

[29] N. B. Cramer, S. K. Reddy, A. K. O'Brien, C. N. Bowman, *Macromolecules* **2003**, *36*, 7964.

[30] S. K. Reddy, N. B. Cramer, C. N. Bowman, *Macromolecules* **2006**, *39*, 3681.

[31] A. Priola, F. Ferrero, G. Gozzelino, M. Panetti, *La Chimica e L'Industria* **1984**, *66*, 471.

[32] F. Romani, E. Passaglia, M. Aglietto, G. Ruggeri, *Macromolecular Chemistry and Physics* **1999**, *200*, 524.
[33] J. Gonzalez de la Campa, Q.-T. Pham, *Makromolekulare Chemie* **1981**, *182*, 1415.
[34] Y. Camberlin, J. P. Pascault, J. Gonzalez de la Campa, Q. T. Pham, *European Polymer Journal* **1980**, *16*, 1031.
[35] M. Laleg, Y. Camberlin, D. Gulino, J. P. Pascault, *European Polymer Journal* **1982**, *18*, 821.
[36] M. A. Golub, *Journal of Polymer Science, Polymer Letters Edition* **1974**, *12*, 615.
[37] C. S. Marvel, K. G. Clarke, H. K. Inskip, W. K. Taft, B. G. Labbe, *Industrial and Engineering Chemistry* **1953**, *45*, 2090.
[38] A. A. Oswald, *ACS, Division of Petroleum Chemistry, Preprints* **1966**, *1*, 155.
[39] J. I. Cunneen, *Journal of the Chemical Society* **1947**, 36.
[40] J. I. Cunneen, *Journal of the Chemical Society* **1947**, 134.
[41] J. I. Cunneen, *Rubber Chemistry and Technology* **1953**, *26*, 370.
[42] J. I. Cunneen, C. G. Moore, B. R. Shephard, *Journal of Applied Polymer Science* **1960**, *3*, 11.
[43] J. I. Cunneen, F. W. Shipley, *Journal of Polymer Science* **1959**, *36*, 77.
[44] J. I. Cunneen, *Journal of Applied Chemistry* **1952**, *2*, 353.
[45] J. I. Cunneen, (British Rubber Producers Research Association). Patent: US 2506997, **1950**.
[46] J. I. Cunneen, W. P. Fletcher, A. N. Gent, R. I. Wood, (British Rubber Producers' Research Assoc.). Patent: GB 820261, **1959**.
[47] G. E. Serniuk, (Standard Oil Development Corporation, USA), Patent: US 2589151 A2, **1952**, p. 12.
[48] G. E. Serniuk, F. W. Banes, M. W. Swaney, *Journal of the American Chemical Society* **1948**, *70*, 1804.
[49] A. A. Oswald, K. Griesbaum, W. A. Thaler, B. E. Hudson, Jr., *Journal of the American Chemical Society* **1962**, *84*, 3897.
[50] B. Ameduri, K. Berrada, B. Boutevin, R. D. Bowden, *Polymer Bulletin* **1993**, *31*, 1.
[51] B. Boutevin, Y. Hervaud, G. Mouledous, *Polymer Bulletin* **1998**, *41*, 145.
[52] U. Gorski, K. Maenz, D. Stadermann, *Angewandte Makromolekulare Chemie* **1997**, *253*, 51.
[53] E. Klemm, U. Gorski, *Angewandte Makromolekulare Chemie* **1993**, *207*, 187.
[54] E. Passaglia, F. Donati, *Polymer* **2007**, *48*, 35.
[55] U. Gorski, E. Klemm, *Angewandte Makromolekulare Chemie* **1995**, *224*, 125.
[56] U. Gorski, E. Klemm, *Angewandte Makromolekulare Chemie* **1998**, *254*, 11.
[57] A. Priola, F. Ferrero, M. Panetti, *Pitture e Vernici* **1983**, *59*, 85.
[58] A. A. Oswald, K. Griesbaum, B. E. Hudson, Jr., J. M. Bregman, *Journal of the American Chemical Society* **1964**, *86*, 2877.
[59] W. A. Thaler, A. A. Oswald, B. E. Hudson, Jr., *Journal of the American Chemical Society* **1965**, *87*, 311.
[60] J. L. McFarling, J. F. Kircher, *International Journal of Applied Radiation and Isotopes* **1967**, *18*, 345.
[61] T. Posner, *Berichte der Deutschen Chemischen Gesellschaft* **1905**, *38*, 646.
[62] S. Boileau, B. Mazeaud-Henri, R. Blackborow, *European Polymer Journal* **2003**, *39*, 1395.
[63] U. Gorski, E. Klemm, D. Gorski, R. Maertin, (Friedrich Schiller Universität, Jena, D), Patent: DE 296288 A5, **1991**, p. 3.
[64] B. Mazeaud, S. Boileau, R. Blackborow, (BP Chimie S. A., FR), Patent: FR 2630449 A1, **1989**, p. 16.
[65] D. Teyssie, C. Vancaeyzeele, O. Fichet, S. Boileau, R. Blackborow, H. P. Rath, A. Lange, H. Pfistner, H. Mach, M. Hiller, (BASF A.-G.), Patent: WO 2006042711 A1, **2006**, p. 49.
[66] A. G. Ajaz, *Rubber Chemistry and Technology* **1995**, *68*, 481.
[67] J. Pytela, M. Sufcak, *PU Latin America 2001, Conference Papers, Sao Paulo, Brazil, Aug. 28-30* **2001**, P24/1.

[68] B. Ameduri, B. Boutevin, M. Nouiri, *Journal of Polymer Science, Part A: Polymer Chemistry* **1993**, *31*, 2069.
[69] B. Boutevin, E. Fleury, J. P. Parisi, Y. Pietrasanta, *Makromolekulare Chemie* **1989**, *190*, 2363.
[70] B. Boutevin, Y. Hervaud, M. Nouiri, *European Polymer Journal* **1990**, *26*, 877.
[71] G. Boutevin, B. Ameduri, B. Boutevin, J.-P. Joubert, *Journal of Applied Polymer Science* **2000**, *75*, 1655.
[72] K. F. Mueller, (Ciba-Geigy A.-G., Switz.). Patent: EP 115253 A1, **1984**, p. 21.
[73] F. Schapman, J. P. Couvercelle, C. Bunel, *Polymer* **1998**, *39*, 4955.
[74] F. Schapman, J. P. Couvercelle, C. Bunel, *Polymer* **2000**, *41*, 17.
[75] F. Schapman, J. P. Couvercelle, C. Bunel, *Polymer* **2001**, *42*, 7503.
[76] F. Schapman, J.-P. Couvercelle, C. Bunel, *European Polymer Journal* **2002**, *38*, 1979.
[77] F. Schapman, J. P. Couvercelle, C. Bunel, *Polymer* **1998**, *39*, 973.
[78] F. Schapman, J. P. Couvercelle, C. Bunel, *Polymer* **1998**, *39*, 965.
[79] S. Garin, L. Lecamp, B. Youssef, C. Bunel, *European Polymer Journal* **1998**, *35*, 473.
[80] L. Lecamp, B. Youssef, C. Bunel, *European Polymer Journal* **1997**, *33*, 1021.
[81] Y. Eckstein, E. J. Berger, *ACS, Organic Coating Appl. Pol., Preprints* **1983**, *48*, 23.
[82] J. Justynska, Z. Hordyjewicz, H. Schlaad, *Polymer* **2005**, *46*, 12057.
[83] F. Schapman, B. Youssef, E. About-Jaudet, C. Bunel, *European Polymer Journal* **2000**, *36*, 1865.
[84] L. Poussard, F. Burel, J.-P. Couvercelle, C. Loutelier-Bourhis, C. Bunel, *Journal of Applied Polymer Science* **2006**, *100*, 3312.
[85] D. H. Carey, G. S. Ferguson, *Macromolecules* **1994**, *27*, 7254.
[86] P. D. Mumbauer, D. H. Carey, G. S. Ferguson, *Chemistry of Materials* **1995**, *7*, 1303.
[87] R. C. L. Dutra, V. L. Lourenco, M. F. Diniz, M. F. P. Azevedo, R. V. Barbosa, B. G. Soares, *Polymer Bulletin* **1996**, *36*, 593.
[88] P. Jansen, M. Amorim, A. S. Gomes, B. G. Siaresm, *Journal of Applied Polymer Science* **1995**, *58*, 101.
[89] P. Jansen, A. S. Gomes, B. G. Soares, *Journal of Applied Polymer Science* **1996**, *61*, 591.
[90] P. Jansen, E. F. Silva, A. S. Gomes, B. G. Soares, *Macromolecular Reports* **1995**, *A32*, 655.
[91] P. Jansen, B. G. Soares, *Polymer Degradation and Stability* **1996**, *52*, 95.
[92] M. I. B. Tavares, P. Jansen, B. G. Soares, *Polymer Bulletin* **1996**, *37*, 215.
[93] P. Jansen, F. G. Garcia, B. G. Soares, *Journal of Applied Polymer Science* **2003**, *90*, 2391.
[94] P. Jansen, B. G. Soares, *Journal of Applied Polymer Science* **2000**, *79*, 193.
[95] P. Jansen, B. G. Soares, *Journal of Applied Polymer Science* **2002**, *84*, 2335.
[96] B. G. Soares, F. F. Alves, M. G. Oliveira, A. C. F. Moreira, *Journal of Applied Polymer Science* **2002**, *86*, 239.
[97] B. G. Soares, F. F. Alves, M. G. Oliveira, A. C. F. Moreira, F. G. Garcia, M. d. F. S. Lopes, *European Polymer Journal* **2001**, *37*, 1577.
[98] M. G. Oliveira, A. C. O. Gomes, M. S. M. Almeida, B. G. Soares, *Macromolecular Chemistry and Physics* **2004**, *205*, 465.
[99] M. G. Oliveira, B. G. Soares, *Journal of Applied Polymer Science* **2001**, *82*, 38.
[100] B. G. Soares, M. G. Oliveira, *Kautschuk Gummi Kunststoffe* **2003**, *56*, 396.
[101] B. G. Soares, A. S. Sirqueira, M. G. Oliveira, M. S. M. Almeida, *Kautschuk Gummi Kunststoffe* **2002**, *55*, 454.
[102] A. S. Sirqueira, B. G. Soares, *Macromolecular Materials and Engineering* **2007**, *292*, 62.
[103] B. G. Soares, F. O. Cario, Jr., *Journal of Applied Polymer Science* **2006**, *99*, 14.
[104] M. G. Oliveira, B. G. Soares, C. M. F. Santos, M. F. Diniz, R. C. L. Dutra, *Macromolecular Rapid Communications* **1999**, *20*, 526.
[105] A. S. Sirqueira, B. G. Soares, *European Polymer Journal* **2003**, *39*, 2283.
[106] A. S. Sirqueira, B. G. Soares, *Journal of Applied Polymer Science* **2002**, *83*, 2892.
[107] A. S. Sirqueira, B. G. Soares, *Journal of Macromolecular Science, Part B: Physics* **2007**,

46, 639.
[108] J. Justynska, H. Schlaad, *Macromolecular Rapid Communications* **2004**, *25*, 1478.
[109] A. Gress, A. Volkel, H. Schlaad, *Macromolecules* **2007**, *40*, 7928.
[110] J.-F. Lutz, H. Schlaad, *Polymer* **2008**, *49*, 817.
[111] F. Ciardelli, M. Aglietto, E. Passaglia, F. Picchioni, *Polymers for Advanced Technologies* **2000**, *11*, 371.
[112] F. Donati, Master Degree thesis, University of Pisa (Pisa), **2000**.
[113] F. R. Mayo, *Journal of the American Chemical Society* **1943**, *65*, 2324.
[114] S. Beuermann, N. Garcia, *Macromolecules* **2004**, *37*, 3018.
[115] M. D. Zammit, T. P. Davis, G. D. Willett, K. F. O'Driscoll, *Journal of Polymer Science, Part A: Polymer Chemistry* **1997**, *35*, 2311.
[116] G. Henrici-Olive, S. Olive, *Makromolekulare Chemie* **1963**, *68*, 219.
[117] G. Henrici-Olive, S. Olive, *Makromolekulare Chemie* **1966**, *96*, 221.
[118] M. Kamachi, D. J. Liaw, S. Nozakura, *Polymer Journal* **1981**, *13*, 41.
[119] K. F. O'Driscoll, M. J. Monteiro, B. Klumperman, *Journal of Polymer Science, Part A: Polymer Chemistry* **1997**, *35*, 515.
[120] A. Valdebenito, M. V. Encinas, *Polymer* **2005**, *46*, 10658.
[121] D. Colombani, *Progress in Polymer Science* **1997**, *22*, 1649.
[122] M. L. Coote, T. P. Davis, *Progress in Polymer Science* **2000**, *24*, 1217.
[123] M. Kamachi, *Advances in Polymer Science* **1981**, *38*, 55.
[124] G. Moad, D. H. Solomon, *Australian Journal of Chemistry* **1990**, *43*, 215.
[125] Y. Geng, D. E. Discher, J. Justynska, H. Schlaad, *Angewandte Chemie, International Edition* **2006**, *45*, 7578.
[126] Z. Hordyjewicz-Baran, L. You, B. Smarsly, R. Sigel, H. Schlaad, *Macromolecules* **2007**, *40*, 3901.
[127] J. Justynska, Z. Hordyjewicz, H. Schlaad, *Macromolecular Symposia* **2006**, *240*, 41.
[128] A. Levent Demirel, H. Schlaad, *Polymer* **2008**, *49*, 3470.
[129] I. K. Voets, A. de Keizer, M. A. C. Stuart, J. Justynska, H. Schlaad, *Macromolecules* **2007**, *40*, 2158.
[130] F. Ciardelli, M. Aglietto, M. B. Coltelli, E. Passaglia, G. Ruggeri, S. Coiai, *NATO Science Series, II: Mathematics, Physics and Chemistry* **2004**, *175*, 47.
[131] F. Ciardelli, S. Coiai, E. Passaglia, A. Pucci, G. Ruggeri, *Polymer International* **2008**, *57*, 805.
[132] F. Ciardellli, A. Altomare, M. Aglietto, S. Bronco, V. Castelvetro, E. Passaglia, G. Ruggeri, E. Taburoni, *La Chimica e L'Industria* **2003**, *85*, 57.
[133] M. Aglietto, F. Ciardelli, E. Passaglia, G. Ruggeri, G. Suffredini, P. Marcucci, E. Mentasti, (Belantro International Corporation, Panama). Patent: WO 9935172 A1, **1999**, p. 39.
[134] F. Ciardelli, E. Passaglia, S. Coiai, (Università di Pisa, Italy). Patent: WO 2004113399 A2, **2004**, p. 30.
[135] E. Passaglia, S. Coiai, M. Aglietto, G. Ruggeri, M. Ruberta, F. Ciardelli, *Macromolecular Symposia* **2003**, *198*, 147.
[136] M. A. Golub, *Pure and Applied Chemistry* **1972**, *30*, 105.
[137] A. F. Halasa, H. E. Adams, *Journal of Polymer Science, Polymer Symposia* **1970**, *No. 30*, 169.
[138] G. Greig, J. C. J. Thynne, *Transactions of the Faraday Society* **1966**, *62*, 379.
[139] M. Noguera, L. Rodriguez-Santiago, M. Sodupe, J. Bertran, *Journal of Molecular Structure* **2001**, *537*, 307.
[140] R. E. Benesh, R. Benesh, *Journal of the American Chemical Society* **1955**, *77*, 5877.
[141] J. B. Donnet, E. Custodero, in *The Science and Technology of Rubber, 5th edition* (Eds.: J. E. Mark, B. Erman, F. R. Eirich), Elsevier Academic Press, San Diego, **2005**, pp. 367.
[142] G. Heinrich, M. Kluppel, *Advances in Polymer Science* **2002**, *160*, 1.
[143] S. Wolff, *Kautschuk Gummi Kunststoffe* **1981**, *34*, 280.

[144] R. Rauline, (Michelin S.à.S.), Patent: EP 0501227 A1, **1992**, p. 18.
[145] W. M. Hess, *Rubber Chemistry and Technology* **1991**, *64*, 386.
[146] W. M. Hess, G. C. McDonald, E. Urban, *Rubber Chemistry and Technology* **1973**, *46*, 204.
[147] J. B. Donnet, E. Custodero, *Carbon* **1992**, *30*, 813.
[148] J. B. Donnet, E. Custodero, T. K. Wang, *Kautschuk Gummi Kunststoffe* **1996**, *49*, 274.
[149] G. Kraus, J. Jansen, *Kautschuk Gummi Kunststoffe* **1978**, *31*, 569.
[150] R. H. Bradley, I. Sutherland, E. Sheng, *Journal of Colloid and Interface Science* **1996**, *179*, 561.
[151] A. I. Medalia, G. Kraus, in *The Science and Technology of Rubber, 2nd Edition* (Eds.: J. E. Mark, B. Erman, F. R. Eirich), Elsevier Academic Press, San Diego, **1994**, p. 300.
[152] T. C. Gruber, T. W. Zerda, M. Gerspacher, *Carbon* **1993**, *37*, 1209.
[153] W. M. Hess, G. C. McDonald, *Rubber Chemistry and Technology* **1983**, *56*, 892.
[154] D. Creeden, *The Carbon Aggregate* **1997**, *4*, 1.
[155] Y. Chevallier, J. C. Morawski, Patent: EP 0157703 A1, **1984**.
[156] L. R. Evans, W. H. Waddell, *Kautschuk Gummi Kunststoffe* **1995**, *48*, 718.
[157] A. I. Medalia, L. W. Richards, *Journal of Colloid and Interface Science* **1972**, *40*, 233.
[158] D. F. Twiss, *Journal of the Society of Chemical Industry, London* **1925**, *44*, 106.
[159] S. Wolff, M. J. Wang, E. H. Tan, *Rubber Chemistry and Technology* **1993**, *66*, 163.
[160] E. M. Dannenberg, *Rubber Chemistry and Technology* **1986**, *59*, 512.
[161] E. M. Dannenberg, H. J. Collyer, *Journal of Industrial and Engineering Chemistry* **1949**, *41*, 1607.
[162] G. Kraus, *Science and Technology of Rubber, Vol. 1*, F.R.Eirich Academic Press, New York, **1978**.
[163] J. O'Brien, E. Cashell, G. E. Wardell, V. J. McBrierty, *Macromolecules* **1976**, *9*, 653.
[164] R. A. Beebe, M. H. Polley, W. R. Smith, C. B. Wendell, *Journal of the American Chemical Society* **1947**, *69*, 2294.
[165] Z. Rigbi, *Kautschuk Gummi Kunststoffe* **1993**, *46*, 36.
[166] D. Rivin, *Rubber Chemistry and Technology* **1963**, *36*, 729.
[167] D. Rivin, *Rubber Chemistry and Technology* **1971**, *44*, 307.
[168] W. D. Schaeffer, W. R. Smith, M. H. Polley, *Industrial and Engineering Chemistry* **1953**, *45*, 1721.
[169] J. Le Bras, *Journal of Applied Polymer Science* **1983**, *22*, 525.
[170] M. E. Abu-Zeid, Y. A. Youssef, *Journal of Applied Polymer Science* **1986**, *31*, 1575.
[171] W. F. Watson, *Journal of Industrial and Engineering Chemistry* **1955**, *47*, 1281.
[172] R. S. Rajeev, S. K. De, *Rubber Chemistry and Technology* **2002**, *75*, 429.
[173] S. Wolff, *Rubber Chemistry and Technology* **1996**, *69*, 325.
[174] H. M. Smallwood, *Journal of Applied Physics* **1944**, *15*, 758.
[175] E. Guth, O. Gold, *Physical Reviews* **1938**, *53*, 322.
[176] G. Kraus, *Journal of Polymer Science, Part B: Polymer Letters* **1970**, *8*, 601.
[177] A. I. Medalia, *Journal of Colloid and Interface Science* **1970**, *32*, 115.
[178] S. Wolff, U. Goerl, M. J. Wang, W. Wolff, *European Rubber Journal* **1994**, *176*, 16.
[179] M. J. Wang, S. Wolff, J. B. Donnet, *Rubber Chemistry and Technology* **1991**, *64*, 714.
[180] S. Wolff, M. J. Wang, *Rubber Chemistry and Technology* **1992**, *65*, 329.
[181] Y. Bomal, P. Cochet, B. Dejean, I. Gelling, R. Newell, *Kautschuk Gummi Kunststoffe* **1998**, *51*, 259.
[182] Y. Bomal, P. Cochet, B. Dejean, J. Machurat, *Rubber World* **1993**, *6*, 33.
[183] S. Shiga, M. Furuta, *Rubber Chemistry and Technology* **1985**, *58*, 1.
[184] A. Westlinning, S. Wolff, *Kautschuk Gummi Kunststoffe* **1966**, *19*, 470.
[185] S. Wolff, *Kautschuk Gummi Kunststoffe* **1969**, *22*, 367.
[186] S. Wolff, *Kautschuk Gummi Kunststoffe* **1970**, *28*, 7.
[187] S. Wolff, K. Burmester, *Kautschuk Gummi Kunststoffe* **1976**, *29*, 691.
[188] S. Wolff, H. Pohnisch, P. Hoffmann, *Kautschuk Gummi Kunststoffe* **1975**, *28*, 379.

[189] H. G. Kilian, H. Schenk, S. Wolff, *Colloid and Polymer Science* **1987**, *265*, 410.
[190] S. Wolff, *Kautschuk Gummi Kunststoffe* **1988**, *41*, 674.
[191] S. Wolff, *Kautschuk Gummi Kunststoffe* **1974**, *27*, 511.
[192] G. M. Cameron, M. W. Ranney, K. J. Sollman, *SGF Publicerande* **1973**, *No. 43*, VIII.
[193] M. W. Ranney, G. M. Cameron, B. W. Lipinski, *Kautschuk Gummi Kunststoffe* **1973**, *26*, 409.
[194] M. W. Ranney, C. A. Pagano, *Rubber Chemistry and Technology* **1971**, *44*, 1080.
[195] M. W. Ranney, K. J. Sollman, G. M. Cameron, *Kautschuk Gummi Kunststoffe* **1975**, *28*, 597.
[196] L. P. Ziemianski, C. A. Pagano, M. W. Ranney, *Rubber World* **1970**, *163*, 53.
[197] F. Thurn, S. Wolff, *Kautschuk Gummi Kunststoffe* **1975**, *28*, 733.
[198] M. J. Wang, S. Wolff, *Rubber Chemistry and Technology* **1992**, *65*, 715.
[199] S. Wolff, *Kautschuk Gummi Kunststoffe* **1979**, *32*, 760.
[200] A. R. Payne, *Reinforcement of Elastomers, Vol. (unique)*, Intersciences, New York, **1965**.
[201] A. R. Payne, *Journal of Applied Polymer Science* **1962**, *6*, 57.
[202] A. R. Payne, *Journal of Applied Polymer Science* **1962**, *6*, 368.
[203] W. P. Fletcher, A. N. Gent, *Rubber Chemistry and Technology* **1954**, *27*, 209.
[204] A. R. Payne, R. E. Whittaker, *Rubber Chemistry and Technology* **1971**, *44*.
[205] T. Riccò, in *Caratterizzazione Meccanico-Dinamica di Materiali Polimerici*, Pacini Editore S.p.A., Gargnano (BS), **2005**, pp. 107.
[206] A. Lion, C. Kardelky, P. Haupt, *Rubber Chemistry and Technology* **2003**, *76*, 533.
[207] P. G. Maier, D. Goritz, *Kautschuk Gummi Kunststoffe* **1996**, *49*, 18.
[208] E. M. Dannenberg, *Rubber Chemistry and Technology* **1975**, *48*, 410.
[209] E. M. Dannenberg, J. J. Brennan, *Rubber Chemistry and Technology* **1966**, *39*, 597.
[210] N. Nagata, T. Kobatake, H. Watanabe, A. Ueda, A. Yoshioka, *Rubber Chemistry and Technology* **1987**, *60*, 837.
[211] F. Tsutsumi, M. Sakakibara, N. Oshima, *Rubber Chemistry and Technology* **1990**, *63*, 8.
[212] L. Mullins, *Rubber Chemistry and Technology* **1969**, *42*, 339.
[213] L. Mullins, N. R. Tobibn, *Journal of Applied Polymer Science* **1965**, *9*, 2993.
[214] M. Gerspacher, C. P. O'Farrell, L. Nikiel, H. H. Yang, *Rubber Chemistry and Technology* **1996**, *69*, 786.
[215] L. Nikiel, M. Gerspacher, H. Yang, C. P. O'Farrell, *Rubber Chemistry and Technology* **2001**, *74*, 249.
[216] D. J. Schuring, *Rubber Chemistry and Technology* **1980**, *53*, 600.
[217] D. J. Schuring, S. Futamura, *Rubber Chemistry and Technology* **1990**, *63*, 315.
[218] S. K. Clark, in *International Rubber Conference*, Proc. Soc. Rubber Ind. Japan, Tokyo, **1975**, pp. 325.
[219] T. Kempermann, *Rubber Chemistry and Technology* **1981**, *55*, 391.
[220] A. C. Patel, J. T. Byers, *ACS, Rubber Division, Preprints* **1980**, *Paper n.48*.
[221] M. Gerspacher, C. P. O'Farrell, H. H. Yang, L. Nikiel, *Rubber World* **1999**, *220*, 27.
[222] E. R. Fitzgerald, J. D. Ferry, *Rubber Chemistry and Technology* **1982**, *5*, 1569.
[223] G. G. A. Bohm, M. N. Nguyen, *Journal of Applied Polymer Science* **1995**, *55*, 1041.
[224] M. Gerspacher, L. Nikiel, H. H. Yang, C. P. O'Farrell, G. A. Schwartz, *Kautschuk Gummi Kunststoffe* **2002**, *55*, 596.
[225] C. J. Lin, W. L. Hergenrother, E. Alexanian, G. G. A. Bohm, *Rubber Chemistry and Technology* **2002**, *75*, 865.
[226] C. J. Lin, T. E. Hogan, W. L. Hergenrother, *Rubber Chemistry and Technology* **2004**, *77*, 90.
[227] S. Mihara, R. N. Datta, W. K. Dierkes, J. W. M. Noordermeer, in *Technical Meeting - ACS, Rubber Division, 172nd* (Ed.: A. C. Society), Cleveland, Ohio, **2007**, pp. mihara1/1.
[228] J. P. Greenstein, M. Winitz, *Chemistry of the amino acids, Vol. 1 page 7 and Vol. 3 page 1879*, John Wiley and Sons, New York, **1961**.

[229] R. Salle, Q.-T. Pham, *Journal of Polymer Science, Polymer Chemistry Edition* **1977**, *15*, 1799.
[230] V. D. Mochel, *Journal of Polymer Science, Part A: Polymer Chemistry* **1972**, *10*, 1009.
[231] V. D. Mochel, W. E. Claxton, *Journal of Polymer Science, Part A: Polymer Chemistry* **1971**, *9*, 345.
[232] F. Ziaee, H. S. Mobarakeh, M. Nekoomanesh, H. Arabi, *e-Polymers* **2008**, *118*, 1.
[233] N. ten Brummelhuis, C. Diehl, H. Schlaad, *Macromolecules* **2008**, *41*, 9946.
[234] Z. I. Kulitski, L. M. Terman, V. F. Tsepalov, V. Y. Shlyapintokh, *Russian Chemical Bulletin* **1963**, *12*, 230.
[235] E. Passaglia, M. Marrucci, G. Ruggeri, M. Aglietto, *Gazzetta Chimica Italiana* **1997**, *127*, 91.
[236] M. A. Golub, *Journal of Polymer Science, Polymer Letters Edition* **1974**, *12*, 295.
[237] M. A. Golub, *Macromolecules* **1969**, *2*, 550.
[238] M. A. Golub, *Rubber Chemistry and Technology* **1978**, *51*, 677.
[239] M. A. Golub, R. J. Gargiulo, *Journal of Polymer Science, Polymer Letters Edition* **1972**, *10*, 41.
[240] M. A. Golub, J. Heller, *Journal of Polymer Science, Part B: Polymer Letters* **1966**, *4*, 469.
[241] M. A. Golub, C. L. Stephens, *Journal of Polymer Science, Part A-1: Polymer Chemistry* **1968**, *6*, 763.
[242] M. A. Golub, M.-T. Sung, *Journal of Polymer Science, Polymer Letters Edition* **1973**, *11*, 129.
[243] M. A. Golub, *Journal of Polymer Science, Polymer Chemistry Edition* **1981**, *19*, 1073.
[244] N. Grassie, A. Heaney, *Journal of Polymer Science, Polymer Letters Edition* **1974**, *12*, 89.
[245] M. A. Golub, *Journal of Polymer Science, Polymer Chemistry Edition* **1980**, *19*, 1073.
[246] R. Peters, M. v. Duin, G. Kwakkenbos, Y. Mengerink, R. v. Benthem, C. d. Koster, P. J. Schoenmakers, S. v. d. Wal, *Journal of Chromatography A* **2008**, *1201*, 151.
[247] R. Peters, D. Tonoli, M. v. Duin, J. Mommers, Y. Mengerink, A. T. M. Wilbers, R. v. Benthem, C. d. Koster, P. J. Schoenmakers, S. v. d. Wal, *Journal of Chromatography A* **2008**, *1201*, 141.
[248] M. Bellander, B. Stenberg, S. Persson, *Journal of Applied Polymer Science* **1999**, *73*, 2799.
[249] L. Gonzalez, A. Rodriguez, A. Marcos, C. Chamorro, *Rubber Chemistry and Technology* **1996**, *69*, 203.
[250] L. D. Loan, *Rubber Chemistry and Technology* **1967**, *40*, 149.
[251] B. M. E. van der Hoff, *Applied Polymer Symposia* **1968**, *7*, 21.
[252] T. Zytoski, A. Fischer, *J. of Am. Chem. Soc.* **1997**, *119*, 12869.
[253] V. Grinshpun, A. Rudin, *Journal of Applied Polymer Science* **1986**, *32*, 4303.
[254] S. Mori, T. Suzuki, *Journal of Liquid Chromatography and Related Technologies* **1981**, *4*, 1685.
[255] B. Trathnigg, *Progress in Polymer Science* **1995**, *20*, 615.
[256] F. Schapman, J. P. Couvercelle, C. Bunel, *Polymer* **1999**, *41*, 17.
[257] M. Gordon, J. S. Taylor, *Journal of Applied Chemistry* **1952**, *2*, 493.
[258] E. A. DiMarzio, J. H. Gibbs, *Journal of Polymer Science* **1959**, *40*, 121.
[259] I. Uematsu, K. Honda, *Rep. Prog. Polymer Physics Japan* **1965**, *8*, 111.
[260] I. Uematsu, K. Honda, *Rep. Prog. Polymer Physics Japan* **1966**, *9*, 254.
[261] J. M. Barton, *Journal of Polymer Science, Part C: Polymer Symposia* **1970**, *30*, 573.
[262] H. Daimon, H. Okitsu, J. Kumanotani, *Polymer Journal* **1975**, *7*, 460.
[263] I. Havlicek, J. Biros, J. Podesva, J. Hrouz, *Polymer Bulletin* **1981**, *4*, 9.
[264] J. Podesva, J. Biros, *Makromolekulare Chemie* **1981**, *182*, 3341.
[265] J. Furukawa, A. Nishioka, *Journal of Polymer Science, Part B: Polymer Letters* **1971**, *9*, 199.
[266] J. Furukawa, Y. Iseda, K. Haga, N. Kataoka, T. Yoshimoto, T. Imamura, Y. Shido, A. Miyagi, K. Tanaka, K. Sakamoto, *Journal of Polymer Science, Part B: Polymer Letters*

1969, *7*, 561.
[267] J. Furukawa, A. Nishioka, T. Kotani, *Journal of Polymer Science, Part B: Polymer Letters* **1970**, *8*, 25.
[268] G. E. Ham, *Journal of Macromolecular Science, Part A: Chemistry* **1975**, *A9*, 461.
[269] G. E. Ham, *Journal of Macromolecular Science, Part A: Chemistry* **1975**, *A9*, 1281.
[270] G. Liu, Z. Meng, W. Wang, Y. Zhou, L. Zhang, *Journal of Physical Chemistry B* **2008**, *112*, 93.
[271] M. Hirooka, T. Kato, *Journal of Polymer Science, Part B: Polymer Letters* **1974**, *12*, 31.
[272] R. B. Beevers, E. F. T. White, *Journal of Polymer Science, Part B: Polymer Letters* **1963**, *1*, 171.
[273] W. H. Howard, *Journal of Applied Polymer Science* **1961**, *5*, 303.
[274] K. H. Illers, *Kolloid z. Z. Polym.* **1963**, *190*, 16.
[275] M. Hirooka, H. Yabuuchi, J. Iseki, Y. Nakai, *Journal of Polymer Science, Part A-1: Polymer Chemistry* **1968**, *6*, 1381.
[276] K. Yokota, *Progress in Polymer Science* **1999**, *24*, 517.
[277] Y. Iwakura, F. Toda, H. Suzuki, *Journal of Organic Chemistry* **1967**, *32*, 440.
[278] Y. Iwakura, F. Toda, H. Suzuki, *Journal of Polymer Science, Part A: Polymer Chemistry* **1967**, *5*, 1599.
[279] V. Bottiglione, M. Morcellet, C. Loucheux, *Makromolekulare Chemie* **1980**, *181*, 485.
[280] C. Methenitis, J. Morcellet-Sauvage, M. Morcellet, *Polymer Bulletin* **1984**, *12*, 133.
[281] C. Methenitis, J. Morcellet-Sauvage, M. Morcellet, *Polymer Bulletin* **1984**, *12*, 141.
[282] C. Methenitis, J. Morcellet-Sauvage, M. Morcellet, C. Loucheux, *Convegno Italiano Scienza Macromolecole, [Acts], 6th* **1983**, *2*, 1.
[283] M. Morcellet, C. Loucheux, *Macromolecules* **1982**, *15*, 890.
[284] J. Morcellet-Sauvage, M. Morcellet, C. Loucheux, *Makromolekulare Chemie* **1981**, *182*, 949.
[285] J. Morcellet-Sauvage, M. Morcellet, C. Loucheux, *Makromolekulare Chemie* **1982**, *183*, 821.
[286] J. Morcellet-Sauvage, M. Morcellet, C. Loucheux, *Makromolekulare Chemie* **1982**, *183*, 831.
[287] C. Methenitis, J. Morcellet, G. Pneumatikakis, M. Morcellet, *Macromolecules* **1994**, *27*, 1455.
[288] F. Sanda, M. Nakamura, T. Endo, *Chemistry Letters* **1997**, 175.
[289] F. Sanda, M. Nakamura, T. Endo, *Journal of Polymer Science, Part A: Polymer Chemistry* **1998**, *36*, 2681.
[290] F. Sanda, M. Nakamura, T. Endo, *Macromolecules* **1996**, *29*, 8064.
[291] F. Sanda, M. Nakamura, T. Endo, T. Takata, H. Handa, *Macromolecules* **1994**, *27*, 7928.
[292] T. E. Hopkins, K. B. Wagener, *Advanced Materials* **2002**, *14*, 1703.
[293] H. Kudo, F. Sanda, T. Endo, *Macromolecular Chemistry and Physics* **1999**, *200*, 1232.
[294] H. Kudo, F. Sanda, T. Endo, *Macromolecules* **1999**, *32*, 8370.
[295] J. P. Gao, J. P. Chen, Z. Y. Wang, *Journal of the American Chemical Society* **1995**, *117*, 5377.
[296] T. Nakano, Y. Okamoto, K. Hatada, *Journal of the American Chemical Society* **1992**, *114*, 1318.
[297] Y. Okamoto, M. Nishikawa, T. Nakano, E. Yashima, K. Hatada, *Macromolecules* **1995**, *28*, 5135.
[298] W. L. Senn Jr., *Analytica Chimica Acta* **1963**, *29*, 505.
[299] A. R. Katritzky, D. E. Weiss, *Journal of the Chemical Society, Perkin Transactions II* **1975**, 27.
[300] A. R. Katritzky, D. E. Weiss, *Journal of the Chemical Society, Perkin Transactions II* **1975**, 21.
[301] A. R. Katritzky, D. E. Weiss, *Journal of the Chemical Society, Chem. Communication* **1974**,

401.
[302] B. Trathnigg, X. Yan, *Chromatographia* **1992**, *33*, 467.
[303] E. M. I. Barrall, C. J. R, J. F. Johnson, *Journal of Applied Polymer Science* **1968**, *12*, 1373.
[304] AIM, *Fondamenti di Scienza dei Polimeri, Vol. 1*, 2nd ed., Pacini Editore S.p.a., **1998**.
[305] A. L. Segre, M. Delfini, F. Conti, A. Boicelli, *Polymer* **1975**, *16*, 338.
[306] H. Sato, T. Ishikawa, K. Takebayashi, Y. Tanaka, *Macromolecules* **1989**, *22*, 1748.
[307] H. Sato, K. Takebayashi, K. Tanaka, *Macromolecules* **1987**, *20*, 2418.
[308] I. C. McNeill, W. K. Stevenson, *Polymer Degradation and Stability* **1985**, *10*, 247.
[309] K. Suchocka-Galas, *European Polymer Journal* **1990**, *26*, 1203.
[310] J. L. Binder, *Industrial and Engineering Chemistry* **1954**, *46*, 1727.
[311] A. J. Durbetaki, C. M. Miles, *Analytical Chemistry* **1965**, *37*, 1231.
[312] E. Passaglia, S. Coiai, G. Giordani, E. Taburoni, L. Fambri, V. Pagani, M. Penco, *Macromolecular Materials and Engineering* **2004**, *289*, 809.
[313] E. Passaglia, S. Coiai, L. Ricci, F. Ciardelli, *Macromolecular Symposia* **2004**, *218*, 61.
[314] T. Scholl, H. J. Weidenhaupt, H. W. Engels, (Bayer A.-G., Germany). Patent: EP 489313 A1, **1992**, p. 15.
[315] T. Scholl, J. Trimbach, (Bayer A.-G., Germany). Patent: DE 19961522 A1, **2001**, p. 8.
[316] T. Scholl, (Bayer A.-G., Germany). Patent: EP 1101789 A1, **2001**, p. 10.
[317] T. Scholl, U. Eisele, J. Trimbach, S. Kelbch, (Bayer A.-G., Germany). Patent: EP 974616 A1, **2000**, p. 13.
[318] T. Scholl, J. Trimbach, W. Nentwig, R. Engehausen, (Bayer A.-G., Germany). Patent: DE 10049964 A1, **2002**, p. 8.
[319] T. Scholl, R. Peter, R. Steiger, P. Wendling, J. Trimbach, A. Koski, (Bayer A.-G., Germany). Patent: EP 1101794 A1, **2001**, p. 10.
[320] T. Scholl, J. Trimbach, (Bayer A.-G., Germany). Patent: DE 19920788 A1, **2000**, p. 6.
[321] T. Scholl, J. Trimbach, (Bayer A.-G., Germany). Patent: EP 1000971 A1, **2000**, p. 12.
[322] T. Scholl, J. Trimbach, (Bayer A.-G., Germany). Patent: DE 19914848 A1, **2000**, p. 8.
[323] T. Scholl, J. Trimbach, (Bayer A.-G., Germany). Patent: EP 1130034 A2, **2001**, p. 9.
[324] L. G. Wideman, K. J. Pyle, R. R. Smith, P. H. Sandstrom, (The Goodyear Tire & Rubber Company, USA). Patent: EP 1221461 A1, **2002**, p. 11.
[325] L. G. Wideman, K. J. Pyle, R. R. Smith, P. H. Sandstrom, (The Goodyear Tire & Rubber Company, USA). Patent: EP 1191058 A1, **2002**, p. 12.
[326] S. Gandon-Pain, (Michelin S.à.S.). Patent: FR 2854404 A1, **2004**, p. 41.
[327] M. Breza, I. Kortisova, Z. Cibulkova, *Polymer Degradation and Stability* **2006**, *91*, 2848.
[328] Z. Cibulkova, P. Simon, P. Lehocky, J. Balko, *Polymer Degradation and Stability* **2005**, *87*, 479.
[329] H. W. Engels, *Kautschuk Gummi Kunststoffe* **1994**, *47*, 12.
[330] N. M. Huntink, R. N. Datta, A. Talma, J. W. M. Noordermeer, *Journal of Applied Polymer Science* **2006**, *100*, 853.
[331] E. Klein, Z. Cibulkova, V. Lukes, *Polymer Degradation and Stability* **2005**, *88*, 548.
[332] R. P. Lattimer, E. R. Hooser, R. W. Layer, C. K. Rhee, *Rubber Chemistry and Technology* **1983**, *56*, 431.
[333] J. Bowman, M. Da Via, M. E. Pattinelli, P. Tortoreto, *Kautschuk Gummi Kunststoffe* **2004**, *57*, 31.
[334] P. Tortoreto, C. Arcoleo, M. Da Via, J. Bowman, in *TyreTech 2000 Congress Acts*, *9th edition*, Warsaw, Poland, **2000**, pp. 16/1.
[335] P. Tortoreto, M. Da Via, *Industria della Gomma* **2001**, *45*, 33.
[336] R. Clausius, *Journal des Mathematiques de Paris* **1862**, *VII*, 209.
[337] B. T. Poh, C. S. Te, *Journal of Applied Polymer Science* **2000**, *77*, 3234.
[338] J. Froehlich, W. Niedermeier, H. D. Luginsland, *Composites, Part A: Applied Science and Manufacturing* **2005**, *36A*, 449.
[339] C. Dubisson, Y. Fukumoto, L. S. Hegedus, *Journal of the American Chemical Society* **1995**,

117, 3697.